WORKING FOR A HEALTHY FUTURE

HISTORICAL RESEARCH REPORT

Research Report TM/79/15
1979

Investigation into the dust deposition pattern in the respiratory tract. Final report on CEC Contract 6244-00/8/101

Emmett PC

WORLD HEALTH ORGANISATION
COLLABORATING CENTRE
FOR OCCUPATIONAL HEALTH

HISTORICAL RESEARCH REPORT
Research Report TM/79/15
1979

Investigation into the dust deposition pattern in the respiratory tract. Final report on CEC Contract 6244-00/8/101

Emmett PC

INSTITUTE OF OCCUPATIONAL MEDICINE
Research Avenue North, Riccarton, Edinburgh, EH14 4AP
Tel: +44 (0)870 850 5131 Fax: +44 (0)870 850 5132
e-mail publications@iomhq.org.uk

Report No. TM/79/15
(EUR.P36)
CEC Contract
6244-00/8/101
UDC 539.215.4

FINAL REPORT ON CEC
CONTRACT 6244-00/8/101

INVESTIGATION INTO THE DUST DEPOSITION PATTERN IN THE RESPIRATORY TRACT

P.C. Emmett

August 1979

Price:
£20.00 (UK)
£25.00 (Overseas)

Report No. TM/79/15 (EUR. P36)
CEC Contract 6244-00/8/101

I N S T I T U T E O F O C C U P A T I O N A L M E D I C I N E

INVESTIGATION INTO THE DUST DEPOSITION PATTERN IN THE RESPIRATORY TRACT

by

P.C. Emmett

FINAL REPORT ON CEC RESEARCH CONTRACT 6244-00/8/101

Duration of project: September 1974 to August 1978

Research work carried out with financial aid from the Commission of the European Communities.

Medical Branch,
Institute of Occupational Medicine,
Roxburgh Place,
EDINBURGH
EH8 9SU

(Tel. 031-667-5131)

August 1979

CONTENTS

LIST OF TABLES AND FIGURES

Report No. TM/79/15

INSTITUTE OF OCCUPATIONAL MEDICINE

FINAL REPORT ON CEC CONTRACT 6244-00/8/101

INVESTIGATION INTO THE DUST DEPOSITION PATTERN IN THE RESPIRATORY TRACT

by

P.C. Emmett

SUMMARY

The deposition and short-term clearance characteristics of monodisperse aerosol particles (size range 4·5 - 13 μm diameter) in the human respiratory tract have been investigated in eighteen human volunteer subjects.

The primary aim of the study has been to define accurately the upper size limit of dust which is able to penetrate below the larynx and to deposit subsequently in the dead space airways. It is this size fraction of dust which may be important in the aetiology of chronic bronchitis. The experimental problems of obtaining an accurate sample of the inhaled aerosol and of controlling the physiological conditions of aerosol administration have been given particular emphasis, in order to improve on the suitability and accuracy of existing experimental techniques. A new type of apparatus has been constructed which accurately samples the aerosol to be inhaled by a subject and at the same time ensures a rigorous control of the physiological conditions of aerosol administration.

The sampling part of the device employs a simple mechanical servomechanism which consists in essence of two spirometers in mutual balance. The most important advantages of the new method are: 1. its proven accuracy even at the largest particle size employed (13 μm diameter); 2. the future possibility of studying polydisperse dusts without in any way affecting the accuracy of the result; 3. its cost effectiveness in terms of high accuracy at low cost compared with, for example, that of aerosol sampling techniques based on optical scatter.

The experimental and historical background to the present work is discussed in order to emphasise the areas in which previous research might be open to misinterpretation and to illustrate gaps in the knowledge of aerosol behaviour in the human respiratory tract.

The regional distribution of the inhaled particles within the respiratory tract has been estimated using an indirect technique, the accuracy of which depends, in part, on certain widely accepted assumptions. The method is based on the monitoring of the clearance of inhaled radioactive particles over a period of about one day. By assuming that the material cleared within this period represents only those particles which initially deposited on the ciliated dead space airways, the relative proportions of respiratory zone and dead space aerosol deposition may be estimated. A profile scanning technique

for distinguishing between adjacent and overlapping anatomical regions has been employed (HOLMA, 1967), which is considered to be a more suitable method for this purpose than the fixed radiation detector systems employed elsewhere.

The total deposition results of the present work are generally lower than those of other workers, with one exception, in a limited region of comparison, rising only slowly from a mean value of about 80% of the inhaled aerosol at 4·5 μm particle diameter to about 88% at 13 μm, percentages being expressed in relation to the inhaled aerosol and averaged over three subjects at each particle size. Mouthwash recovery ranged from below 1% to just over 9% in the same particle size range. These figures are also lower than those reported by other workers and it is suggested that mouthpiece design and dimensions may be the most important causative factors. Aerosol losses in the laryngeal/pharyngeal region have been carefully measured and exhibit the largest scatter of observations of any anatomical region studied, suggesting an important role for the glottal opening. The mean values at each size ranged from 9% to 42%, which is lower than those reported by LIPPMANN and ALBERT (1969), whose results exhibited considerably greater scatter. Considering the rapidly increasing trend in these losses with increasing particle size it seems unlikely that particles more than several microns greater than the largest particle size employed in the present work (13 μm diameter) are able to penetrate below the larynx in significant amounts.

Estimated percentage aerosol deposition on the dead space airways maintains a fairly constant level throughout most of the particle size range studied, rising from about 21% at 4·5 μm to about 36% at 6·7 μm and remaining at about this level up to and including 13 μm particle diameter. The estimated levels of one-day retention are higher than those of LIPPMANN and ALBERT (1969) but agree well with the one published result of STAHLHOFFEN et al. (1979). Good agreement has also been obtained with the fractional retention values reported by FOORD et al. (1978) in a limited region of particle size overlap. The present results for respirable dust are about 45% retention (relative to inhaled aerosol) at ~24 hours and 4·5 μm particle diameter, declining steadily to about 8½% at 10·4 μm and about 6½% at 13 μm particle diameter. However, while these results would appear to indicate that the larger particles are able to penetrate to the respiratory zone of the lungs far more effectively than had hitherto been considered possible by most investigators, the rapid decline in the independently obtained laryngeal/tracheal clearance curves does not support this finding. Moreover, an analysis of the present data using a simple filter model of the respiratory tract demonstrates that the regional aerosol deposition results are wholly inconsistent with the expected behaviour of airborne particles in the respiratory zone. It is therefore concluded that the measured levels of one-day retention at large particle sizes are being caused by an incomplete clearance of particles which initially deposited on the dead space airways.

The ramifications of the above conclusion with respect to

existing respirable dust sampling curves are discussed and it is recommended that the results of the present work should be regarded only as an upper deposition limit, in the case of respirable dust, and a lower deposition limit in the case of that dust fraction which deposits on the dead space airways.

An interesting secondary phenomenon has also been observed: the clearance curves exhibit distinct non-random fluctuations. By means of fixed and double radiation detectors placed over the laryngeal and tracheal region of the throat, it has been established that the fluctuations are not merely an artefact of the primary measuring detector and have their origin from somewhere below the trachea, not solely in the larynx itself. The possible biological and physical factors that may be implicated in the causation of the clearance pulses are discussed.

1. INTRODUCTION

The definition of a safe or acceptable level of dust exposure requires some knowledge of the amount and site of deposition of dust in the human respiratory tract, under a variety of conditions, and its subsequent rate of clearance. Calculation of these dust filtration characteristics is complicated and consensus has not yet been established (TAULBEE and YU, 1975). If possible, therefore, they are best determined experimentally.

While useful information may be obtained by use of models or hollow casts of the upper respiratory tract, the technique would be difficult to apply to the more intricate lower respiratory tract (SCHLESINGER and LIPPMANN, 1972). The use of artificially ventilated excised lungs is also limited, for reasons of availability and technique (MITCHELL, 1975). Accurate assessment of the degree of a dust hazard therefore requires experimental work involving live subjects, preferably human.

Such experimental work is often concerned with the measurement of the total amount of dust which deposits in the respiratory tract relative to that inhaled, termed total deposition. It is also possible to combine this with the indirect estimation of the relative amount of dust which deposits within specific zones of the respiratory tract, termed regional deposition, by the use of radioactive aerosols (LIPPMANN and ALBERT, 1969).

Although many experiments have been performed to measure total deposition the scatter of observations has been considerable (DAVIES, 1974). Besides individual variations, such scatter may be due in part to poor aerosol sampling techniques and in part to a failure to define or control those factors, such as breathing rate, which determine the rate of aerosol deposition in the subject. Because of these experimental difficulties very few total deposition experiments have been performed at particle diameters greater than several micrometers. Still fewer experiments have been performed to investigate regional deposition (LIPPMANN, 1977; FOORD et al, 1978).

It is the purpose of the present work to extend reliable knowledge of total and regional aerosol deposition and clearance characteristics in the human respiratory tract to the highest practical particle diameter. In this chapter essential background knowledge is reviewed.

1.1 Description of human respiratory tract

(i) Morphology and patterns of airflow

For the purposes of the present discussion the human respiratory tract will be divided into three zones: 1. the nasopharynx, oral passages and larynx; 2. the dead space airways, extending from the trachea to the terminal bronchioles, 3. the respiratory zone, where the gas exchange units, or alveoli, are situated.

Air which enters the nose encounters a greater resistance to flow than it does in the mouth, passing through the large narrow channels of the nasal cavities. The lateral walls of the cavities consist of folded turbinates whose role may be to expose the incoming air to the maximum surface area and hence enhance the nasal aerosol filtration efficiency (PROCTOR and SWIFT, 1971). Air which enters the mouth will tend to encounter less resistance to flow but possesses a potentially more variable cross-section, mainly determined by the position of the tongue and soft palate. Whether inhaled by either route, air is fully warmed and moistened by the time it enters the major bronchi (PROCTOR, 1964).

It is the larynx that mainly determines entry conditions for flow into the trachea. According to Macklem and Mead, (1967), the larynx, together with the mouth and trachea, accounts for about half the viscous resistance to breathing. The degree of glottal opening in the larynx varies according to whether the subject is inspiring or expiring, according to lung volume, and according to the level of exercise (STANESCU et al, 1972). Below the larynx there is less variability at given lung volume.

The conducting airways repeatedly branch in a generally dichotomous manner. The most widely used description of this branching system is that of Weibel, (1963). In Weibel's 'model A' symmetrical branching system, the number of branches, n, at a given generation, q, is given by,

$$n = 2^q \qquad \text{..... equation 1.1.1}$$

The trachea is defined as the zeroth generation(Table 1.1.1).

Table1.1.1: Weibel model 'A'; Regular dichotomy system, lung volume 4·8 l at ~3/4 maximum inflation

generic term	generation number	number per generation	diameter mm.	length mm.	cumulative length *1 mm.	cross-sect. area per generation cm.²	volume per generation cm.³	cumulative volume cm.³	surface area per generation *1 cm.²	cumulative surface area *1 cm.²	Reynolds' Number *1 *2
TRACHEA	0	1	18·0	120·0	120·0	2·54	30·5	30·5	67·8	67·8	1,510
MAIN BRONCHUS	1	2	12·2	47·6	167·6	2·33	11·3	41·8	36·8	104·6	1070
LOBAR BRONCHUS	2	4	8·3	19·0	186·6	2·13	4·0	45·8	19·1	123·7	797
	3	8	5·6	7·6	194·2	2·00	1·5	47·2	10·9	134·6	573
SEGMENTAL BRONCHUS	4	16	4·5	12·7	206·9	2·48	3·5	50·7	30·8	165·4	370
CARTILAGINOUS BRONCHI	5	32	3·5	10·7	217·6	3·11	3·3	54·0	38·0	203·4	230
↓	6	64	2·8	9·0	226·6	3·96	3·5	57·5	50·4	253·8	145
	7	128	2·3	7·6	234·2	5·10	3·9	61·4	67·0	320·8	92
	8	256	1·86	6·4	240·6	6·95	4·5	65·8	95·7	416·5	55
	9	512	1·54	5·4	246·0	9·56	5·2	71·0	134	550·8	33
↓	10	1,024	1·30	4·6	250·6	13·4	6·2	77·2	191	741·9	20
TERMINAL BRONCHUS	11	2,048	1·09	3·9	254·5	19·6	7·6	84·8	277	1,019	11
BRONCHIOLES	12	4,096	0·95	3·3	257·8	28·8	9·8	94·6	413	1,433	7
↓	13	8,192	0·82	2·7	260·5	44·5	12·5	106	607	2,040	3·6
	14	16,384	0·74	2·3	262·8	69·4	16·4	123	886	2,927	2·2
↓	15	32,768	0·66	2·0	264·8	113	21·7	145	1,315	4,242	1·2
TERMINAL BRONCHIOLE	16	65,536	0·60	1·65	266·5	180	29·7	175	1,980	6,222	0·7
RESPIRATORY BRONCHIOLES	17	131,072	0·54	1·41	267·9	300	41·8	217	3,096	9,318	0·37
↓	18	262,144	0·50	1·17	269·0	534	61·1	278	4,888	14,206	0·19
↓	19	524,288	0·47	0·99	270·0	944	93·2	371	7,932	22,138	0·10
ALVEOLAR DUCTS	20	1,048,576	0·45	0·83	270·9	1,600	140	510	12,400	34,538	0·06
↓	21	2,097,152	0·43	0·70	271·6	3,220	224	735	20,865	55,403	0·03
↓	22	4,194,304	0·41	0·59	272·1	5,880	350	1,085	34,146	89,549	0·01
ALVEOLAR SAC	23	8,388,608	0·41	0·50	272·6	11,800	591	1,675	57,658	147,208	< 0·01

*1 calculated by present author. *2 at 10 litres minute volume.

However, the high degree of morphologic asymmetry in the conducting airways should always be borne in mind. Convenient mathematical descriptions may sometimes obscure certain physical realities, such as the variation of branching angle from generation to generation (HORSFIELD et al, 1967).

The total cross-sectional area of the conducting airways increases directly with generation number and, consequently, the airflow which initially tends to be turbulent in the large airways is almost certainly laminar in the smaller airways. The nature of airflow in an airway is normally characterized by the Reynold's number Re, which expresses the relative magnitudes of the purely inertial and viscous forces in a fluid, and for a cylinder is given by,

$$Re = \frac{\rho . L . Vo}{\eta} \qquad \text{..... equation 1.1.2}$$

Where, ρ is the mass density of fluid
L is the diameter of the cylinder
Vo is the mean fluid flow rate
η is the viscosity of the fluid

Reynold's numbers in the human respiratory tract vary from about 0.01 in an alveolar sac, to about 1,500 in the trachea, depending on breathing pattern (Table 1.1.1). In the small airways (<2mm dia.) it is therefore highly likely that the flow which advances into the respiratory zone is of the Poisseuille type, i.e. the velocity distribution is parabolic, the velocity being a maximum in the centre of each airway. Very little mixing between the advancing tidal and the surrounding sheaths of expiratory reserve and residual air is therefore likely to occur (DAVIES et al, 1972), and the flow tends to be reversible (MUIR et al, 1971). Transfer of aerosol between these volumes in the small airways, therefore takes place mainly by virtue of the intrinsic particle mobility.

The dead space airways are considered to end at the terminal bronchioles, beyond which lie the alveolated airways,

or respiratory bronchioles. The terminal bronchioles are termed generation 16 in the Weibel model and beyond this point the airways are virtually free of cilia. Total airway cross-sectional area increases greatly in the respiratory bronchioles and still more quickly on entering the alveolar ducts and alveoli. There are something like 3×10^8 alveolar units in the normal adult lung.

(ii) Clearance mechanisms

Short-term clearance is generally taken to be synonymous with mucociliary clearance, but it is by no means established that there exists no longer term mucociliary phase. Camner and Philipsson (1978) demonstrated completion of a short-term clearance phase in humans within about one day after aerosol administration, but the work of Gore and Patrick (1978) has raised the possibility of a much longer term retention of particles in the trachea and first bifurcation of the conscious rat. Similarly, it cannot be stated with certainty that there exists no rapid phase of alveolar clearance, although this is considered to be unlikely by most investigators (MORROW, 1977). Moreover, Stahlhoffen et al (1979) have reported the results of the longer-term clearance of 0·6 μm diameter particles which were deposited overwhelmingly in the respiratory zone, observing no rapid phase component in the clearance curve.

Van As (1977) has recently reviewed some of the inconsistencies in the concept embodied by the term 'mucous sheet', first coined by Lucas and Douglas (1934). There is conflicting evidence as to whether this 'sheet' is in fact continuous or not (STURGESS, 1977), as has often been assumed (HATCH and GROSS, 1964). Moreover, there is still much controversy concerning the true composition of the 'mucous sheet' and the role of mucus proper, i.e. the secretory product of mucous glands and goblet cells, in it. In the present work the term 'ciliary transport fluid' will be used throughout, in order to avoid confusion.

The ciliary transport fluid is propelled towards the trachea by the combined beating action of the cilia, which line most of the dead space airways from the zeroth to about the sixteenth airway generation. While the structure

and function of the individual cilia have been examined in some detail (DALHAM, 1956), the mechanism of their combined behaviour remains poorly understood. In particular, the direction and speed of the transport process in relation to its variation with airway dimension is almost wholly undetermined. The importance of this information lies in its influence on the thickness of the ciliary transport fluid as it 'ascends' the dead space airways (ASSMUNDSSON and KILBURN, 1970).

Longer term clearance processes are believed to involve mainly alveolar macrophages and the pulmonary lymphatic system. However, the present work is concerned purely with short-term clearance phenomena, therefore longer term mechanisms will not be discussed further.

1.2 Behaviour of aerosols in the human respiratory tract

The term aerosol, an imprecise one, may be applied to any small particle which remains airborne for a reasonable time. Typical aerosols would therefore include dusts, smokes, sprays and mists, but generally exclude fumes and gases, although the distinction is not entirely clear-cut. All practical aerosols are actually poly-disperse, that is their diameters span a range of values. According to Fuchs and Sutugin (1966), an aerosol may be regarded as 'practically mono-disperse' when its geometric standard deviation is less than or equal to 12.

(i) Aerosol deposition mechanisms

All terrestrial particles experience the gravitational force. A spherical particle settling in air under the influence of gravity attains a terminal velocity, V_t, when the resistive and gravitational forces are just equal. The resistive force Fd, may be calculated using the well-known Stoke's equation, at low values of particle Reynold's number, Re_p (i.e. $Re_p < \sim 0{\cdot}05$).

$$Fd = 3\pi \eta \, d.V_T \qquad \ldots\ldots\ldots \text{ equation 1.2.1}$$

where, η, is the viscosity of air

d, is the particle diameter

Neglecting buoyancy forces and equating resistive and gravitational forces, the terminal velocity is given by,

$$V_T = \frac{\rho . d^2 . g}{18 \eta} \qquad \ldots\ldots\ldots \text{ equation 1.2.2}$$

where, ρ , is the particle density

g , is the acceleration due to gravity

Therefore, in a fluid of given viscosity particle density as well as optical diameter must be considered in characterizing the dynamic behaviour of an aerosol particle. It is convenient to accomplish this by defining its aerodynamic diameter, which is the diameter of a unit density sphere having the same terminal velocity as the particle in an identical medium.

For very large particles when the particle Reynold's number is high, equation 1.2.2 may be inaccurate. Similarly, for very small particles, those whose diameters are comparable to the mean free path of the surrounding air molecules, 'slip-correction factors' must be applied. However, in the size range of particles in the present study equation 1.2.2 will suffice.

When a particle is non-sperical but of well defined shape, a shape correction factor may be applied (ALLEN, 1974). However, when the particle is of highly irregular shape, or, of essentially regular shape but possessing an irregular or deformed surface, its aerodynamic diameter is difficult to predict and may be best determined by direct observation of falling speed.

When a particle is carried by a moving airstream which changes in speed or direction, it experiences a lag in its motion relative to the airstream by virtue of its own

inertia. The nature of the dependence of inertial effects on the particle density and diameter may perhaps be most easily calculated by considering the elementary case of a particle projected into a still air system at time $t = 0$, with an initial velocity, v_o. The inertial force is at all times opposed by the drag force on the particle, therefore for a sphere,

$$m.\frac{dv}{dt} = -3\pi\eta v.d \quad \ldots\ldots\ldots \text{ equation 1.2.3}$$

where, m, is the particle mass

v, is the particle's instantaneous velocity in the x-direction relative to the air-system $\left[\therefore v=\frac{dx}{dt}\right]$

(other nomenclature as above)

$$\therefore \frac{dv}{v} = \frac{-3\pi\eta d}{m} . dt = -\frac{dt}{\tau} \quad \text{where, } \tau = \frac{m}{3\pi\eta d},$$

and is termed the relaxation time of the particle

$$\therefore \int_{v_o}^{v} \frac{1}{v} . dv = \frac{-1}{\tau} . \int_0^t dt$$

where, v is the particle velocity at time, t.

$$\therefore \left[\ln(-v)\right]_{v_o}^{v} = -\frac{t}{\tau}$$

$$\ln v - \ln v_o = \ln\left(\frac{v}{v_o}\right) = \frac{-t}{\tau}$$

since, $\ln e^x = x$,

$$\therefore v = v_o . \exp\left[\frac{t}{\tau}\right]$$

After τ seconds the particle has slowed to $\frac{1}{e}$ of its initial value, v_o, possessed at the time of projection into the air-system.

The quantity most often used to represent the inertial behaviour of particles in variable flow regimes is the particle

stop distance, So,

now, $v = \frac{dx}{dt}$,

and from equation 1.2.3,

$$m \cdot \frac{dv}{dx} \cdot \frac{dx}{dt} = -3\pi\eta d \cdot \frac{dx}{dt}$$

$$\therefore m \int_{v_o}^{0} dv = -3\pi\eta d \int_{0}^{S_o} dx$$

$$\therefore v_o = \frac{3\pi\eta d}{m} \cdot So = \frac{So}{\tau}$$

$$\therefore So = v_o \tau \quad \text{..... equation 1.2.4}$$

Now since, $\tau = \frac{m}{3\pi\eta d} = \frac{\rho d^2}{18\eta}$

$$\therefore So = \frac{\rho d^2 v_o}{18\eta} \quad \text{..... equation 1.2.5}$$

Therefore, like the particle terminal velocity, v_T, So depends on particle diameter squared. Indeed, equation 1.2.5 may be re-written more simply as,

$$So = \frac{v_T . v_o}{g} \quad \text{..... equation 1.2.6}$$

and equation 1.2.2 may be re-written as,

$$v_T = \tau g \quad \text{..... equation 1.2.7}$$

Another important force which must be considered for very fine dusts is that induced by the Brownian motion of the gas molecules which surround each particle. However, in the size range of the present study the diffusive force is negligibly small. In the special case of fibrous aerosols, where the dimension of the particle may be a significant fraction of that of the containment vessel, the possible effects of interceptive deposition must be considered. In

the present work only spherical particles having diameters of negligible size in relation to the smallest human airway have been used and interceptive effects may be ignored.

Aerosols formed by the mechanical dispersal of a volatile liquid, invariable carry a substantial electric charge (WHITBY and LIU, 1966). Enhanced aerosol deposition may occur through the induction of electrical image forces or by the mutual repulsion of charged particles, termed the space-charge effect. The latter is highly dependent on the aerosol number concentration. Yu and Chandra (1978) have calculated the rate of deposition of 1 μm diameter particles in the human respiratory tract and conclude that the particle number density must be of the order of 10^5 particles per cubic centimetre before space-charge effects need to be considered. This is a far higher particle concentration than occurs in the present work.

For very fine aerosols it is possible that enhanced particle deposition might occur in the respiratory tract as a result of the induction of an electrical image force on the airway walls. Recent evidence for submicron particles supports this view (MELANDRI et al, 1977). However, it may be shown by elementary calculation that image forces are likely to be negligible even for the smallest particle size used in the present work (4·5 μm diameter).

According to Yu (1977), the image force, Fi, experienced by a spherical particle in a cylindrical vessel is given by,

$$Fi = \frac{Q^2 r^2}{16 \pi R^4 \epsilon_o (R-r)^2} \qquad \text{.... equation 1.2.8}$$

where, Q = total charge on particle
r = radial distance of particle from the cylinder axis
R = radius of cylinder
ϵ_o = permittivity of free space

Putting Q = y.e, where e is the fundamental unit of electronic charge and y is the number of such charges on each particle, equation 1.2.8 may be written as,

$$F_i = y^2 K$$

where $$K = \frac{q^2 r^2}{16 \pi R \epsilon_o (R - r)^2}$$

As an example, let R be the radius of the smallest airway in the Weibel model, where R ≃ 0·2 mm. Let $r = 10^{-2}$. R = 2μm, since if the image forces are small over this range in such a small airway, they are likely to be small elsewhere in the respiratory tract.

$$K = \frac{q^2 R^2 10^{-4}}{16 \pi R^2 \epsilon_o (R - 10^{-2} . R)^2}$$

Putting $e = 1{\cdot}6 \times 10^{-19}$ Coulombs, $\epsilon_o = 8{\cdot}85 \times 10^{-12}$ Farads $metre^{-1}$ gives, $K \simeq 1{\cdot}4 \times 10^{-17}$ Newtons.

The magnitude of the gravitational force, F_g, is given by,

$$F_g = m.g \quad \text{(nomenclature as above)}$$

Which for a unit density particle of diameter 4·5μm, gives a value $F_g \simeq 4{\cdot}7 \times 10^{-13}$ Newtons. Therefore, for Fi to be comparable to F_g, y must have a value of $(F_g / K)^{\frac{1}{2}}$, which in this case is approximately $1{\cdot}8 \times 10^2$ charges per particle. This is about an order of magnitude greater than the number of elementary charges measured elsewhere to reside on identical aerosol particles to those of the present study (FRY, 1970). It is therefore unlikely that electrostatic deposition is of any significance in this case. Precautionary measures were nevertheless taken to neutralize the test aerosol, described in Chapter 3, part 2 (iv).

A number of other forces exist which may act on an airborne particle, but only diffusiophoretic and thermal forces could be of conceivable relevance here. Diffusiophoretic forces act when there is a diffusional transfer of gases from

regions of high to low gas concentrations. In the human lung such diffusive transfer does occur, but owing to the simultaneous transfer of nearly equal numbers of O_2 and CO_2 molecules in opposite directions, it is considered unlikely by most investigators that diffusiophoretic forces are of much significance (HIDY and BROCK, 1969).

For thermal forces to act on a particle a temperature gradient must exist. In the human lung the temperature may be regarded as a nearly uniform 37°c throughout. The temperature in the oral cavity may often be several degrees below this figure and it is possible that very small thermal forces act on inhaled particles. However, since the residence time of particles in the oral cavity is always very small, even during quiet breathing, it is unlikely that thermal deposition forces are of any significance.

Overall then, it is the two basic forces of nature, gravity and inertia, that are likely to be of most significance in determining the respiratory tract deposition of the aerosol particles of the present study. Both depend on the square of particle diameter and the importance of each is likely to be considerably influenced by physiological factors.

(ii) Physiological factors in aerosol deposition

In the following discussion the influence of respiratory physiology on aerosol deposition will be considered only insofar as it affects the contribution of the two primary deposition mechanisms, gravitational settling or sedimentation, and inertial impaction. Inertial deposition of particles may occur in the respiratory tract wherever there is a change in the magnitude or direction of gas flow. Such changes occur most frequently in the upper airways and human head. Besides being influenced by the mean inspired or expired flow rates, it is likely that subtle changes in the configuration of upper respiratory tract anatomy are also important. Such anatomic variability has already been mentioned (1.1(i)); in particular, the constriction of the glottal opening during expiration is certain to increase peak flow velocities in the larynx and is therefore likely to lead to enhanced inertial deposition in, and possibly beyond, this region.

The importance of inertial deposition at the carinal ridge of the bifurcations has frequently been emphasised (SCHLESINGER et al. 1977). However, little attention has been given to the possible inertial deposition of particles arising from the existence of turbulent eddy currents and secondary swirling motions in the respiratory tract, as has been recently pointed out (HAMILL, 1979). Such deposition is often termed, perhaps misleadingly, 'turbulent diffusion'. Variations in the glottal opening during breathing may be of considerable importance in this respect and conceivably be a major source of both inter- and intra-subject variability.

Anatomical variability may also occur in the nasal cavity, but since the present work involved purely mouth-breathing experiments this will not be considered further.

According to the experimental results of Schlesinger and Lippmann(1972), who measured aerosol deposition in hollow casts of the human tracheo-bronchial tree, inertial impaction is not important beyond about the first ten airway generations. As was described above, airflow rates are slower and particle residence times longer in the smaller airways. This lowers the probability of inertial deposition and raises that of gravitational deposition. Therefore, as aerosol losses due to inertial impaction decrease, those due to sedimentation are likely to increase, towards the smaller airways (TAULBEE and YU, 1975).

The amount of aerosol which deposits in the respiratory zone of the lungs relative to the amount of aerosol inhaled at the mouth, will be determined by two factors, other influences being equal: 1. the amount of aerosol entering the respiratory zone; 2. the deposition efficiency in the respiratory zone. Since with increasing particle size more aerosol is likely to be lost in the dead space airways, aerosol exposure to the respiratory zone decreases. Yet since the deposition efficiency in the respiratory zone increases with particle size there must be a point at which the deposition there is a maximum. The peak alveolar deposition has normally been predicted to lie between 2-4 μm particle diameter, although this has never been confirmed experimentally (TASK GROUP ON LUNG DYNAMICS, 1966). Moreover,

it seems not to have always been appreciated that since the amount of aerosol loss in dead space is likely to vary considerably with breathing pattern, the alveolar peak may not always be at a fixed particle size (HEYDER et al, 1975).

Tidal volume and breathing rate rarely change in isolation from one another. A high level of exercise may result in an increase in both (SILVERMAN et al, 1951). At higher breathing rates there will be increased particle impaction in the dead space airways; since particle residence times are then lower it is likely that there is a simultaneous decrease in sedimentation losses. Therefore, whether or not there is a change in the aerosol exposure level in the respiratory zone will depend on the relative importance of inertial and gravitational deposition in the dead space airways. At higher breathing rates there will also be shorter particle residence times in the respiratory zone and consequently a lower aerosol deposition efficiency.

It is most important to distinguish between a change in respiratory zone deposition efficiency and a change in the absolute amount of aerosol which deposits there per unit time. For example, a doubling of breathing rate may well result in about a halving of the respiratory zone deposition efficiency, but since double the amount of dust enters the respiratory tract, and something probably close to double may enter the respiratory zone, the change in the absolute amount of dust which deposits in the respiratory zone may be slight.

The influence of tidal volume on aerosol deposition is not always entirely dependent on the fact that inhaled particles are taken 'deeper' into the lung (LIPPMANN, 1977). The increase in penetrance of particles which have already entered the respiratory zone, to the level of the alveolar ducts, with even a substantial increase in lung volume, is only of the order of a few millimetres (Table 1.1.1). At a given breathing rate some of the importance of tidal volume may also lie in the relative proportions of the inhaled aerosol which occupy the dead space airways and the respiratory zone. Since during quiet breathing a typical tidal volume is something like 600 ml (COMROE et al, 1955), the dead space

airways may well account for a substantial fraction of this. At higher tidal volumes the dead space airways become a smaller fraction and a higher relative amount of aerosol deposits in the respiratory zone.

The influence of the degree of lung inflation on aerosol deposition is still controversial. Heyder et al (1975) claim that it is the functional residual capacity (FRC) which mainly determines the observed differences in total deposition between subjects. However, Davies et al (1977) argue that total deposition correlates better with the residual volume (RV), since FRC includes the expiratory reserve volume (ERV), 'which changes more with age'. Such arguments depend on a number of anatomical imponderables, such as relative numbers and size of alveoli between subjects. Other anatomical factors such as variations in upper respiratory tract morphology, both between and within subjects, appear to have been neglected.

In measuring the total and regional deposition of aerosols in the respiratory tract the influence of the amount of aerosol which is transferred from the tidal to the expiratory reserve or the residual air must be considered (HEYDER, 1971). During the steady breathing of an aerosol of uniform inhaled concentration, the concentration of aerosol in the respiratory zone increases until a steady state level is reached. At this point the rate at which aerosol is transferred into the respiratory zone is just equal to the rate at which it deposits there. This process is termed the 'wash-in'. On cessation of aerosol inhalation, airborne particles may be observed in the expired air in ever decreasing amounts for several breaths. This process is termed the 'wash-out' (DAVIES et al, 1972). Consequently, for aerosol particles small enough to remain airborne in the breath which follows that in which they were first inhaled, it is necessary to specify whether total deposition is being measured before or after steady-state equilibrium has been established. Because of the relatively high levels of total deposition measured for particles larger than 4·5 μm (LIPPMANN and ALBERT, 1969; FOORD et al, 1978), it is unlikely that steady-state influences are important above this size (see Chapter 3, part 2(i)).

The temperature and humidity of the inspired air must be also considered as a possible factor in aerosol deposition. If the particles are inhaled from air at ambient temperature, normally about 17°c cooler than the lungs and not completely saturated even at this lower temperature, there exists the possibility of the condensation of water vapour on their initially cooler surfaces. Some total deposition experiments have been conducted at room temperature and humidity (LIPPMANN and ALBERT, 1969; FOORD et al, 1978) while others have for technical reasons required the inspired air to be at ~ 37°c and ~ 100% relative humidity (HEYDER et al, 1973). Such influences are discussed further in Chapter 3, part 3.2.(iv).

Finally, attention is drawn to a potentially important means by which inertial aerosol deposition in the respiratory tract may be enhanced that appears to have been overlooked in the literature. Relative inertially-induced movement between an inhaled airborne particle and its carrier airstream may arise quite independently of the changes in the magnitude or direction of the airflow relative to the 'fixed' human respiratory tract, if the individual is himself accelerated relative to the earth's inertial frame of reference. The magnitude of such an effect relative to the gravitational force, may be seen crudely by considering the ability of the human being to jump into the air, overcoming gravity, for short periods. Considering that occupational dust exposure must occur against a backcloth of work and therefore movement, such effects may merit investigation. In particular, the rapid mechanical vibrations induced in an individual by hand-held machine tools should be considered since these may simultaneously give rise to a high local dust concentration. It should therefore be borne in mind that the laboratory derivation of aerosol deposition curves for the stationary subject may not necessarily be readily applied to the work situation, even when differences in aerosol character and breathing conditions have been taken into account.

1.3 Criteria for defining aerosol hazard to the human respiratory tract

The induction of lung disease through the inhalation of airborne matter may be due to a multitude of factors: individual

susceptibility; toxicity of dust; solubility of dust; amount of dust deposited in diseased region; residence time of dust in deseased region. In the present work the latter two factors are of most relevance.

Perhaps the two most notable contemporary examples of aerosol hazard evaluation are those of the mining and atomic energy industries. Of particular concern in both industries is the dust fraction that is able to penetrate to the respiratory zone of the lungs. In a miner's lungs this dust fraction may give rise to silicosis or pneumoconiosis, while for a worker in the atomic energy industry the radiation dose arising from inhaled radionuclides is highly dependent on their pulmonary residence time. In establishing dust hazard criteria it is desirable to determine the dose-response characteristics of each dust. This requires the environmental sampling of the dust in question such that the individual or average dose to the employees may be determined. Dose-response correlation will be greatest when only that fraction of dust which would deposit in the region of the lungs of most interest is included in the sample (JACOBSEN et al, 1970). As the region of most interest and relevance, historically, has been the respiratory zone of the lungs, a size-fraction of dust has been defined which purports to represent that fraction of the total inhaled dust which deposits in the respiratory zone under normal working conditions (ORENSTEIN, 1960). This dust fraction is usually termed, perhaps rather misleadingly, 'respirable dust'. Although definitive respirable dust sampling criteria have been adopted by a number of nations (Figure 1.3.1), it is important to appreciate that the relative amount of dust which deposits in the respiratory zone is likely to be highly dependent on the breathing pattern adopted. It is also important to appreciate the historical origin of these criteria, for their basis is only partly empirical. Currently, the possibility of establishing sampling criteria for 'inhalable dust' is being considered (OGDEN and BIRKETT, 1977). Interest has also been expressed concerning the size fraction of dust which deposits in the dead space airways (ROGAN et al, 1973) which could be implicated in the aetiology of chronic bronchitis. For such new criteria to be established

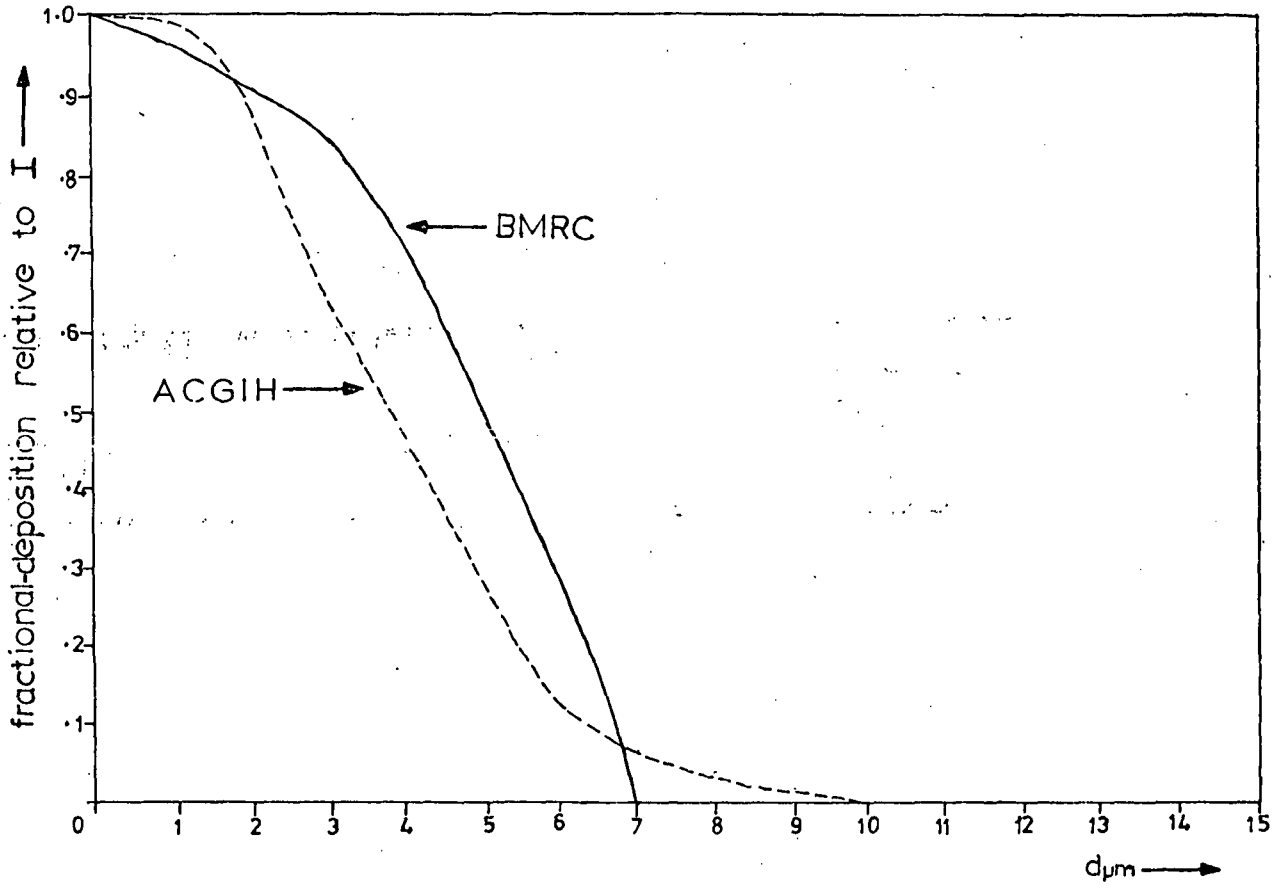

Figure 1.3.1: Respirable dust sampling criteria in U.K. (BMRC) and U.S.A. (ACGIH). (I represents inhaled aerosol).

more experimental work is required concerning the fate of the larger inhaled particles in the respiratory tract.

In Chapter 2, the historical origin of existing dust sampling criteria is reviewed from the viewpoint of the experimental work on which they were partly based.

2. HISTORICAL AND EXPERIMENTAL BACKGROUND

The possibility of a relationship between the inhalation of airborne matter and lung disease has long been recognised (GALEN, 129-199). However, it was not until late into the industrial revolution, by which time industrially derived aerosols were ubiquitous, that serious attempts were made to quantify the airborne hazard and to investigate the nature of pulmonary defence mechanisms. Although the history of such work has been described many times (HATCH and GROSS, 1964; STUART, 1973) and the experimental findings have often been applied to practical problems of industrial health (TASK GROUP ON LUNG DYNAMICS, 1966), the techniques used to obtain these results have rarely been examined (DAVIES, 1974). The emphasis placed in the present work on experimental accuracy and control may be better understood in this context.

In 1868, LISTER reported that air lost its power to cause putrefaction when mixed with blood by virtue of its having passed into the lungs. The observation was taken as evidence of the air purification properties of the lungs. This was seemingly corroborated by TYNDALL, who in 1870 reported on one of his earlier experiments which he believed had demonstrated the 'deeper portions of expired air' (probably what would now be called the expiratory reserve air) to be entirely free of inhaled airborne matter. As described by OWENS (1923), Tyndall's work was widely misinterpreted to mean that the lung acts as a perfectly efficient filter of all dusts. Although OWENS (1923) clarified the interpretation of these results and had also shown Tyndall's experimental technique to be insufficiently sensitive to detect very fine particles, in the intervening years the belief that the lungs act as a highly efficient dust filter became widespread and this view still persists in many modern textbooks of medicine and physiology:

> 'Particles below 1 μm in size are nearly the only ones to penetrate into the pulmonary depths.... Their deposition rate in alveolar spaces is very high, exceeding 90% of the total number of small particles inhaled, for any respiration rate and depth.' L. DAUTREBANDE in 'Microaerosols', 1962.

2.1 Total Deposition

The first attempt to measure total aerosol deposition in man, i.e. the total amount of aerosol which deposits expressed as a fraction or percentage of the total amount of aerosol

inhaled, was that of SAITO et al. (1912). The size distribution of dust employed and the breathing pattern of the subjects were not well defined however. Similar comments apply to the works of BAUMBERGER (1923) who attempted to measure differences in the total deposition values of tobacco smoking subjects 'puffing' and 'inhaling'. Baumberger was the first to employ an electrostatic precipitator, which enabled the exhaled aerosol to be collected without the problems that can arise when exhaling through a resistive filter. The electrostatic precipitator was later used in experiments conducted by SAYERS et al. (1924), but the first experiments to measure total deposition at a well defined breathing pattern were those of DRINKER et al. (1928). Their experiments serve usefully to illustrate the more fundamental experimental problems that may be encountered when attempting to measure total deposition.

According to the simple definition of total deposition mentioned above, other factors being equal, there are only two quantities which need to be measured: the total amounts of aerosol inhaled and exhaled by a subject. Ideally, the aerosol to be inhaled should be sampled as closely as possible to its point of entry into the subject, in order to avoid particle losses in any connecting pipework. The exhaled aerosol must be separately collected, or sampled, and mixing with any dead space aerosol in the apparatus, together with actual losses of exhaled aerosol in this dead space, should be minimised. In the apparatus of DRINKER et al. (1928), the aerosol to be inhaled was sampled remotely from the subject, thus allowing the possibility of high particle losses in the connecting pipework, particularly at large particle sizes. The separation of inhaled and exhaled flows, using flap valves, may have resulted in significant losses of exhaled aerosol before it could be collected. The overall tendency would therefore be for total deposition to be overestimated.

Many later total deposition experiments employed methods possessing similar or equivalent drawbacks (C.E. BROWN, 1931; VAN WIJK and PATTERSON, 1940; WILSON and LA MER, 1948; LANDAHL, 1950; DAUTREBANDE, 1957). The scatter of these

observations has been considerable (DAVIES, 1964).

ALTSHULER et al. (1957) introduced a new aerosol sampling technique based on optical scatter from a monodisperse aerosol which overcame many of the disadvantages mentioned above. The aerosol concentration was measured, as a function of time, close to the point of entry into the subject. By relating this to simultaneous recordings of respiratory flow rates and volumes, the relative amounts of inhaled and exhaled aerosol were calculated. Altshuler's basic apparatus was much improved by MUIR and DAVIES (1967) since no co-operation from the subject was needed for the manipulation of valves. Still further improvements have been made by HEYDER et al. (1973), (1975), particularly with regard to the application of analogue computing techniques in the automatic calculation of results.

Despite these improvements the optical scatter technique still imposes a few limitations. Measurement of the exhaled aerosol is more difficult than measurement of that inhaled, since the concentration of aerosol falls rapidly from the beginning of an expiration and the estimation of the true average is difficult (DAVIES, 1974). This is the converse of the aspiration sampling problem when it is, in general, harder to obtain accurate estimates of the total inhaled aerosol than total exhaled. Large particle sizes are particularly difficult to study using the technique.

2.2 Regional Deposition and Clearance

Techniques for measuring regional deposition have a more recent history. Two distinct experimental approaches have been adopted. One is based on the fractionation of the expired air into separate volumes and the amounts of aerosol contained within each are then measured. BROWN et al. (1950) first used the technique for this purpose and their results have probably been applied more extensively than any other in the derivation of international exposure standards (TASK GROUP ON LUNG DYNAMICS, 1966). For this reason their work merits some attention.

The experiments of BROWN et al. (1950) are acknowledged by many to have been misconceived (MERCER, 1973; LIPPMANN and

ALTSHULER, 1976). Central to these misconceptions is the assumption that the aerosol concentration measured at a given expired volume can be directly related to the amount of aerosol deposition that has occurred at a given depth, or region, in the lungs. Those who have reviewed their work have usually pointed to the weakness of assuming that aerosol particles follow the same course in the lungs as gases, which neglects the greater diffusibility of gases. In essence, this means there will be an error in the estimation of the amount of aerosol which can be said to have penetrated no further than the dead space airways. More fundamental objections to their methods have sometimes been overlooked. Their basic equations used in the calculation of deposition results from the raw experimental data are mutually inconsistent. A few of these inconsistencies were pointed out by ALTSHULER (1959).

The other technique for measuring regional deposition is that first described by ALBERT et al. (1955). It is based on measurements of the proportion of inhaled radioactive particles cleared from the lungs at about one day after aerosol administration. At an earlier date, WILSON and LA MER (1948) used radioactive particles in an attempt to measure regional deposition, but the method was based on the premise that by placing a collimated radiation detector over a section of the lung periphery, a representative measure of relative respiratory zone deposition could be obtained. It is apparent from Wilson and La Mer's paper (1948), that they well understood the approximate nature of the technique. Nevertheless, their work also merits attention because of its extensive use in the derivation of internationally accepted dust exposure standards (TASK GROUP ON LUNG DYNAMICS, 1966).

Wilson and La Mer's data (1948) from seven subjects were averaged to obtain a plot of 'relative axillary count' versus optical particle radius. The meaning of 'relative axillary count' must be made clear for it has sometimes been misinterpreted. It represents the number of detector counts per minute per μCi of inhaled radioactivity, averaged over the seven subjects. This is quite distinct from the amount of pulmonary deposition relative to the amount of aerosol inhaled. As was

pointed out by Wilson and La Mer, it is quite impossible to obtain any information on total respiratory zone deposition, from this data alone, relative to the inhaled aerosol. In a monograph on pulmonary deposition and retention, HATCH and GROSS (1964) cite Wilson and La Mer's data and describe their plot of 'relative axillary count' versus particle radius as 'the percentage deposition values in relation to particle size'.

A still earlier misinterpretation of Wilson and La Mer's data (1948) appears in the paper of BROWN et al. (1950). In this, Wilson and La Mer's 'relative axillary count' also appears as a 'percentage deposition' ordinate, but the higher deposition peak (there were actually two) is plotted at a level of 55%, not the 87% or so, of HATCH and GROSS (1964). The origin of the 55% value may be found in Wilson and La Mer's paper (1948). As this particular expression of their data has been extensively applied to theoretical and practical problems of industrial health, its origin merits clarification.

As has already been mentioned in the present review, Wilson and La Mer had stated in their paper (1948) that no information could be obtained from their axillary detector results on the amount of respiratory zone deposition relative to the amount of aerosol inhaled. In an attempt, literally, to 'determine this order of magnitude' they adopted two crude calibration schemes: one based on the calibration of their axillary detector in terms of absolute units of radioactivity; the other, based on measurements of blood radioactivity concentrations. The former method gave rise to the 55% value, but 27½% would have been equally valid since they had rather arbitrarily decided that their calibration 'pad' represented both lungs rather than the one nearest to the detector, the further one being excluded according to their description of the technique. The latter method gave rise to a range of retention values falling between 18% and 63% of the inhaled aerosol. The highly approximate nature of both these methods was clearly stated by Wilson and La Mer (1948).

The interpretation put on Wilson and La Mer's data (1948) by BROWN et al. (1950) is repeated in many of the reviews of the literature (DAUTREBANDE, 1954; STUART, 1973). Moreover

the same misinterpreted data have been used by Committee 2 of the TASK GROUP ON LUNG DYNAMICS, which sat in 1965 under the auspices of the ICRP* in order to provide a sound basis for inhaled radionuclide dosimetry and setting of international exposure limits. In their report (1966) the Wilson and La Mer data (1948) appear as in the paper of BROWN et al. (1950). As can be seen in Fig.2.2.1,a theoretical curve for percentage respiratory zone deposition (designated 'pulmonary zone deposition' in the report) for mouth breathing, was derived from the Wilson and La Mer data (1948) after making certain adjustments for particle hygroscopicity. Equivalent theoretical curves for nasal breathing were derived from the experimental results of BROWN et al. (1950). This was long after ALTSHULER (1959) had first questioned the basic equations that appeared in BROWN et al. (1950). The work of the ICRP Task Group forms the basis of current international exposure standards for inhaled radionuclides.

The radioactive aerosol technique, described by ALBERT et al. (1955), for the measurement of regional deposition was later developed by the same principal author and his later co-worker Lippmann (LIPPMANN and ALBERT, 1969). The technique is based on the assumption that the non-respiratory zone of the lung clears more quickly than the respiratory zone, by virtue of its being largely ciliated. The radioactive aerosol technique presents many technical difficulties which are described in later chapters. The results of LIPPMANN and ALBERT (1969) and those of the other two groups who have collected data in this field are discussed in Chapter 4.

Besides work on the aggregate clearance of inhaled particles in which the fundamentals of clearance mechanisms are often of only indirect interest, there have been many studies of the basic mechanism of mucociliary clearance and measurements of specific clearance rates in the ciliated airways. These investigations fall broadly into two categories: histological study of tissue excised from animals and man and the study of clearance rates in live subjects. It is beyond the scope of the present review to describe work on long-term clearance or to review the literature which deals with the esentially

* International Committee on Radiological Protection.

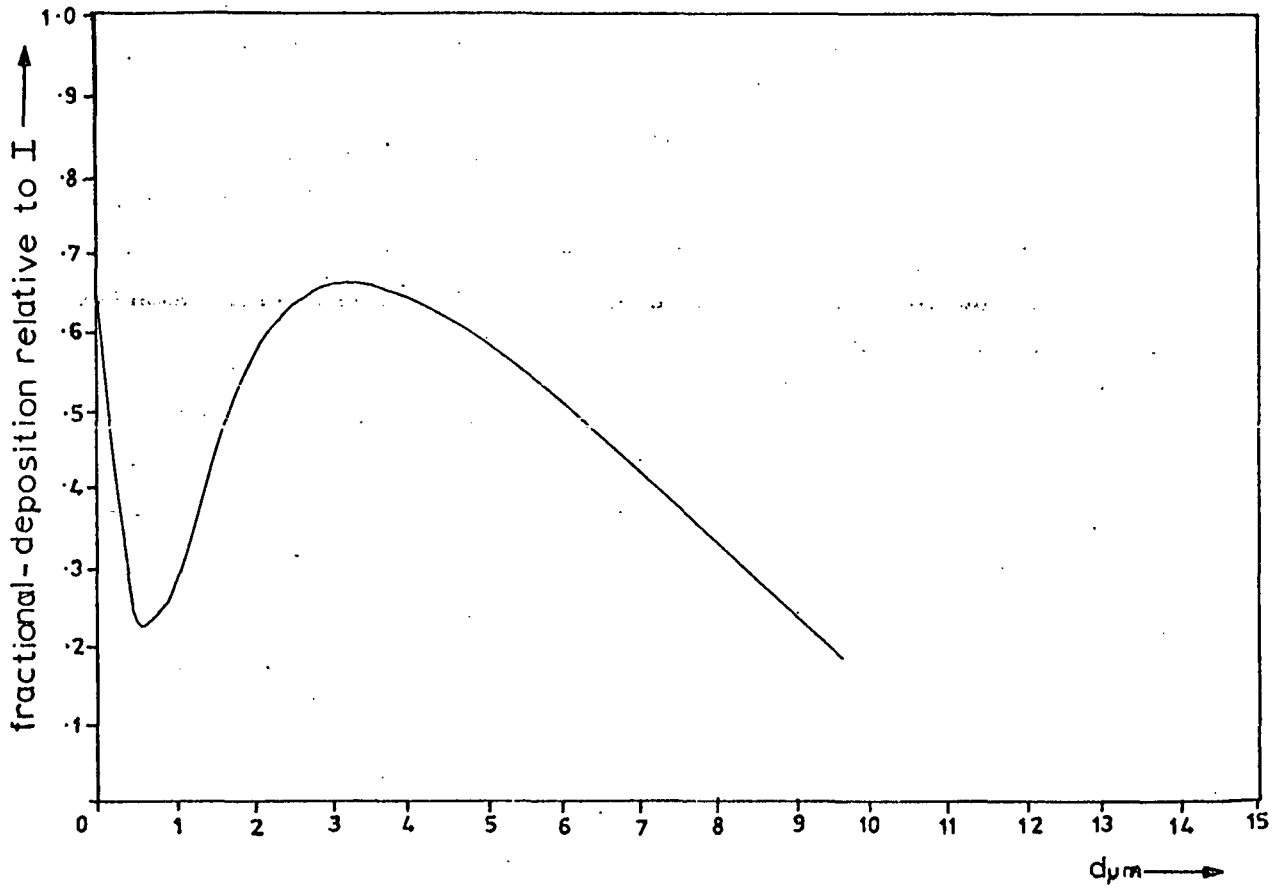

Figure 2.2.1: Task Group respirable dust curve. Theoretical curve at 15 breaths $min.^{-1}$, 750 cc tidal volume. I represents aerosol entering trachea.

mechanistic ciliary properties.

From histological study it has been possible to obtain information of limited reliability on clearance rates in airways of various diameters in animals and man (DALHAMN, 1956; ASSMUNDSSUN and KILBURN, 1970). This is possible because the cilia beat with a degree of independence from the central nervous system and may continue to beat for some time after death. The limitations to the reliability of this approach arise because of the inevitable experimental interference with the delicate balance of clearance fluids and ciliary beating (SLEIGH, 1977).

In conclusion, this review has considered some of the experimental techniques used to obtain the results of the most important investigations into the deposition and clearance of inhaled particles. The reliability of many of these techniques has been questioned and some errors in the interpretation of certain widely quoted results have been indicated.

3. EXPERIMENTAL METHODS

3.1 Particles

This section describes the techniques that were developed to produce a monodisperse test aerosol (coefficient of variation < 10%). The particles consisted of polystyrene labelled with a γ-emitting isotope, Technetium^{99m} (Tc^{99m}), whose half-life of radioactive decay is six hours. The latter is a convenient figure for measurements over a period of about one day. Polystyrene particles have been used in many human aerosol inhalation studies conducted elsewhere (BOOKER et al., 1967; THOMSON and PAVIA, 1969; FOORD et al., 1978). BLACK and WALSH (1970), reported on the work of EVANS (1967), who observed no obvious short-term toxic effects in in vitro cell studies. At an earlier date, SCHOENBERG et al. (1961) studied the phagocytosis of polystyrene particles in the reticulo-endothelial system of the rabbit and concluded they were metabolically inert and non-toxic to the host.

The advantages of employing monodisperse particles in a human aerosol inhalation study are essentially twofold. Firstly, if the mass of aerosol which deposits in a particular region of the respiratory tract is estimable, it is possible to express this value as a fraction of the total inhaled mass, directly. If a polydisperse aerosol is used, the size distribution of each deposition fraction must be measured in order to determine the fractional deposition of each component size, but this is rarely possible. It cannot be assumed that the deposition fractions measured at a mean diameter of polydisperse aerosol, whether it is derived in relation to number, area, or mass, are necessarily equal to the deposition fraction that would be measured using a monodisperse aerosol of the same number, area, or mass, diameter. In the case of a practically monodisperse aerosol, differences between mean diameters expressed in terms of mass, area and number, are minimal. Assuming a log-normal distribution, i.e. one in which the relative frequency plotted against $\log_e$ of size is normally distributed, the diameter, $\bar{d}m$, of the particle having a mass equal to the average mass of the sample, is given by:

$$\ln.\bar{d}m \quad \ln.\bar{d} + 3{\cdot}5 \ln.^2 \sigma g \qquad \text{.....equation 3.1.1}$$

where $\bar{d}$ is the count-mean diameter, $= \frac{1}{N} \sum_{i}^{o} ni.di$

and N = number of particles in sample

ni = number of particles of diameter di

σg = geometric standard deviation of the sample.

For $\sigma g = 1{\cdot}1$, the difference in value between $\bar{d}m$ and $\bar{d}$ is $0{\cdot}14$ μm at $\bar{d} = 4{\cdot}5$ μm and $0{\cdot}42$ μm at $\bar{d} = 13{\cdot}0$ μm, which is the size range used in the present study. The deposition fractions measured at a given value of $\bar{d}$ for a practically monodisperse aerosol may therefore be assumed to be close to the value of the same deposition fractions that would be measured for a perfectly monodisperse aerosol ($\sigma g = 1$) of the same diameter.

The second main advantage in employing a monodisperse test aerosol is that the difference between particle deposition measured in terms of particle number and particle mass is minimal (HEYDER, 1971). This allows comparison of results with those of similar studies based on measurements of inhaled and exhaled particle number concentrations (HEYDER et al., 1973, 1975).

(i) Aerosol generation principles

Monodisperse polystyrene particles labelled by chemical chelation with Tc^{99m} were produced using a commercially available spinning-top aerosol generator (Research Engineers Ltd.). In this technique the solution to be atomized is fed via a fine needle, at a constant rate, to the centre of an air-driven spinning-top. The feed solution spreads rapidly across the flat surface of the top and is angularly accelerated to the edges at a rate which depends on the rotational frequency (Fig. 3.1.1). The solution first forms a ligament as it leaves the edge (i), the ligament then elongates (ii) and finally disintegrates into two or more droplets (iii), (PHILIPSON, 1973). The smaller droplets are termed satellites and the larger droplets termed primaries. By equating the forces on the primary droplet due to angular acceleration and surface tension and determining an empirical constant of proportionality between them, the following relationship has been derived which is useful in estimating

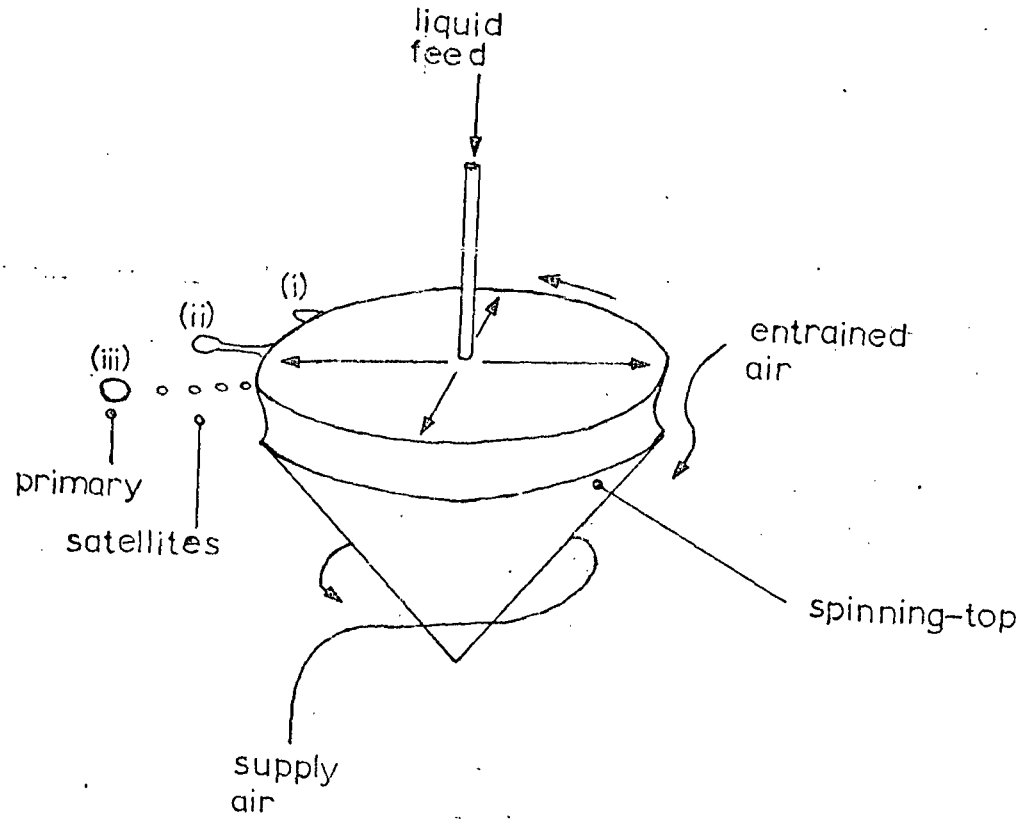

Figure 3.1.1: Spinning - top.

the primary droplet diameter, dp, at a particular rotational frequency (MAY, 1949):

$$dp = \frac{4{\cdot}5}{\omega}\left(\frac{T}{D.\rho}\right)^{\frac{1}{2}} \qquad \text{.....equation 3.1.2}$$

where, ω = angular velocity of spinning-top in radians sec.$^{-1}$

T = surface tension of droplet in dynes cm.$^{-1}$

D = diameter of the top at its surface in cm.

ρ = density of feed solution in gms cc.$^{-1}$

dp = primary droplet diameter in cm.

There is a practical upper limit to spinning-top speed normally determined by the maximum available air-flow. It is therefore usual practice to produce smaller particles, termed secondaries, by evaporating off the bulk of the primary droplet, leaving behind a smaller, solid, residue. The diameter, ds, of the secondary particle depends on the concentration of solute in the initial solution and is given by:

$$ds = dp\left[\frac{10^{-3}.C}{\rho_s}\right]^{\frac{1}{3}} \qquad \text{.....equation 3.1.3}$$

where, C = wt.vol.$^{-1}$ concentration of solute in feed solution in gms l.$^{-1}$

ρs = density of solute in gms ml.$^{-1}$

ds = secondary particle diameter in centimetres.

dp = primary particle diameter in centimetres.

MAY (1949) stated that the satellite particles are about four times as numerous as the primaries and about one quarter of their diameter. In the present work a mean size ratio of $0{\cdot}41 \pm {\cdot}04$ (10 observations $\pm$ standard error of the mean) over a size range of 4·5-13·0 μm diameter was determined (see part (iii) below for sizing technique).

The monodispersity of the resultant aerosol is dependent on a number of factors (WHITBY, 1965). An important one is the separation of the feed needle tip from the spinning-top surface, since if this is too great partial droplet formation may occur at the needle orifice. Accurate centralization of the feed needle tip is also important, otherwise the feed solution tends to spread non-uniformly over the spinning-top

surface. Both these requirements necessitate some form of fine-control positioning mechanism for the feed needle. Another influence on aerosol monodispersity is the steadiness and rate of feed of solution to the spinning-top (RYLEY, 1959).

The MAY (1949) apparatus (Research Engineers Ltd.) incorporates an automatic satellite removal system which employs the Bernoulli principle and is based on the fact that the satellite particles are projected a lesser distance from the spinning-top edge than the primaries. In practice the system is not always workable because of the poor optimization of suction flow rate with satellite diameter. Moreover, if updraught or downdraught collection of aerosol is employed, the satellite removal system may be ineffective owing to disruption of air flow in the region of droplet formation.

3.1 (ii) Description of aerosol generation and labelling

In attempting to measure the clearance of radioactive particles from the lungs it is essential to employ a radioactive label that is stable in the watery fluids that line the dead space airways. For this reason the radioactive label, Tc^{99m}, was chemically chelated into the polystyrene molecules as tetraphenylarsonium pertechnetate by the method of FEW et al. (1970). In this procedure the labelling is performed while the polystyrene is still in solution, before aerosol production. The radioactive label is therefore incorporated throughout the volume of each particle, not just on the surface, and the amount of radioactivity per particle varies as the particle mass. The overall process was not very efficient and relatively high amounts of radioactivity (~ 30mCi) had to be used at the initial stage.

The solution from which the particles were produced consisted of 1% (weight for volume) polystyrene dissolved in a mixture of xylene and methyl iso-butyl ketone of 4:1 volume to volume ratio. The ketone was included to retard the evaporation of xylene over the spinning-top surface which otherwise resulted in the excessive accumulation of polystyrene residue and consequent degradation of particle size uniformity. Production time was always limited to below 20 minutes as impacted polystyrene tended to accumulate on the spinning-top

housing, which eventually interfered with its operation (BLACK and WALSH, 1970). Solution feed rate to the spinning-top was optimised at below a nominal value of 0·5 cc min.$^{-1}$ as above this the particle size uniformity was found to be unacceptably poor (> 10% coefficient of variation). No more than 10 cc of solution could therefore be sprayed and this necessitated the use of a feed system in which the volume of liquid dead space was minimal.

As was described in 3.1 (i), there are several important practical requirements for the production of a monodisperse aerosol. To solve the problem of feeding the radioactive solution at a predetermined and steady rate with minimal liquid dead space losses, the apparatus illustrated in Figure 3.1.2 was devised. It was found that mechanical injector and peristaltic pumps tended to produce spasmodic fluctuations in feed rate. To smooth the liquid feed a simple damping mechanism was used in conjunction with a mechanical injector pump (C.F. Palmer Ltd.). Water was fed at a predetermined rate into a coil of silastic rubber tubing. The coil served both as a reservoir for the incoming water and as a damper of any sudden variations in its feed rate. The silastic coil was connected to a 10 ml. pipette which contained the radioactive solution, thus forming an air-tight system. Owing to the hydrostatic pressure of liquid in the pipette, the air pressure in it was initially negative. This steadily grew more positive as liquid feeding progressed and the hydrostatic pressure of the solution diminished. Water movement in the silastic coil therefore continuously compensated for the pressure changes and in consequence, the average feed at the needle orifice (internal diameter $\simeq$ 400 μm) was normally a fraction of about 0·6 of the predetermined value. The latter was always set at 0·5 cc min.$^{-1}$, giving a value at the feed needle head always equal to or lower than this and an average rate of about 0·3 cc min.$^{-1}$. As the radioactive solution was completely expelled from the pipette there were no liquid dead space losses.

Research Engineers Ltd. supply a device to control the positioning of the feed needle, known as a spider, but this is cumbersome and inaccurate in use and has the disadvantage that

aerosol losses tend to occur on it during aerosol production. If radioactive particles are produced it is unsafe to make adjustments during a production run, as is often necessary. Full external fine-positioning control was accomplished in the present work by means of the device illustrated in Figure 3.1.2. In this, four screwed thread rods were mounted crosswise to a central perspex collar, which housed the feed needle. The four free ends of the rods protruded through the walls of a perspex box which housed the spinning-top unit. Feed needle positioning control was achieved by rotation of butterfly nuts attached to the rod ends. Rotation of opposite pairs of butterfly nuts in concurrent directions resulted in movement of the needle along the axis of the rod in question, with no alteration in the height of the needle or in its position in a direction perpendicular to this axis. Contrawise rotation of any opposite pair of butterfly nuts resulted, owing to a slight central inflection at the crossbar midpoint, in either upward or downward movement of the needle, depending on whether such rotation was an inwards or outwards screwing motion.

The automatic satellite removal system (MAY, 1949), was found to be unsatisfactory in a number of respects, for reasons already mentioned, and was therefore blocked off. This was found not to have any adverse effect on the aerosol monodispersity. Both primary and satellite particles were collected by means of the updraught collection system illustrated in Figure 3.1.2. The particles were swept upwards in airstreams which converged at two millipore filters (Millipore Filter Corporation) on which they were collected. In order to ensure no external leakage of radioactive particles the updraught collection airflow rate was always set at a greater value than that of the air supply to the spinning-top stator. The air pressure in the production unit was therefore always negative and the induced air inflow was directed via a multi-hole collar which surrounded the spinning-top housing, in order to provide an additional collection updraught. Millipore filters of nominal pore diameter equal to that of the expected satellite diameter were used. These filters are resistant to xylene vapour and the coefficient of variation in pore diameter is claimed by the manufacturers to be less than $\pm$ 5%. The degree of particle

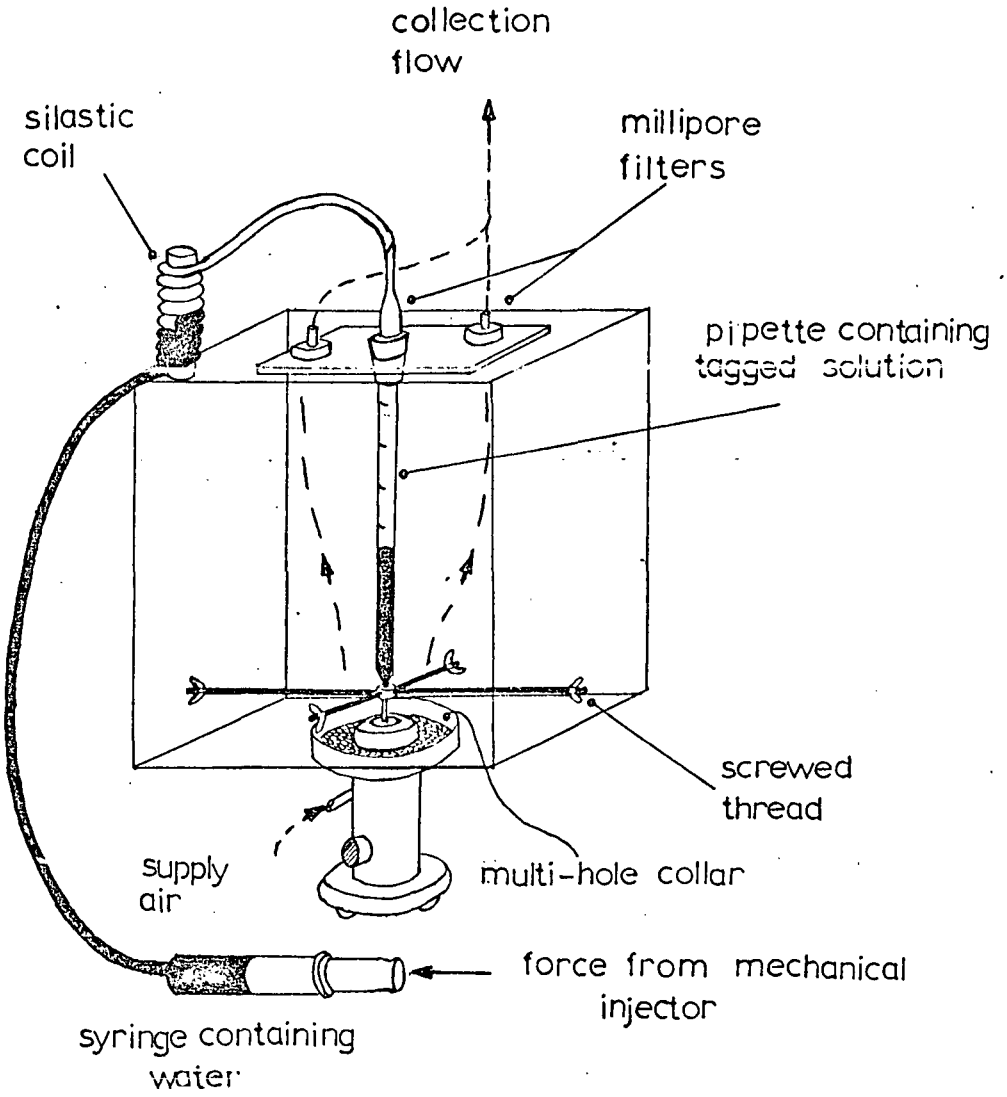

Figure 3.1.2: Aerosol generation apparatus.

penetration through the millipore filters was checked directly in the present work by measuring the radioactivity associated with an additional millipore filter placed in-line with that of a main collection filter (see 3.2 (i)). The results indicated a particle collection efficiency close to 100%.

In order to ensure good particle size reproducibility between production runs a calibration curve of air supply flow, in arbitrary units of rotameter scale, versus count-mean particle diameter was derived (Figure 3.1.3). Direct comparison with the theoretical values of particle diameter predicted using equations 3.1.1 and 3.1.2 is not strictly valid in this case, owing to the possible effects of blocking the satellite removal port on the spinning-top rotational frequency at a given air supply rate.

Before an aerosol production run the spinning-top and its housing were cleared of excess polystyrene. The spinning-top surface was roughened using medium grade carborundum powder which facilitated the wetting of its surface by the spraying solution (MAY, 1949). The entire aerosol production unit was housed in a fume cupboard in the interests of radiological safety (Figure 3.1.4).

It was necessary to remove the satellite particles from the sample after a production run. This was accomplished by making use of the fact that primary particles fall more quickly in a fluid than the satellites. Using a centrifuge it was possible to quicken their rates of fall. Ten separate centrifuging operations were performed for each sample and the clear portion of liquid, which contained mostly satellites, was removed after each run. The appropriate levels and durations of centrifuge spin were determined empirically. By such means it was found that the proportion of satellites in the sample could be reduced to 2.5% $\pm$ 2.4% by mass (mean of 18 observations $\pm$ standard deviation) from the initial value always greater than 27%.

Finally, the required amount of radioactivity was drawn off from the sample and placed in 1·2 ml of ethanol ready for administration to the subject. Aerosol administration techniques and procedures are described in section 3.2.

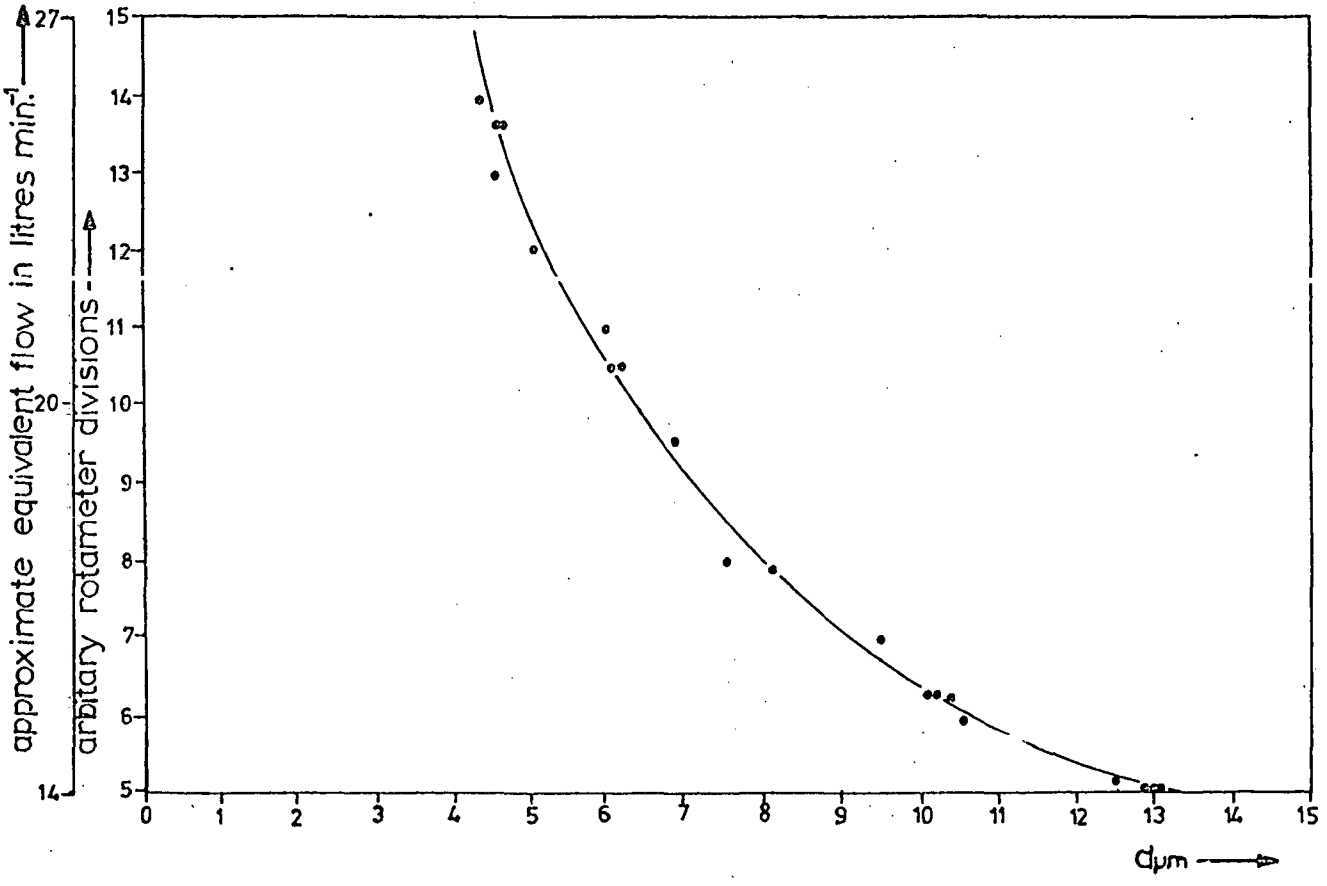

Figure 3.1.3: Particle diameter (μ m) vs supply flow (line drawn by eye fit).

Figure 3.1.4: Photograph of aerosol generation apparatus in fume cupboard.

(iii) Particle characterisation and in vitro leaching

The count-mean diameter of a sample of 200 particles was determined after an experiment using a Timbrell double-image micrometer and particle size analyser (Fleming Instruments Ltd.). The sample was taken from slides placed in the main spraying chamber of the aerosol administration apparatus, which enabled estimates of the proportions of aggregates and satellites in the sample to be determined simultaneously. The calibration accuracy of the sizing instrument was periodically checked using a standard calibration slide.

The count-mean diameters of the particles were found to be log-normally distributed (Figure 3.1.5). It was more convenient to express the particle size uniformity in terms of the coefficient of variation, α , (α = standard deviation, σ , ÷ count mean diameter, $\bar{d}$) than geometric standard deviation, σg. According to FUCHS and SUTUGIN (1966), $\alpha \simeq \ln \sigma g$, for small values of α .

(a) Aerodynamic diameter

For purposes of comparison between the aerosol deposition results of the different research groups it is useful to express such results in terms of the aerodynamic diameters of the aerosol particles employed in each case. The aerodynamic diameter of a particle is defined as the diameter of a unit density sphere having the same falling speed as the particle in an identical fluid. At a given size it is dependent on particle shape and density.

The density of polystyrene has been quoted at 1·06 gms cc^{-1} (BLACK and WALSH, 1970). However, the possibility of the inclusion of some gas or vapour at the moment of particle formation should not be excluded. Particle density was therefore checked directly.

Polystyrene particles of ~ 10 μm count-mean diameter, which have conveniently short settling times in liquids, were placed in a temperature stabilised ethanol (ρ = 0·789 gms ml^{-1} at 20°c)*

* C.R.C. Handbook of Chemistry and Physics, 1968.

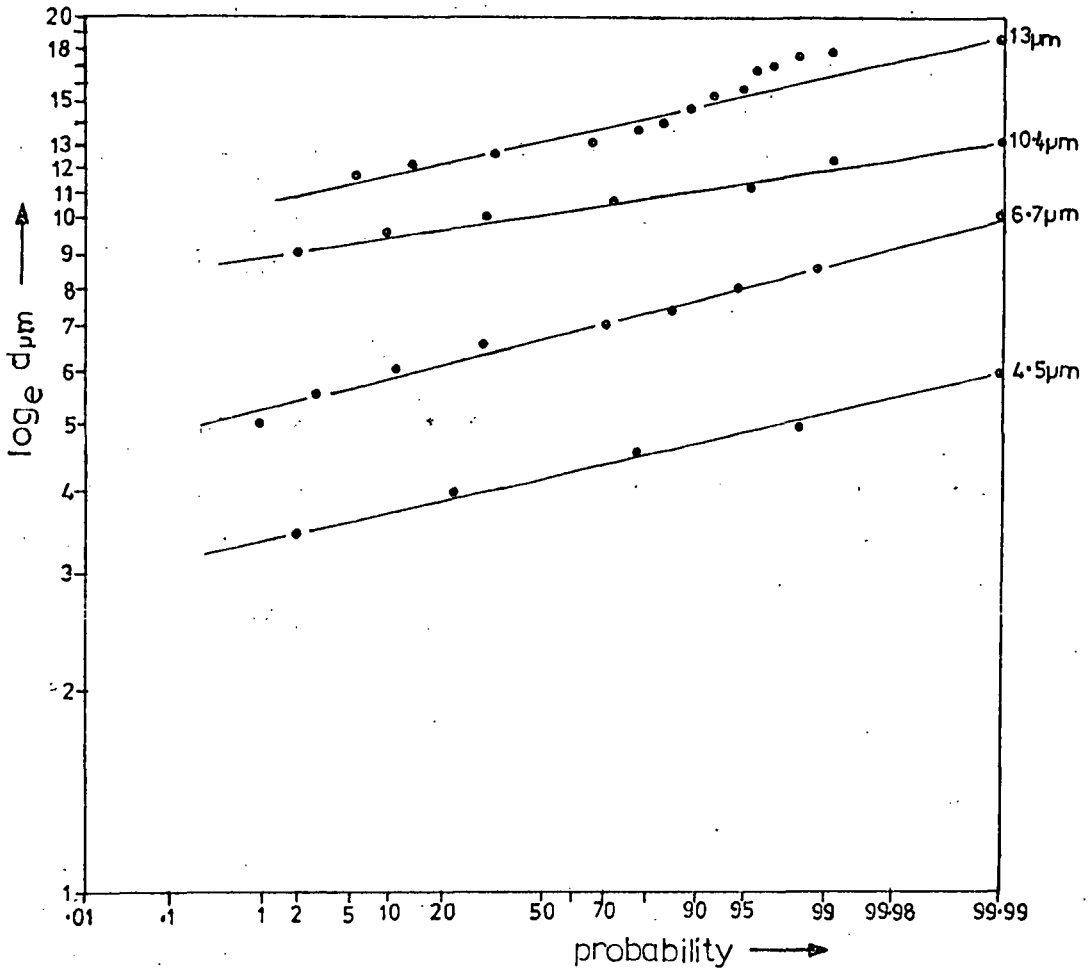

Figure 3.1.5: Particle size distributions; $\log_e$ particle diameter (μm) vs probability.

based solution whose density could be modified by the addition of known volumes of glycerol triacetate (ρ = 1·156 gms ml^{-1} at 20°c)*. At a solution density of 1·06 gms ml^{-1} and temperature of 20°c, particle buoyancy resulted in slight upwards movement of the particles after several hours. Gravitational settling could just be observed after twenty-four hours at a solution density of 1·03 gms ml^{-1} and steady temperature of 20°c. According to Archimedes' principle, the upthrust on a particle is equal to the weight of an equivalent volume of fluid which is just supported at rest. When the particle is also just supported at rest, in relation to the fluid, the densities of fluid and particle are equal. It was therefore concluded that at this particle diameter the polystyrene density lay in a range 1·03 - 1·06 gms ml^{-1} at a temperature of 20°c. Particles of 4·5 μm diameter were also checked, using the same procedure, and were found to have densities in the same range.

Figure 3.1.6 shows an electron micrograph of a typical particle sample. Although the overall shape of the particles is shown to be essentially spherical, they are severely indented. Many are 'apple-shaped', having large single indentations. Particles produced from the unlabelled polymer also tended to be 'apple-shaped' but were less severely indented. The possibility was considered that the fluid resistance experienced by such particles would differ from that of spherical particles of identical mass to a degree that would significantly influence their falling speeds in air.

The falling speeds of microscopic particles are difficult to measure experimentally and particle shape factors are equally difficult to treat theoretically (ALLEN, 1974). Two experimental approaches were adopted: one based on a macroscopic simulation of the microscopic surface irregularities; the other based on direct measurement of the falling speeds of the microscopic particles in which spherical 'control' particles were used. The purpose of the former approach was to give an indication of whether such surface irregularities were likely to be at all significant; that of the latter was to quantify any

* C.R.C. Handbook of Chemistry and Physics, 1968.

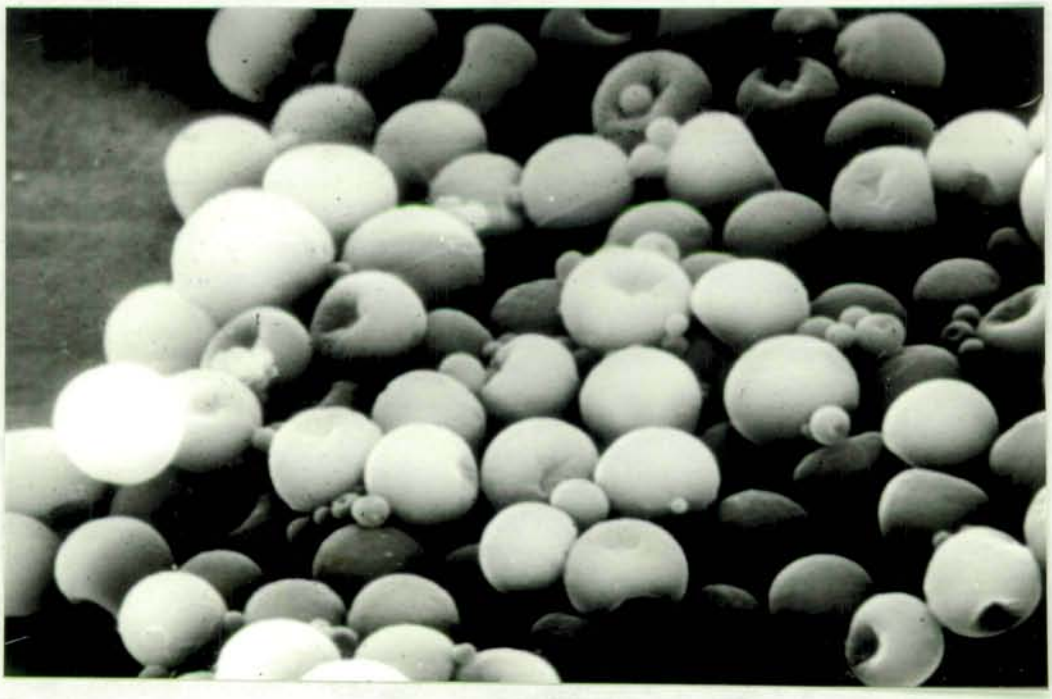

Figure 3.1.6: Electron micrograph of 6.7 μ m (dia.) particles showing their non - sphericity.

such effect as directly as possible, using the actual polystyrene particles.

A plasticine particle of 1·2 cm diameter, having an expanded polystyrene interior for increased buoyancy, was used to determine the effects of three distinct surface characteristics on its falling speed in glycerol (absolute viscosity = 1,450 centipoise @ 20°c)*. The Reynolds number of the particle in glycerol was below 0·05, which is low enough for Stokes' law to remain valid (see Ch.1, part 2(i)). The plasticine extension of the particle was moulded into: (i) a sphere; (ii) an 'apple-shape' with smooth exterior; (iii) an 'apple-shape' with severely indented exterior. It was the latter which was considered to most closely approximate to the appearance of the polystyrene particles observed on the electron micrographs. Falling speeds were measured over a distance of 20·5 cm in a graduated cylinder containing the glycerol, the temperature remaining constant throughout. The respective falling speeds were: (i) 0·894 $\pm$ ·018 cm sec.$^{-1}$; (ii) 0·805 $\pm$ ·022 cm sec.$^{-1}$; (iii) 0·695 $\pm$ ·011 cm sec.$^{-1}$, each figure being the mean of eight observations $\pm$ the standard error of the mean. This large (~22% at the extremes) variation indicated that particle surface irregularities were indeed of some consequence, at least on a macroscopic scale.

To investigate the effects of particle surface irregularity on the microscopic scale an attempt was made to measure the bulk settling rate of particles in olive oil (ρ = 0·918 gms cc^{-1} @ 15°c, absolute viscosity = 84 centipoise @ 20°c)*. The major difficulty of such experiments lies in the near impossibility of eliminating thermal motions in the settling fluid. A further difficulty is the fact that owing to the spread of sizes present, even in samples of good size uniformity (coefficient of variation < 10%), the falling edge of the sample in solution, or hydrosol, tends to be more representative of the falling speed of the lower end of the overall particle size distribution than that of the count-mean size. An attempt was made to eliminate these

* C.R.C. Handbook of Chemistry and Physics, 1968.

systematic errors by using particles of human serum albumen, which appeared to be smooth and spherical, as controls.

The falling speed of a particle in a fluid in the laminar flow region may be predicted using the Stokes' equation in the form

$$v_p = K.dp^2.\Delta\rho_p \quad \text{.....equation 3.1.4}$$

$$v_a = K.da^2.\Delta\rho_a \quad \text{.....equation 3.1.5}$$

where v_p, v_a = the falling speed of perfectly spherical polystyrene or albumen particles in cm.sec.$^{-1}$

dp, da = the diameter in centimetres of the polystyrene or albumen particles.

$\Delta\rho_p, \Delta\rho_a$ = the difference in density between the polystyrene or albumen particles and the fluid medium, in gms cc $^{-1}$.

$K = \frac{g}{18\eta}$ where g is the acceleration due to gravity in cm.sec^{-2} and η is the fluid viscosity in poise.

For particles having surface irregularities falling in a fluid subject to thermally induced fluid motions, the distance of fall of the falling edge of perfectly monodisperse hydrosols of polystyrene or albumen particles may be written as

$$Dp = Kdp^2.\Delta\rho_p.t.Sp - K' \quad \text{.....equation 3.1.10}$$

$$Da = Kda^2.\Delta\rho_a.t.Sa - K' \quad \text{.....equation 3.1.11}$$

where Dp, Da = observed distance of fall of falling edge of the polystyrene or albumen hydrosol in cm.

Sp, Sa = the dimension less drag coefficients which equal unity for a perfect sphere.

K′ = the distance of thermally induced upwards shift in the falling edge of the polystyrene or albumen hydrosol, in centimetres.

t = period of settlement in seconds.

When Dp $\simeq$ Da, over the same period of settlement t,

$$\frac{Dp}{Da} \simeq \frac{dp^2 . \Delta\rho p . Sp}{da^2 . \Delta\rho a . Sa} \qquad \text{.....equation 3.1.12}$$

In practice, perfect hydrosol monodispersity is unobtainable. It was therefore necessary to measure the count-mean diameter not of the whole sample, but of those particles which lay at the falling edge of the hydrosol in the fluid medium, dpe and dae, for polystyrene and albumen particles, respectively.

for, Dp $\simeq$ Da and Sa = 1, $\qquad Sp \simeq \frac{Dp.\ dae^2\ \Delta\rho a}{Da\ dpe^2\ \Delta\rho p}$ .....equation 3.1.13

It is not claimed that experimental error was eliminated using this technique. There would undoubtedly be errors in the estimation of the location of the falling edge of the hydrosol in both cases. However, because the two samples were placed in almost identical geometrical and temperature environments the systematic error would tend to be of similar magnitude for each. The purpose of conducting the experiment was to provide what was considered to be a reasonable quantitative indication of the magnitude of the effect on a microscopic scale.

Using equation 3.1.13 to determine values of Sp eliminated the need for absolute viscosity measurements. Variations in viscosity due to temperature changes did not therefore affect the result.

Polystyrene and albumen particles of various sizes were tried until an approximate match in their falling speeds in olive oil was achieved. The count-mean diameters for the polystyrene and albumen samples were $\bar{d}p$ = 13·1 μm, (coefficient of variation = 8·9%) and $\bar{d}a$ = 8·6 μm (coefficient of variation = 5·2%). The count-mean diameters of the polystyrene and albumen particles sampled, by means of a syringe, at the falling edges of their respective hydrosols after one day of free settling were $\bar{d}pe$ = 12·6 $\pm$ ·002 μm (5 observations $\pm$ standard error of the mean), and $\bar{d}ae$ = 8·2 $\pm$ 0·008 μm (5 observations $\pm$ standard error of the mean).

The hydrosols were left to settle out over a period of

about one day, when movement in the falling edges was usually about 8 mm. Both samples were placed in 5 mm bore glass tubing, sealed at one end, marked with an external scale. The tubes were placed adjacently in a beaker of water in order to ensure their temperatures would be nearly equal at all times. Five separate runs were performed. No aggregation was observed in either sample removed from the falling edges of the hydrosols.

For final determination of Sp, it was necessary to measure the density of the albumen particles, ρ_a. This was done using a procedure similar to that described above for polystyrene particles, except solutions of acetone and carbon tetrachloride were employed. It was found that ρ_a lay in the range 1·26 - 1·27 gms ml^{-1} and the mean figure of this range was used in equation 3.1.13 to determine Sp. The result was Sp = ·77 $\pm$ ·02 (mean of 5 observations $\pm$ standard error of the mean) indicating that particle shape factors were of comparable importance for both microscopic and macroscopic particles. The aerodynamic diameter of the particles could not therefore be taken as equal to their count-mean diameter. The implications of this result for purposes of comparing the aerosol deposition and clearance data of different research groups are discussed in Chapter 4, part 2(ii).

(b) In vitro leaching

The degree of radioactive leaching from the particles was measured initially in vitro. Particles of 4·5 μm diameter were produced using the methods described above, including the centrifuging stage. One volume was left to stand for about one day in ethanol solution alone, at ambient temperature (~ 20°c), the other was dried of ethanol and placed in distilled water alone at a temperature of 37°c, also for about one day.

At the end of the leaching period both solutions were centrifuged and the bulk of clear liquid was removed from each sample for radioassay. Two measurements were performed in each case. The degree of leaching in distilled water was measured to be within 0·03% of the initial activity in the water sample (~ 1·5 mCi), after allowing for isotope decay. For ethanol, the degree of leaching was considerably higher, at 2·6% of the initial activity. For this reason the period for which the

particles were stored in ethanol prior to an experiment was always kept to a minimum (~ 20 minutes). The possibility of an *in vivo* leaching of the particles is discussed in 3.3 (ii).

3.2 Measurement of total deposition and control of physiological conditions of aerosol administration

(i) Total deposition

Total deposition is defined here as

$$f_D(I) = \frac{D}{I} \qquad \text{.....equation 3.2.1}$$

where $f_D(I)$ is the total respiratory tract deposition, D, expressed as a fraction of the amount of aerosol inhaled by a subject, I, over one or more whole breaths.

alternatively $f_D(I)$ may be expressed as

$$f_D(I) = \left[1 - \frac{I}{E}\right] \qquad \text{.....equation 3.2.2}$$

where E = the amount of aerosol exhaled by a subject over one or more whole breaths.

In this context, a whole breath is defined as an inspiration to a volume, V_T litres (37°c, and 100% relative humidity), followed by expiration of the same volume, where V_T is termed the tidal volume of the subject. If inspired and expired volumes are not equal, or nearly equal, in every breath, it is not possible to measure, or closely estimate, $f_D(I)$, by this definition.

The amounts I, D, E, may be expressed in terms of mass, surface area, number, or radioactivity, of an aerosol. For a monodisperse aerosol (coefficient of variation < 10%) it is assumed that the values of $f_D(I)$ calculated on each such basis are nearly equal (see 3.1). The distinction between the simple definition of $f_D(I)$ in equations 3.2.1, 3.2.2, and the more complicated steady-state definition of total deposition, was discussed in Chapter 1. The difference is not important at that particle size above which no aerosol can be recovered in the expired tidal air of the breath which follows that in which the aerosol was first inhaled. Owing to the small percentage of tidal air known to be involved in the breath to breath tidal and

reserve air mixing process (HEYDER and DAVIES, 1971), and the relatively high (> ·7) values of $f_D(I)$ measured in the present work at the smallest particle diameter employed, 4·5 μm, it is unlikely that steady-state influences are of any significance at or above this size.

Accurate measurement of $f_D(I)$ requires accurate measurement of I and E. Some of the experimental difficulties likely to be encountered when attempting to measure total deposition were described in Chapter 2. Large particle sizes are particularly difficult to study owing to their greater tendency to deposit by gravitational settling or inertial impaction, in the aerosol administration apparatus. Referring to Figure 3.2.1 and firstly considering the problem of estimating the amount of aerosol inhaled by a subject, it may be evident that the sampling configuration illustrated in (i) has certain merits. The sampled aerosol is obtained close to the point of entry into the subject and is therefore likely to be representative. Moreover, if the instantaneous sampling flow rate, fs, could be made at all times equal to the instantaneous inspiratory flow rate, fi, then owing to its inherent symmetry nearly equal aerosol losses would occur in both arms of the Y-piece and the amount of aerosol drawn through the sampling port would be nearly equal to that inspired by the subject.

LANDAHL and his co-workers (1947, 1948, 1950, 1951, 1952) were the first investigators to employ a Y-piece sampling configuration in human aerosol inhalation experiments and, as far as can be ascertained from the literature, were the only ones to have done so. However, in their experiments the onus was always on the subject to maintain an inspiratory flow that was at all times equal to a constant sampling flow. Moreoever, the necessity imposed on the subject of having to move to a separate port in order to exhale made this task especially difficult (LANDAHL and HERRMANN, 1948). An improved approach might be to derive a sampling flow that was somehow made to 'slave' to the inspiratory flow, which was allowed to vary.

Figure 3.2.1 (ii) illustrates how this might be achieved in principle, for radioactive particles. An airflow meter, M, measures total flow into the system which is at all times equal

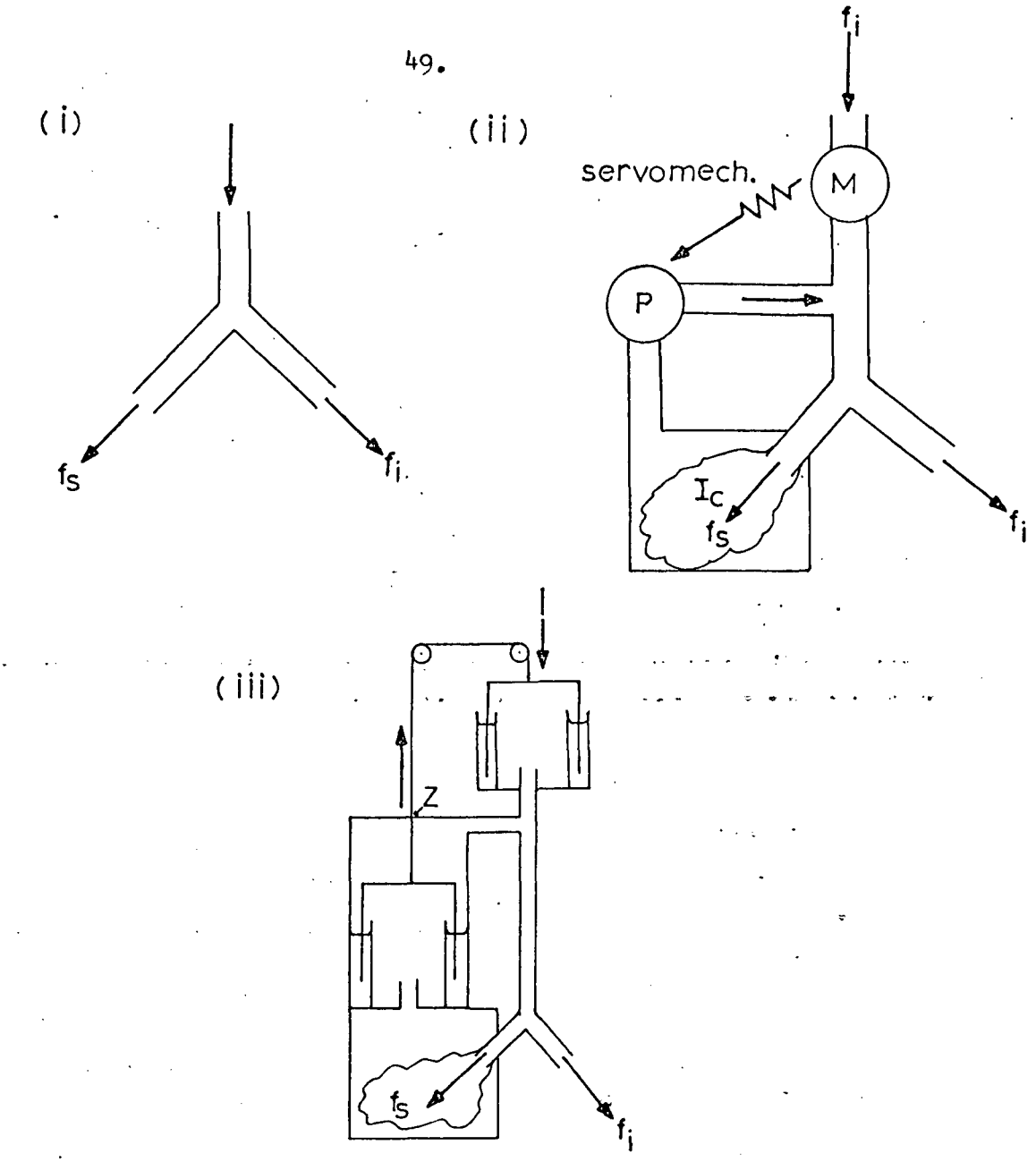

Figure 3.2.1: Aerosol sampling configurations.

to the total outflow derived by the subject, S. By some undefined servomechanism, the pump, P, derives an equal flow at the sampling port and returns this back into the system in order not to affect the relationship between total inflows and outflows. During this process the radioactive particles are drawn into a collection bag, Ic, for later radioassay. Servomechanisms based on pneumotachographic or other similar measurements of inspired flow were rejected on the grounds that this might seriously diminish the amount of aerosol able to reach the subject, particularly at large particle sizes. Spirometers provide a simple and trouble-free means of measuring gas flow (MERCER, 1973). By using a pair of nearly identical spirometers in the configuration illustrated in Figure 3.2.1 (iii), these sampling principles are brought closer to practical realisation. Several difficulties remain, however. Besides the difficulty of sealing at 'Z', on the figure, after a number of inspirations the sampling bag would expand to the limits of its capacity and, similarly, the spirometers would eventually reach the limits of their movement. Also, the exhaled aerosol must somehow be collected. Figure 3.2.1 (iv) illustrates the final design at least as regards aerosol sampling. In this apparatus movement between spirometers was transmitted via pulley wheels attached to a freely rotatable shaft, which could be easily sealed at 'X' on the figure. The expansion of the collection bag, Ic, during an inspiration, was compensated for by an equal volume of contraction during an expiration, by means of pump P, acting via a filter and solenoid valves S1, S2. Rather than separately correct for the inspiratory movement of the spirometers (A and B in the figure), the contraction of the collection bag Ic during an expiration, was used to achieve this in a single action. Thin walled neoprene-rubber collection bags were used in order to ensure that attenuation of radiation during radioassay would be negligibly small (see 3.3(ii)d).

The mode of action was as follows: at the end of an inspiration the valves V1, V2, moved to the positions shown in Figure 3.2.1(iv)b. The subject was then free to expire via the expiratory port of V1 into an expiratory collection bag, Ec. Expired volumes were measured by spirometer C, shown in the figure. The solenoid valves S1, S2, re-directed the suction

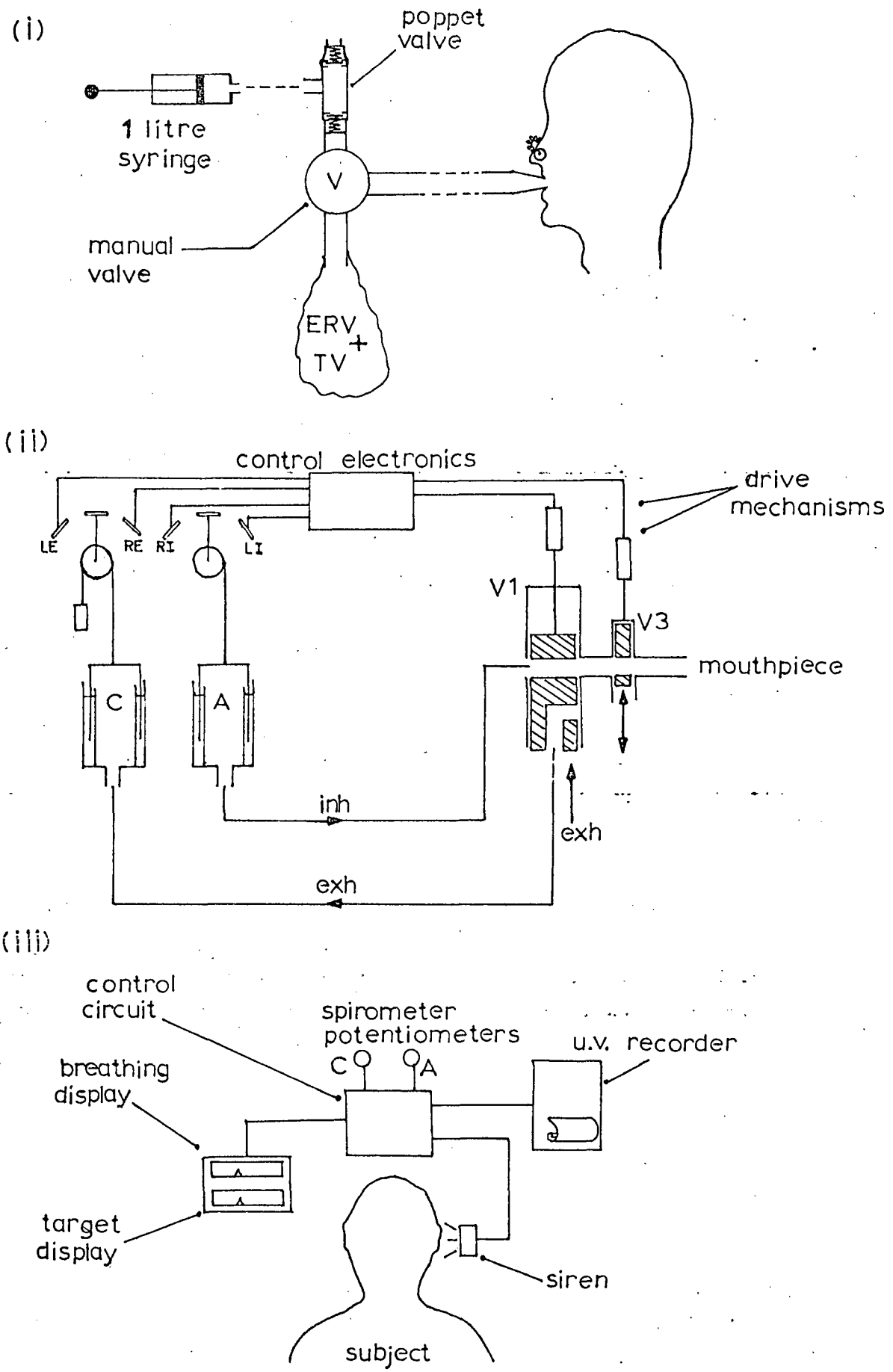

Figure 3.2.2: Breathing control.

flow of pump P at the beginning of an expiration (to be distinguished from the end of an inspiration), which resulted in a contraction of the expiratory collection bag Ec. On commencement of this contraction, the pressure within spirometer B fell below that of atmospheric and its downwards movement was induced. This movement was facilitated by the opening of valve V2, which permitted a compensatory inflow of air into the apparatus. The downwards movement of spirometer B, during expiration, was accompanied by an equal and opposite movement of spirometer A. Contrary to the situation which existed during an inspiration, spirometer B then led the movement of the spirometer pair and the apparatus was essentially in reverse operation.

It was also necessary to re-set the position of spirometer C, following an expiration. This was achieved in a manner similar to that described above for spirometers A and B, except that the processes operated only during an inspiration. In this case, valves V1, V2, moved into the position shown in figure 3.2.1(iv)a, at the end of an expiration. Both the inspiratory and expiratory re-setting processes could be halted at a predetermined point by means of the proximity switches R1 and RE, respectively, illustrated in Figure 3.2.2. These were magnetically actuated open/close switches (Radiospares Components Ltd.) and the actuating magnet was radially mounted on the spirometer pulleys. The radial arms of the pulleys were slightly weighted in order to counterbalance variations in spirometer flotation weight.

Millipore filters (see 3.1(ii)) were used to collect the radioactive particles within the collection bags during the re-setting processes. Millipore filter holders (Millipore Filter Corporation) incorporating an 'o' ring for effective sealing were also used. A direct check for possible particle penetration was made by placing a filter of a nominal pore diameter (3 μm) equal to that of the collection bag filters, in-line with that of the suction feed tube of the expiratory collection bag. An aerosol containing both primary particles (~ 6·5 μm diameter) and satellites (~ 30% by mass, ~ 2·6 μm diameter) was sprayed into the main chamber of the apparatus and a period of simulated breathing was undertaken (by a method described in 3.2 (iii)b).

The radioactivity measured on the in-line filter (< 50pCi) was 0·13% of that measured on the main collection filter (~ 40μCi) indicating a collection efficiency of nearly 100%.

(ii) Breathing control and valve actuation

The apparatus described above does not represent the final system. Neither the mechanism of valve actuation at the end of an inspiration or expiration, nor the method used to control the breathing pattern of the subject during aerosol administration have yet been described.

(a) Valve actuation

Actuation of the respiratory valve(s) used to separate inhaled and exhaled aerosol flows is one of the most difficult experimental problems in human aerosol inhalation research (WALSH et al., 1977). Its importance lies mainly in the danger of misdirecting a portion of the exhaled aerosol through the inspiratory port of the apparatus. The concentration of the exhaled aerosol falls rapidly from the beginning of an expiration (MUIR, 1967) and if at this time a small volume of the expired flow were to be misdirected, an error in the estimation of the exhaled aerosol would result, the magnitude of which might be far greater than the actual fraction of the misdirected expired volume would suggest, particularly at large particle sizes.

A number of approaches to the problem of valve actuation have been adopted by other investigators. ALTSHULER et al. (1957) used manually operated valves to separate inspired and expired aerosol flows, with the accompanying danger of subject error and excessive breath-holding. DENNIS (1950, 1971) introduced a valve sensitive to pressure changes at the mouthpiece, but the delay between the application of pressure signal and completion of valve movement was high (~ 200 milliseconds). A much improved pressure sensitive valve has recently been developed which uses sensitive pressure sensors and rapid-action solenoid actuators (WALSH et al., 1977). The authors state that the time delay between generation of a signal at the mouthpiece and completion of valve movement was reduced to about 40 milliseconds, which resulted in a measurable volume of mis-

directed expired air of less than 5% of tidal volume. This delay is close to that (~ 50 milliseconds), measured for a compressed-air driven valve V3 (Figure 3.2.2(ii)) constructed for use in the present work, which was found to be the best that could be achieved. One of the main objectives of the present work was to measure total deposition at the largest particle sizes able to penetrate below the larynx. At such particle diameters, which turned out to be greater than equal to 13 μm (see Chapter 4), the error due to the misdirection of exhaled aerosol is likely to be far greater than that which obtains when using aerosol particles of about half this diameter (FOORD et al., 1978). Considering the relatively high falling speeds of 13 μm diameter unit density spherical particles ($V_T \sim 0{\cdot}54$ cm. sec^{-1} in air) it is possible that the majority of exhaled particles at this size are returned from the trachea, which is almost vertical during aerosol administration, and main bronchi, whose total volume is only about 42 ml (WEIBEL, 1963). This figure is comparable with the expected volume of misdirected expired flow at a tidal volume of one litre. It was therefore considered necessary to adopt a method of valve actuation that would prevent any of the expired flow from being misdirected, at all.

Before describing this method it will first be necessary to discuss the other major problem encountered in human aerosol inhalation experiments, that of breathing pattern control, since to some extent the same techniques have been applied in solving both.

(b) Breathing control

The possible influences of breathing pattern on the deposition probability of inhaled particles were discussed in Chapter 1. A symmetrical 'clipped sawtooth' breathing pattern was adopted and aerosol administration was initiated at the subject's functional residual capacity, which had been measured previously (Figure 3.2.3). It should be appreciated that when a subject breathes via an apparatus respiration may become more conscious than it would be normally and some form of artificial control might in any case be required. The reason for adopting a fixed tidal volume and breathing rate was to standardise the residence time of

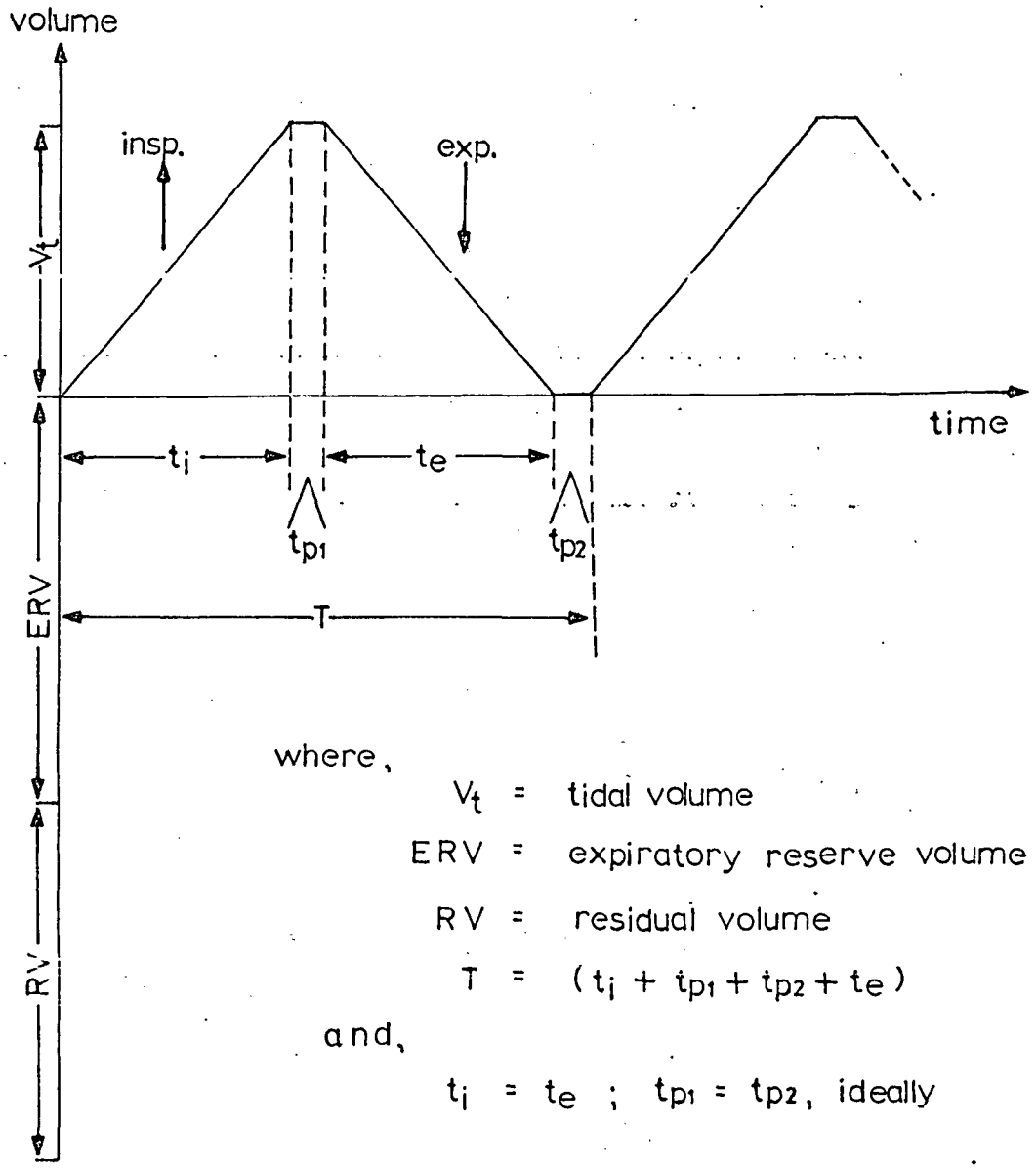

where,

V_t = tidal volume

ERV = expiratory reserve volume

RV = residual volume

$T = (t_i + t_{p1} + t_{p2} + t_e)$

and,

$t_i = t_e$; $t_{p1} = t_{p2}$, ideally

Figure 3.2.3: Standard breathing pattern.

particles in the respiratory tract between different breaths. Specific air flow rates and the average residence time in different airways must also be considered. In common with the work of HEYDER et al. (1973) and DAVIES et al. (1972), the instantaneous airflow was made equal to the mean airflow over times ti, te, (Figure 3.2.3), where ti = te, ideally. This greatly simplifies the problem of standardisation between different research groups. Aerosol administration was initiated at the functional residual capacity of the subject because this most closely represented the lung volume during normal breathing at rest, or quiet breathing. It may also be the lung volume at which the total deposition between different subjects can be equalised, at least at small particle sizes (HEYDER et al., 1975). The complicated considerations involved in this problem were discussed in Chapter 1.

The problem of breathing control is particularly acute in experiments involving the inhalation of radioactive particles. Once these have been administered to the subject there can be no opportunity for a second attempt, if at all, until the radioactivity has almost entirely decayed. It is therefore essential to adopt a procedure that is simple and effective in use, even for previously untrained subjects.

The apparatus shown in Figure 3.2.2(i) was used to set lung volumes prior to aerosol administration. The subject first completed a maximal expiration and then inspired a fixed volume of air, equal to expiratory reserve volume plus tidal volume, from a rubber bag. Wearing a noseclip throughout the procedure, the subject then transferred to the mouthpiece of the main apparatus and preceded aerosol inhalation proper with an expiration. The procedure was practised several times before an experiment to ensure that no air would be inspired or expired during transferal.

Control of the two main respiratory parameters, tidal volume and breathing rate, presents a more severe practical problem. As was discussed above, it is particularly important to ensure that inspired and expired volumes are equal in any breath. Yet it has been stated by both DAVIES et al. (1972) and HEYDER et al. (1973), that even experienced subjects cannot ensure that this is achieved. If the expired volume is less than that

inspired in any breath, then the volume difference will be erroneously measured to have been completely deposited. Part of the problem of breathing control may be that the subject is often required to attempt simultaneous control and co-ordination of different variables. An improved approach might be to place one of these variables under automatic control, thus allowing the subject to concentrate more on the control of the remaining variable. The obvious candidate for automatic control is tidal volume, since this can be controlled by means of volume limits, whereas automatic flow rate control might necessitate some means of artificial respiration.

Automatic tidal volume control was achieved by means of magnetically actuated volume limit switches operating in conjunction with a mouthpiece blocking-valve, V3 (Figure 3.2.2 (ii)). Although this same expedient is closely related to the more complicated problem of respiratory valve actuation, for the sake of clarity, its role in breathing control will first be considered separately.

Referring to Figure 3.2.2 (ii), A and C are the spirometers used for the detection of inspired and expired volumes, respectively (nomenclature as in Figure 3.2.1 (iv)). Spirometer C was thermostatically maintained at a temperature of 37°c. LI, LE, represent proximity limit switches (crossover type, Radiospares Components Ltd.), whose position was adjusted relative to RI, RE, (the resetting process limit switches mentioned in 3.2 (i)), to obtain the desired tidal volume, defined at 37°c and 100% relative humidity. Inspired and expired volumes were equalised by appropriate adjustment of LI, allowing for gas expansion in the lungs, assumed to be at 37°c and 100% relative humidity, from ambient temperature and humidity. The temperature of the air in the aerosol administration apparatus was measured prior to an experiment by means of a mercury-in-glass thermometer, permanently housed within it. The inspired air was always very nearly saturated with water vapour owing to the presence of a water-filled spirometer in the apparatus. Although a small amount of ethanol vapour was also present its partial pressure contribution was negligible. A slight lowering of temperature ($< 2^{\circ}c$) occurred because of ethanol evaporation: this needed

about 60 calories of latent heat of vaporisation, compared to the 30 or more calories of heat required to change the temperature of air within the spraying chamber by $1^{o}c$. Correction factors were calculated using the ideal gas equation in the form

$$Vi = \left[\frac{273 + ti}{273 + te} \cdot \frac{760 - Pe}{760 - Pi}\right] \cdot Ve \quad \text{.....equation 3.2.3}$$

where, ti = temperature of inspired air in degrees centigrade
te = temperature of expired air = $37^{o}c$ (after warming).
Pe = saturation vapour pressure of water at $te^{o}c$
Pi = saturation vapour pressure of water at $ti^{o}c$
Vi = volume of inspired air at $ti^{o}c$ and 100% relative humidity

The expired air was assumed to be at $37^{o}c$ and 100% relative humidity because of uncertainty in the amount of cooling and condensation that might occur before its exit from the mouth (WALKER et al., 1961). This assumption was of no consequence because of subsequent re-heating and re-saturation of expired air in the wetted expiratory collection bag (Figure 3.2.5), which was almost instantaneous (less than 1·6 calories of heat are needed to raise the temperature of 1 litre of air by $5^{o}c$). It was possible to check the equality of inspired and expired volumes using a simple bag-in-a-box breathing simulator (see 3.2 (iii)b). In the resting subject the volume of inspired air, temperature and humidity notwithstanding, exceeds that expired by less than 1% in any breath, owing to unequal exchange of carbon dioxide and oxygen in the lungs (COMROE et al., 1955). Over ten breaths this could amount to about 10% of the tidal volume or about 100 ml at a tidal volume of 1·0 litre. As this figure was small in comparison with a typical functional residual capacity of about 2 litres, the effect was ignored. It should be appreciated that this volume error is distinct from the error which results from the misdirection of the early portion of expired air (see above). Its significance lies not with the calculation of total deposition as such, but with the control of the lung volume of the subject during aerosol administration. It should also be borne in mind that in the absence of automatic volume control a drift of at least this order is to be expected from breath to

breath: this would not only result in a change in lung volume throughout aerosol administration, but also cause an error in the measurement of total deposition.

Referring again to Figure 3.2.2 (ii), and considering only at this stage the role of the respiratory control valve, V3, and its positions at various stages in one breathing cycle: V3 was a rapid-action blocking valve which prevented airflow through the mouthpiece by closing at the end of an inspiration or expiration, determined when the magnet actuators on the spirometer pulley arms reach the limit switches LI, LE, respectively. At the instant that V3 closed, the subject received a signal to change from expiration to inspiration, or vice-versa. Referring to Figure 3.2.2 (iii), this signal was applied by a miniature siren situated close to the subject's right ear which sounded for as long as the subject took to respond. Its purpose was to minimise the duration of breath-holding. The mean figure for the latter, for all subjects, was 0·38 sec. (σ = ·14 sec., 20 observations).

The respiratory flow control system is shown in Figure 3.2.2 (iii). This incorporated a pair of miniature edge-level indicators, one of which, termed the target display, was connected to a sawtooth wave generator of adjustable wave frequency and amplitude. It could therefore be used for a variety of tidal volumes and flowrates. Mounted directly above this was an identical indicator, termed the breathing display, whose indicator followed the movements of the inspiratory and expiratory spirometers A and C in each half cycle, adjustable for scale. The subject had therefore to match the movement of the two indicators. This proved to be more effective than a metronome in controlling breathing rates. For those subjects in the main study of particle size at constant respiratory pattern (breathing rate = 10 breaths minute $^{-1}$, tidal volume = 1·0 litre) the mean figure was 10·16 breaths minute $^{-1}$ (13 observations, σ = 0·26 breaths min.$^{-1}$). The method was less successful in controlling the relative durations of an inspiration (ti) and an expiration (te) within a single breath. Most subjects consistently inspired more rapidly than they expired, the mean figure being te = 1·22 ti (20 observations,

$\sigma = 0{\cdot}4$). In some individuals this tendency was particularly pronounced (see Tables 4.2.2 and 4.2.4).

The breathing patterns of each subject were recorded by means of a U.V. light-sensitive paper recorder (S.E. Electronics Ltd.). Only the excursions of the inspiratory spirometer were recorded as this was all that was necessary to derive the times, ti, tp_1, and T from which te could be estimated by assuming $tp_1 = tp_2$ (Figure 3.2.3).

(c) Overall operation of apparatus

In the first part (a) of this section the problem of respiratory valve actuation was described, with particular emphasis on the necessity of preventing any of the initial portion of expired air from entering the inspiratory port. For the sake of clarity the method of breathing control was described separately, in part b. The overall operation of the apparatus is described below insofar as it is relevant to the problem of respiratory valve actuation.

Figure 3.2.4 is an attempt to represent the overall operation of the apparatus, the nomenclature being the same as before. The blocking valve V3 is again of central importance. Its purpose in this instance, besides that of assisting in the control of the tidal volume of the subject, was to enable the main respiratory valve V1 to change its position when a signal to change from inspiration to expiration, or vice-versa, was indicated to the subject, in anticipation of the subject's response. Since V1 changed position before any changes on the part of the subject, and since after V3 had blocked the mouthpiece it could only be opened again by application of the appropriate pressure signal by the subject, there was no possibility of any misdirection of expired aerosol.

It should be noted that while the position of V1 was determined only by the limit switches LI, LE, V3 was under combined automatic and subject control. Referring as before to Figure 3.2.4, the position of the respiratory valves and spirometers during an inspiration was as shown in (i). During the early period of inspiration the position of the expiratory spirometer, C, was re-set in the manner described above (see

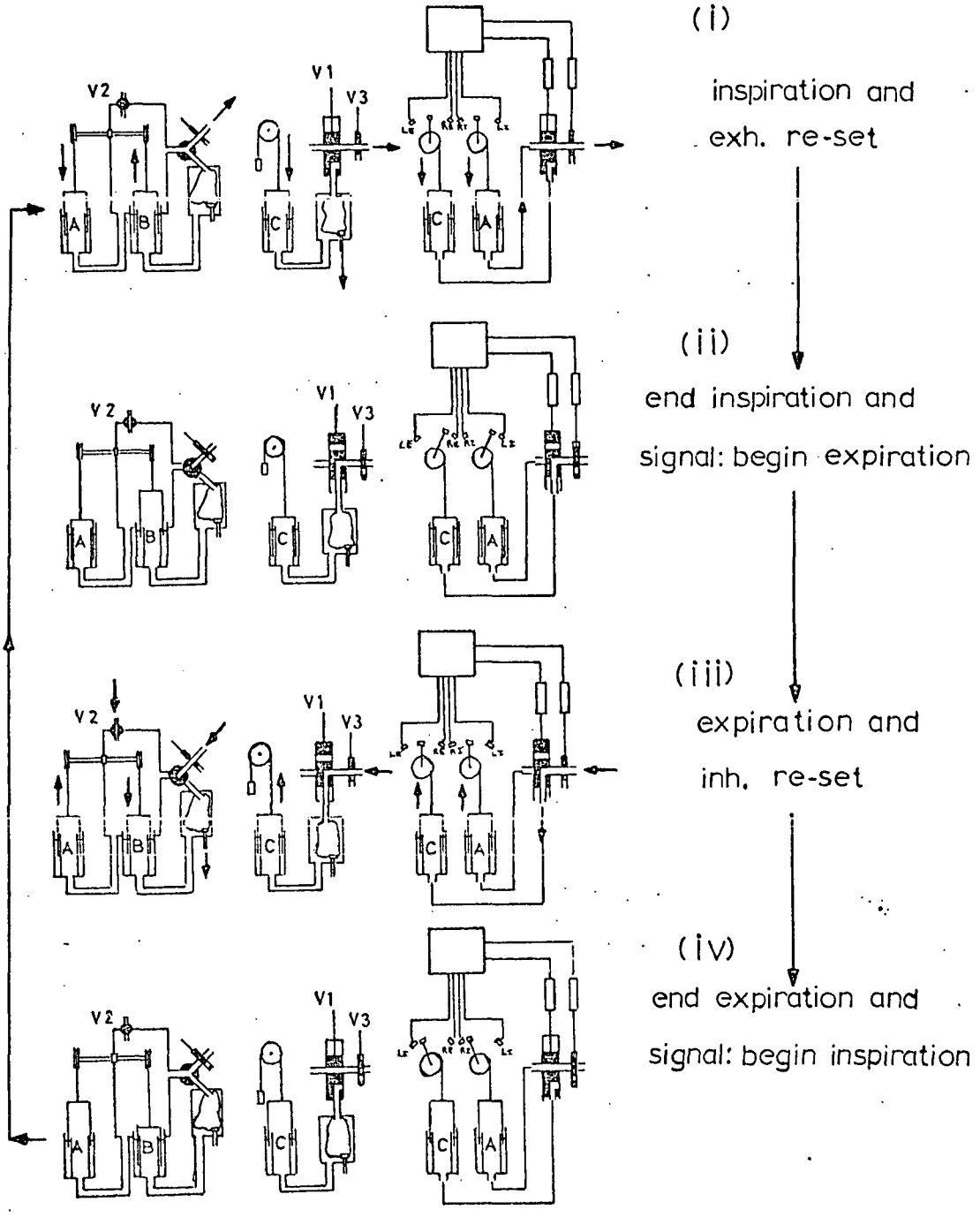

Figure 3.2.4: Overall operation of apparatus.

(see 3.2 (i)). The end of inspiration (ii) occurred when the magnet actuator on the pulley of spirometer A, reached LI. At this point the main respiratory valve V1 moved into the expiratory position and V3 closed, blocking the mouthpiece. Simultaneously the subject had received a signal to begin an expiration, in the manner described in part b of this section. At this point, V3 was under subject control and when the subject responded to the applied stimulus by expiring, micromanometer probes detected the resultant pressure change (operational threshold = + 0.2 mmH_2O), which caused V3 to be opened by the electro-pneumatic control apparatus (Figure 3.2.5). V3 did not open if the subject continued to apply only a negative pressure at the mouthpiece. At the instant that V3 opened, defined as the beginning of an expiration, the spirometer re-setting process was initiated for spirometers A and B (iii). The end of expiration (iv) occurred when the magnet actuator on the pulley of spirometer C, reached LE. At this point the main respiratory valve, V1, moved into the inspiratory position and V3 closed, blocking the mouthpiece. Simultaneously the subject had received a signal to begin an inspiration. At this point, V3 was once more under subject control and when the subject responded to the applied stimulus by inspiring, micromanometer probes detected the resultant pressure change (operational threshold = -0.2 mmH_2O) and V3 was opened. V3 did not open if the subject continued to apply only a positive pressure. At the instant that V3 opened, defined as the beginning of an inspiration, the spirometer re-setting process was initiated for spirometer C (iv).

As a safety feature it was considered necessary to incorporate some means of preventing a change in the direction of respiratory excursion before the limit switches, LI and LE, had been reached by the magnet actuators; i.e. during modes (i), (iii), in Figure 3.2.4. To this end, if a small positive pressure of +0.05 mmH_2O, in the case of an inspiration, or of -0.05 mmH_2O, in the case of an expiration, occurred, V3 closed until the correct pressure was re-applied. Inevitably, if such an error was committed by a subject, a small volume of aerosol would be misdirected during the delay (~ 50 milliseconds) between the application of signal and completion of valve movement. In the event, the additional facility was not needed on

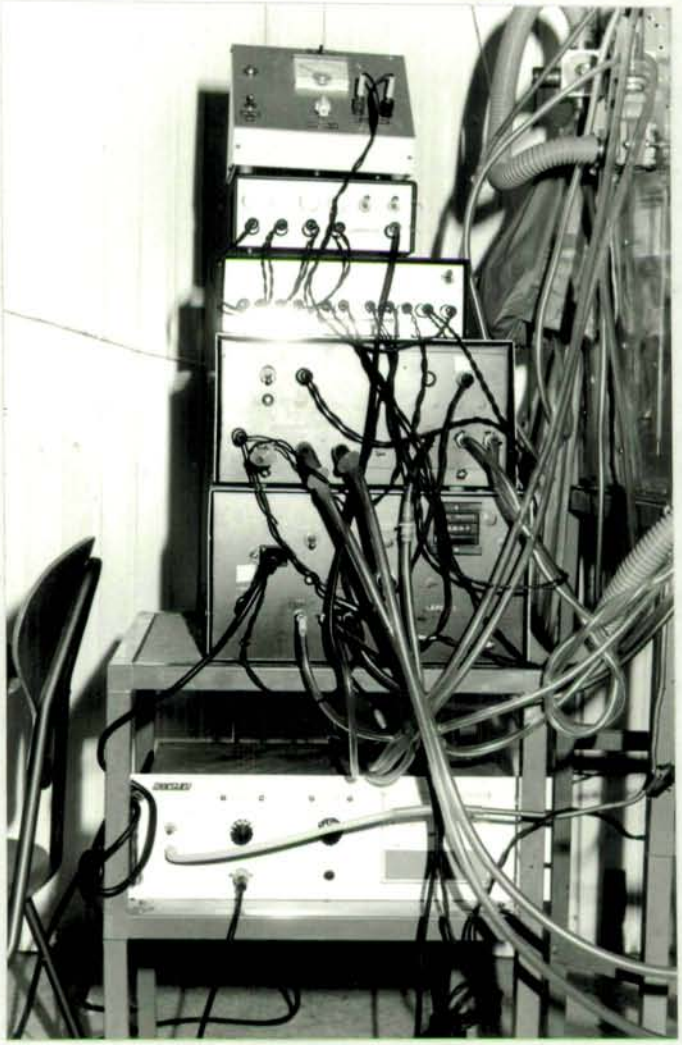

Figure 3.2.5: Photograph of electro - pneumatic control.

a single occasion during the study.

The respiratory valves V1, V3, and the respiratory flow rate control device are shown in Figure 3.2.6.

3.2 (iii) Treatment of dead space errors and testing of sampling accuracy

(a) Dead space errors

Errors due to dead space losses were important above a particle diameter of about 10 μm and had therefore to be taken into account (Table 3.2.1). Two types of dead space error were distinguished in the treatment: those due to particle losses in the mouthpiece during expiration; and those due to particles which remained airborne long enough in the dead space to be passed into the inspiratory or expiratory collection bags. The latter quantity, kn, was estimated from the known volume of mouthpiece and sampling tube dead space, 25 ml in both cases, and the amount of aerosol known to have penetrated beyond the line b′, shown on Figure 3.2.7 (i) (see equation 3.2.6). Aerosol losses in the mouthpiece during expiration were estimated by assuming equal loss efficiencies in both directions of flow; hence the losses in each direction were assumed to depend only on the relative aerosol concentrations and average particle residence times in the mouthpiece during inspiration and expiration. Owing to the smallness of these losses their values could be approximated using equation 3.2.5.

The equation (3.2.2) for the calculation of total deposition, $f_D(I)$ becomes,

$$f_D(I) = \left(1 - \left[\frac{Ic-Kn+DS'-li}{Ec-Kn+le}\right]\right) = \left[\frac{Ic-(Ec+DS-DS')}{Ic-Kn+DS'-li}\right] \quad \text{...equation 3.2.4}$$

$$\text{and,} \quad li \simeq \left(\frac{Ic}{Ic+Ec}\right)\left(\frac{ti}{ti+te}\right) DS \quad \text{.....equation 3.2.5}$$

$$Kn \simeq \left(\frac{0{\cdot}025}{V_T}\right)(Ic+DS') \quad \text{.....equation 3.2.6}$$

$\bar{d}\mu m$	DS′±σ% of I	DS±σ% of I
4·55	0·45±·22	0·53±·92
6·74	1·79 ±·46	1·26 ±·88
10·45	5·70 ±·89	4·44 ±1·41
13·04	7·00±·93	7·15±·45

Table 3.2.1: Dead space losses in mouthpiece (DS) and sampling tube (DS′) averaged over three subjects at each particle size ($\bar{d}\,\mu m$). (Subjects of variable particle size study only).

Figure 3.2.6: Photograph of respiratory control valves and breathing control apparatus.

where, Ic = amount of aerosol drawn into inspiratory collection bag

Ec = amount of aerosol passed into expiratory collection bag

K_n = average amount of aerosol per breath which occupies the mouthpiece or sampling tube at the end of an inspiration, times the number of breaths, n.

li = aerosol losses in the sampling tube or mouthpiece, assumed equal during an inspiration.

le = aerosol losses in mouthpiece over all expirations

DS = total inspiratory and expiratory aerosol losses in the mouthpiece, assumed to equal (li + le)

DS' = total aerosol losses in sampling tube

ti = average duration of inspiration

te = average duration of expiration

V_T = tidal volume in litres at 37°c and 100% RH.

One type of dead space error was ignored in this treatment. This was the sampling error which results by virtue of the valve, V3, which closed shortly before V1 and spirometer B (Figure 3.2.4), occupying a finite volume. Their combined effect was estimated to lead to an underestimate of less than 0·4% in the amount of aerosol inhaled by the subject.

The amounts of aerosol deposited in the various dead space regions of the apparatus and collection bags were assessed by measuring the relative amounts of radioactivity associated with each. At the end of aerosol administration the mouthpiece, sampling tube, and connecting tubing to the expiratory collection bag, were swapped. The collection bags were removed and folded into geometrically identical containers for radioassay. Attenuation of γ-radiation through the walls of the folded rubber bags was only slight (< 5%) using Tc^{99m} (photopeak energy = 140 keV) and in any case about equal in each bag and sample. Radioassay of samples was performed using a whole body monitor, details of which are given in 3.3.

(b) Testing of sampling accuracy

Owing to the sensitivity of the aerosol sampling system to minor air leakages the air-tightness of the apparatus was always checked before an experiment by withdrawing a known volume of

air from the system and checking this against spirometer deflection , as measured on linear scales fixed parallel to the spirometer-bell attachment strings (Figure 3.2.8 (i)). A previously calibrated brass syringe (1·0 litre) was used in this and was always pumped about ten times in order that the cumulative effect of a minor leak would be apparent.

All spirometers were constructed from thin aluminium sheet in order that their mechanical response to pressure change would be as rapid as possible. This response was measured by means of a pneumotachograph (Fleisch No. 4) connected to the mouthpiece. Flow rates at the mouthpiece could then be compared to the volume changes calculated from the movement of the inspiratory spirometer A, measured by means of a potentiometer attached to its pulley wheel. Figure 3.2.9 shows the results for airflow rates of 32 and 41 litres minute^{-1}, which confirmed that spirometer response was satisfactory at air flow rates greater than those likely to be encountered in the experiments (target rates = 13-20 litres minute^{-1}).

As the overall accuracy of a total deposition measurement depended on a multitude of factors it was considered necessary to devise a method of checking it as directly as possible. To this end, the apparatus shown in Figure 3.2.7 (ii) was used to measure the accuracy of aerosol sampling and collection over a number of breaths. It was also useful in determining the aerosol delivery efficiency at a given particle size and moreover served as a direct check on the accuracy of volume control since the volume of air in the collection bag D, changed considerably over a number of breaths for only a small inspired and expired volume inequality. The aerosol which was 'inhaled' into the collection bag D, either settled out or was passed into the expiratory collection bag Ec. The actual quantity of 'inhaled' aerosol could therefore be derived from measurements of the radioactive contents of the expiratory collection bag Ec, and bag D, taking into account the dead space losses.

The measured quantity of 'inhaled' aerosol was then compared to that predicted from equation 3.2.8.

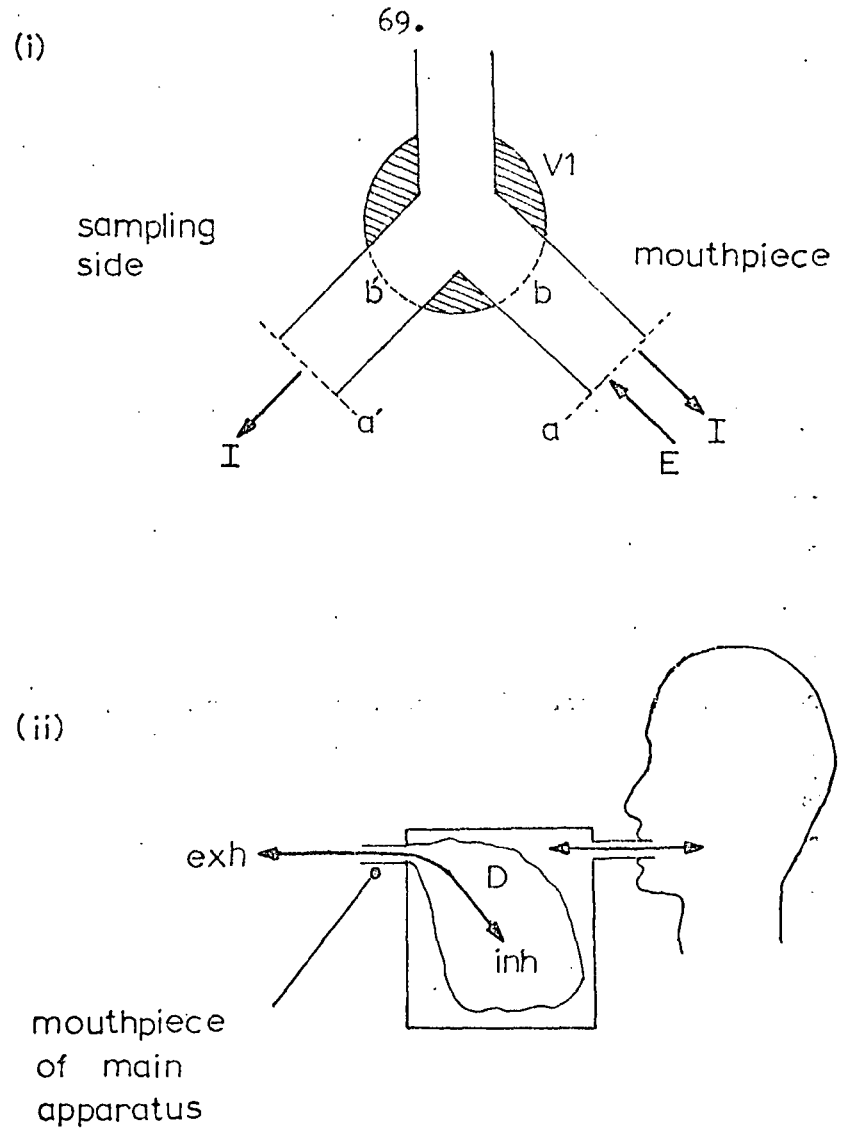

Figure 3.2.7: Dead space and accuracy test.

(i)

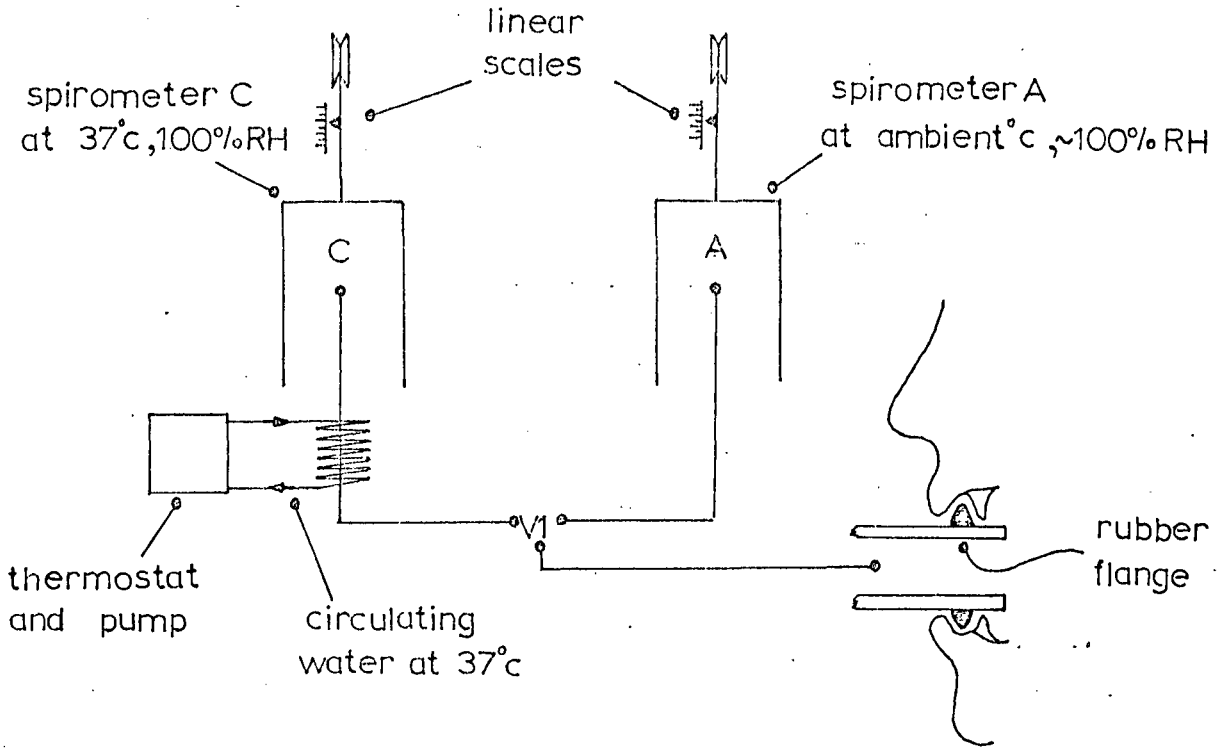

(ii)

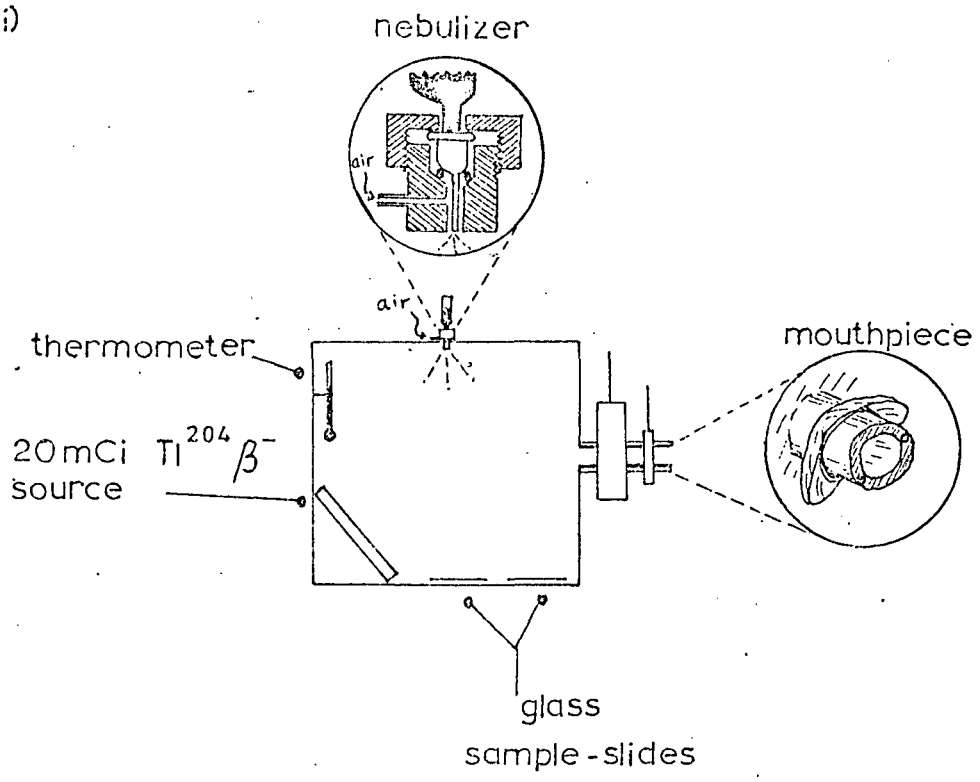

Figure 3.2.8: Constructional aspects of apparatus.

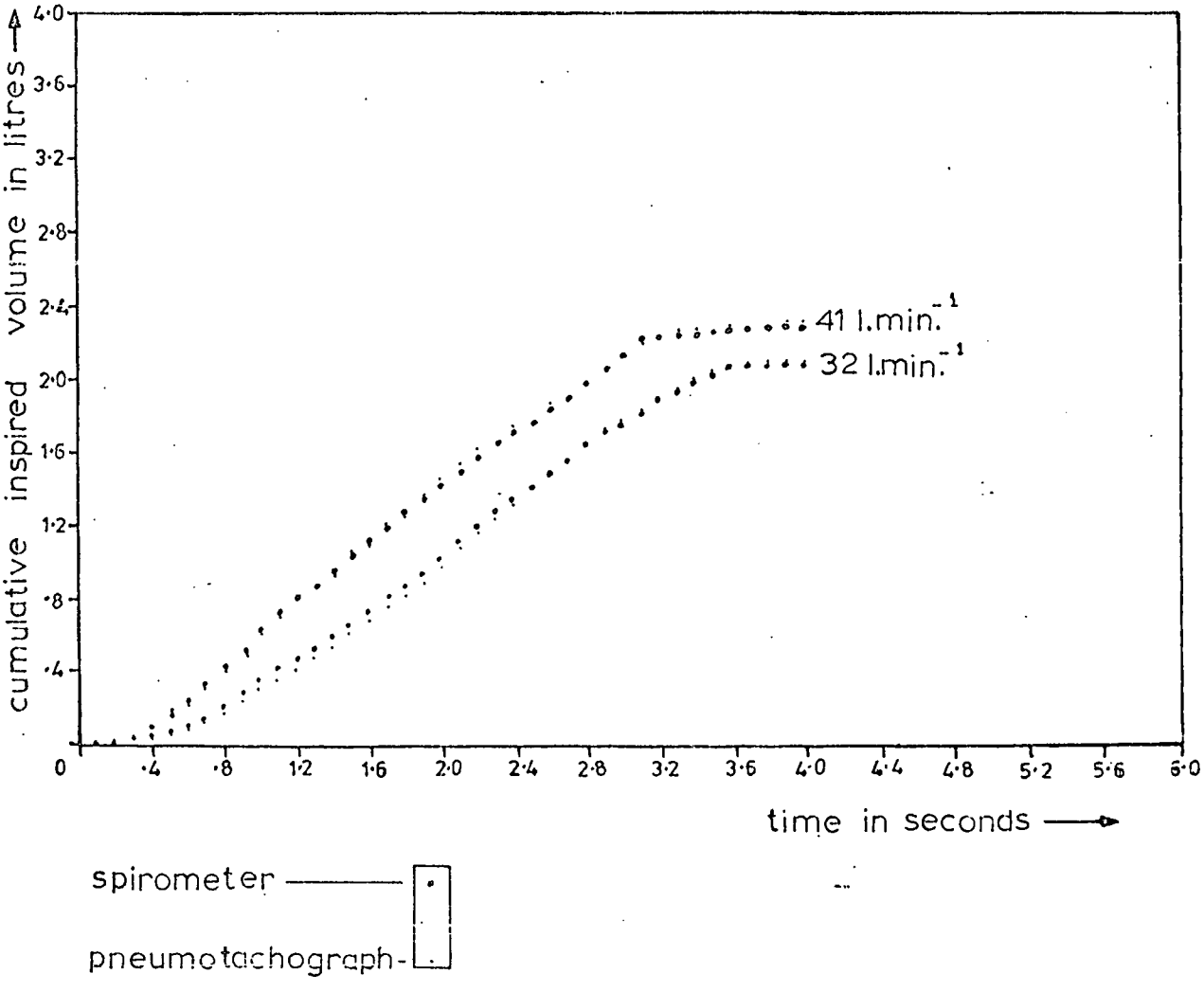

Figure 3.2.9: Spirometer response.

I measured = (Ec-Kη+1e+Dc) .....equation 3.2.7

I predicted = (Ic-Kη+DS'-1i) .....equation 3.2.8

where, Dc = amount of aerosol deposited in the collection bag D

and, 1e = (DS-1i)

(other nomenclature having the same meaning as above).

The results of nine such observations, all at a tidal volume of one litre and mean breathing rate of approximately 10 breaths minute^{-1}, are given in Table 3.2.2, having a satisfactory accuracy at all particle sizes. The mean predicted figure, expressed as a percentage of the measured figure, was 100·02 $\pm$ 0·8%, ($\pm$ standard error of the mean, σ = 2·4%).

(iv) Re-dispersion of particles and aerosol characterization

The techniques employed for the generation and characterization of monodisperse polystyrene particles were described in 3.1. However, as these particles were re-dispersed at a later stage for aerosol administration, full characterization of the aerosol actually inhaled by the subject required consideration of changes in its bulk aerodynamic properties after secondary dispersal.

(a) Re-dispersion

The particles were re-dispersed in the aerosol administration apparatus by incorporating them into 1·2 ml of ethanol, which was subsequently dispersed as a fine mist by means of an air-jet nebulizer (Figure 3.2.8 (ii)). The nebulizer was operated by a small pump which aspirated from the ambient air at a rate of 12 litres minute^{-1}, such that nebulization was normally completed within about ten seconds. The assumption was that the ethanol droplets, most of which would contain one particle, quickly evaporated leaving the dry, airborne polystyrene particles. In such circumstances it was considered inadvisable to rely solely on theoretical predictions of droplet lifetimes. There was the possibility, for example, of water vapour condensation on the particles immediately following dispersion, owing to the lowering of their temperature relative to that of the surrounding air as

nominal particle dia.μm	test no.	Ipredicted as % Imeasured
4·5	1	100·18
6·5	2	102·10
4·5	3	98·96
6·5	4	95·37
4·5	5	97·76
4·5	6	103·80
4·5	7	100·86
9·5	8	101·46
13·0	9	99·57
6·44	means	100·02

Table 3.2.2: Testing of sampling accuracy - results.

the ethanol evaporated. However, experimental observation of fine droplet evaporation is a difficult problem (PORSTENDÖRFER et al., 1977). In order to make such observations as directly as possible the apparatus shown in Figure 3.2.10 was used to trap a portion of sprayed particles in a viscous oil (silicone oil, kinematic viscosity = 200 centistokes), for subsequent microscopic examination.

A sample of polydisperse polystyrene particles, in 0·5 ml. of ethanol solution was sprayed into a 28 litre perspex box which was kept saturated with water vapour. When spraying was completed, after about ten seconds, a tap was turned to allow in a displacement flow of air into the box and force a portion of the aerosol through a narrow orifice. At the orifical exit the particle laden airstream impacted into a fine jet of the oil and those particles that were captured became trapped in a reservoir directly below. The purpose of using the oil jets was to encapsulate the particles in a fluid as rapidly as possible, thus arresting any evaporation process and facilitating their direct microscopic examination. That the technique was effective in achieving this was confirmed by placing oil-impaction jets at about one centimetre from the nebulizer nozzle, when ethanol was sprayed on its own. Ethanol droplets in a variety of sizes could be observed on microscopic examination of the fluid. On microscopic examination of the particles collected in the manner described above, no liquid residue could be discerned. Liquid droplets were distinguishable from solid particles because of their good sphericity which contrasted sharply with the surface irregularity of the polystyrene particles. As a final check, ethanol was also sprayed on its own into the box. No droplets were observed in the fluid.

The absence of any fluid around the particles also indicated an absence of any significant water vapour condensation on the particles. As the particles must have undergone considerable cooling during ethanol evaporation, this result suggests that condensation of water vapour on the particles on entering the warmer, saturated, respiratory tract, is also of no consequence.

The volume of alcohol sprayed into the apparatus for aerosol administration was determined as that which would not result in

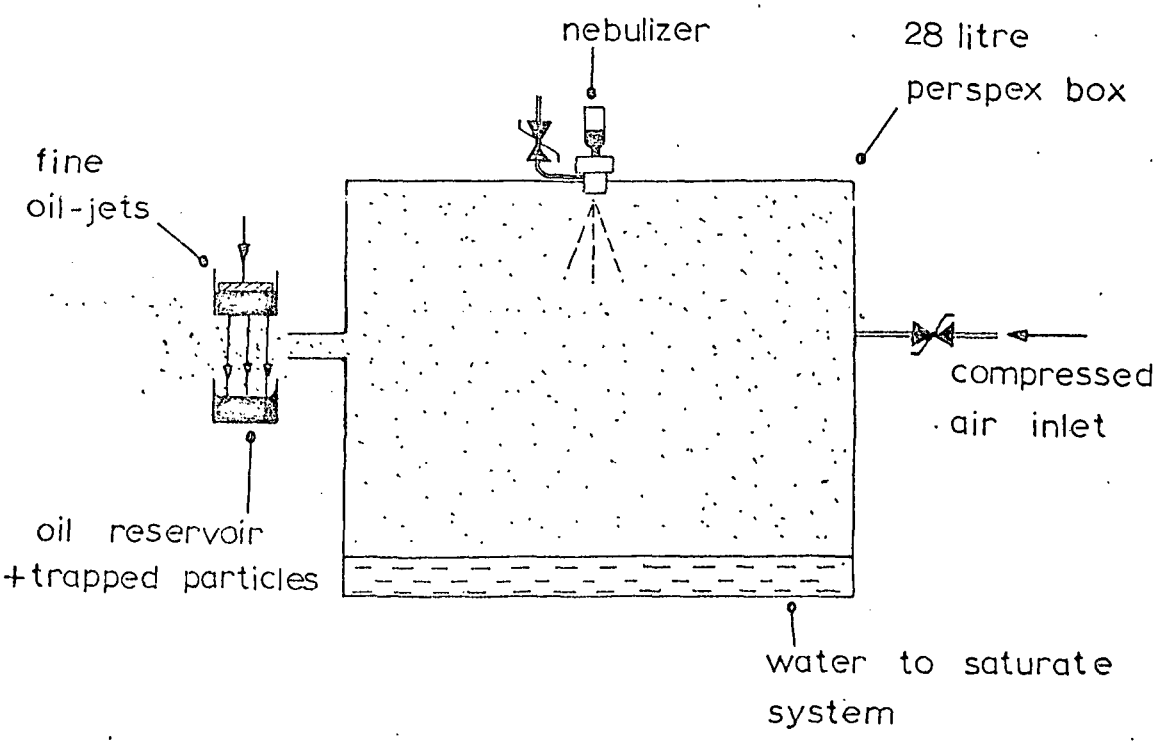

Figure 3.2.10: Testing of particle dryness following dispersion.

any respiratory discomfort for the majority of subjects (ethanol concentration ~ 13·3 milligrams litre^{-1} or ~ 1% by volume). HOLMA (1967) reported that the inhalation of ethanol vapour had no effect on rates of short-term clearance in rabbits at concentrations as high as 5% by volume. In the present work, ethanol was also found to have no obvious bronchial constriction or dilation effects. The maximum expiratory flow at 50% of forced vital capacity (MEF 50%) for two subjects was measured before and after they had inhaled alcohol vapour at a concentration of 13·3 milligrams litre^{-1} over ten breaths. The results before and after alcohol inhalation were, respectively, (1) 3·76 $\pm$ ·014, 3·88 $\pm$ ·019; (2) 4·26 $\pm$ ·011, 4·25 $\pm$ ·002, all results being the mean $\pm$ the standard error of 3 observations, flow rates being expressed, at body temperature and pressure, in litres second^{-1}.

Average aerosol delivery efficiency over ten breaths, expressed as the amount of aerosol inhaled by the subject relative to the amount sprayed into the apparatus, ranged from approximately 1% at a particle diameter of 13 μm, to nearly 5% at a particle diameter of 4·5 μm. Alternatively expressed as the percentage decrease in aerosol concentration in the actual volume of air inhaled by a subject, the figures were at least 9% and 45% for 13 μm and 4·5 μm particles, respectively. As this decrease normally occurred over a period of at least one minute of breathing, the decrease in aerosol concentration over a period of one breath (3-4·5 seconds) was small. The mass of aerosol deposited in the subjects was typically in the region of 100 μgm, corresponding to particle numbers of between 10^5 and 2 x 10^6, or an average inhaled concentration of between 5 - 100 particles per cubic centimetre. In the region of 10 μCi of radioactivity was normally delivered to the subject, although this sometimes varied owing to a degree of unpredictability in the particle labelling efficiency and was set at about twice this figure for some selective applications. Radiation dose was set as low as possible, consistent with reasonable counting statistics. Relevant aspects of radiation counting statistics are discussed in 3.3. Radiation dose given to the lungs varied according to the proportion of clearance. The maximum dose given to the lungs, assuming complete retention, varied from

approximately 2 m.rem to 17·5 m.rem, but 5 m.rem typically. In many cases, most of the particles deposited in the lungs were rapidly translocated to the abdomen. Assuming complete clearance to the transverse colon, the radiation dose to this organ again varied from approximately 2 m.rem to 17·5 m.rem, and 5 m.rem typically. Three subjects participated in repeat studies and in their case total radiation dose in each of the above organs was below 15 m.rem. Conversion factors from absolute radioactivity to radiation dose given to specific organs were taken from ICRP report No. 17 'Protection of the Patient in Radionuclide Investigations' (1971).

(b) Aerosol characterization

The possible influence of electrical charges on airborne particle deposition was discussed in Chapter 1. Although it was considered unlikely to be an influence in the particle size range of the present study (4·5 - 13·0 μm diameter), the electrical neutralisation of the test aerosol was attempted by exposing it to a mixture of positive and negative free ions generated by an ionizing radiation source. Owing to a degree of uncertainty in the published literature as to the time taken to achieve a Boltzmann distribution of free ions, the strength of source used was set considerably higher than was considered absolutely necessary (TAKAHASHI and KUDO, 1973). It was not possible to measure the charge distribution of the test aerosol directly. The radiation source used consisted of a 5 x 25 cm rectangular metal foil impregnated with approximately 20 m.Ci. of Thallium^{204}, which is a pure β-emitter (energy = 0·77 MeV) and has a conveniently long half-life of radioactive decay ($T_{\frac{1}{2}}$ = 3·9 years). It was housed in a lead-lined box which had a hinged lid to facilitate radiation exposure during an experiment (Figure 3.2.8 (ii)).

The time in seconds, tb, taken to achieve a Boltzmann charge distribution was estimated using the equation of GUNN (1954).

$$tb = \frac{1}{4\pi e N \mu} \qquad \text{.....equation 3.2.9}$$

where, e = fundamental unit of electronic charge (esu).

N = small ion pair density (number cc^{-1}).

μ = small ion mobility in $cm.^2 V^{-1} sec.^{-1}$

Values of ion pair density corresponding to a given β-radiation source in a given volume were taken from the empirical data of TAKAHASHI and KUDO (1973). A value of $\mu = 1{\cdot}4$ $cm.^2 V^{-1} sec.^{-1}$ was used, which is the average mobility of positive and negative ions quoted by BRICARD and PRADEL (1966), giving a value for tb of 1·6 seconds. This value should only be taken as an order of magnitude estimate as equation 3.2.9 was not intended, strictly, to apply to particle diameters above about 3 μm. It is however within an order of magnitude of the value of tb predicted by FRY (1970), who employed a β-radiation source of similar strength, but with much shorter particle residence times (~ 1 second) near it. In the present work, there was normally greater than a 30-second delay between the end of particle dispersal and the first intake of aerosol by the subject.

It should be appreciated that the purpose of such electrical neutralisation was not to eliminate such effects entirely, but merely to standardise them between separate experiments.

Besides defining the size, shape, density and electrical charge characteristics of the particles, it was also necessary to consider the relative proportions of satellite and aggregated particles present in the aerosol inhaled by each subject. Since satellite particles fall more slowly than their corresponding primaries it is likely that their relative concentration would increase with time after initial dispersal, with a more pronounced effect at increasing particle size. The effect was measured at 10·4 μm and 13 μm particle diameters by aspirating for one minute, about 30 seconds after particle dispersal, through a millipore filter attached to the mouthpiece of the aerosol administration apparatus. The relative proportions of satellites to primaries on the filter, N_{s1}/N_{p1}, was then compared to that measured on glass slides, N_{s2}/N_{p2}, placed on the floor

of the main spraying chamber. Two such tests were performed for each size and the average result expressed as $\left[\frac{Ns1}{Np1} \times \frac{Np2}{Ns2}\right]$, which gave a figure of 2·3, 2·8, for 10·4 μm and 13 μm diameter particles, respectively. The ratio of satellites in any given particle sample at these sizes was calculated as the product of this factor and the proportion of satellites measured on glass slides placed on the floor of the spraying chamber during aerosol administration. In only two cases (KD, TDW), at particle diameters ≥ 10·4 μm, did this value exceed 2%. Differential settling of satellites and primaries at the two sizes studied below 10·4 μm, was found to be negligible over a period of two minutes. The relative proportions of satellites and primaries for all experiments are listed in Table 3.2.3.

Aggregation of particles was not generally significant above a particle diameter of 4·5 μm because of the relatively fewer numbers dispersed from solution. At 4·5 μm particle diameter, the proportion of particles sprayed as singlets fell in a range 80%-95%, of the total number of entities, the average value being 88·3%. The majority of those particles not dispersed as singlets were either doublet or triplet entities (Table 3.2.3). The proportions were obtained by microscopic analysis of glass slides which had been placed on the floor of the spraying chamber during aerosol administration. The degree of aggregation was reduced as far as possible by minimising the number concentration of particles in the ethanol spraying solution and by subjecting it to several minutes of vibration in an ultrasonic bath prior to aerosol administration. Owing to a rapid decline in aerosol production efficiency with low polymer concentrations, a lower limit to particle number concentration in the ethanol spraying solution was imposed and a finite degree of particle aggregation was unavoidable.

The effects of particle agglomeration may be examined using the semi-empirical relationship of Stöber (1972) which applies to chain-like aggregares of particles:

subject	d μm	coeficient of variation	primaries % mass	singlets % by no.	doublets + triplets % by no.
DCFM	4·55	9·01	n.d.	n.d.	n.d.
AM	4·58	5·65	92·2	87·5	11·9
AR	4·53	8·80	95·0	82·6	13·0
group av.	4·55	7·82	93·6	85·1	12·5
HG	7·00	10·00	96·4	96 0	4·0
RB	6·32	7·10	97·8	72·8	17·9
PCE	6·90	8·03	n.d.	n.d.	n.d.
group av.	6·74	9·37	97·1	84 4	11·0
PT av.	10·38	5·90	98·2	97·3	2·7
PH	10·44	5·06	99·0	100·0	0
KD	10·53	5 31	89·9	94·5	5·5
group av	10·45	5·42	95·7	97·3	2·7
TDW	12·86	4·74	91·3	98·0	2·0
JH	13·05	8·60	98·9	96·2	3·8
AD	13·23	10·15	98·9	100·0	0
group av	13·04	7·83	96·4	98·1	1·9
ATM	4·50	6·93	99·5	91·6	8·4
FH	4·49	7·95	98·2	95·0	5·5
RH	4·48	9·00	98·4	95·5	4·5
group av	4·49	7·96	98·7	94·0	6·1
VC	4·58	7·05	98·7	91·0	9·0
MS av	4·60	7·41	97·9	83·3	12·3
JV	4·64	8·22	96·9	89·7	9·6
group av.	4·61	7·51	97·8	88·0	10·3

nd = not determined

Table 3.2.3: Particle characterization.

$$dae = K.\rho^{\frac{1}{2}}.n^{\frac{1}{6}}.d \quad \text{.....equation 3.2.10}$$

where, K = a constant of proportionality

ρ = 'primary' particle density

n = number of 'primary' particles in the agglomerate

d = 'primary' particle diameter

dae = aerodynamic diameter of the agglomerate

Using a value of K = 1, which lies closely between the empirical values observed by KOPS et al. (1975) and STÖBER (1972), this gives a value of dae = 5·05 μm for doublets, and dae = 5·4 μm for triplets, at d = 4·5 μm. The overall effect of particle aggregation in the proportions observed in the present work at 4·5 μm, is therefore likely to be small.

(v) Construction of apparatus and control electronics

Only a brief description of certain constructional aspects, considered relevant, will be attempted here.

It was important that the subject's mouth was effectively sealed over the mouthpiece during aerosol administration. Since the diameter of mouthpiece used was in any case made relatively wide (2·5 cm), in order to minimise airflow resistance, the resultant stretching of the subject's lips favoured good sealing. As an additional safeguard a rubber flange was incorporated into the mouthpiece (Figure 3.2.8). The right and left edges of the flange were elongated in order to prevent 'side-breathing' by the subject. The flange was fitted about one centimetre along the mouthpiece such that the latter normally penetrated to a distance of about three centimetres into the subject's mouth.

The subject sat in a chair, of variable height, such that his back was slightly off-vertical during aerosol administration, as shown in Figure 3.2.11, which also shows the complete aerosol administration apparatus.

From the description of the breath to breath operating sequences described earlier in this chapter it may be apparent that an electro-pneumatic control system of considerable complexity was required. It was also essential that high reliability was achieved, because of the one-off nature of the

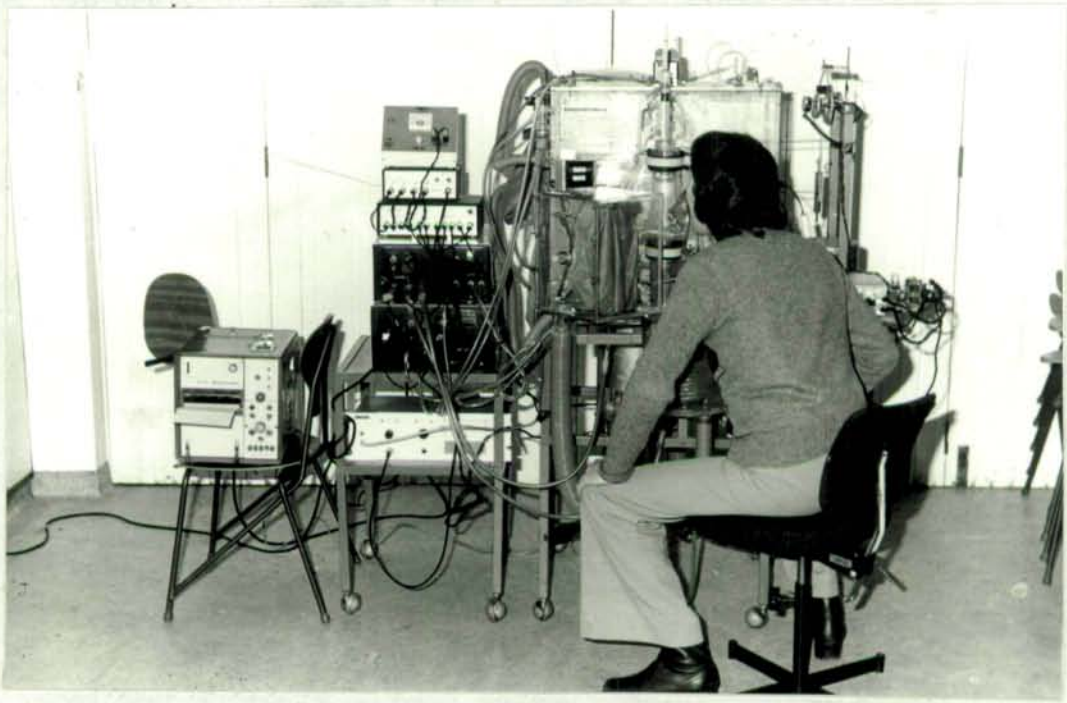

Figure 3.2.11: Photograph of a subject breathing on aerosol administration apparatus.

experiments. A circuit that employed as few discrete components as possible was used in order to minimise the probability of a failure occurring in the whole system.

Pressure changes were detected using a commercially available micromanometer (Mercury Electronics Ltd.).

3.3 Measurement of regional aerosol deposition and clearance

(i) Definitions

While the total deposition fraction may be measured by direct means, because of its relative inaccessibility it is necessary to employ indirect techniques in the estimation of the regional distribution of this fraction within the respiratory tract.

In Chapter 1 the essentially continuous nature of the respiratory tract was described and the difficulty of defining specific boundaries between regions was emphasised. Yet some practical means of distinction must be adopted when it becomes necessary to consider the aerosol filtration characteristics of each region separately. However, if indirect techniques are employed such distinctions ought not to presume an automatic correspondence between the anatomical region under consideration, however precisely it is defined, and the deposition fraction measured empirically. For these reasons purely functional definitions of regional deposition fractions were employed which related as closely as possible to the experimental methods used for the derivation of each:

1. fw(I) That fraction of the inhaled aerosol which could be recovered by washing of the mouth shortly after the end of aerosol administration, normally within 1-2 minutes.

2. fs(I) That fraction of the inhaled aerosol removed to the stomach, by swallowing, between the first and second readioactive lung burden measurements, the second performed normally 9-12 minutes after the end of aerosol administration. The purpose of measuring fs(I) was to estimate aerosol losses in the pharyngeal and laryngeal regions which could

not be recovered in fw(I), but neither could be strictly counted as a lung deposit.

3. fc(I) That fraction of the inhaled aerosol cleared from the lungs between the second and final radioactive lung burden measurements, the final measurement normally being performed 20-22 hours after the end of aerosol administration. If it is assumed that only that fraction of the inhaled aerosol which initially deposited on the ciliated airways was cleared, and completely cleared, during this period, fc(I) is that fraction.

4. $f_R(I)$ That fraction of the inhaled aerosol retained in the lungs at the time of the final radioactive lung burden measurement.

These fractions and all others relating to aerosol deposition in the present work, have been written in the general form,

$$fx(y) = \frac{x}{y} \qquad \text{..... equation 3.3.1}$$

where, x is the magnitude of the quantity under consideration expressed as a fraction of another quantity, y, expressed in the same units as x,

hence,

$$fw(I) = \frac{W}{I} \qquad \text{..... equation 3.3.2}$$

$$fs(I) = \frac{S}{I} \qquad \text{..... equation 3.3.3}$$

$$fc(I) = \frac{C}{I} \qquad \text{..... equation 3.3.4}$$

$$f_R(I) = \frac{R}{I} \qquad \text{..... equation 3.3.5}$$

and, $f_D(I) = fw(I) + fs(I) + fc(I) + f_R(I)$ ... equation 3.3.6

W, was measured in arbitrary detector counts and expressed directly as a fraction of I. S, C and R, were measured firstly as fractions of quantities other than I, and then converted to

fractions of I, by means of the following equations,

$$f_S(I) = f_{S(c+R+s)}.(f_D(I)-f_W(I)) \quad \text{..... equation 3.3.7}$$

$$f_C(I) = f_{C(c+R)}.(f_D(I)-f_W(I)-f_S(I)) \quad \text{..... equation 3.3.8}$$

$$f_R(I) = f_{R(c+R)}.(f_D(I)-f_W(I)-f_S(I)) \quad \text{..... equation 3.3.9}$$

where, $f_{S(c+R+s)}$, $f_{C(c+R)}$, and $f_{R(c+R)}$, were estimated from measurements of whole body radioactivity.

and, $f_{C(c+R)}+f_{R(c+R)}=1$ ..... equation 3.3.10

(ii) Measurement techniques

(a) Mouth and throat deposits

Radioactive particles deposited in the mouth during aerosol administration were removed by means of the apparatus illustrated in Figure 3.3.1. Several pressurised water-jets were directed upwards into the subject's mouth from a 50 ml syringe, in order to ensure that any particles removed would be washed downwards into the collection vessel. Mouthwash duration was normally about thirty seconds. Gargling methods were rejected as these were found to be more likely to lead to swallowing, which in this case it was desirable to avoid as far as possible. The radioactive content of the mouthwash collection vessel was measured in arbitrary detector counts. For each radioassay the vessel was placed in a standard position within the detector and the amount of fluid was always made up to a standard level. Further details of radioassay procedures are given below (3.3 (ii) e).

In the determination of dust-exposure standards it is desirable to have some knowledge of the proportion of aerosol which is able to penetrate beyond the larynx at a given particle size or breathing pattern. Estimation of the proportion of inhaled aerosol which deposits in the laryngeal region presents severe practical difficulties however. In particular, the subject is able to remove some or all of the initial throat deposit before it can be measured. LIPPMANN and ALBERT (1969)

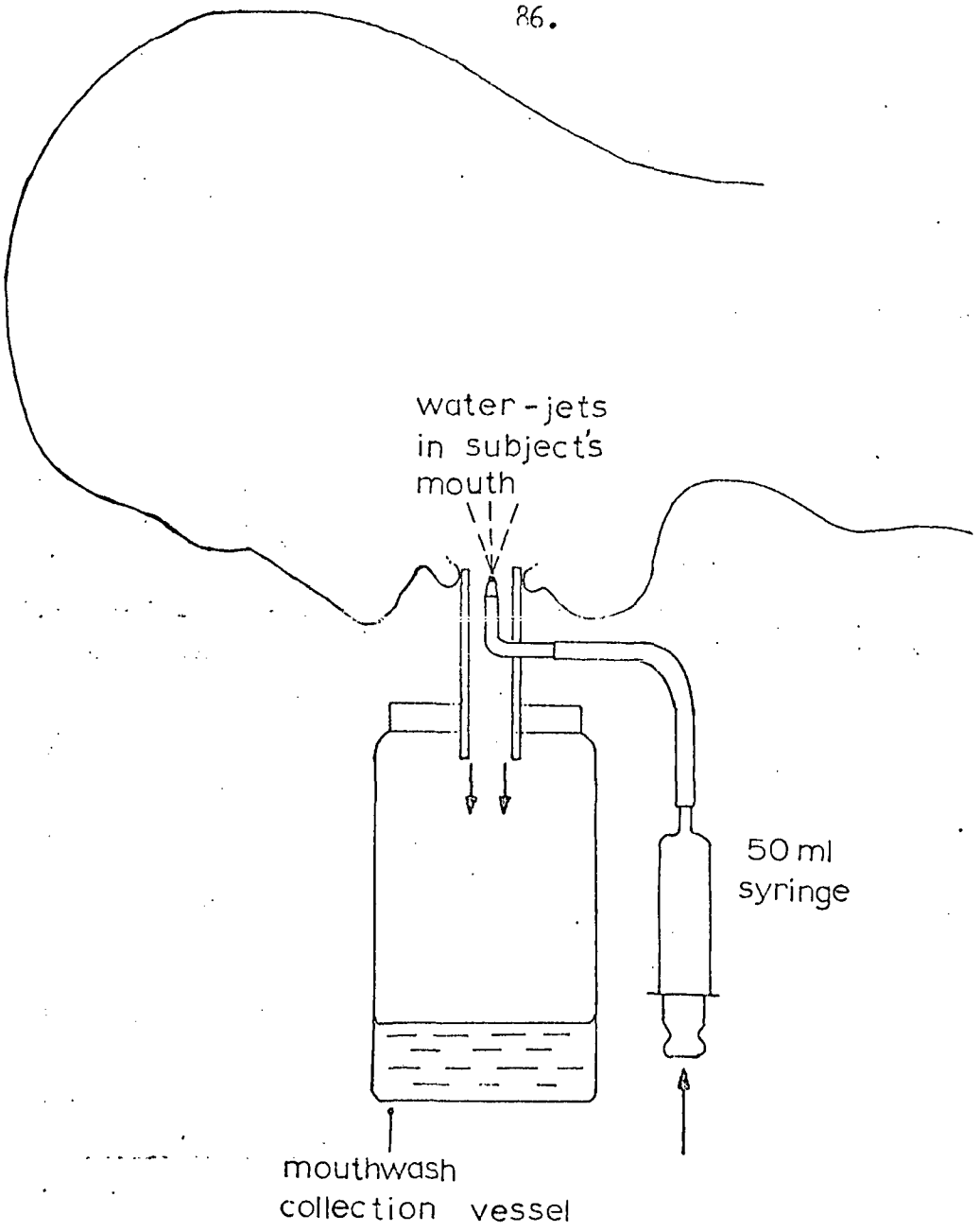

Figure 3.3.1: Mouthwash apparatus.

were the first to attempt such measurements. In their technique the throat and lung deposits were measured in sequence, the lung being the first to be measured. In the present work, in order to minimise the time available for swallowing, the measurement of initial lung and throat deposits was performed in a single manoeuvre. This eliminated the need for measurements of absolute radioactivity in the subject's throat since the throat deposit could be expressed directly as a fraction of the total deposit, in arbitrary detector counts. No conscious or deliberate coughing or swallowing was reported by any subject in this early period after aerosol administration. Moreover, it was possible by means of the technique to detect whether a significant amount of radioactivity had actually been swallowed before the first radioactive body-burden measurement. None was observed for any subject. Further details of the method are given in 3.3(ii)c.

(b) Retained and cleared fractions

The fraction of the inhaled radioactive particles cleared from or retained in the lungs of a subject at a given time ought not to automatically be assumed to correspond to the fractions of aerosol which initially deposited in the largely ciliated non-respiratory, and non-ciliated respiratory, zones of the lung. The reasons for this were discussed in Chapter 1. The definition of an aerosol deposition fraction in terms of levels of retention or clearance at specific times therefore enables the behaviour of aerosols in the respiratory tract to be described using the minimum number of assumptions.

In order to obtain the levels of lung retention at a given time, ideally, the total radioactive contents of both lungs should be measured. However, owing to an arbitrary degree of anatomical overlap between the lungs and those organs through which swallowed radioactivity must eventually traverse, notably the stomach, duodenum and transverse colon, this would appear to be impossible to achieve in practice even when using detectors of the highest available resolution. By resolution it meant the ability of a detector to distinguish between regions. If the resolution of an instrument is increased it is normally at the expense of a decrease in sensitivity which is

most often measured in terms of the number of detector counts above background per absolute unit of radioactivity measured. In a clearance study such difficulties are further compounded by the necessity of monitoring the radioactive lung burden for relatively long periods, since this requires the use of an initial radioactive lung burden that is high enough to leave a detectable magnitude of radioactivity at the end of the clearance period. Detectors of relatively high sensitivity are normally employed in lung clearance studies (LIPPMANN and ALBERT, 1969; CAMNER, 1971; MORSY et al., 1978; FOORD et al., 1978). These may detect relatively low lung burdens, considered ethically acceptable for administration to healthy volunteer subjects, but only at the cost of a relatively poor detector resolution. A compromise is therefore normally required between detector resolution and sensitivity such that a reasonably large fraction of the lung burden may be measured while it is at the same time ensured that there is no significant contribution to detector counts from radioactivity that has already been passed down the oesophagus.

With the exception of CAMNER (1971), the other workers mentioned above employed radiation detectors placed in a stationary position relative to the subject's chest. The main disadvantage of such an approach is that the magnitude of the abdominal contribution to detector counts is subject to a degree of uncertainty for any given measurement, with the attendant consequence that more of the lung radioactive burden may be excluded than was absolutely necessary. FOORD et al. (1977) have demonstrated the large inter-subject differences and rapid temporal variations in the abdominal contribution to fixed detector count rates. CAMNER (1971) employed a linear scanning detector to measure rates of short-term clearance. The advantage of this approach is that a one-dimensional profile of whole body radioactivity is obtained from which it is possible to estimate the relative radioactive contents of lung and abdomen and their degree of mutual overlap for a given detector resolution. A similar technique was employed in the present work, details of which are given below.

(c) Use of profile scanner in the estimation of deposition fractions and clearance rates

The profile scanner used in the present work is illustrated in Figure 3.3.2. The apparatus was essentially that described by TOTHILL and GALT (1971), who conducted a quantitative analysis of its performance. Two diametrical detectors were positioned above and below the subject, which reduced variations in detector response along any vertical line between them. The detectors consisted of thallium activated sodium-iodide crystals, optically coupled to single photomultiplier tubes. Parallel slit lead collimators were fitted and their width could be varied to give a range of spatial responses and resolutions. The subject lay in a supine position approximately mid-way between the detector-pair and could be moved at a pre-determined rate, in a horizontal plane, such that the full body length was scanned.

The two photomultiplier outputs were first amplified and then passed via a mixer into a multi-channel spectrum analyser operated in the multi-scaling mode. In essence, this mode of operation enabled the detector output for a given period, at a particular time, to be assigned a particular location or channel number in the analyser memory corresponding to the particular position of the scanner trolley at that time. A whole body profile of the radioactive distribution within the subject could therefore be obtained, an illustrative example of which is shown in Figure 3.3.3. By setting the analyser counting period or dwell time, to one second, and setting the scanner trolley speed to one centimetre per second, each point on the scan profile, of which there were 200, corresponded to a one centimetre trolley movement. The calibration accuracy of the apparatus was periodically checked using a stop watch, both with and without a subject on the scanner trolley. Total scan time was 200 seconds which was sufficient to obtain 4,000-5,000 detector counts per μCi of inhaled radioactivity. Only some 50 seconds of this period were spent actually scanning the lungs, in which time only a small degree of clearance would be likely to occur. From a series of such profiles a lung clearance curve for each subject was derived, by a method described below, each point on the curve being derived from one

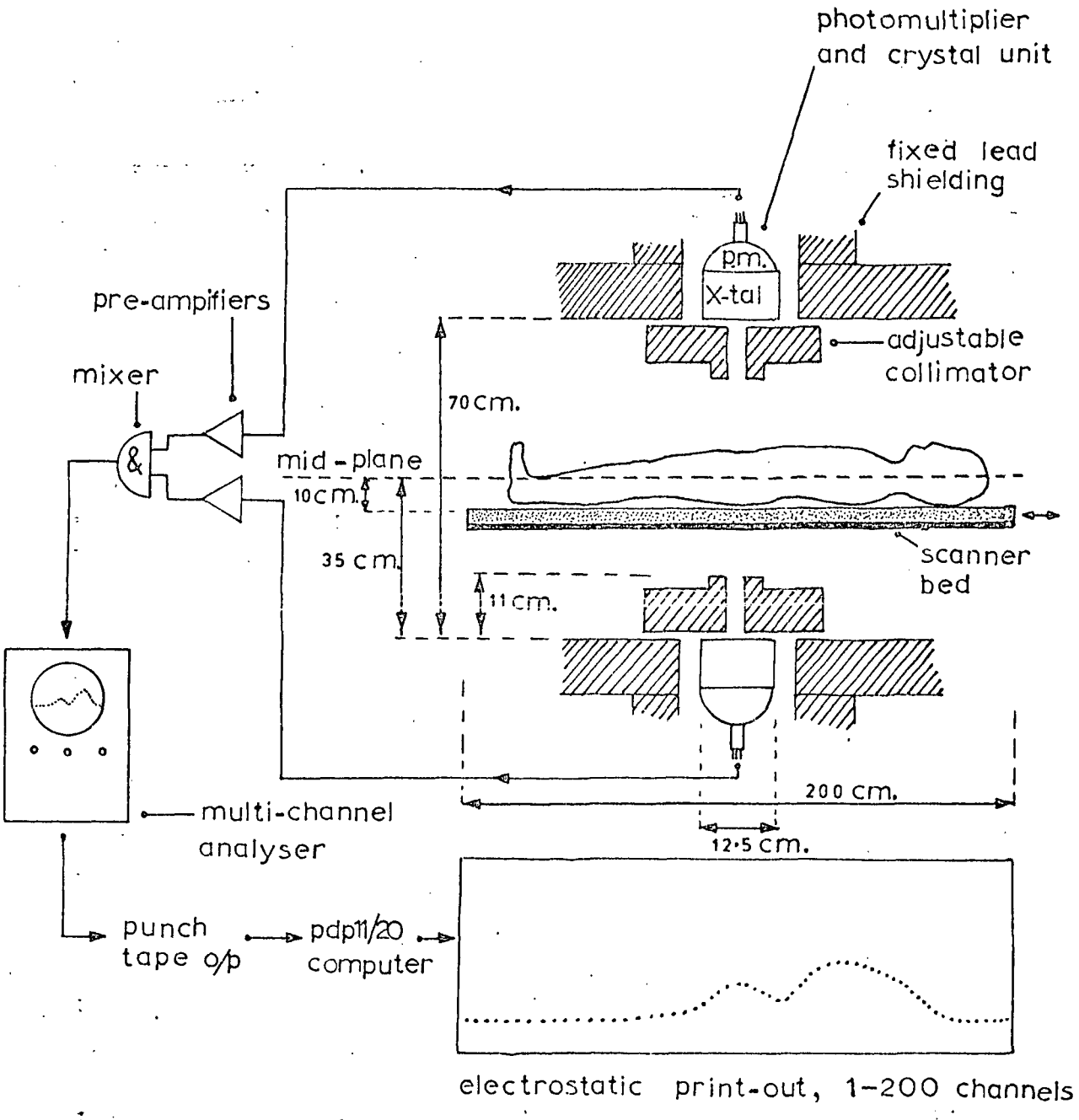

Figure 3.3.2: Profile scanner.

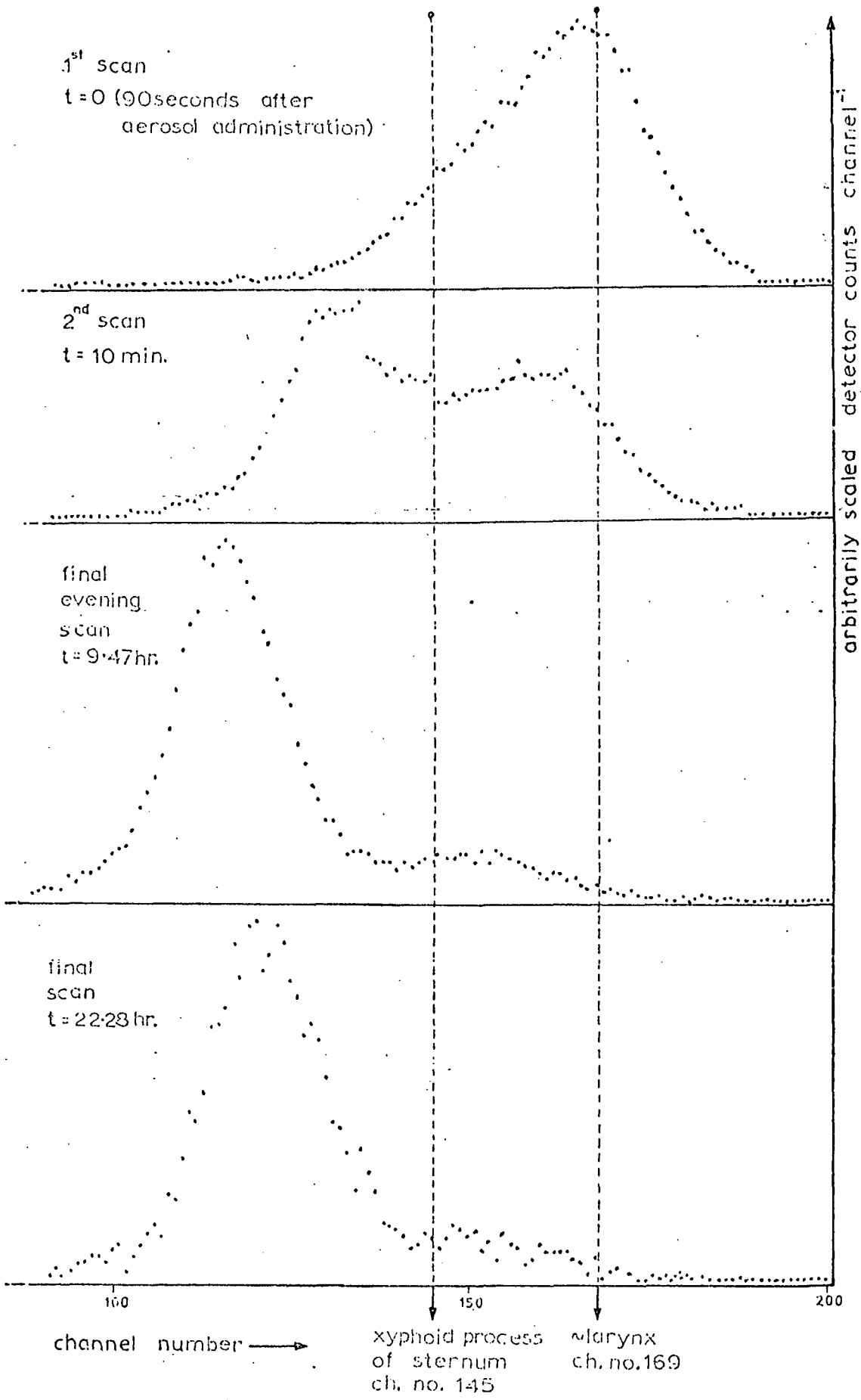

Figure 3.3.3: Example of profile scans obtained at various times (t). Subject PT1, $\bar{d}$ = 10·21 μm.

profile scan. From the magnitude of lung retention averaged over the three final scans, normally performed 20-22 hours after aerosol administration, values for $f_{c(c+R)}$, $f_{R(c+R)}$, were derived (equations 3.3.(8-10)). Owing to the large number of scan profiles obtained for each subject, which varied from 20-50, corrections for background radiation and isotope decay were performed on each profile by means of a PDP 11/20 computer (Digital Equipment Corporation). The unprocessed profile scan data were first stored on punched tape and then transferred to a magnetic storage disc. Figures for background radiation and time of scan were fed into the computer via a teletype and a computer program (HANNAN, 1978) applied the necessary corrections to each data point of the profile, printing the corrected version on an electrostatic printer. The figure for background radiation, normally between 1,500-2,500 detector counts, was derived from the average of five or more scans performed during the clearance period without a subject on the trolley. The coefficient of variation in background detector counts was always within $\pm$ 5% of the average value during the scanning period. Relevant aspects of radiation counting statistics are discussed in 3.3(ii)d.

As the lung clearance measurements were performed in a hospital department where radioisotopes were in frequent use, care was taken to ensure that the subject was not contaminated by this environment, as far as possible. The subject was instructed to wear shoes when it was necessary to venture into the hospital corridor and to remove them before a scan. Scanning of the experimental operatives who had been in the hospital for several hours confirmed that there was normally no pick-up from airborne radioactive contamination detectable above normal background radiation. Before use it was necessary to set an 'energy-window' on the multi-channel analyser such that only those scintillation photons that had arisen mainly as a result of photoelectric absorption of Tc^{99m} γ-photons (photopeak energy = 140 KeV) in the scintillator crystal were included in the data output. This ensured greater overall accuracy by preferential exclusion of background radiation, at slight cost in terms of sensitivity due to exclusion of scintillation photons that had arisen mainly as a result of Compton

interactions within the scintillation crystal or subject.

As was described above, a compromise is needed between detector resolution and sensitivity such that as large a portion of the lungs is measured with a minimal contribution from swalled radioactivity. In this, it is essential to have some means of knowing the contribution of the cleared radioactivity and its distribution within the abdomen at various times after aerosol administration, for a given detector resolution. Such knowledge cannot be obtained by calculation alone but must be determined empirically. In order to determine the optimum collimator slit-width, profile scans were performed using two volunteer subjects who had been intravenously injected with Tc^{99m} labelled human serum albumen microspheres. These subsequently became trapped in the pulmonary fine-capillary structure and their distribution on the whole body profile was compared to that of Tc^{99m} labelled polystyrene particles taken orally (i.e. swallowed). Slit widths from 2 to 20 centimetres were tried. At a slit-width of 2 centimetres the advantage in terms of lung/abdominal overlap appeared minimal in comparison with the results obtained at a slit-width of 5 centimetres, when detector sensitivity was some six times greater. Lung/abdominal profiles were barely distinguishable above a collimater width of 8 centimetres, but appeared satisfactory for both subjects at 5 centimetres (Figure 3.3.4(i) and (ii)). At an isotopic photopeak energy of 140 KeV the mid-planar resolution, defined as the width of a profile peak at half its maximum height obtained by scanning a point source at the mid-line of the mid-plane, is approximately three times the slit width (TOTHILL, 1974). For a slit width of 5 centimetres this implies that for radioactivity placed at the boundary of an organ, its contribution to detector counts will not fall below half its peak value until the detectors have moved approximately 7·5 centimetres off a vertical line above the boundary.

This contribution will fall to zero at a distance,

$$do = q\left[\frac{d}{a} - 1\right] \quad \text{.....equation 3.3.11}$$

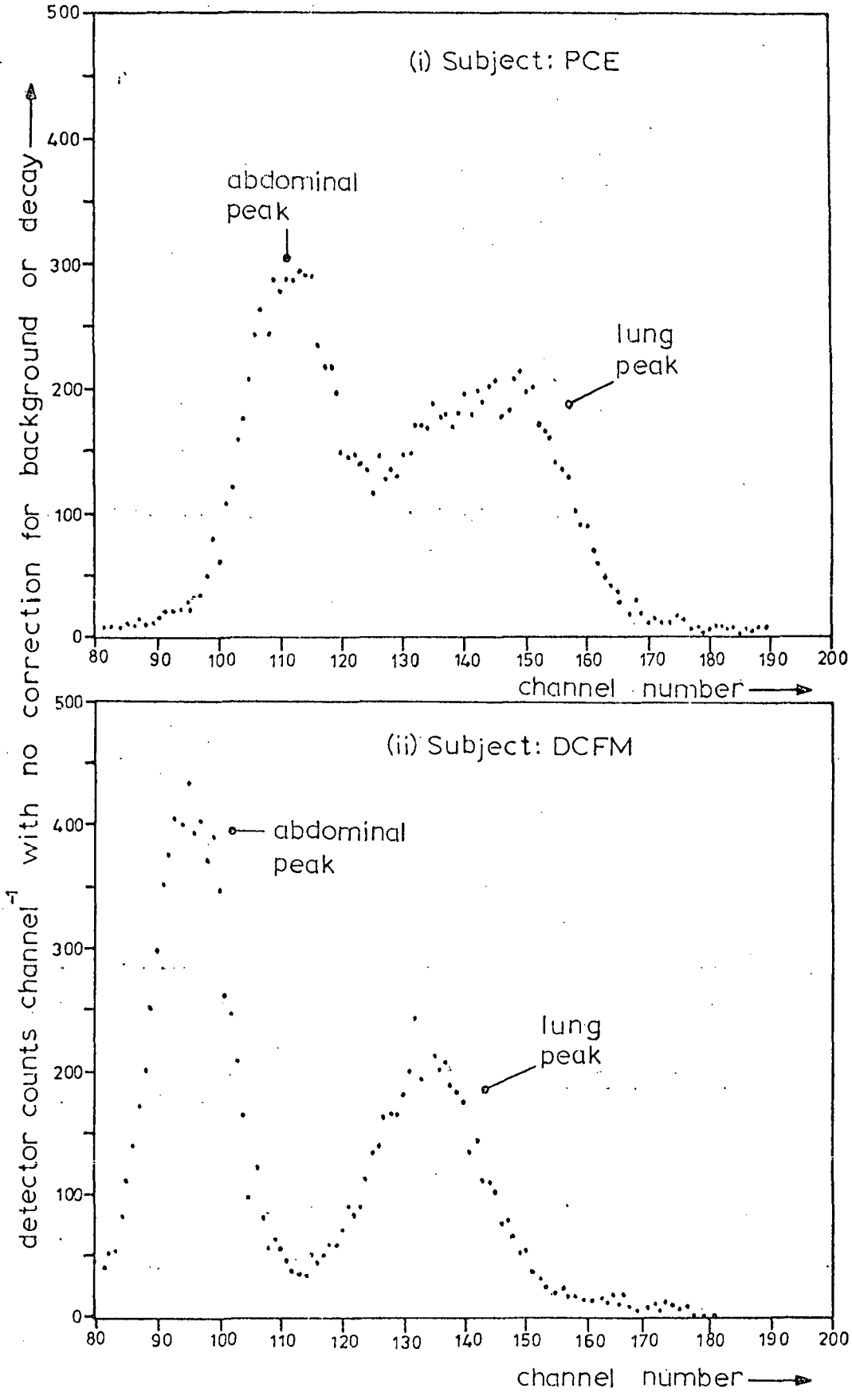

Figure 3.3.4: Slit width optimisation - results for two subjects at 5cm. collimator slit width.

Also, the full width half maximum resolution, R, could be approximated by,

$$R = do + q \quad \text{..... equation 3.3.12}$$

where, q = collimator slit width (5 centimetres)

d = distance from the crystal to mid-plane

a = collimator length (11 centimetres)

do = distance in a horizontal plane from the slit edge to the point at which the contribution of a point source at the mid-line of the mid-plane is zero.

At the mid-plane (d = 35 centimetres), this gives a value do = 10·9 centimetres. Consequently, even if all swallowed radioactivity remained at the nearest point to the lungs, i.e. in the stomach, the portion of the lungs scanned by the region of maximum detector response could still be between about one half to two thirds of the total and yet still exclude the abdominal contribution. Variation in spatial response in a vertical plane parallel to the collimator slits is discussed in 3.3(ii)d. The relatively small degree of lung/abdominal overlap on the scan profiles at a slit width of 5 centimetres shown in Figure 3.3.4, is consistent with these predictions. Collimator slit-width was set at 5 centimetres for all measurements.

Figure 3.3.5(i) shows the characteristic shape of a scan profile obtained as soon as possible after aerosol administration, normally within 1-2 minutes. The channel number of the small 'hump' on the otherwise smooth larger peak always corresponded, to within approximately 2 centimetres, to the position of the subject's larynx relative to the scanner trolley. After completion of the first scan, the subject was asked to gargle and swallow several times with drinking water. Following this procedure the second profile scan, normally performed within 8-10 minutes after the first, had the characteristic shape shown in Figure 3.3.5(ii). The laryngeal 'hump' transfers to the abdominal region, with no selective deposit remaining in the laryngeal region discernible on the scan profile. This indicated that the period of time between the first and second scans was sufficient for material deposited in the laryngeal region to have been cleared, by whatever means, and passed

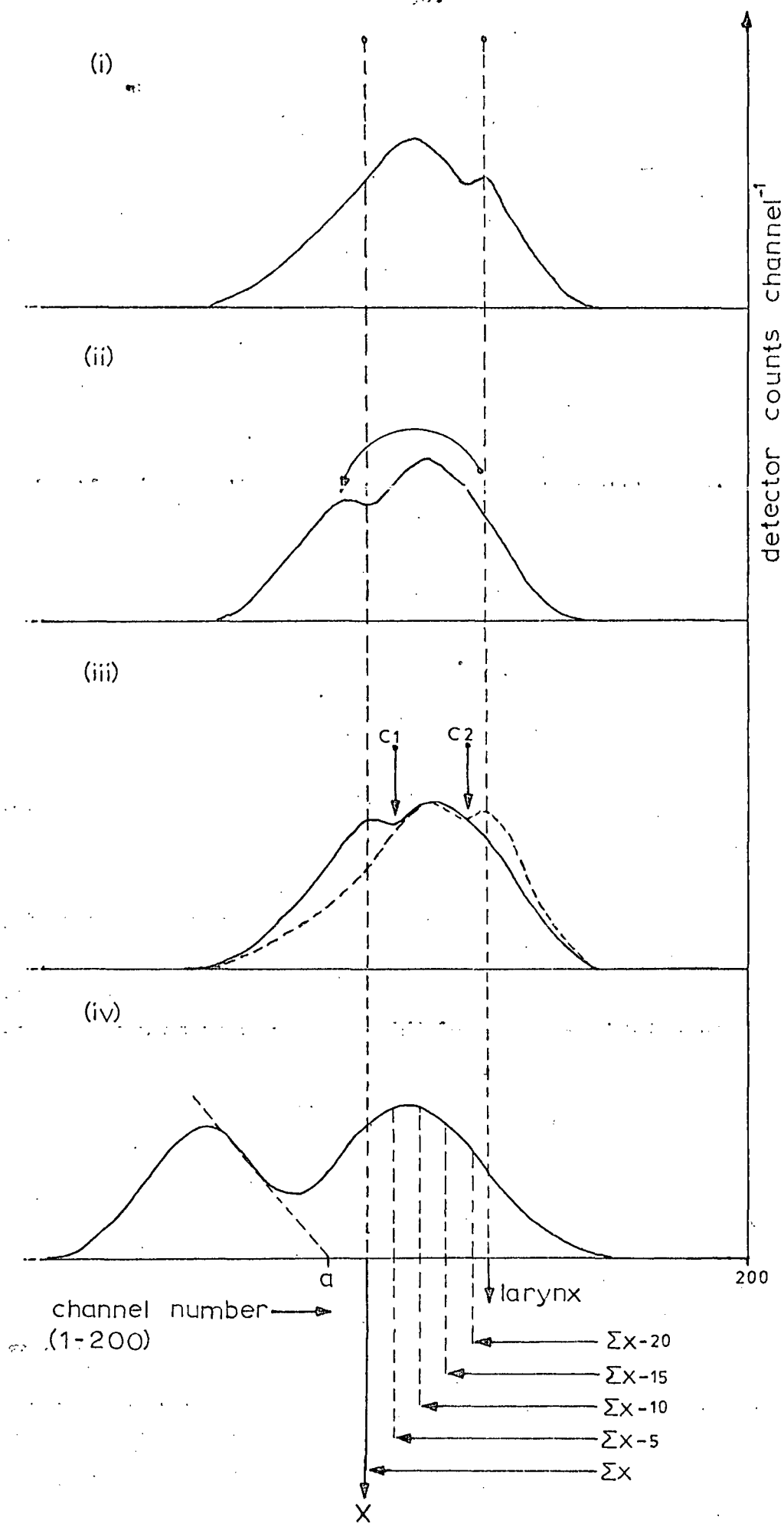

Figure 3.3.5: Profile scan analysis.

down the oesophagus.

The magnitude of the laryngeal 'hump' was obtained by subtracting the channel counts of the second profile summed over channels (0 - C1) from the corresponding ones of the first, where C1 was a standard reference point obtained by superimposing the two profiles and determining the point at which they converged (Figure 3.3.5(iii)). There were actually two points of convergence, C1 and C2. Summation and subsequent profile subtraction could therefore have been made either over channels (C2 - 200) or (0 - C1). In practice it was normally found to make no difference on which side the subtraction was executed, indicating an insignificant change in count rate, or sensitivity, due to the changed spatial distribution of the radioactive particles.

In obtaining the laryngeal/pharyngeal deposit, fs(I), by such means, an element of cleared upper-tracheal deposit below the larynx was included. Estimation of this deposit by, for example, planimetric analysis of the first scan profile,would not overcome this difficulty as it could not be assumed that some of the 'hump' was not due to selective tracheal losses immediately below the larynx. Assuming a tracheal ciliary transport rate of one centimetre per minute (GOODMAN et al., 1978), the approximate maximum boundaries of the region thought to be included by adoption of this method may be as shown in Figure 3.3.6. In practice it is unlikely that the material included extended this far below the larynx owing to the additional clearance delay introduced by the larynx itself. While it is technically possible to estimate the laryngeal/pharyngeal initial deposit by means of fixed radiation detectors (LIPPMANN and ALBERT, 1969), the profile scanner has the clear advantage that it may be confirmed directly from the scan profile whether or not a significant amount of radioactivity has been swallowed before the first measurement. However, it should be appreciated that any differences between the estimates for 'throat losses' of different research groups may be due not only to differences in technique, but also to differences in the definition of this fraction.

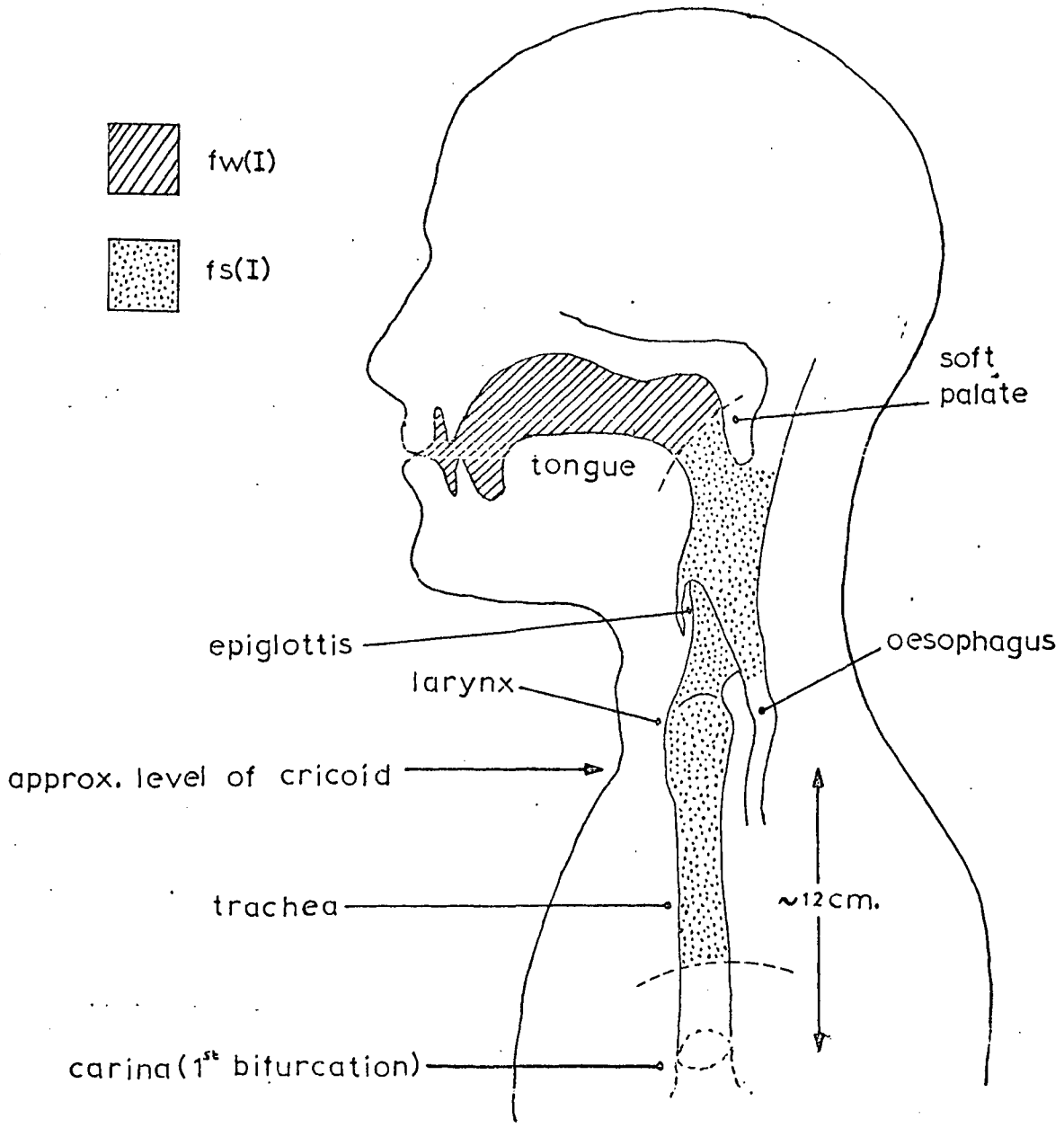

Figure 3.3.6: Regional deposition fractions fw(I), fs(I)
-approximate maximum boundaries of inclusion.

The initial value of the lung deposit from below or just below the larynx, was derived from the second scan profile performed 9-10 minutes after the end of aerosol administration. There may have been a finite fraction of tracheal deposit cleared in this period, most of which would be included in the fraction, fs(I). This magnitude may be estimated from the lung clearance curves averaged over three subjects at each particle size(Figures 4.3.1-4, Chapter 4). In the particle size range studied (4·5 - 13·0 μm diameter), this magnitude was between 2-4% of the initial deposit over the first ten minutes of clearance after aerosol administration, the largest particle size exhibiting the most rapid clearance as might be expected. In terms of the amount of aerosol inhaled by a subject these magnitudes reduce to, (fc(I) + fs(I)) x (2-4%) which gives values in the range 1·5-2·0% in the particle size range studied. In addition to the two profile scans performed 1-2 and 9-12 minutes after aerosol administration, between these times, approximately 4-5 minutes after aerosol administration, measurements of tracheal radioactivity immediately below the larynx were conducted using a fixed radiation detector system. A second such measurement was made immediately following the second profile scan, about 11-14 minutes after aerosol administration. These measurements were actually initiated for a quite different purpose, explained below, and not all subjects were measured. Details of the method are given in 3.3(iii). By estimating the area of the tracheal clearance curve bounded by these times, the magnitude of the deposit which had passed through the trachea in that interval could be estimated in relation to the magnitude of the deposit subsequently cleared through the trachea, i.e. to fc(I). These estimates confirmed those obtained from the averaged profile scan clearance curves, giving average values at each particle size in the range 0·3-1·6% for the deposit cleared between the first and second tracheal measurements, expressed as a percentage of the amount of aerosol inhaled by the subject (Table 3.3.1). These percentages amounted to only a small fraction of fs(I) at any particle size (see Chapter 4). It is not possible to reach conclusions as to the proportions of aerosol which initially deposited in the pharynx or larynx separately, owing to

$\bar{d}$ µm	subject	% of I	average % of I
13·04	A D	1·9	1·52
	J H	1·1	
4·49	ATM	0·4	0·31
	F H	0·1	
	R H	0·5	
10·45	P T 2	1·0	0·85
	K D	0·7	
4·61	MS 1	0·2	0·44
	MS 2	0·6	
	J V	0·5	

Table 3.3.1 : Estimation of amount cleared between first two throat meas. Particle size range 4·5 – 13 µm.

uncertainty concerning the amount of clearance from the larynx before the first, fixed detector, throat clearance measurement. However, it may be observed that owing to the small proportion of radioactive particles estimated to have been cleared in the first 9-12 minutes after the end of aerosol administration, the striking differences between these results and those reported by ALBERT et al. (1967); LIPPMANN and ALBERT (1969); ALBERT and LIPPMANN (1973), cannot be explained in terms of differences in the definition of deposition and clearance fractions. Differences in technique must therefore be considered. This is discussed further in Chapter 4.

Figure 3.3.3 shows scan profiles for one subject at successively greater times after aerosol administration. The regions containing cleared and retained radioactivity are readily discernible on the later scan profiles.

Planimetric analysis of the scan profiles (CAMNER, 1971) was rejected on the grounds that assumptions would be required concerning the shape of the purely abdominal or lung profiles in the region of overlap. Instead, the lung contribution was obtained by summation of all counts to the right of an anatomical reference point, marked 'X' on Figure 3.3.5, a certain number of channels beyond which it was considered that the abdominal contribution would be negligible. Before each experiment the subject's chest was marked close to the xyphoid process of the sternum bone, such that the position of the mark relative to the scanner trolley, and hence to the scan profile, could be conveniently determined. Five separate clearance curves were initially derived from the whole series of scan profiles for each subject: Σx, Σx-5, Σx-10, Σx-15, Σx-20; each of which, except for Σx, were derived by summation of five fewer channels than the preceding clearance curve (Figure 3.3.5(iv)). The same section of the lung profile would therefore be included in the determination of each point on the curves, provided the anatomic reference point had been accurately measured. It should be noted that by adopting this method of analysis, the derived levels of retention may well exceed unity for certain periods as material is cleared upwards into the selected summation region of the profile scan prior to removal into the

abdominal region. The effect is likely to be most pronounced over the smallest summation sections (e.g. Σx-20, Figure 3.3.7).

As might be expected the clearance curve based on the highest number of detector counts, i.e. Σx, exhibited the least scatter of points, and that based on the smallest, i.e. Σx-20, exhibited the largest. An example is shown in Figure 3.3.7. However, the scatter was greater than anticipated on a purely statistical basis, discussed in 3.3(ii)d. Moreover it appeared not to be entirely random but often formed distinct peaks along the curves when several successive points were close, which became more pronounced on those derived on scan profile sections at successively greater distances from the reference point, 'X', implying an association with the upper reaches of the lungs, towards the trachea. The possible origin of this phenomenon is discussed below and in Chapter 4. This scatter reduced considerably for the final profile scans, 20-22 hours after aerosol administration, although by this time purely statistical scatter was more important. A small range of values for $f_{C(C+R)}$, $f_{R(C+R)}$, was therefore possible and it was considered necessary to adopt a standard criterion for the selection of the summation section to be employed in the derivation of these values, in each case. As the position of the abdominal peak on the scan profile was of most importance in determining the degree of lung/abdominal overlap, the criterion adopted was derived by projecting the right-hand side of the abdominal peak, which was in all cases discernible, to the channel number scale baseline at 'a', Figure 3.3.5(iv). In the event of a small quantity of abdominal radioactivity residing at 'a', in the subject, it would be approximately ten channels further along the profile before its contribution to detector counts fell to nought. The summation point was therefore selected as that which was greater than ten channels from 'a'. This was normally either Σx-5 or Σx-10, and in a few cases, Σx-15. The proportion of total initial lung counts included in the derivation of the selected clearance curves averaged 52 $\pm$ 24% (mean $\pm$ standard deviation).

A comparison between the methods used to obtain the lung clearance curve from the scan profiles was made in one subject (Figure 3.3.8(i)). One clearance curve was derived using a

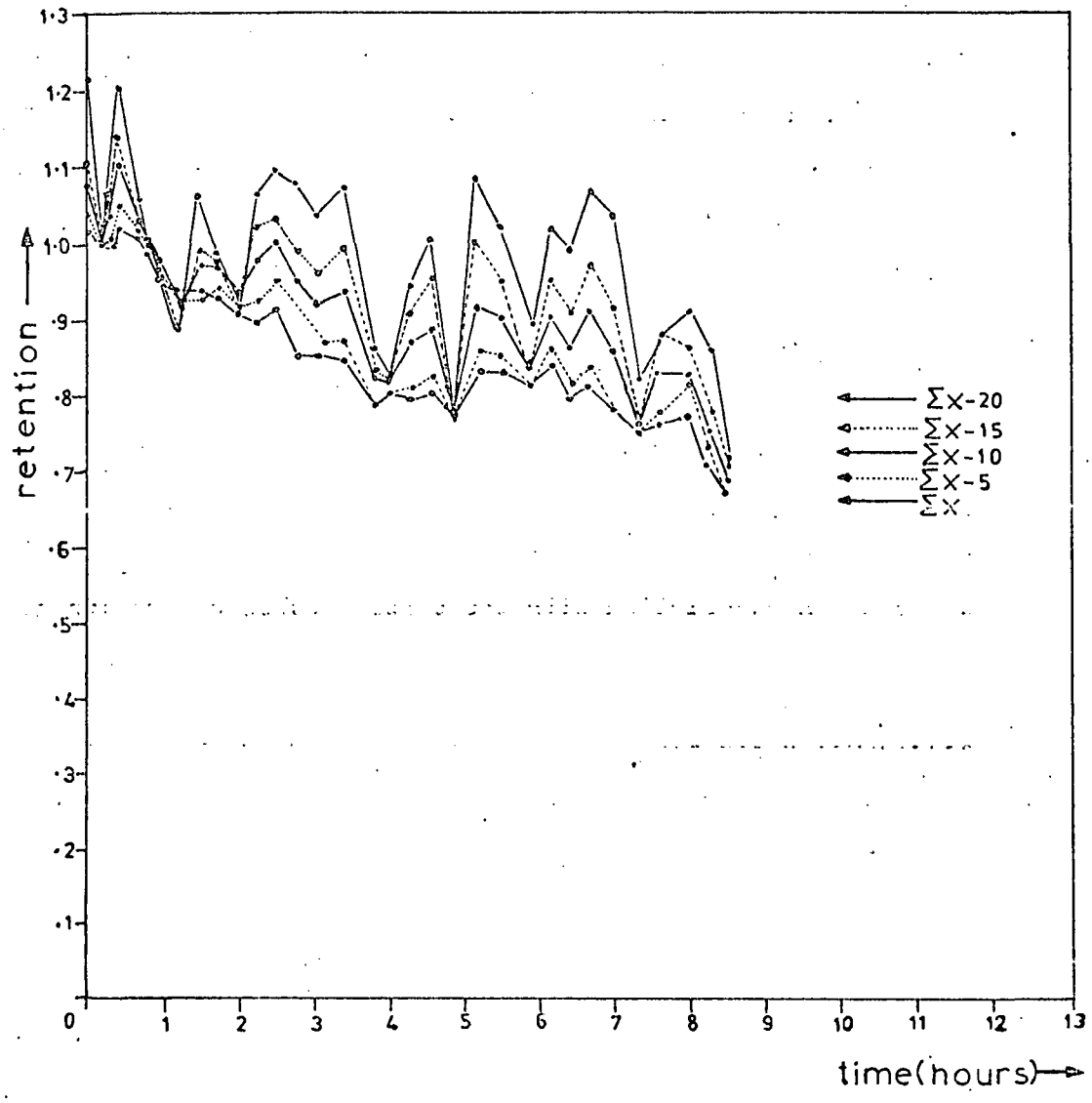

Figure 3.3.7: Example of family of clearance curves obtained for one subject (AM), $\bar{d} = 4.67\,\mu m$.

planimetric method based essentially on the assumption of symmetry between the right and left halves of the abdominal and lung sections of the scan profiles. The other clearance curve was derived from the same profiles using the summation method described above. As shown in the figure the scatter of points is far less for the curve derived by the planimetric method and is similar to those reported by CAMNER (1971). A larger scatter of points was observed whenever the summation method was employed. Individual and group average clearance curves are presented in Chapter 4, part 3.

It was considered that the clearance pulses may have arisen as a result of an experimental artefact, although none was known that could satisfactorily explain such non-random behaviour. To investigate the possibility that the phenomenon was due to genuine variations in the radioactive content of the lung section being scanned, for one subject, a single fixed radiation detector was placed vertically over the throat at regular intervals during the clearance period. The detector consisted of a scintillation crystal (Nuclear Enterprises Ltd.), optically coupled to a photomultiplier tube and was mounted in a cylindrical brass collimator (bore = 6·5 centimetres) at a depth of 8 centimetres. The photomultiplier output was fed into a counter-ratemeter and single channel analyser (J and P Engineering Ltd., type MS310) and the number of detector counts obtained over a two-minute counting period was recorded manually. Figure 3.3.8(ii) shows the result obtained after application of the appropriate corrections for radiation background and isotope decay. The reasonable degree of temporal matching between the scanning and fixed detector clearance pulses indicates that the clearance pulses were indeed associated with the distribution of radioactivity in the subject. The phenomenon was further investigated in other subjects and more refined methods of measuring the clearance of radioactive particles in the throat were developed. These are described in 3.3(iii).

(d) Limitations of profile scanning

The use of a profile scanner in the estimation of the deposition and retention of radioactive particles in the respiratory tract has been described above, but not its

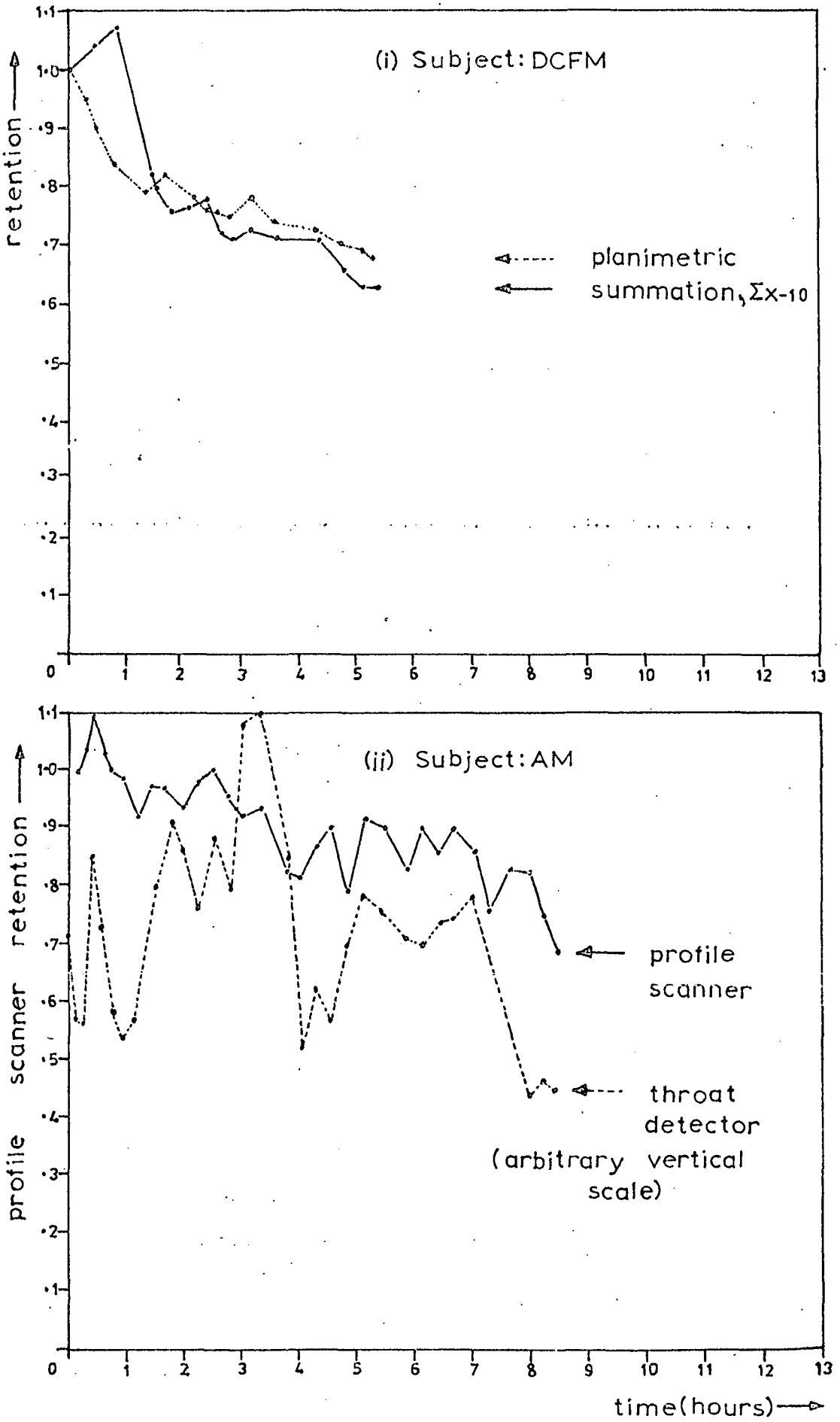

Figure 3.3.8: Comparison of methods of profile analysis (i) and observation of clearance fluctuations (ii).

limitations. These are difficult to quantify and involve complex considerations.

An important limitation was that the spatial response of the scanner was not entirely uniform but varied in a complicated way according to the photopeak energy of isotope used, the mode of combining detector counts from each detector output, and the degree of variation in tissue scatter from point to point (TOTHILL and GALT, 1971). Spatial response was measured using a hardboard phantom of approximately unit density, to simulate tissue scatter. A Tc^{99m} point source was placed at various points within the phantom and a profile scan was performed for each source position, the settings being the same as they would for a profile scan of an actual subject. The total detector counts for each scan were corrected for background and isotope decay and expressed as percentages of the counts obtained after scanning the point source at the mid-line of the mid-plane between the detectors (Figure 3.3.9). Point to point variations of nearly 70% were observed. However it should be appreciated that such variations would only be of any consequence when the initial spatial distribution of radioactivity differed significantly from that of the final. The fraction of initial radioactive lung burden which was retained in the lungs would be measured with the same overall sensitivity throughout all profile scans, other factors being equal, if the spatial distribution was constant throughout. This would not be the case with the total lung burden as it would include that fraction to be later cleared from the lungs, which would be unlikely to have the same spatial distribution as the retained fraction at any time. Quantification of the overall effect presents great difficulties owing to the variety of unknown anatomic and particle distribution factors. It should be borne in mind that it is the initial distribution of deposited particles in the lungs that is important, not their distribution during the clearance process which has no bearing on final point determination. If the particles were initially deposited in the small airways (< 2mm diameter), their spatial distribution might be expected to closely resemble that of the fraction later retained in the lungs, which would reside wholly or mainly in the non-ciliated respiratory zone

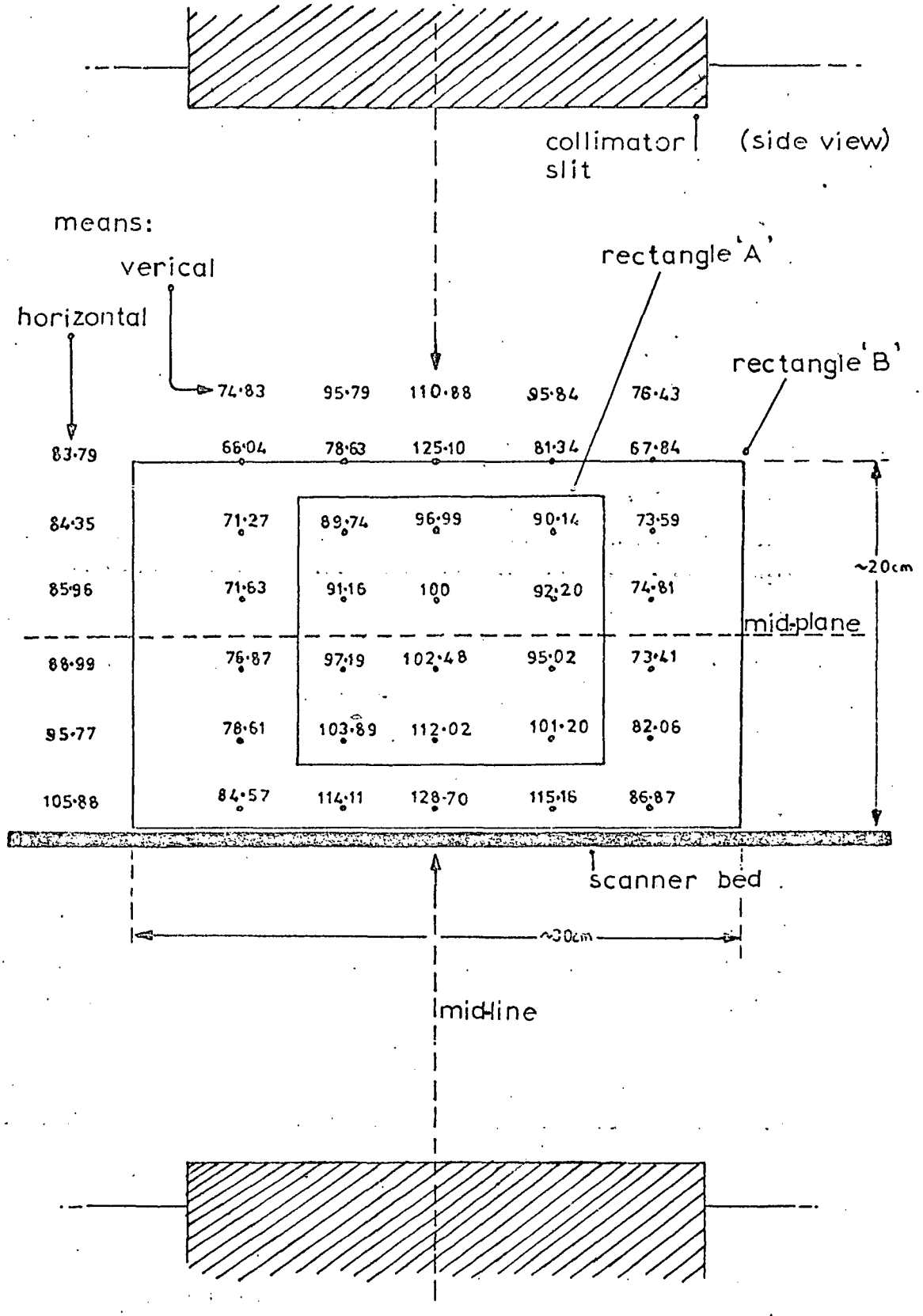

Figure 3.3.9: Spatial response of profile scanner.

of the lungs. It is therefore likely that the effect was most important at large particle sizes, where penetration to both the small airways and respiratory zone is small. In this case the initial particle distribution of the fraction to be later cleared from the lungs would tend to be more centralised than that of the retained fraction, which would therefore tend to be more peripheral. The overall effect may be quantified in a crude worst-case manner by assuming that the fraction to be later cleared has an initial uniform distribution entirely enclosed within the rectangle A, Figure 3.3.9, while that of the retained fraction is uniformly distributed in the remaining area, B. Taking the average of all percentage values in each area gives 86·15% and 97·67%, for areas B and A, respectively. The radioactivity in area A is therefore 'overestimated' by approximately 13% relative to that in area B, which is considerably less than the maximum point to point variation. In practice it is probable that even at large particle sizes there is a finite degree of overlap between the initial distribution of retained and, later, cleared fractions, hence the overestimate of the latter compared to the former would be lower than 13%. It should be noted that this figure is a percentage of the cleared deposition fraction, not of the amount of inhaled aerosol, I.

Using the profile scanner it was uniquely possible to obtain direct evidence of the magnitude of the combined effects of variations in detector spatial response and tissue attenuation, not over the thoracic cage alone, but over the whole body. This was accomplished by plotting the total detector counts over the whole of each profile scan, corrected for radiation background and isotope decay, over the whole series of scans obtained for each subject. Fixed radiation detectors which measure a selected part of the body cannot readily be used for this purpose. Variations in the measuring sensitivity of the cleared fraction due to its movement from the chest to the abdomen might be expected to be comparable if not actually greater than those arising from differences in the spatial distribution of radioactivity within the thoracic cage, owing to its initial concentration into the regions bounded by the stomach and small intestines. The results for all subjects are shown in

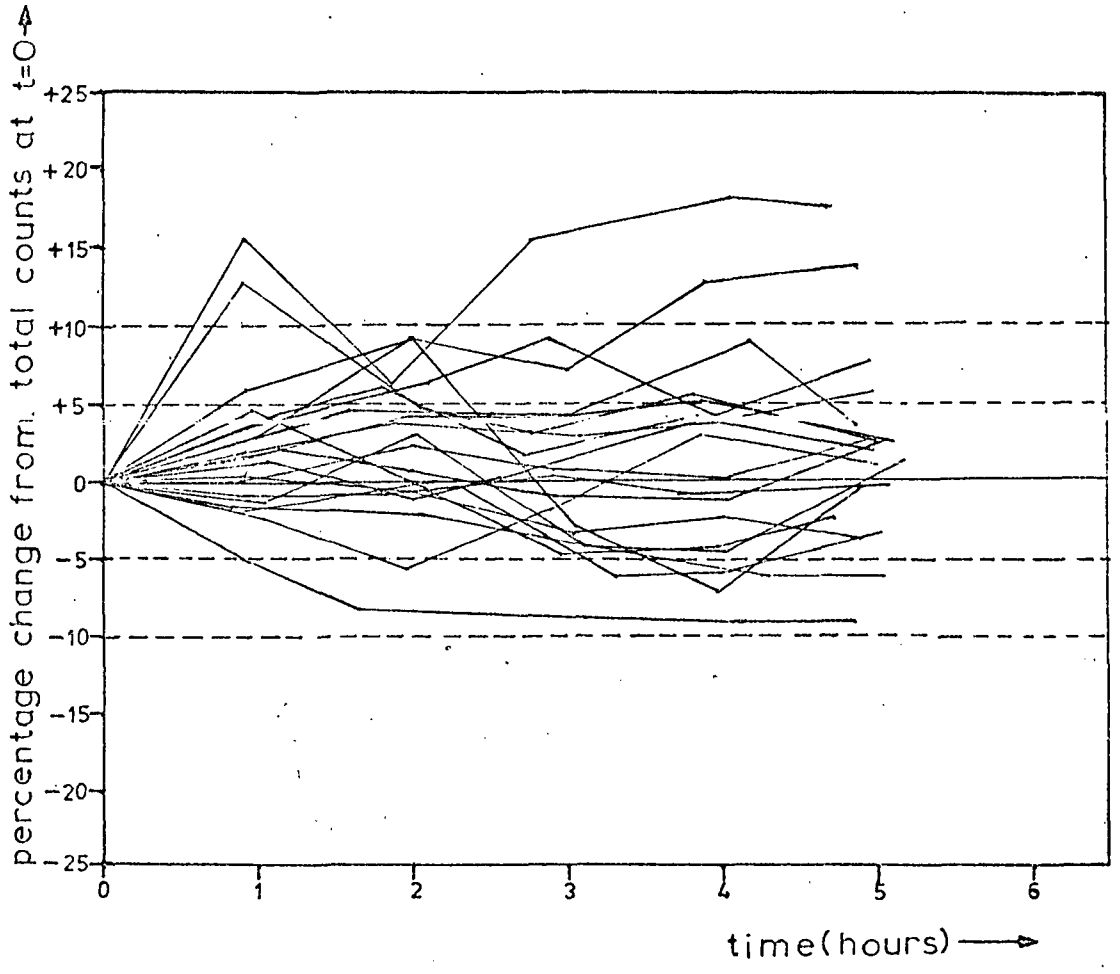

Figure 3.3.10: Variation in total count rate over first five hours for all subjects.

Figure 3.3.10. It has been assumed that no faecal clearance of radioactivity occurred during the first five hours after aerosol administration. The percentage variation in total detector counts was shown to normally be within 5%, rarely exceeding 10%, of the initial value, indicating that the percentage error in the estimation of the clearance and retention fraction, fc (c+R), fR(c+R), would be comparably small, and still smaller in terms of the amount of aerosol inhaled by a subject, I.

It should be noted that some of the variation shown in Figure 3.3.10 would undoubtedly have arisen as a result of errors in the positioning of the subject on the scanner trolley. As far as possible the subject was always centralised on the same horizontal line relative to the detectors, but subject movement during a scan (duration = 200 seconds) could never be entirely eliminated. Intrinsic variation and drift in the detectors and associated electronics could be accurately monitored by scanning several standard radioactive samples throughout the measuring period, under conditions of constant geometry. Detector drift rarely exceeded 5% of the initial value from first to final scan, which was approximately double the typical percentage variation from scan to scan. Further details are given below. The results shown in Figure 3.3.10 therefore indicate that the variation in detector spatial response and tissue attenuation were not serious limiting factors in the accuracy of the determination of the retention, clearance and deposition fractions, using the profile scanner. This, coupled with the considerable advantages of profile scanning over fixed detector methods, makes the method the most appropriate for lung clearance studies.

Radioactive decay is a random process and there is therefore a degree of uncertainty in the accuracy of any measured value that is dependent on the number of recorded detector counts per unit time, the number of repeat measurements, and whether or not the final value has been obtained from measurement of additional quantities, e.g. background radiation, in which there is also a random variation.

The standard error or standard deviation, σ , of individual values about their mean may be estimated, by assuming a Poisson distribution, using,

$$\sigma_N = \sqrt{\bar{N}} \simeq \sqrt{N}, \text{ if } \sigma \text{ is small} \quad \ldots\ldots \text{ equation 3.3.13}$$

where, N = number of detector counts

$\bar{N}$ = average number of detector counts over an infinite series of measurements each of which were obtained over equal periods of time.

The standard error of the mean of m independent measurements is given by,

$$\sigma_{\bar{N}m} = \frac{\sigma_N}{\sqrt{m}} \quad \ldots\ldots\ldots \text{ equation 3.3.15}$$

where, $\bar{N}m$ is the average value of N over m measurements.

Expressed in terms of the relative standard error, $\nu_{\bar{N}}$, or coefficient of variation about the mean of m measurements this becomes,

$$\nu_{\bar{N}m} = 100\,\frac{\sigma_{\bar{N}m}}{\bar{N}m} = \frac{100}{\bar{N}m}\left(\frac{\bar{N}m}{m}\right)^{\frac{1}{2}}\% \quad \ldots\ldots\ldots\ldots \text{ equation 3.3.15}$$

The standard error, σ_{1-2} , of the sum or difference of two independent measurements is given by (TOPPING, 1965),

$$\sigma_{1-2} = (\sigma_1^2 + \sigma_2^2)^{\frac{1}{2}} \quad \ldots\ldots\ldots\ldots \text{ equation 3.3.16}$$

where, σ_1 , σ_2 , are the standard errors of each measurement.

Using equations 3.3.13 and 3.3.14 to determine $\sigma_{\overline{1-2}m}$, the standard error of the difference of two measurements over m independent observations, gives,

$$\sigma_{\overline{1-2}m} = \left(\frac{N_{\overline{1+2}m}}{m}\right)^{\frac{1}{2}} \quad \ldots\ldots\ldots\ldots \text{ equation 3.3.17}$$

and from equation 3.3.15,

$$\nu_{\overline{1-2}m} = \frac{100}{N_{\overline{1-2}m}}\left(\frac{N_{\overline{1+2}m}}{m}\right)^{\frac{1}{2}}\% \quad \ldots\ldots\ldots\ldots \text{ equation 3.3.18}$$

where, $N_{\overline{1+2}_m}$, $N_{\overline{1-2}_m}$ = the average sum or difference of detector counts over m independent measurements, each of which were obtained over equal periods of time.

Calculated from equation 3.3.18, values of $N_{\overline{1-2}_m}$ needed to be in the region of 3,500 detector counts, equivalent to approximately 0·78 μCi of whole body radioactivity at the time of the final scan, or about 12 μCi at the time of aerosol administration, to ensure that $V_{\overline{1-2}_m}$ was within ± 2% of the mean value that would be obtained from an infinite series of measurements, with a probability of 0·683 that the average value over 3 observations, (m = 3), would fall within this range, or a probability of 0·955 that it would fall within twice this range. These were considered to be the acceptable levels of uncertainty. In some cases $V_{\overline{1-2}_m}$ exceeded 2%, the highest value being 3·01%, the average being 1·81%, owing to a certain degree of unpredictability in the aerosol delivery efficiency of the aerosol administration apparatus and in the value of total deposition, $f_D(I)$, for any subject.

(e) Use of profile scanner in the measurement of radioactive samples and detection of in vivo leaching

All radioactive samples were positioned at a standard vertical and horizontal position relative to the scanner detectors, for radioassay. The aerosol collection bags (see 3.2(iii)), were folded into almost flat, geometrically identical, cardboard envelopes, such that the entire sample was scanned at a constant height.

Radioactive attenuation through the walls of each sample container was small, estimated to be less than 6% and in any case approximately equal for each sample. For samples containing liquids (mouthwash), a calibration factor was derived in a separate experiment involving reference sources. Three independent measurements of each sample were taken and one sample, the inspiratory collection bag, was scanned repeatedly throughout the measuring period (20-22 hours) as a check on the stability of the profile scanner electronics. The drift in the latter only occasionally exceeded 5% from first to final scan, which was approximately double the typical percentage

variation in sample counts, from scan to scan. A correction factor for amplifier drift was applied on the basis of the mean percentage change over three scans of the inspiratory collection bag, performed at the beginning and end of the period.

By means of a standard reference source of known absolute radioactivity, it was possible to calculate the radiation dose administered to the subject. Calculation of total deposition and its subdivisions did not depend on a knowledge of absolute radioactivity, because all samples were measured with the same counting efficiency, or detector sensitivity, and only relative counts for each needed to be determined.

The inaccuracy in the measurement of the radioactive samples due to random statistical variations in emitted radiation was negligibly small, because these were measured shortly after aerosol administration when only a small amount of radioactive decay had occurred. The exception to this was when the radioactivity of a sample was extremely small ($< \sim 2\%$) in relation to that of the aerosol inhaled by the subject, I. In this case although the coefficient of variation $\sqrt{}$, calculated from equation 3.3.18, might be relatively high ($> \sim 5\%$), it was still negligibly small in relation to I.

Profile scanning is of considerable advantage in the detection of possible *in vivo* leaching of radioactivity from labelled particles since if radioactivity is removed from one zone it inevitably appears in another. According to HARPER *et al.* (1966) the physiological behaviour of pertechnetate compounds is similar to that of iodine which is selectively concentrated in the thyroid and salivery glands and the stomach, transferal occurring via the bloodstream. With the exception of the stomach such concentrations would be readily discernible on the scan profiles if of at all significant magnitude. Moreover, any radioactive content in the bloodstream would be apparent as an excess of counts above background over those channels on the scan profile corresponding to the position of the subject's legs on the scanner trolley. Such concentrations or excesses of radioactivity were not observed for any subject. The possibility of urinary excretion of leached radioactivity was investigated in one subject (A R), by collecting the total

urinary output for eight hours after aerosol administration. The urinary sample was measured for possible radioactive content using the profile scanner, but the detector counts were found to be at the background level.

(iii) Observation of tracheal and laryngeal clearance

The origin of these observations was described in 3.3(ii)c. A single detector was used in the first instance in an attempt to observe ciliary clearance in the throat of one subject (Figure 3.3.8(ii)). However, this detector was insufficiently well collimated to guarantee effective exclusion of the uppermost section of lung, that nearest the first rib of the subject, which extends typically to a line approximately four centimetres above the manubrium sterni at the chest mid-line, as observed on chest radiographs. Consideration was given to the origin of the clearance pulses and the possibility that they arose as a consequence of a periodic accumulation and emptying of ciliary transport fluid within the larynx was investigated. A fixed, double, radiation detector apparatus was constructed: one detector was positioned over the subject's larynx (T_a); while the other was situated over a region just below the cricoid cartilage of the larynx (T_b), such that a short section of the trachea would be included in its field of view and the upper lung lobes would be wholly excluded (Figure 3.3.11(i) and (ii)). If the clearance pulses were arising as a consequence of a periodic accumulation and emptying of ciliary clearance fluid within the larynx in an otherwise 'smooth' clearance process, two distinct clearance curves would be obtained: one characteristic of the genuine variations in amounts of radioactivity entering the larynx; the other characteristic of some other process occurring within the larynx itself. If, on the other hand, the clearance pulses were reflected in genuine variations in the distribution of radioactive particles entering the larynx, the larynx itself playing only a minor modifying role, two similarly pulsatile clearance curves would be obtained which were out of phase by the time of ciliary transit between the two detectors. Figure 3.3.12 shows the first result (subject A D) using the double detectors, which is highly consistent with the latter view.

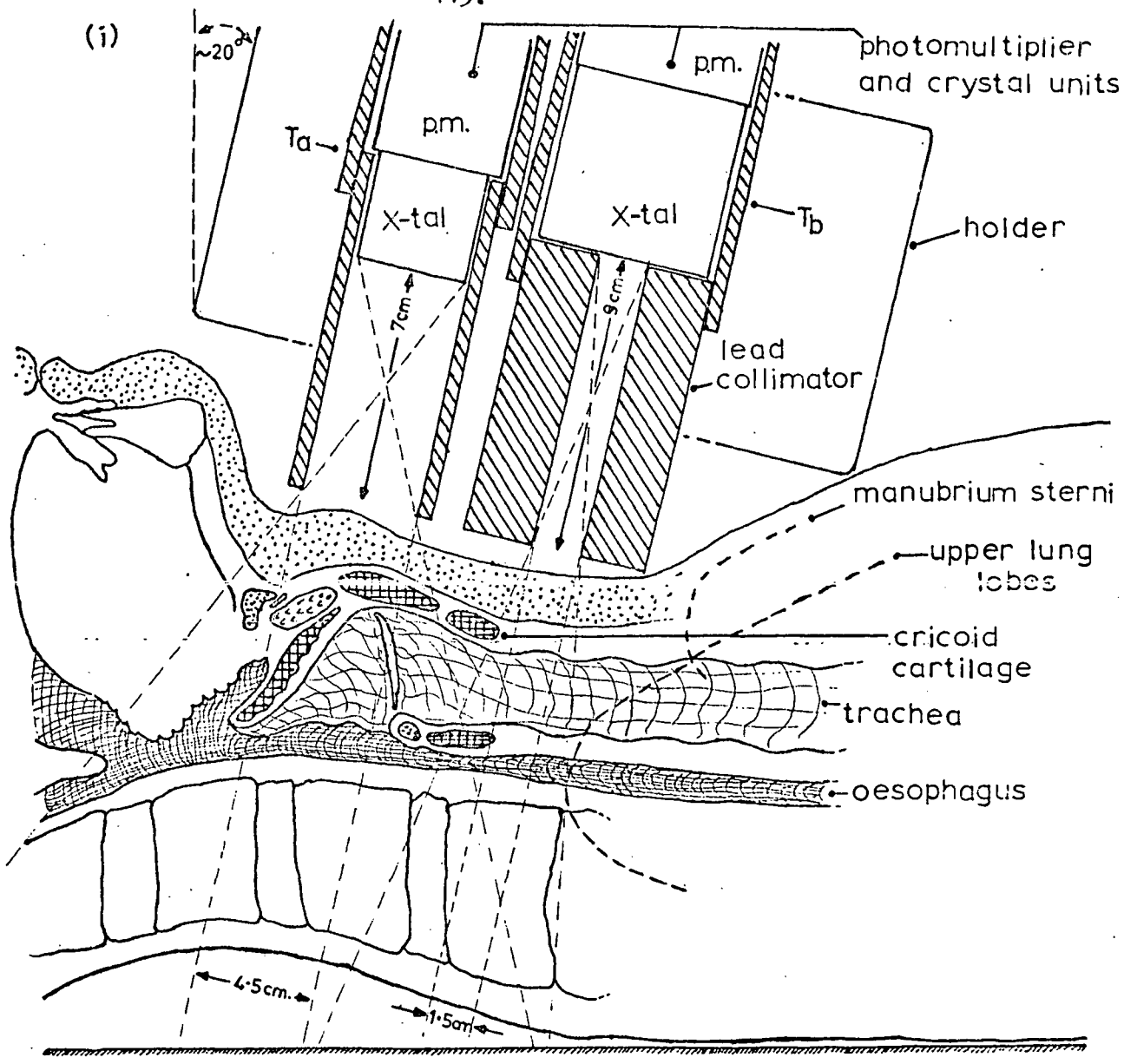

(ii)

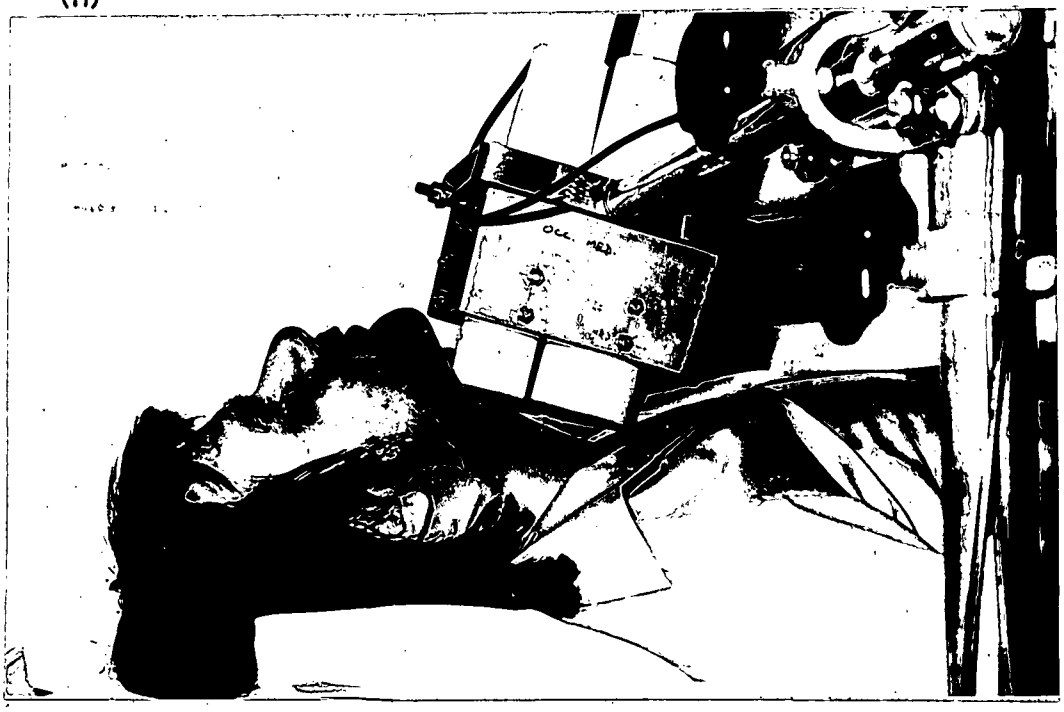

Figure 3.3.11: Throat clearance detectors.
Sectional view (i); Photograph of subject (ii).

The same detector configuration was used for all subjects studied subsequent to subject A D, Figure 3.3.12, and similar results were obtained in many cases (see Chapter 4). Owing to intersubject anatomical variations an apparatus designed for a supposedly average subject could never be completely effective in all cases. The collimator design and dimensions were selected following examination of a number of chest radiographs, both lateral and frontal (N.C.B., medical survey unit). From these, a typical value of four centimetres for the distance of vertical separation between the upper lung lobes and top of the manubrium sterni at the chest mid-line, was determined. This leaves very little room for the placing of a detector between the cricoid cartilage of the larynx and the uppermost part of the lungs. Advantage had therefore to be taken of the area of tissue between the right and left upper lung lobes, by placing a slit-collimated detector at a slight inclination ($\sim 20^{o}$) over this region, in order to detect tracheal clearance (Figure 3.3.13). Collimator design and positioning of the purely laryngeal detector was more straightforward (Figure 3.3.11(i)). In many cases, particularly at large particle sizes, the bulk of material was cleared within the first few hours after aerosol administration, as measured by the profile scanner. The tracheal and laryngeal detectors confirmed these rapid clearances and moreover their detector count rate was later observed to fall to the background level, thus confirming that there had been no inclusion of radioactivity in the upper lung lobes.

Inevitably, because such a small area of the respiratory tract was observed during any measurement, radiation counting statistics were often poor, particularly towards the end of the clearance period. The 95% confidence limits have been indicated on all throat clearance figures. It should also be noted that the clearance pulses cannot be explained in terms of passage of single or small groups of particles beneath the detectors. There were normally fewer than two detector counts per particle through the measuring period, which is distinct from and considerably lower than, the number of photon emissions per particle per unit time ($\leqslant 4$ per second), as estimated from:

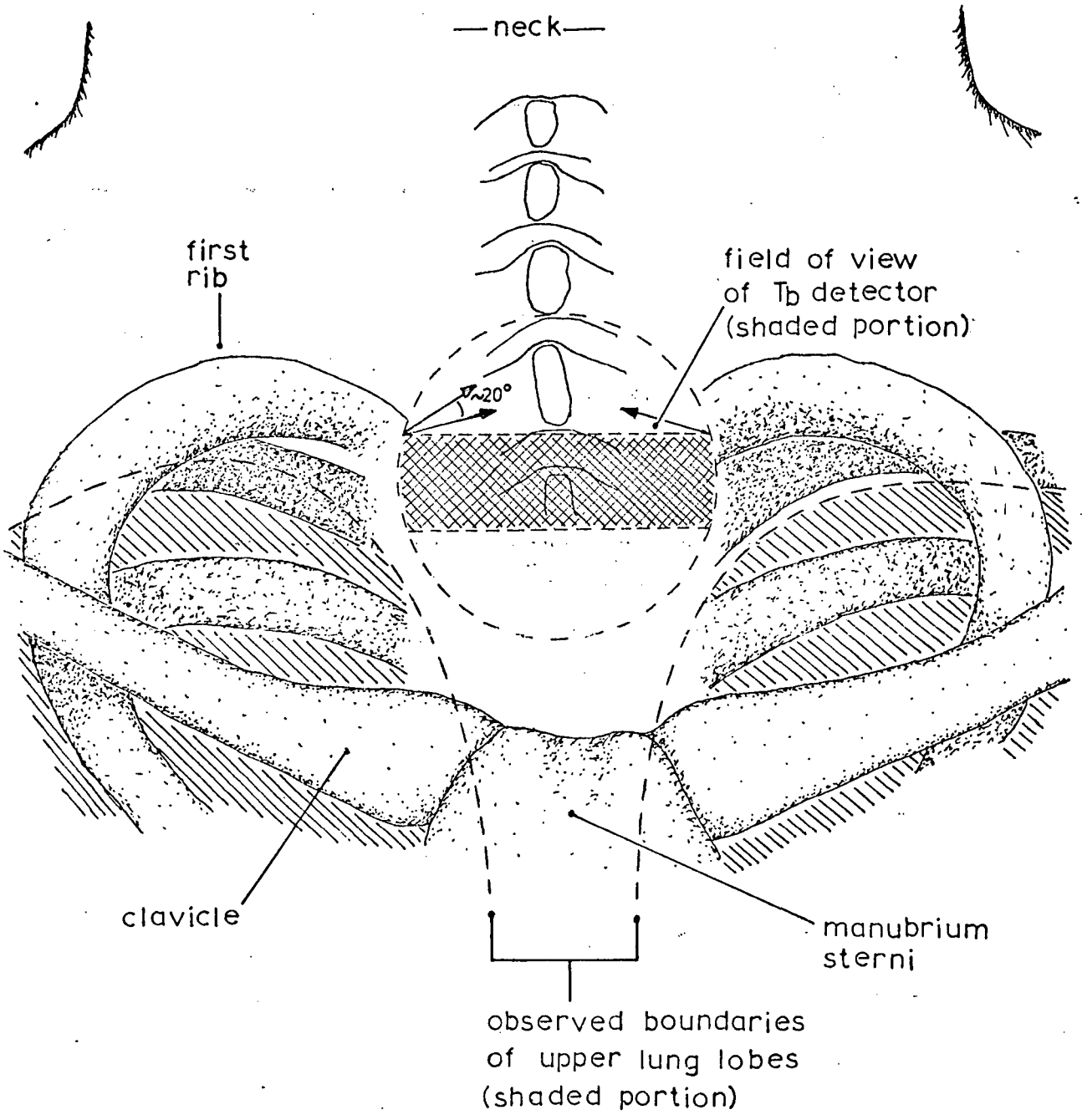

Figure 3.3.13: Shaded tracing from a chest X-ray (1:1 scale) illustrating difficulty of positioning the T_b detector over trachea.

$$Nc = \sum_{n=1}^{x} \frac{Cn}{Nn} = \frac{\sum_{n=1}^{x} Cn \cdot tm}{fc(I) \cdot Nx \cdot x \cdot td} \quad \text{.....equation 3.3.19}$$

where, Nc = the number of detector counts for one particle present beneath the detectors for td.

td = time of detector measurement (~ 0.033 hour)

tm = time of total measuring period (~ 9 hours continuously)

x = number of measurements over period tm.

Nx = number of particles inhaled by the subject

Nn = number of particles present beneath the detectors during the period of measurement, tm.

Cn = total detector counts over each period of measurement, td, corrected for radiation background and isotope decay

$\sum_{n=1}^{x} Cn$ = total detector counts of each measurement, Cn, summed over all measurements, x .

Being single detectors, there was a greater variation in throat detector response with source depth than for the profile scanner. The hypothetical range of vertical movement for a source within the trachea or larynx would be in the region of two centimetres. If a point source moved this distance from an initial position ten centimetres from the detector crystal, the response would vary by some 30%, expressed as a percentage of the maximum. However, it is improbable that such a range of movement, in a vertical direction, would occur in the trachea (assumed horizontal) from one measurement to the next. In the larynx the situation is less certain, but the close matching, both temporal and in terms of relative magnitudes, obtained between the laryngeal and tracheal clearance curves suggests that the effect of any depth response variation was not large.

As the purpose of making the observations was essentially qualitative, no attempt was made to determine absolute or relative magnitudes of radioactivity being cleared at different times. The rates of rise and fall of the clearance pulses and their degree of matching in the larynx and trachea, were considered to be of most interest. For this reason as many

observations per unit time as possible were made for each subject. Four consecutive throat detector measurements, each of two minutes' duration, were interspersed with a single profile scan, giving an interval of 8-10 minutes between each set. Before either type of clearance measurement the subject swallowed a mouthful of drinking water to assist in the clearance of material lodged in the pharynx. Clearance measurements of one form or the other were therefore conducted continuously for a long period, normally 8-9 hours after aerosol administration.

The throat clearance results are presented and discussed in the next chapter.

3.4 Subjects and experimental procedures

Consent to perform the experiments was obtained from the M.R.C. Isotope Advisory Panel (at the time of writing now under the auspices of the D.H.S.S.) and the local ethical committee of the hospital in which the experiments were conducted. The radiation doses administered to the subjects (average ~ 4 m.rem to any organ) was considerably less than that given in a typical chest X-ray. A total of eighteen male volunteer subjects participated in a total of twenty experiments and the nature of the work was fully described to each. Their physiological and lung function data are listed in Table 3.4.1. Only a few subjects reported symptoms of respiratory infection on the day of an experiment and those concerned have been indicated in the table.

Each smoker subject was requested not to smoke on the day before, or on the day of, an experiment. Instructions to subjects as regards swallowing and coughing, during and shortly after aerosol administration, were described in 3.3(ii). No special instructions were given as regards coughing after the second profile scan since if this were an important factor in the natural clearance process of a subject it was considered desirable to allow it. However, only one subject (V C), a smoker, was observed to find it necessary to occasionally cough throughout the continuous part clearance measuring period (8-9 hours). During the latter period the subjects spent approximately half their time in a supine position. The possibility of a gravitational influence on ciliary clearance

subject	age years	height m.	weight kg.	FeV^1 l. *	FVC l. *	VC l. *	ERV l. *	A.	B.	C.
DCFM	45	1·86	71	4·32	5·70	nd	nd	110·8	NS	N
AM	29	1·71	67	4·75	5·75	6·02	2·17	121·8	NS	N
AR	26	1·67	68	3·07	3·55	3·60	1·30	80·8	NS	Y
gp.av.	33·3	1·74	68·7	4·04	5·00	4·81	1·74	104·5		
HG	30	1·86	94	4·50	6·07	5·94	1·48	102·3	NS	N
RB	26	1·83	81	4·85	5·88	6·33	1·95	110·2	NS	Y
PCE	26	1·80	78	4·80	6·28	6·02	nd	111·6	NS	N
gp. av.	27·3	1·83	84·3	4·72	6·08	6·10	1·72	108·0		
PT	55	1·72	67	3·20	4·60	4·84	1·65	94·1	NS	N
PH	25	1·78	57	5·07	2·48	5·24	2·10	117·9	LS	N
KD	28	1·76	70	4·28	5·10	5·32	2·20	104·4	NS	N
gp. av.	36·0	1·75	64·7	4·18	4·06	5·13	1·98	105·5		
TDW	46	1·80	84	3·65	4·96	nd	1·42	98·6	PS	N
JH	31	1·70	63	3·95	4·70	4·75	1·90	103·9	NS	N
AD	25	1·72	64	4·25	5·85	5·76	2·52	106·3	NS	N
gp.av.	34·0	1·74	70·2	3·95	5·17	5·26	1·95	102·9		
ATM	33	1·86	68	5·34	6·50	6·70	2·32	124·2	NS	N
FH	28	1·89	72	5·42	7·00	6·89	3·14	117·8	NS	Y
RH	33	1·87	81	5·37	6·30	6·65	1·76	124·9	NS	N
gp.av.	31·3	1·87	73·7	5·37	6·60	6·75	2·41	122·3		
VC	54	1·80	76	4·00	5·30	5·56	2·78	117·6	PS	N
MS	38	n.d.	n.d.	4·90	5·40	5·40	2·00	n.d.	NS	N
JV	38	1·78	79	3·78	5·48	5·00	1·27	96·9	LS	N
gp.av.	43·3	1·79	77·5	4·23	5·39	5·32	2·02	107·3		
pop.av.	34·2	1·79	72·9	4·42	5·38	5·63	2·00	108·5		
s.d.	9·7	0·07	9·1	0·71	1·08	0·85	0·53	11·9		

A. = % of predicted FeV^1 N = no NS = non smoker
B. = smoking history Y = yes LS = light smoker
C. = respiratory infection PS = pipe smoker
* = b.t.p.s. nd = not determined

Table 3.4.1: Physiological data.

cannot be excluded. However, because of the relatively large number of clearance measurements considered necessary for each subject (~ 100) in order to observe the rapid clearance fluctuations, this was considered to be an unavoidable situation.

Aerosol administration was normally initiated at about the same time of day (11.30 a.m. - 1.30 p.m.) for each subject and the clearance measurements were performed continuously for a period normally in the range 8-9 hours, with a final measurement (3 profile scans) at 20-22 hours after aerosol administration. All mouthpieces were thoroughly cleaned with disinfectant before an experiment, in the interests of hygiene.

4. RESULTS AND DISCUSSION

4.1 Calculation and organization of results

As was described in Chapter 3, part 2(iv)b, in some cases the proportion of satellite particles inhaled by a subject exceeded 2% by mass, or radioactivity. At the largest particle sizes, owing to the small levels of lung retention measured, it was considered desirable to attempt to express the results for two subjects (KD and TDW) in terms of those which would be obtained if primary particles alone had been inhaled. In both cases the procedure demonstrated that the corrections were always a small fraction of I (< 5%; Table 4.1.1).

The total deposition of an aerosol containing both primary and satellite particles is given by,

$$f_D(I) = \frac{(Ip + Is) - (Ep + Es)}{(Ip + Is)} \quad \ldots\ldots\ldots \text{equation } 4.1.1$$

where, Ip or Is, denotes the amount of primary or satellite particles inhaled, respectively.

Ep or Es, denotes the amount of primary or satellite particles exhaled, respectively.

$$\therefore \quad f_D(I) = \frac{(Ip - Ep) + (Is - Es)}{(Ip + Is)}$$

since, $f_D(I) = \frac{I - E}{I}$

$$\therefore \quad f_D(I) = \frac{(f_D(I)p.\ Ip + f_D(I)s.Is)}{(Ip + Is)}$$

where, $f_D(I)p$ or $f_D(I)s$, denotes the values of $f_D(I)$ for primary or satellite particles, respectively.

$$\therefore \quad f_D(I) = \frac{\left(f_D(I)p + f_D(I)s.\frac{Is}{Ip}\right)}{\left(1 + \frac{Is}{Ip}\right)}$$

which re-arranging leads to,

$$f_D(I)p = f_D(I) + \frac{Is}{Ip}.\ (f_D(I) - f_D(I)s) \ldots \text{equation } 4.1.2$$

subject	particles	$f_{D(I)}$	$f_{W(I)}$	$f_{S(I)}$	$f_{C(I)}$	$f_{R(I)}$
KD.	P+S	·9417	·0946	·4195	·2950	·1326
	P	·9644	·1047	·4605	·3057	·0936
TDW.	P+S	·9299	·0589	·4059	·3906	·0744
	P	·9428	·0636	·4365	·3992	·0434

P = primaries

S = satellites

Table 4.1.1: Satellite corrections.

Therefore, if the difference between $f_D(I)$ and $f_D(I)s$, as estimated from the lower part of the measured total deposition curve (Figure 4.2.1), is small, the difference between $f_D(I)p$ and $f_D(I)$ is also small. This was found to be the case for subjects KD and TDW (Table 4.1.1). The quantity Is/Ip was determined from the slide samples placed on the floor of the main apparatus during aerosol administration, after allowing for the effects of differential settling in the manner already described (see Chapter 3, part 2(iv)b).

The regional deposition fraction of an aerosol containing both primary and satellite particles in region, X, say, is given by,

$$fx(I) = \frac{(Xp + Xs)}{(Ip + Is)} \quad \text{..... equation 4.4.3}$$

where, Xp or Xs, denotes the amount of primary or satellite particles deposited in region X, respectively.

since, $fx(I) = \frac{X}{I}$

$$\therefore \quad fx(I) = \frac{(fx(I)p.\ Ip + fx(I)s.Is)}{(Ip + Is)}$$

which dividing and re-arranging as above, gives,

$$fx(I)p = fx(I) + \frac{Is}{Ip}\ (fx(I) - fx(I)s) \text{...equation 4.1.4}$$

where, $fx(I)p$ or $fx(I)s$, denotes the values of $fx(I)$ for primary or satellite particles, respectively.

If the difference between $fx(I)p$ and $fx(I)s$, as estimated from the lower end of the regional deposition curves (Figures 4.2.2, 4.2.3, 4.2.4, 4.2.5) is small, according to equation 4.1.4 the difference between $fx(I)p$ and $fx(I)$ is also small. The largest correction to any deposition fraction was ~ 4% of I (Table 4.1.1) for subjects KD and TDW. The amended values for these subjects have been plotted in the figures.

The deposition fractions, $f_D(I)$, $f_w(I)$, $f_s(I)$, $f_c(I)$, $f_R(I)$, were measured firstly at a constant breathing pattern (tidal

volume, V_T = 1.0 litre (BTPS); breathing rate = 10 breaths minute^{-1}) over a range of particle diameters (4·5-13·0 μm). Three subjects were studied at each particle size, making a total of twelve subjects for the variable particle size study. Two subjects (DCFM and PCE) were not measured at about one day after aerosol administration. In their case, the lowest point on the clearance curve was used to calculate the final level of retention. The results are presented and discussed in part 2 of the present chapter. In addition, the effects of varying the breathing pattern at a constant particle diameter (4·5 μm) were investigated in nine subjects, three at each pattern, three being in common with the variable particle size study, making a total of eighteen subjects participating in the research. The results of the variable breathing pattern study are presented and discussed in part 2(iv) of the present chapter. The number of subjects who were willing or able to participate in repeat studies and the number of repeat studies possible, was necessarily limited by the extensive time required for each experiment and the cumulative radiation dose administered to them. Two subjects (PT and MS) participated in the reproducibility study, two experiments being performed in each case. The results of the reproducibility study are presented and discussed in part 2(iii) of the present chapter.

For all subjects a lung clearance curve was derived from the series of profile scans. Four studies were performed without any throat clearance measurements, before the relevance of the clearance pulses was fully considered (see Chapter 3, part 3(iii)). Six studies were performed using a single detector, to measure laryngeal clearance, which was described in Chapter 3, part 3(ii)c. Ten studies were performed using the double detector apparatus, which was described in Chapter 3, part 3(iii). The throat clearance results are presented and their origin and significance is discussed, in part 3(ii) of the present chapter.

4.2 Aerosol deposition at variable particle size and breathing pattern

The deposition fractions obtained for the twelve subjects of the variable particle size study are listed in Table 4.2.1

and their individual breathing conditions during aerosol administration in Table 4.2.2. It should be noted that deposition fractions to four decimal places have been quoted in these tables because this is helpful when confirming the accuracy of certain equations, as described later in the text. The 95% confidence limits shown on certain figures have been calculated using 'Student's t-test'.

The total deposition results, $f_D(I)$ versus particle size, are plotted in Figure 4.2.1. These have three notable features: (1) the increase in $f_D(I)$ with increasing particle size is small; (2) a large amount of aerosol is exhaled, particularly towards the larger sizes, compared to the results of other workers (see Figure 4.2.9); (3) there are finite differences between subjects. The most important source of inter-subject variability would appear to be fs(I) (Figure 4.2.3). This is somewhat predictable as the laryngeal/ pharyngeal region has a highly variable geometry and flow rates are high (see Chapter 1, part 1(i)). The first two features may indicate the importance of the relatively large volume of anatomical dead space in the mouth, pharynx, larynx and large airways. Since much of these zones contains a significant vertical volume element and aerosol which enters last, leaves first, residing for only a short period, it appears that the total deposition 'saturates' at or below about 4·5 μm particle diameter, increasing only gradually thereafter.

The deposition fractions fw(I), fs(I), show clear upward trends with increasing particle size (Figures 4.2.2 and 4.2.3). At this point it should be noted that no attempt is made in the present work to plot the deposition fractions as a unique function of an impaction parameter, e.g. particle density x particle diameter^2 x mean flow rate, as some other workers have attempted (LIPPMANN, 1975). Such an approach may well be erroneous because the amount of aerosol depositing in a given region is dependent on the amount which enters, from either direction of flow, as well as its intrinsic aerosol filtration efficiency. It is first necessary to express, if possible, the measured values of deposition in terms of efficiencies, as opposed to fractions, which may require a detailed preliminary

analysis. Moreover, since aerosol deposition is never a unique function of an impaction parameter, for example, a sedimentation parameter might also vary as particle density and particle diameter^2, but inversely as flow, it must be borne in mind that the combination of variables of flow and residence times in the respiratory tract are critical in this respect. In the present work respired flow rates have been held nearly constant, which is therefore not conducive to any attempt at distinguishing the relative importance of sedimentation and impaction. Other approaches have been attempted however (see part 2(iii) of the present chapter).

While the curve of fc(I) (Figure 4.2.4) also shows a generally increasing trend with increasing particle size, this appears to falter at the largest particle sizes. However, it must be remembered that aerosol exposure below the larynx will be considerably reduced owing to the increase in fw(I) and fs(I) (Figure 4.2.8). In this instance, it would be helpful to attempt to express the deposition of the cleared fraction, fc(I), in terms of the absolute aerosol deposition efficiency in the region concerned. Considering the plot of $f_R(I)$ versus particle diameter it appears that the larger sizes are able to penetrate and deposit in the respiratory zone in relatively large numbers (Figure 4.2.5). This is a most unusual result when the relative magnitudes of the other deposition fractions are considered (Figure 4.2.6). If fc(I) is reduced at the larger particle sizes because of greatly decreased aerosol penetrance below the larynx, it might be expected that owing to the fact that the deposition efficiency in the dead space airways is certain to increase greatly at the larger particle sizes, the measured values of fc(I) would be much greater in comparison to $f_R(I)$ than actually turns out to be the case (Figure 4.2.7). At both 10·4 μm and 13 μm particle diameter, $f_R(I)$ is a significant fraction of fc(I). However, the complicated interaction between aerosol exposure and deposition efficiency makes such intuitive analysis uncertain. To analyse this and other questions more rigorously, it is first necessary to formulate a descriptive model of the lung, as a series of discrete filters, which may enable the regional deposition efficiencies to be estimated within reasonable limits.

(i) Definition and description of lung model

Four regional deposition fractions have been measured in the present work: $f_W(I)$, $f_S(I)$, $f_C(I)$, $f_R(I)$. For the purposes of the following analysis it will be assumed that each such fraction represents the fractional deposition value in a particular region, i.e. W, S, C, R, corresponding to the mouth, larynx/pharynx, dead space airways, and the respiratory zone, respectively. The validity of the assumptions will then be considered.

In performing such an analysis it cannot be assumed that the aerosol deposition efficiencies are equal in both directions of flow, for any region, without consideration of the physics of the deposition mechanisms and possible variations in the anatomy of a particular region between inspiration and expiration. For example, it is known that the glottal opening tends to be more constricted during an expiration than an inspiration[11] (see Chapter 1, part 1(i)), which might therefore lead to a correspondingly higher aerosol deposition efficiency in the larynx during an expiration. Similarly, as a consequence of the dichotomous branching geometry of the airways, there might be greater inertial impaction of particles in the dead space region (C) during an inspiration, than an expiration. Effectively, therefore, each deposition region with the exception of the respiratory zone, should be considered to behave as two filters assumed to possess unequal aerosol deposition efficiencies. In the present analysis these filters are denoted by the subscript, i, for an inspiration; W_i, S_i, C_i; and, e, for an expiration: W_e, S_e, C_e.

In addition, it must be considered that not the entire tidal volume of aerosol traverses the filters W, S, and C, during an inspiration. For the mouth and laryngeal/pharyngeal regions the volume of tidal air not making the complete traverse is relatively small (~ 50 ml) and the error introduced by ignoring this volume is likely to be negligible. (It should be noted that the relatively large values of $f_E(I)$ measured at large particle sizes which may well be returned mainly from these regions, do not have a disproportionate effect in the analysis owing to the dependency of regional deposition

efficiencies mainly on aerosol exposure during an inspiration). However, in the case of dead space airways the proportion of tidal air not making the complete traverse may be significant and must therefore be taken into account. According to WEIBEL (1963) the volume of dead space airways (generations 0-16) at about $\frac{3}{4}$ of maximum lung inflation (~ normal inflation level) is 175 ml. This implies that up to about 18% of the inhaled air would fail to reach the respiratory zone at a tidal volume of 1·0 litre (BTPS), assuming plug-type flow. The question of the degree of penetrance to the respiratory zone is complicated by the likelihood that airflow in the smaller airways is of the Poisseuille type (i.e. the plot in two dimensions of the forward flow velocity over an airway cross section possesses a parabolic profile). The consequence of this is that the respiratory zone may be reached by a volume of inspired air that may sometimes be only some half of the dead space volume (BRISCOE et al., 1954). This does not mean that the volume of inhaled air which fails to penetrate to the respiratory zone is always about half the dead space volume, since it is probable that at tidal volumes several times greater than the dead space volume the fraction approaches, $\left[\frac{Vd}{V_T}\right]$, where Vd is the dead space volume and V_T is the tidal volume.

In the formulation of a lung model it must also be remembered that a proportion of the inhaled air, respiratory gas exchange notwithstanding, will become inextricably mixed with the expiratory reserve and residual air already in the lungs (see Chapter 1, part 1(i)). However, experiments using 1 μm diameter particles as tracers of gas flow in the lungs have demonstrated that the amount of such mixing is negligibly small (DAVIES et al., 1972).

The journey of the inhaled aerosol into and out of the respiratory tract may therefore be closely represented by the lung model shown in Figure 4.2.10. The regions W, S, are represented by four discrete in-series filters: W_i , W_e, S_i , S_e, to allow for possible differences in the unidirectional aerosol deposition efficiencies. Alternatively, these may be represented together as a single 'head' filter, H, where $(W_i + S_i) = H_i$, and $(W_e + S_e) = H_e$. The dead space airways

are represented as three filters: two in-series, representing the unidirectional aerosol deposition; and one in parallel with these representing the deposition of the portion of the inhaled aerosol which just fails to penetrate to the respiratory zone. The respiratory zone itself is represented by a single in-series filter, R. The filters, Ci, R, Ce, Cd, may also be represented by a single filter, (C + R), for convenience in some calculations.

Referring to Figure 4.2.10, the algebraic relationships are as given below,

$W = (W_i + W_e)$ ..... equation 4.2.1

$S = (S_i + S_e)$ ..... equation 4.2.2

$H = (W + S) = H_i + H_e$ ..... equation 4.2.3

$H_i = (W_i + S_i)$ ..... equation 4.2.4

$H_e = (W_e + S_e)$ ..... equation 4.2.5

$C = (C_i + C_d + C_e)$ ..... equation 4.2.6

$(C + R) = (C_i + C_d + C_e + R)$ ..... equation 4.2.7

$W_i = (I - I_{Wi})$ ..... equation 4.2.8

$S_i = (I_{Wi} - I_{Si})$ ..... equation 4.2.9

$C_i = (I_{Si}' - I_{Ci})$ ..... equation 4.2.10

$$C_d = (I_{cd} - E_{cd}) \quad \text{..... equation 4.2.11}$$

$$R = (I_{ci} - E_R) \quad \text{..... equation 4.2.12}$$

$$C_e = (E_R - E_{ce}') \quad \text{..... equation 4.2.13}$$

$$S_e = (E_{ce} - E_{se}) \quad \text{..... equation 4.2.14}$$

$$W_e = (E_{se} - E) \quad \text{..... equation 4.2.15}$$

$$D = (I - E) = W_i + S_i + C_i + C_d + C_e + R + S_e + W_e \quad \text{....equation 4.2.16}$$

$$I_{cd} = Y.I_{si} \quad \text{..... equation 4.2.17}$$

$$I_{si}' = (1 - Y).I_{si} = Y'.I_{si} \quad \text{..... equation 4.2.18}$$

$$I_{si} = I_{si}' + I_{cd} \quad \text{..... equation 4.2.19}$$

$$Y = \left[P.\frac{V_d}{V_T}\right] \quad \text{..... equation 4.2.20}$$

where, $0 < P < 1$, and P is the factor which determines the proportion of the dead space volume, V_d, occupied by the inspired air.

A deposition efficiency is defined here as the aerosol deposition in a region divided by the total aerosol flux into that region, i.e.,

$$\epsilon_{wi} = \frac{W_i}{I} \quad \text{..... equation 4.2.21}$$

$$\epsilon_{si} = \frac{S_i}{I_{wi}} \quad \text{..... equation 4.2.22}$$

$$\epsilon_{Hi} = \frac{Hi}{I} \quad \text{..... equation 4.2.23}$$

$$\epsilon_{Ci} = \frac{Ci}{I_{Si}}, \quad \text{..... equation 4.2.24}$$

$$\epsilon_{Cd} = \frac{C_d}{I_{Cd}} \quad \text{..... equation 4.2.25}$$

$$\epsilon_R = \frac{R}{I_{Ci}} \quad \text{..... equation 4.2.26}$$

$$\epsilon_{Ce} = \frac{Ce}{E_R} \quad \text{..... equation 4.2.27}$$

$$\epsilon_{He} = \frac{He}{E_{Ce}} \quad \text{..... equation 4.2.28}$$

$$\epsilon_{Se} = \frac{Se}{E_{Ce}} \quad \text{..... equation 4.2.29}$$

$$\epsilon_{We} = \frac{We}{E_{Se}} \quad \text{..... equation 4.2.30}$$

The relationship between the inspiratory and expiratory aerosol deposition efficiencies of certain regions, and that between ϵ_{Cd} and ϵ_{Ci} , or ϵ_C , are defined by 'q- values', i.e.,

$$\epsilon_{Cd} = q_1 \epsilon_C \quad \text{..... equation 4.2.31}$$

$$\epsilon_{He} = q_2 \epsilon_{Hi} \quad \text{..... equation 4.2.32}$$

$$\epsilon_{Ce} = q_3 \epsilon_{Ci} \quad \text{..... equation 4.2.33}$$

$$\epsilon_{Cd} = q_4 \epsilon_{Ci} \quad \text{..... equation 4.2.34}$$

As the measured values of $f_w(I)$ were generally small at all particle sizes it was considered not to warrant a separate analysis for the case of $\epsilon_{wi} \neq \epsilon_{we}$

When the 'q-values' are unity, the aerosol deposition efficiencies reduce to,

$$\epsilon_{Wi} = \epsilon_{We} = \epsilon_W$$

$$\epsilon_{Si} = \epsilon_{Se} = \epsilon_S$$

$$\epsilon_{Hi} = \epsilon_{He} = \epsilon_H$$

$$\epsilon_{Ci} = \epsilon_{Ce} = \epsilon_C$$

The 'q-values', q_2 and q_3, are of more importance in determining the magnitude of the aerosol deposition efficiencies than q_1 or q_4. It may be shown that the permissible values of q_1 lie in the range, $0 < q_1 < \sim 2$, for small values of ϵ_{Cd}, and $q_4 \simeq \frac{q_1 + q_3}{2}$ .... equation 4.2.35, which is intended as a simple approximation only (Appendix 1).

Considering now the various cases when the 'q-values' are non-unity, it may be shown that ϵ_{Hi} , ϵ_{He} , may be determined from a knowledge of $f_H(I)$, $f_{C+R}(I)$, for a range of possible values of q_2.

Case A: $\epsilon_{Hi} \neq \epsilon_{He}$, $q_2 \neq 1$

now, $H = H_i + H_e = \epsilon_{Hi} . I + \epsilon_{He} E_{ce}$

$$\therefore H = \epsilon_{Hi}\left[I + q_2(I_{Si} - (C+R))\right]$$

dividing by I, substituting $I_{Si} = I(1 - \epsilon_{Hi})$ and re-arranging gives,

$$f_H(I) = \epsilon_{Hi}\left[1 + q_2 (1-\epsilon_{Hi}) - q_2 . f_{C+R}(I)\right]$$

$$\therefore 0 = \epsilon_{Hi} + q_2 (\epsilon_{Hi} - \epsilon_{Hi}^2) - q_2 . f_{C+R}(I) - f_H(I)$$

$$\therefore 0 = a\epsilon_{Hi}^2 - b\epsilon_{Hi} + c \qquad \text{..... equation 4.2.36}$$

where, $a = q_2$

$b = [1 + q_2(1 - f_{C+R}(I)]$

$c = f_H(I)$

Solving the quadratic equation 4.2.36 for ϵ_{Hi} in the normal manner, leads to,

$$\epsilon_{Hi} = \frac{b \pm (b^2 - 4ac)^{\frac{1}{2}}}{2a} \qquad \text{..... equation 4.2.37}$$

Case B: $\epsilon_{Ci} \neq \epsilon_{Ce}$, $q_3 \neq 1$

Now, $C = C_i + C_e + C_d$

$\therefore \quad C = \epsilon_{Ci} I_{Si}' + \epsilon_{Ce} . E_R + \epsilon_{Cd} . I_{Cd}$

putting, $I_{Si}' = Y' . I_{Si}$, $E_R = (I_{Ci} - R)$, $I_{Cd} = Y . I_{Si}$,

gives, $C = \epsilon_{Ci} \left[Y' . I_{Si} + q_3 (I_{Ci} - R) \right] + q_4 . \epsilon_{Ci} . Y . I_{Si}$

putting, $I_{Si} = I(1 - \epsilon_{Hi})$; $I_{Ci} = I_{Si}' . (1 - \epsilon_{Ci})$,

gives, $C = \epsilon_{Ci} \left[Y' . I(1 - \epsilon_{Hi}) + q_3 (I_{Si}' . (1 - \epsilon_{Ci}) - R) + q_4 . \epsilon_{Ci} . YI(1 - \epsilon_{Hi}) \right]$

dividing by I and making similar substitutions and re-arranging gives,

$$fc(I) = \epsilon_{Ci} \left[Y'(1 - \epsilon_{Hi}) + q_3 . Y'(1 - \epsilon_{Hi})(1 - \epsilon_{Ci}) - q_3 f_R(I) \right] + q_4 . \epsilon_{Ci} . Y(1 - \epsilon_{Hi})$$

$$\therefore \quad fc(I) = -\epsilon_{Ci}^2 \left[q_3 . Y' . (1 - \epsilon_{Hi}) \right] + \epsilon_{Ci} \left[Y'(1 - \epsilon_{Hi})(1 + q_3 + \frac{q_4 . Y}{Y'}) - q_3 . f_R(I) \right]$$

$$\therefore \quad 0 = a' \epsilon_{Ci}^2 - b' \epsilon_{Ci} + c' \qquad \text{..... equation 4.2.38}$$

where, $a' = \left[q_3 . Y.(1 - \epsilon_{Hi})\right]$

$b' = \left[(1 - \epsilon_{Hi})(Y' + q_3.Y' + q_4.Y) - q_3 f_R(I)\right]$

or putting $Y' = (1 - Y)$,

$b' = \left[(1 - \epsilon_{Hi})(1 + q_3 + Y(q_4 - 1 - q_3)) - q_3 f_R(I)\right]$

$c' = fc(I)$

Solving the quadratic equation 4.2.38 as above, for ϵ_{Ci}, gives,

$$\epsilon_{Ci} = \frac{b' \pm (b'^2 - 4a'c')^{\frac{1}{2}}}{2a'} \qquad \text{..... equation 4.2.39}$$

When $q_3 = 1$, b' reduces to,

$b' = \left[(1 - \epsilon_{Ci})(2 + Y(q_4 - 2)) - f_R(I)\right]$

Having calculated values of ϵ_{Hi}, ϵ_{Ci}, for the desired values of q_1, q_2, q_3, it is then possible to determine ϵ_R

Now, $\epsilon_R = \frac{R}{I_{Ci}}$

$I_{Ci} = I_{Si}' - C_i = I_{Si}'.(1 - \epsilon_{Ci})$

$I_{Si}' = I_{Si}.Y' = Y'.I(1 - \epsilon_{Hi})$

$$\therefore \epsilon_R = \frac{R}{IY'(1 - \epsilon_{Hi})(1 - \epsilon_{Ci})}$$

$$\therefore \epsilon_R = \frac{f_R(I)}{Y'.(1 - \epsilon_{Hi})(1 - \epsilon_{Ci})} \qquad \text{..... equation 4.2.40}$$

When $q_2 = 1$, ϵ_{Hi} may be replaced by ϵ_H, and when $q_3 = 1$, ϵ_{Ci} may be replaced by ϵ_C, in equation 4.2.40.

It should be noted from equation 4.2.40 that ϵ_R values have their maximum when ϵ_{Hi} and ϵ_{Ci} are also a maximum. Taking the extreme and highly unlikely case of assuming that all losses in regions H and C occur during inspiration only, the values of ϵ_{Hi} and ϵ_{Ci}, may be calculated as follows,

$$\epsilon_H = \frac{H}{I} = f_H(I) \quad \text{..... equation 4.2.41 (case } q_2 = 0)$$

$$C_{Ci} = \frac{C}{I_{Si}'} = \frac{C}{\gamma'.I(1-\epsilon_{Hi})} = \frac{f_C(I)}{(1-\epsilon_{Hi}).\gamma'} \quad \text{... equation 4.2.42 (case } q_3 = 0)$$

Case C: $\epsilon_{Si} = \epsilon_{Se} = \epsilon_S$: $\epsilon_{Wi} = \epsilon_{We} = \epsilon_W$; $q_2 = 1$

Although values of fw(I) were considered too trivial to warrant an analysis of the case $\epsilon_{Wi} = \epsilon_{We}$, it was considered desirable to at least express ϵ_W, ϵ_S , separately, in one case ($q_2 = 1$).

Now, $W = W_i + W_e = \epsilon_W(I + E_{Se})$

and, $E_{Se} = E_{Ce} - S_e = E_{Ce}(1-\epsilon_S)$

$$\therefore f_W(I) = \epsilon_W\left[1 + f_{E_{Ce}}(I)\ (1-\epsilon_S)\right]$$

$$\therefore \epsilon_W = \frac{f_W(I)}{\left[1 + f_{E_{Ce}}(I).(1-\epsilon_S)\right]} \quad \text{..... equation 4.2.43}$$

now, $E = E_{Ce} - H_e = E_{Ce}(1-\epsilon_H)$

(Values of ϵ_H are more convenient to use here, and if $(\epsilon_{Si} + \epsilon_{Wi}) = (\epsilon_{Se} + \epsilon_{We})$ then $\epsilon_{Hi} = \epsilon_{He} = \epsilon_H$).

$$\therefore E_{Ce} = \frac{E}{(1-\epsilon_H)}$$

$$\therefore f_{E_{Ce}}(I) = \frac{f_E(I)}{(1-\epsilon_H)} = \frac{(1 - f_D(I))}{(1-\epsilon_H)} \quad \text{..... equation 4.2.44}$$

Now, $S = S_i + S_e = \epsilon_S(I_{Wi} + E_{Ce})$

and, $I_{Wi} = I(1-\epsilon_W)$

$$\therefore f_S(I) = \epsilon_S\left[(1-\epsilon_W) + f_{E_{Ce}}(I)\right]$$

substituting for ϵ_W using equation 4.2.43 gives,

$$f_S(I) = \epsilon_S \left[\left(1 - \frac{f_W(I)}{\left[1 + f_{E_{Ce}}(I)\ (1 - \epsilon_S) \right]} \right) + f_{E_{Ce}}(I) \right]$$

$$\therefore f_S(I).\left[1 + f_{E_{Ce}}(I)(1 - \epsilon_S)\right] = \epsilon_S\left[1 + f_{E_{Ce}}(I).(1-\epsilon_S)\right] - f_W(I).\epsilon_S + f_{E_{Ce}}(I).\epsilon_S\left[1 + f_{E_{Ce}}(I).(1 - \epsilon_S)\right]$$

$$\therefore 0 = -f_S(I) - f_S(I).f_{E_{Ce}}(I) + f_S(I).f_{E_{Ce}}(I).\epsilon_S + \epsilon_S + f_{E_{Ce}}(I).\epsilon_S - f_{E_{Ce}}(I).\epsilon_S^2 - f_W(I).\epsilon_S + f_{E_{Ce}}(I).\epsilon_S + f_{E_{Ce}}(I)^2.\epsilon_S - f_{E_{Ce}}(I)^2.\epsilon_S^2$$

$$\therefore 0 = -\epsilon_S^2\left[f_{E_{Ce}}(I) + f_{E_{Ce}}(I)^2\right] + \epsilon_S\left[1 + f_S(I).f_{E_{Ce}}(I) + f_{E_{Ce}}(I) + f_{E_{Ce}}(I) - f_W(I) + f_{E_{Ce}}(I)^2\right] - \left[f_S(I) + f_S(I).f_{E_{Ce}}(I)\right]$$

$$\therefore 0 = a''.\epsilon_S^2 - b''.\epsilon_S + c'' \qquad \text{..... equation 4.2.45}$$

where, $a'' = \left[f_{E_{Ce}}(I)(1 + f_{E_{Ce}}(I))\right]$

$b'' = \left[1 - f_W(I) + f_{E_{Ce}}(I)(2 + f_S(I) + f_{E_{Ce}}(I))\right]$

$c'' = \left[f_S(I).(1 + f_{E_{Ce}}(I))\right]$

Solving for ϵ_S in the quadratic equation 4.2.45 gives,

$$\epsilon_S = \frac{b'' \pm (b''^2 - 4a''.c'')^{\frac{1}{2}}}{2a''} \qquad \text{..... equation 4.2.46}$$

It was considered necessary to adopt some means of independently checking the accuracy of the calculated aerosol deposition efficiencies for each subject.

Now, $D = H_i + C_i + C_d + R + C_e + H_e$

$$f_D(I) = \frac{1}{I}\Big[\epsilon_{Hi}.I + \epsilon_{Ci}.Y'.I(1 - \epsilon_{Hi}) + q_4.\epsilon_{Ci}.YI(1 - \epsilon_{Hi}) + \epsilon_R\left(Y'.I(1 - \epsilon_{Hi}) - \epsilon_{Ci}.Y'.I(1 - \epsilon_{Hi})\right) + \epsilon_{Ce}\left(Y'.I(1 - \epsilon_{Hi}) - \epsilon_{Ci}.Y'.I(1 - \epsilon_{Hi}) - \epsilon_R\left(Y'.I(1 - \epsilon_{Hi}) - \epsilon_{Ci}.Y'.I(1 - \epsilon_{Hi})\right)\right) + \epsilon_{He}\left(Y'.I(1 - \epsilon_{Hi}) - \epsilon_{Ci}.Y'.I(1 - \epsilon_{Hi}) - \epsilon_R\left(Y'.I(1 - \epsilon_{Hi}) - \epsilon_{Ci}.Y'.I(1 - \epsilon_{Hi})\right)\right)$$

$$- \epsilon_{Ce}\left(Y'.I(1-\epsilon_{Hi}) - \epsilon_{Ci}.Y'.I(1-\epsilon_{Hi}) - \epsilon_R\left(Y'.I(1-\epsilon_{Hi}) - \epsilon_{Ci}.Y'.I(1-\epsilon_{Hi})\right)\right) + \epsilon_{He}\left(Y(1-\epsilon_{Hi}) - q_4.\epsilon_{Ci}.Y(1-\epsilon_{Hi})\right)\Big]$$

Cancelling I and simplifying gives,

$$f_D(I) = \Big[\epsilon_{Hi} + \epsilon_{Ci}.Y'(1-\epsilon_{Hi}) + q_4.\epsilon_{Ci}.Y(1-\epsilon_{Hi}) + \epsilon_R(Y'(1-\epsilon_{Hi})(1-\epsilon_{Ci})) + \epsilon_{Ce}(Y'(1-\epsilon_{Hi})(1-\epsilon_{Ci})(1-\epsilon_R)) + \epsilon_{He}(Y'(1-\epsilon_{Hi})(1-\epsilon_{Ci})(1-\epsilon_R)(1-\epsilon_{Ce})) + \epsilon_{He}(Y(1-\epsilon_{Hi})(1-q_4.\epsilon_{Ci}))\Big]$$

putting,

$$P_1 = Y'(1-\epsilon_{Hi})$$

$$P_2 = P_1(1-\epsilon_{Ci})$$

$$P_3 = P_2(1-\epsilon_R)$$

$$P_4 = P_3(1-\epsilon_{Ce}) = P_3(1-q_4.\epsilon_{Ci})$$

$$P_1' = Y(1-\epsilon_{Hi})$$

$$P_2' = P_1'(1-q_4.\epsilon_{Ci})$$

Where in the above notation Px, say, represents the aerosol penetrance to region, X.

$$\therefore f_D(I) = \epsilon_{Hi} + P_1.\epsilon_{Ci} + P_1'.q_4.\epsilon_{Ci} + P_2.\epsilon_R + P_3.\epsilon_{Ce} + P_4.\epsilon_{He} + P_2'.\epsilon_{He}$$

$$\therefore f_D(I) = \epsilon_{Hi}[1 + q_2(P_4 + P_2')] + \epsilon_{Ci}[P_1 + q_4.P_1' + q_3.P_3] + \epsilon_R.P_2 \quad \text{..... equation 4.2.47}$$

where,

$$f_H(I) = \epsilon_{Hi}[1 + q_2(P_4 + P_2')]$$

$$f_C(I) = \epsilon_{Ci}[P_1 + q_4.P_1' + q_3.P_3]$$

$$f_R(I) = \epsilon_R.P_2$$

When $q_2 = 1$, ϵ_{Hi} may be replaced by ϵ_H in equation 4.2.47; when $q_3 = 1$, ϵ_{Ci} may be replaced by ϵ_C, and q_4 by q_1.

Using the above equations it is therefore possible to determine whether the predicted values of fractional deposition

tally with the actual.

By an essentially similar process of calculation it may be shown that to include the terms, ϵ_W and ϵ_S, $f_D(I)$ should be written (Appendix 2),

$$f_D(I) = \epsilon_W[1 + P_5 + P_3'] + \epsilon_S[1 - \epsilon_W + P_4 + P_2'] + \epsilon_{Si}[P_1 + q_4.P_1' + q_3.P_3] + \epsilon_R.P_2$$

..... equation 4.2.48

where, $f_W(I) = \epsilon_W(1 + P_5 + P_3')$

$f_S(I) = \epsilon_S(1 - \epsilon_W + P_4 + P_2')$

$f_C(I) = \epsilon_{Ci}(P_1 + q_4.P_1' + q_3.P_3)$

$f_R(I) = \epsilon_R.P_2$

and, $P_1 = Y'(1 - \epsilon_W)(1 - \epsilon_S)$

$P_2 = P_1(1 - \epsilon_{Ci})$

$P_3 = P_2(1 - \epsilon_R)$

$P_4 = P_3(1 - \epsilon_{Ce}) = P_3(1 - q_3.\epsilon_{Ci})$

$P_5 = P_4(1 - \epsilon_S)$

$P_1' = Y(1 - \epsilon_W)(1 - \epsilon_S)$

$P_2' = P_1'(1 - q_4.\epsilon_{Ci})$

$P_3' = P_2'(1 - \epsilon_S)$

(ii) Discussion of calculated regional deposition for variable particle size study

Taking an assumed value of P = 1, giving Y = 0·18, Y′ = 0·82, values of ϵ_C have been calculated for a range of values of q_1, when $q_2 = q_3 = 1$, using equations 4.2.37 and 4.2.38. The individual and group average values of ϵ_H are plotted in Figure 4.2.11. Average values only for ϵ_C are plotted in Figure 4.2.12, with error bars at the 95% confidence limit, for a range of values of q_1, i.e. 0·5, 1, and 2, the latter being an extreme. This demonstrates that the influence of q_1 on ϵ_C values is not large. Putting a reasonable estimate of $q_1 = 1$ throughout subsequent derivations of ϵ_C or ϵ_{Ci}, for a range of values of q_2, q_3, will not therefore introduce a significant error.

Individual and group-average values of ϵ_C for $q_1 = 1$ and $q_3 = q_2 = 1$, are plotted in Figure 4.2.13.

The trend in ϵ_H, ϵ_C, (Figures 4.2.11 and 4.2.13) is generally upwards with increasing particle size, as might be expected. At 10·4 μm particle diameter there appears to be a disproportionate increase in the curve for ϵ_H, but this falls within the observed range of values.

The values of ϵ_H may be further subdivided into values of ϵ_W and ϵ_S (this is not to imply that $\epsilon_H = \epsilon_W + \epsilon_S$, in fact $\epsilon_H = [1 - (1 - \epsilon_W)(1 - \epsilon_S)]$, calculated using equations 4.2.43 and 4.2.46. The individual and group-average values for ϵ_W and ϵ_S are plotted in Figures 4.2.14 and 4.2.15, respectively. ϵ_W manifests a clear upward trend with increasing particle size, as did $f_W(I)$, and ϵ_S, while also showing a generally upwards trend, possesses a similar scatter of points to $f_S(I)$ and gives an obvious clue as to the main source of intersubject variability.

Values of ϵ_R for various values of ϵ_{Ci}, ϵ_{Hi}, or ϵ_C, ϵ_H, may now be calculated from equation 4.2.40. The individual and group-average values of ϵ_R for $q_3 = q_2 = 1$ are plotted in Figure 4.2.16. This shows an obvious downwards trend with increasing particle size. However, the result is somewhat remarkable in the light of an assumed dominance of aerosol sedimentation in the respiratory zone. Before other factors are considered it is first necessary to examine the possibility that the downwards trend in ϵ_R, shown in Figure 4.2.16, is caused by incorrect assumptions in the values of q_3 and q_2. Figure 4.2.17 is a plot of group-average ϵ_R values for a wide range of combinations of values of q_3 and q_2. Whichever values, or combination of values, is selected, the trend in ϵ_R is always downwards with increasing particle size.

The bizarre nature of the trend in ϵ_R may be exemplified by intuitively considering the relationship between the particle falling speed, lung morphology and mean particle residence times in the airways, at the largest particle diameter: 13 μm. According to Stokes' law, a unit density spherical 13 μm particle falls in still air at a rate of approximately 5 mm every second. The diameter of the largest respiratory bronchiole in the Weibel Model is approximately 540 μm. Neglecting airway

orientation influences, airborne particles entering the respiratory region therefore need only to reside about a tenth of a second before depositing. When the mean respired flow rate, f_o, say, is 333 cc sec.$^{-1}$, as in this case, the average time taken for particles to traverse the dead space, V_d, is given by $\left[\frac{V_d}{f_o}\right]$, or 0·55 seconds. Therefore, for a 6 second breathing cycle, the residence time of particles in the respiratory zone would lie in the range 0 - 4·9 seconds, averaging approximately 2·5 seconds. It may therefore be safely concluded that the overwhelming majority of 13 μm particles resided in the respiratory zone for a time far greater than that actually required for deposition to be assured. Yet according to the results plotted in Figures 4.2.16 and 4.2.17, well over half such particles are able to enter and leave the respiratory zone without depositing. It seems only possible to conclude that the measured deposition fractions are incorrect.

Besides possible errors arising in the experimental technique, discussed in Chapter 3, there are two central assumptions that have been made in the derivation of the regional deposition fractions, $f_R(I)$, $f_C(I)$: (1) that an insignificant amount of material which initially deposited in the respiratory zone was cleared from the lungs in the first day after aerosol administration; (2) that an insignificant amount of material which initially deposited on the dead space airways remains there the first day after aerosol administration. Put more simply, if one of these assumptions is incorrect, it implies either that: (1) C is overestimated at the expense of R; or, (2) R is overestimated at the expense of C, respectively. The third possibility, that neither assumption is correct, cannot be excluded. Although in that case the errors resulting from each incorrect assumption would be partly, or wholly, compensatory.

In Chapter 1, part 1(ii), it was concluded that on the basis of recent evidence (GORE and PATRICK, 1978) it was quite possible that assumption (2) above, was incorrect, but probably not assumption (1) (STAHLHOFFEN et al., 1979). If however some of the retained fraction at 13 μm particle diameter was

actually retained outside the respiratory zone, this would have the effect of lowering $\epsilon_R = \left(\frac{R}{I_{Ci}}\right)$ still further. Only if the whole of the measured retained fraction was actually retained outside the respiratory zone, i.e. if there was actually negligible penetrance to the respiratory zone at this size could the ϵ_R values be explained in terms of assumption (2) being incorrect. Before discussing this possibility further the validity of assumption (1) will also be considered.

Let the systematic error in C be Δ, where Δ might be positive or negative, depending on which assumption is correct, or dominant, Δ being positive if there exists a rapid phase of respiratory zone clearance. The systematic error in Δ is therefore $-\Delta$, i.e.

$$f_C^{\Delta}(C + R) = \frac{C + \Delta}{C + R}$$

$$f_R^{\Delta}(C + R) = \frac{R - \Delta}{C + R}$$

Now, $f_C(I) = \frac{C}{C + R} \cdot \frac{C + R}{I}$

$$\therefore f_C^{\Delta}(I) = \frac{C + \Delta}{I} = f_C(I) - f_{\Delta}(I)$$

similarly, $f_R^{\Delta}(I) = \frac{R - \Delta}{I} = f_R(I) - f_{\Delta}(I)$

now, $\epsilon_R = \frac{R}{I_{Ci}}$ ..... equation 4.2.26

and, $I_{Ci} = I_{Ci}' - C_i = Y'.I_{Si} - C_i$

$\therefore I_{Ci} = Y'.I(1 - C_{Hi}) - C$

$$\therefore \epsilon_R = \frac{R}{[Y.I(1 - C_{Hi}) - C_i^{\Delta}]}$$ ..... equation 4.2.49

similarly, $\epsilon_R^{\Delta} = \frac{R^{\Delta}}{[Y.I(1 - C_{Hi}) - C_i^{\Delta}]}$ ..... equation 4.2.50

where, $C_i^{\Delta} = C_i + \left[\Delta . \frac{C_i}{C}\right]$

now, $C = C_i + C_e + C_d$

But if the invalidity of assumption 1 is causing the 'low' values in ϵ_R, then it is likely that the 'real' value of ϵ_R is almost unity at a particle diameter of 13 μm. If 'real' ϵ_R is unity then obviously C_e is zero,

$\therefore C = C_i + C_d$

let $\epsilon_{Cd} = \epsilon_{Ci}$, ($q_1 = 1$). A 'reasonable' value for the ratio $\frac{C_i}{C}$, may therefore be obtained, since,

$C_i = \epsilon_{Ci} . Y' . I_{Si}$

and, $C_d = \epsilon_{Cd} . Y . I_{Si} = \epsilon_{Ci} . Y . I_{Si}$

$\therefore C = \epsilon_{Ci} . I_{Si} . (Y' + Y) = \epsilon_{Ci} . I_{Si}$

$\therefore \frac{C_i}{C} = Y'$

$\therefore C_i^{\Delta} = C_i + Y'\Delta$

which, substituting in equation 4.2.50, gives,

$$\epsilon_R^{\Delta} = \frac{R - \Delta}{[Y' . I(1 - \epsilon_{Hi}) - C_i - Y'.\Delta]} \quad \text{..... equation 4.2.51}$$

Now, if 'real' ϵ_R is almost unity, equation 4.2.49 leads to,

$R = [Y' . I(1 - \epsilon_{Hi}) - C_i]$

substituting for $[Y' . I(1 - \epsilon_{Hi}) - C_i]$ in equation 4.2.51, gives,

$$\epsilon_R^{\Delta} = \frac{R - \Delta}{R - Y'\Delta}$$

$\therefore \epsilon_R^{\Delta}(R - Y'\Delta) = R - \Delta$

$\therefore R(1 - \epsilon_R^{\Delta}) = \Delta(1 - Y' . \epsilon_R^{\Delta})$

$$\therefore \frac{\Delta}{R} = \frac{f\Delta(I)}{f_R(I)} = \frac{(1 - \epsilon_R^{\Delta})}{(1 - Y'\epsilon_R^{\Delta})} \qquad \text{..... equation 4.2.52}$$

Taking ϵ_R^{Δ} max., i.e. that calculated for $q_2 = 1$, $\epsilon_R^{\Delta} = 0{\cdot}203$ at 13 μm particle diameter (see equations 4.2.37, 4.2.39, 4.2.40), and substituting this value of ϵ_R^{Δ} in equation 4.2.52, gives ($Y' = {\cdot}82$, $f_R^{\Delta}(I) = {\cdot}0646$ at 13 μm)

$$f\Delta(I) = {\cdot}956.f_R(I)$$

now, $f_R^{\Delta}(I) = f_R(I) - f\Delta(I) = f_R(I).[1 - {\cdot}956] = {\cdot}044 f_R(I)$

or, $f_R(I) = 22{\cdot}73 f_R^{\Delta}(I) = 1{\cdot}47$, which is impossible

Therefore if an incorrect value in respiratory zone deposition is causing the 'low' values in ϵ_R, then the Δ error must be, at the very least, a substantial fraction of I, if not actually greater, which is impossible.

However, it would superficially appear plausible to explain the 'low' ϵ_R values, in part, in terms of a short-term clearance of particles which initially deposited in the respiratory zone.

If the majority of particles which initially deposited in the respiratory zone were to be cleared from the lungs within the first day after aerosol administration, the resultant clearance curve would have a fairly predictable shape. In the first few hours after aerosol administration the material which initially deposited in the dead space airways would be cleared, let it be assumed. When the material which initially deposited in the respiratory zone was cleared, both the profile scanner and throat clearance curves would register its transit. It is apparent from examination of the profile scanner clearance curves in Figure 4.3.4, that most material is cleared within a short time after aerosol administration; the same result is even more apparent from examination of the corresponding throat clearance curves (Figures 4.3.10 - 4.3.13 and 4.3.17, 4.3.18). In the latter, there is in some cases no clearance whatever registered by the throat detectors from several to nine hours after aerosol administration (subject PT1), despite the fact that other experiments in the present work using smaller

particles have demonstrated that material would indeed be cleared in this time interval given a sufficient aerosol penetrance. This strongly suggests that most material which deposits in the dead space airways at a particle diameter of 13 μm, does so in the first few airway generations. This is inconsistent with the finding of a finite value of respiratory zone penetrance and retention at the largest particle size and suggests no significant short-term respiratory zone clearance. It should be noted that although for some subjects at large sizes (e.g. JH. $\bar{d}$ = 13 μm) there is a finite amount being cleared at 8-9 hours, this does not necessarily imply a finite penetrance to the smaller airways and respiratory zone and may well be caused by a 'delayed' clearance from the large airways.

The implication of both the above analysis of the regional deposition fractions and the evidence of the clearance curves is that aerosol penetrance and subsequent deposition in the respiratory zone was actually negligible at the largest particle size, and that the measured levels of retention are due to an incomplete short-term clearance of particles which initially deposited in the dead space airways. If 13 μm diameter particles were not completely cleared, it seems safe to assume that an unknown proportion of retention at other particle sizes was also caused by a finite dead space retention. This considerably complicates the interpretation of the measured deposition fractions. Considering the situation at 13 μm, if the above conclusion is correct, it may be predicted that ϵ_{Ci} should become unity when the 'real' value of $f_C(I)$, $f_C(I)$ real say, is substituted into the equations, where,

$$f_C(I) \text{ real} = f_C(I) + f_R(I) = 0{\cdot}426 \text{ at } 13\ \mu\text{m particle diameter}$$

This then serves as a test of the mutual consistency of the analysis and the conclusion. Equations 4.2.41 and 4.2.42 are the most appropriate ones to use here since most material will be lost in the head and airways during inspiration if the above conclusion is correct.

$$\epsilon_{Ci} \text{ real} = \frac{f_C(I) \text{ real}}{Y'(1 - f_H(I))} = 0{\cdot}955, \text{ which is close to unity.}$$

At a certain particle diameter between 4·5 - 13 μm, it is possible that there was a finite penetrance to the respiratory zone. However, without a foreknowledge of retention due to purely respiratory zone deposition, which is likely to depend on particle size, it is impossible to further advance the present analysis of these results. The present curve for $f_R(I)$ may therefore only be regarded as an upper limit to respiratory zone aerosol deposition.

Comparing these results to those of other workers (Figure 4.2.9), it is apparent that there is reasonable agreement in $f_R(I)$ and $f_C(I)$ with the one result of STAHLHOFFEN et al. (1979), and in $f_R(C + R)$ with FOORD et al. (1978), in a limited region of particle size overlap and conditions of aerosol administration, but the results for $f_R(I)$ of LIPPMANN and ALBERT (1969) appear to be in much closer agreement with existing respirable dust sampling curves, although there appears to be more scatter of observations in the results of the latter.

The influence of particle shape, as well as size, should be borne in mind, however (see Chapter 3, part 1(iii)a). All the above mentioned groups used similar particle production techniques to those of the present study and their data may well be comparable, but caution should be exercised until more information is available concerning particle shape factors.

Aerosol losses in the mouth ($f_W(I)$) are lower in the present work than those reported by FOORD et al. (1978), who used a one centimetre diameter mouthpiece, and LIPPMANN and ALBERT (1969), whose subjects clamped their teeth onto tabs at the centre-line of the mouthpiece in some tests and closed their teeth and lips around the external rim of the mouthpiece (diameter not specified) in others. The results for $f_H(I)$ ($= f_W(I) + f_S(I)$) are reasonably close to those of STAHLHOFFEN et al. (1979), who used a two centimetre diameter mouthpiece (c.f. 2·5 centimetres in the present work). It is therefore possible that mouthpiece diameter and design is an important factor in determining the magnitude of aerosol losses in the mouth, but more experiments are clearly needed before reaching a firm conclusion.

Of all four groups, the widely quoted (MERCER, 1975) observations of LIPPMANN and ALBERT (1969) exhibit the most scatter in any deposition fraction. In the light of the experience obtained in the present work, the following explanatory comments may be helpful:

A. $f_D(I)$: The inhaled aerosol was not measured directly by LIPPMANN and ALBERT (1969), $f_D(I)$ being obtained indirectly by measurement of D ($I = D + E$). This requires careful measurement of the radioactive content of the lungs using whole body (or whole lung) counting systems (EHRET et al., 1964). While the variation in point to point counting sensitivity of their detectors has been described by ALBERT et al., 1965, the details of how the arbitrary detector count rate was converted into a measure of the radioactive content of the whole thoracic cage, in absolute units, are too vaguely described to form a sound basis for judging the overall accuracy of the method.

B. $f_W(I)$: The mouthpiece design favoured high mouth losses and changed during their experiments.

C. $f_S(I)$: The difficulties encountered when attempting to measure this fraction were described in Chapter 3, part 3. In the method of LIPPMANN and ALBERT (1969), the collimator design was such as to be unlikely to separately resolve the laryngeal/pharyngeal region from the upper lung lobes (see Figure 3.3.11). Some of the high values shown on Figure 4.2.9(iii) may therefore be caused by the inclusion of some lung radioactivity, while on the other hand some of the low values may be caused by a failure to prevent swallowing between the end of aerosol administration and the time of measurement of the laryngeal/pharyngeal deposit. It is possible to argue this point both ways because of possible inter-subject differences in anatomy and positioning.

D. Clearance: The rapid fall-off in retention often observed by LIPPMANN and ALBERT (1969) and ALBERT and LIPPMANN (1973), in contrast to the results of many other studies (BOOKER et al., 1967; CAMNER and PHILIPSON, 1978; PAVIA and THOMSON, 1976; STAHLHOFFEN et al., 1979), indicates that the initial laryngeal/pharyngeal deposit may have been included in their initial values of lung retention. This would be consistent with the possibilities discussed in point C above.

The results for total deposition $f_D(I)$, in the present work, are lower than those of both FOORD et al. (1978) and LIPPMANN and ALBERT (1969), but agree better at the smaller particle sizes with those of STAHLHOFFEN et al. (1979). Although the results for $f_D(I)$ in the present work show a generally increasing trend with increasing particle size, the relative amounts of aerosol exhaled at the larger sizes are quite high for some subjects. The aerosol which occupies the mouth, pharynx, trachea, and main bronchi (total volume ~ 100 cc), may be a significant contributor in this respect. It should also be borne in mind that aerosols in the respiratory tract obey a 'last in, first out' principle (MUIR, 1967). The residence time of particles which fail to penetrate even to the intrathoracic dead space airways is therefore the smallest of any part of the respiratory tract. Moreover, because of the nature of flows in a typical breathing cycle, these particles are also carried in the slowest flows of any part of the cycle duration, which must also lower the probability of deposition by inertial impaction.

(iii) Discussion of results of variable breathing pattern study

In the generally accepted understanding of the deposition aerosols in the particle size range of the present study, there are two main deposition mechanisms: inertial impaction and sedimentation. Other factors being equal, the former is velocity dependent, the latter, time dependent. In investigating the relative importance of each mechanism it would be desirable to hold the effects of one constant while the other was allowed to vary. Variations of the physiological parameters which define breathing pattern; tidal

volume and breathing frequency, are of little use in this respect since both residence time and respired flow rates change together when there is a change in either physiological parameter. It is not possible to vary the residence time of particles in a lung airway without a simultaneous variation in the mean air flow velocity through it (except by breath-holding).

However, by adopting breathing patterns 1 and 2, shown in Figure 4.2.18, it is at least possible to investigate the importance of the time-dependent deposition mechanisms in the respiratory zone. This is accomplished by using the same breathing flow rates in both patterns. The aerosol deposition efficiency in the dead space airways during an inspiration and expiration, which depends on breathing flow rate, is therefore constant in both cases. The aerosol penetrance to the respiratory zone (I_{Ci}) is consequently a constant fraction of I and the effects of varying the particle residence times (by varying tidal volume) in the respiratory zone, on ϵ_R, may be examined. (It should be noted that in the calculation of ϵ_R, ϵ_{Ci} must also be determined. This depends on C, which may not be exactly equal in the results of both patterns because of a difference in C_e (not ϵ_{Ce}). However, since C_e makes about an order of magnitude smaller contribution to C, than C_i, even at the smallest particle diameter, the error in ϵ_{Ci} and hence ϵ_R is probably negligible. It should also be noted that although the fraction, C_d, is a different fraction of C, between the two patterns, this is allowed for in the calculation of ϵ_R by using the appropriate values of Y′). Pattern 3 is another variation which allows the effects of a change in breathing flow rate to be examined by a comparison between the values of ϵ_{Ci}, ϵ_{Ce}, obtained from the results of pattern 2.

Three subjects were studied for each pattern, all at 4·5 μm particle diameter, which was considered to be about the highest size that could be employed in a study of the time-dependency of aerosol deposition in the respiratory zone. The deposition fractions obtained are listed in Table 4.2.3 and plotted in Figure 4.2.19. The individual and group-average breathing conditions are listed in Table 4.2.4. The calculated regional deposition efficiencies, ϵ_H, ϵ_C, ϵ_R, for values of $q_2 = q_3 = 1$,

are plotted in Figures 4.2.20, 4.2.21, 4.2.22, respectively.

Values of ϵ_R show no obvious increase between patterns 1 and 2, despite the fact that the mean particle residence time was some 50% higher in pattern 1, than 2. Values of ϵ_R in pattern 3 also show no obvious differences over those of pattern 1, although it should be borne in mind that the relative aerosol exposure to the respiratory zone is slightly different to those of patterns 1 and 2.

In view of the strong possibility of a finite retention of particles in the dead space airways about one day after aerosol administration, the results of the breathing pattern study must be treated with some caution. In particular, it is possible, for example, that there are differences in ϵ_R between patterns 1 and 2, being masked by a large proportional contribution of dead space retention. Whatever the cause, the analysis of the preceding section has demonstrated that the deposition fractions, and therefore efficiencies, cannot be correct. It is therefore doubtful if any useful information can be derived from this aspect of the present work.

(iv) Reproducibility of aerosol deposition fractions

Owing to limitations of radiation dose and the considerable time spent by each subject involved in the study, it was not possible to perform repeat observations in more than a strictly limited number of subjects (MS and PT). Nonetheless, agreement between the two repeat runs was generally good in both cases (Table 4.2.5). Values of $f_D(I)$ are almost exactly equal, as are all the other deposition fractions for subject, MS. For subject, PT, there appears to be an increase in $f_S(I)$ at the expense of $f_C(I)$. This again indicates the importance of the larynx as a source of variability in a subject. The reproducibility of the clearance curves is discussed in the next section of the present chapter.

4.3 Short-term clearance results

(i) Profile scanner clearance curves

The individual and group-average (averages calculated at hourly intervals) profile scanner clearance curves are plotted

in Figures 4.3.1-4.3.4. The averages alone are shown in Figure 4.3.5. By means of the vertical scale shown in the latter figure, the times taken to clear specific percentages of the initial deposit below the larynx have been calculated, plotted in Figure 4.3.6. Although all individual clearance curves exhibit a marked scatter of points, whose possible origin is discussed below, all manifest a clear downwards trend with increasing time and a virtual levelling-off after several hours, particularly at large particle sizes.

This indicates that the larger particle sizes tend to deposit in the upper airways to be cleared quickly, while the smaller particles penetrate more deeply into the lungs and are cleared more slowly. The results shown in Figure 4.3.6 indicate that the percentage of the initial deposit cleared is a reasonably constant fraction of the final amount cleared, at any particle size, for the early part of the clearance period. This may imply that the relative amounts of aerosol depositing in very large airways tends to be a reasonably constant fraction of the total deposit below the larynx, at any size.

There is no obvious evidence in these curves of a delayed short-term clearance from the respiratory zone. The final point determination at 20-22 hours after aerosol administration is invariably close to the levels of retention measured the previous night, indicating only a small degree of clearance in the intervening period.

The observation of a very rapid fall-off in retention in the first few minutes after aerosol administration by ALBERT and LIPPMANN (1973), is not supported by the present data, which are more consistent with the results of BOOKER et al. (1967) and STAHLHOFFEN et al. (1979). It is possible that full account was not taken by ALBERT and LIPPMANN (1973) of the material which initially deposits in the laryngeal/pharyngeal region. This is shown in the present work to be a significant deposit at all particle sizes employed and, also, to be rapidly translocated to the stomach.

(ii) Throat clearance curves

The origin and purpose of the throat clearance measurements was described in Chapter 3, part 3(iii). As many measurements per unit time as possible were made in order to resolve the very rapid clearance fluctuations. The throat clearance curves for those subjects with only a single detector placed over the larynx are presented in Figures 4.3.7-4.3.12, and those for subjects with the double detector arrangement, in Figures 4.3.13-4.3.22. In the figures showing the double detector results, T_a curves refer to laryngeal measurements, T_b, to the tracheal. Two sets of curves are presented in each case: a plot of total counts obtained in a two-minute counting period (i) (after allowing for a radiation background and isotope decay); and a plot of the average recorded counts over four successive two-minute counting periods (ii). The latter enables the slower phase changes to be more rapidly discerned.

The throat clearance curves obtained at the large particle sizes (PT1, Figure 4.3.12; PT2, Figure 4.3.17; AD, Figure 4.3.13; KD, Figure 4.3.18), with the possible exceptions of subjects JH, Figure 4.3.11 and PH, Figure 4.3.10, (a smoker), manifest a rapid fall-off in count rate after only several hours, as might be expected. The throat clearance curves for subject, PT, obtained at different dates (c.f. Figure 4.3.12 and 4.3.17(i), T_a curve), are markedly similar. In the case of subject, MS, the T_a, T_b, curves (Figures 4.3.20 and 4.3.21) obtained at different dates and averaged over four consecutive measurements (ii) show some agreement, particularly over the first two hours, but this is not obviously apparent in the non-averaged curves (i). In Figure 4.3.20(i), (MS1), any agreement between the T_a/T_b, curves obtained on the same date is somewhat obscured by the rapidity of the clearance fluctuations, but is apparent on the averaged curves (ii).

The double detector curves for subject, AD, manifest the most obvious temporal phase-lag agreement between the T_a/T_b curves (Figure 4.3.13(i) and (ii)), while those for subjects ATM, RH, KD, (Figures 4.3.14, 4.3.16, 4.3.18, respectively), are uncertain over both curves (i) and (ii). Subjects, FH, VC, JV,

(Figures 4.3.15, 4.3.19, 4.3.22, respectively) show no obvious signs of matching between T_a and T_b. However, all these clearance curves exhibit temporal variations that are often non-random, indicating they are of systematic origin. The absence of phasic matching in the T_a/T_b curves of some subjects indicates that changes in the distribution of particles whilst they reside in the tracheal/laryngeal region may be of importance in some cases, while the excellent phasic matching in other cases is good evidence for the existence of large variations in the distribution of particles over the airway walls before they are cleared into the trachea. This would be consistent with the limited observations of MORROW (1965), who placed a single detector above the carinal ridge of the trachea and observed a single clearance 'oscillation', having a period of about one hour. Some non-random clearance fluctuations were also observed by ALBERT et al. (1965).

It therefore seems justifiable to consider the origin of the fluctuations in relation to the deposition and clearance processes of the human respiratory tract. However, it is pointed out that the following discussion is intended only as helpful speculation.

Although there will undoubtedly be a local variation in the initial distribution of inhaled particles over the airways, particularly at the bifurcations, it would seem improbable that such local variations could persist during the ciliary transport process and arrive at the trachea 'intact'. YEATES et al. (1975) have observed the tracheal transit of several impaction 'boli', shortly after dust insufflation, so it is just possible that some of the early peaks observed in the present work have such an origin. Despite this, the observations of non-random clearance fluctuations even up to nine hours after aerosol administration makes it highly unlikely that their sole origin lies in the initial particle distribution. It is generally accepted that sedimentation is the dominant deposition mechanism in the smaller airways (TAULBEE and YU, 1975), which would tend to leave a fairly uniform deposit over the airway walls. The possibility of a local variation in the sedimentation deposit is hard to predict, but even if such deposits existed they

would be unlikely to persist during the long ciliary transport process. Moreover, the slower phase clearance fluctuations observed in the present work must also be considered. In many subjects there is a slow but large rise in count rate, followed by a slow fall, followed by another rise. It would seem improbable that in the intervening period of low count rate between peaks represents a specific region of the airways in which negligible particle deposition occurred. Presumably, the ciliary transport fluid entering the trachea at any given time has its origin over a wide range of different airway paths. It seems inconceivable that each of these different paths, at a given point, experience a simultaneous failure in the particle deposition mechanisms. It may therefore be more reasonable to consider the possibility of a biological modification to the inhaled particle distribution.

A number of biological factors may exert a possible influence on the relative amounts of inhaled particles entering the trachea at different times. Perhaps the most obvious is the likelihood that the thickness of the ciliary transport fluid increases as it 'ascends' the airways (HILDING, 1965). This arises because material is being cleared from a large area ($\sim 0{\cdot}5 m^2$) into the comparatively small area of the trachea. It has even been postulated that a fluid 're-sorption' must occur in the larger airways in order to accommodate this large volume of cleared fluid (KILBURN, 1968). A degree of mixing and overlapping of fluid layers from daughter airways may therefore occur at the bifurcations. This would have the effect of raising the specific radioactivity per unit area of an inhaled radio-aerosol. However, since such changes would be necessarily slow in character they may perhaps only account for the more gradual changes observed in the present work.

Another possible biological modifying influence on the inhaled particle distribution is that of the secretion of mucus from the mucous glands that are found most frequently in the large airways. Such an influence would depend on there being an irregularity in the mucus emissions as well as a subsequent delaying effect on the clearance process.

Finally, there is the more direct possible influence of the cilia themselves. If their beat frequency were to undergo large temporal variations in the large airways or trachea, clearance fluctuations might result. However, aside from the slow diurnal changes, more rapid fluctuations have never been reported by those involved in the direct measurement of clearance rates in the trachea and elsewhere (SACKNER et al., 1973; BATEMAN et al., 1978).

In conclusion, no definitive explanation of the observed clearance fluctuations can be offered, but the balance of arguments would seem to favour a mainly biological cause.

$\bar{d}_{\mu m}$	subject	$f_{D(I)}$	$f_{W(I)}$	$f_{S(I)}$	$f_{C(I)}$	$f_{R(I)}$
	DCFM	7020	·0088	0	·2579	·4353
	AM	7945	·0087	·0265	·2331	·5262
	AR	·8776	·0116	·2555	·2210	·3895
4.55	group av.	·7914	·0097	·0940	·2373	·4503
	HG	·7882	·0105	·1362	·3528	·2887
	RB	·8946	·0215	·1460	·3468	·3803
	PCE	·7490	0	0	·3745	·3745
6.74	group av.	·8106	·0107	·0941	·3580	·3478
	PT *	·9050	·0325	·4525	·3537	·0636
	PH	·9281	·0367	·3565	·4386	·0963
	KD	·9644	·1047	·4605	·3057	·0936
10.45	group av.	·9325	·0589	·4232	·3650	·0845
	TDW	·9428	·0636	·4365	·3992	·0434
	JH	·8647	·1682	·2870	·3276	·0819
	AD	·8382	·0492	·3636	·3573	·0681
13·04	group av.	·8819	·0937	·3624	·3613	·0646

* = average of 2 results

Table 4.2.1: Deposition fractions in variable particle size study.

$\bar{d}_{\mu m}$	subject	f_b	t_{p1}	inh : exh	e.r.v. + V_f
	DCFM	9·17	·70	1:2·20	n.d.
	AM	10·09	·62	1:2·50	3·17
	AR	10·15	·31	1:0·96	2·30
4·55	group av.	9·15	·54	1:1·89	2·74
	HG	10·27	·25	1:1·19	2·48
	RB	10·07	·34	1:1·71	2·95
	PCE	10·12	·25	1:0·94	n.d.
6·74	group av.	10·15	·28	1:1·28	2·72
	PT *	10·21	·32	1:0·98	2·65
	PH	10·03	·30	1:1·00	3·10
	KD	10·60	·24	1:1·29	3·20
10·45	group av.	10·28	·29	1:1·09	2·98
	TDW	9·81	·49	1:0·67	2·42
	JH	9·94	·27	1:0·95	2·90
	AD	9·90	·26	1:1·09	3·52
13·04	group av.	9·88	·34	1:0·90	2·95

n.d. = not determined

* = average of 2 results

Table 4.2.2: Individual breathing conditions (f_b = 10 breaths $min.^{-1}$, V_T = 1·0 l.) in variable particle size study.

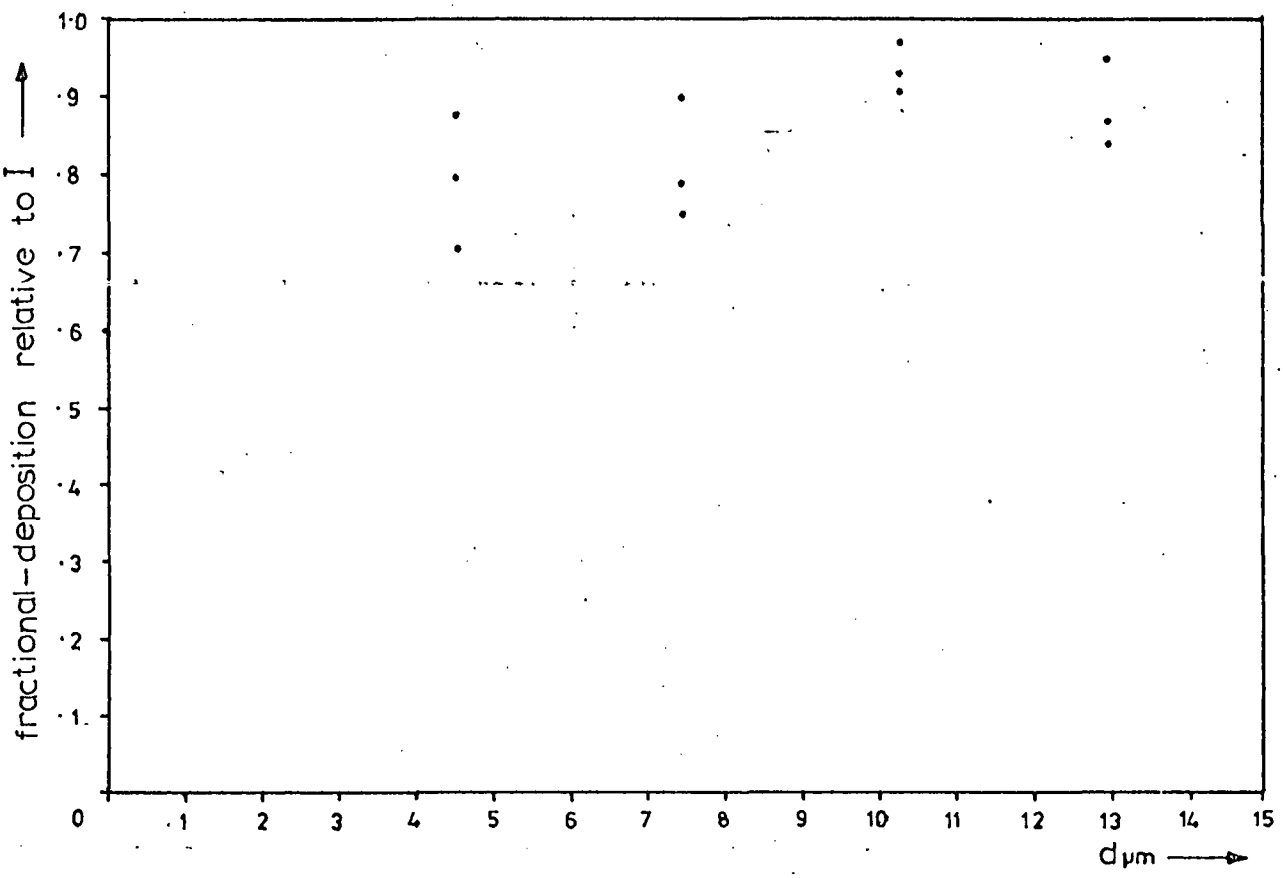

Figure 4.2.1: $f_D(x)$ vs particle diameter (μm).

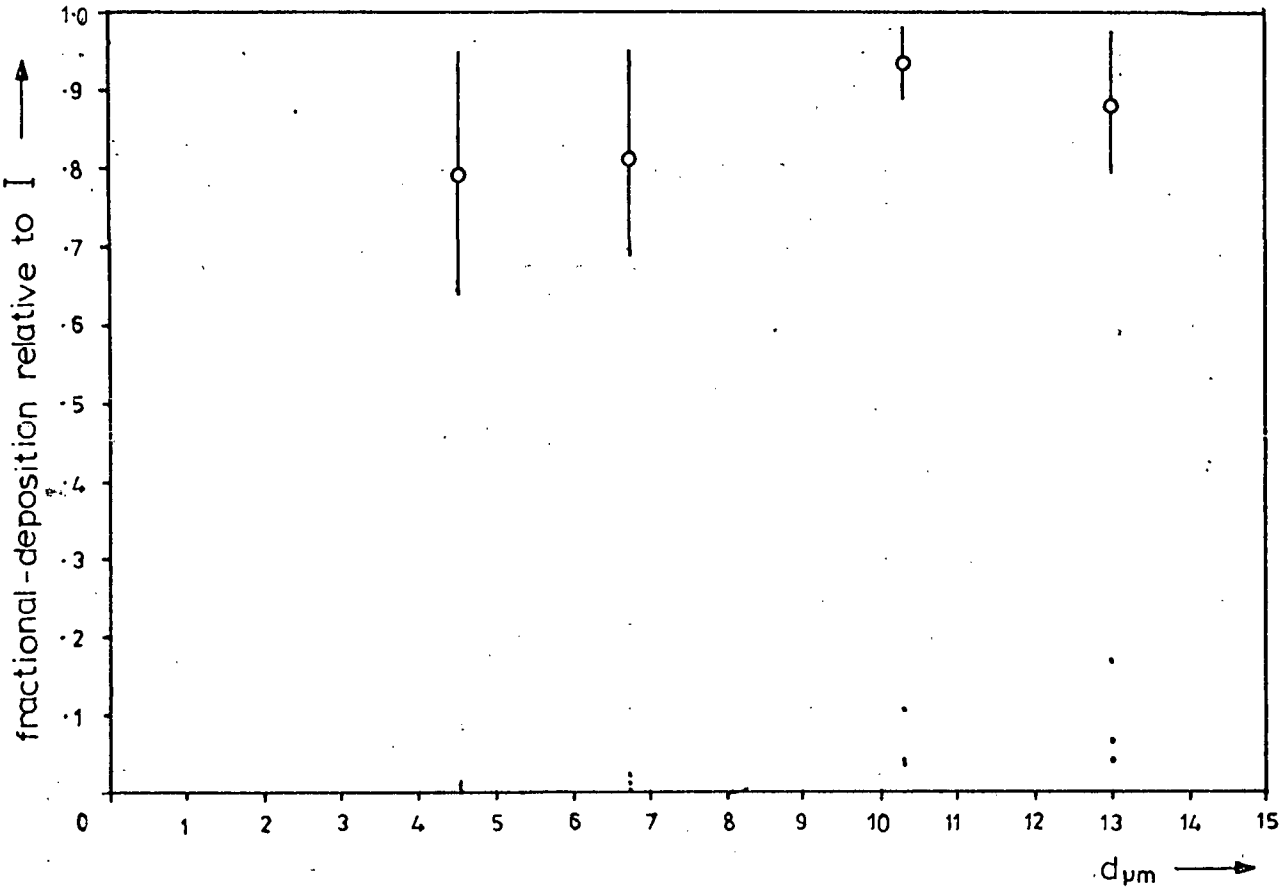

Figure 4.2.2: $f_w(x)$ vs particle diameter (μm). Bars on $f_D(x)$ indicate 95% confidence limits about mean.

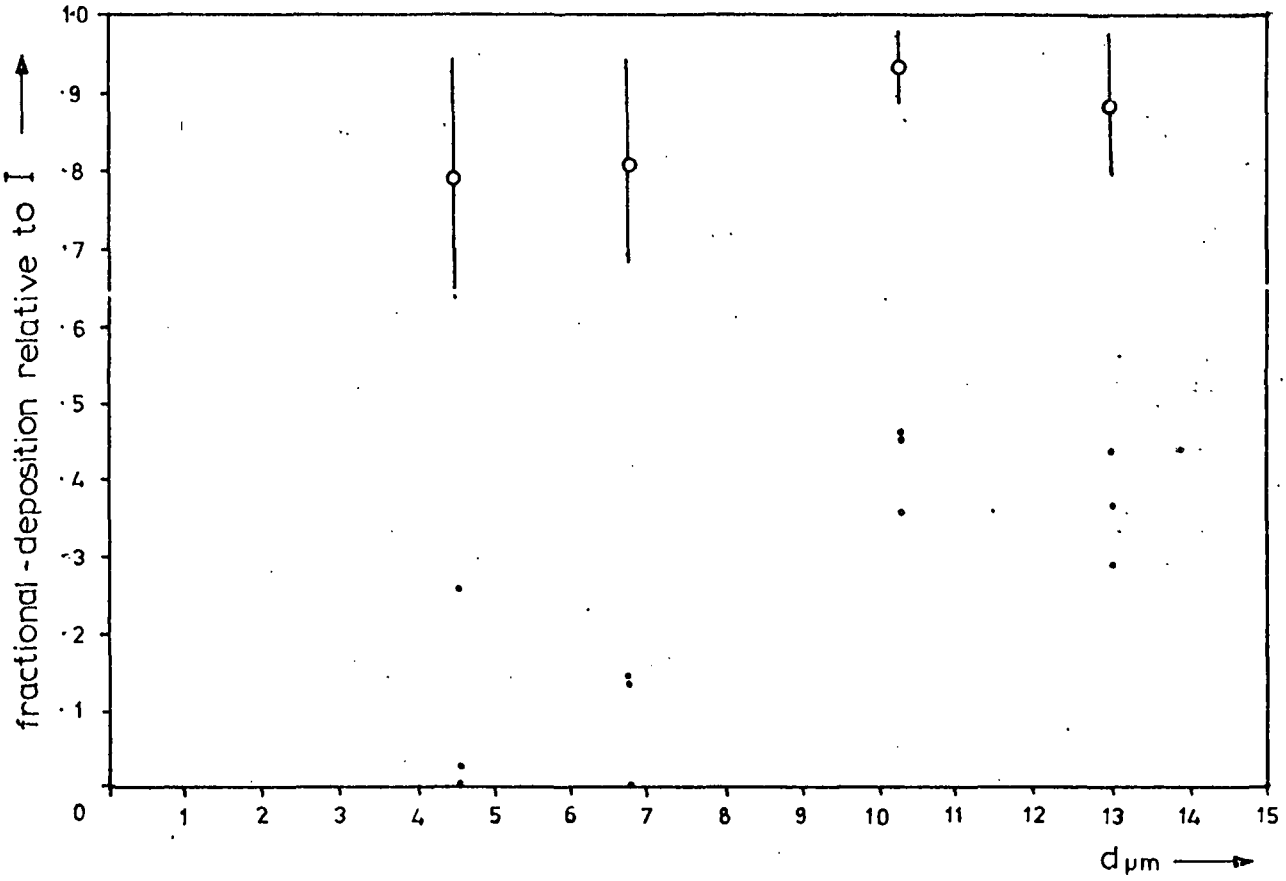

Figure 4.2.3: $f_s(x)$ vs particle diameter (μm). Bars on $f_b(x)$ indicate 95% confidence limits about mean.

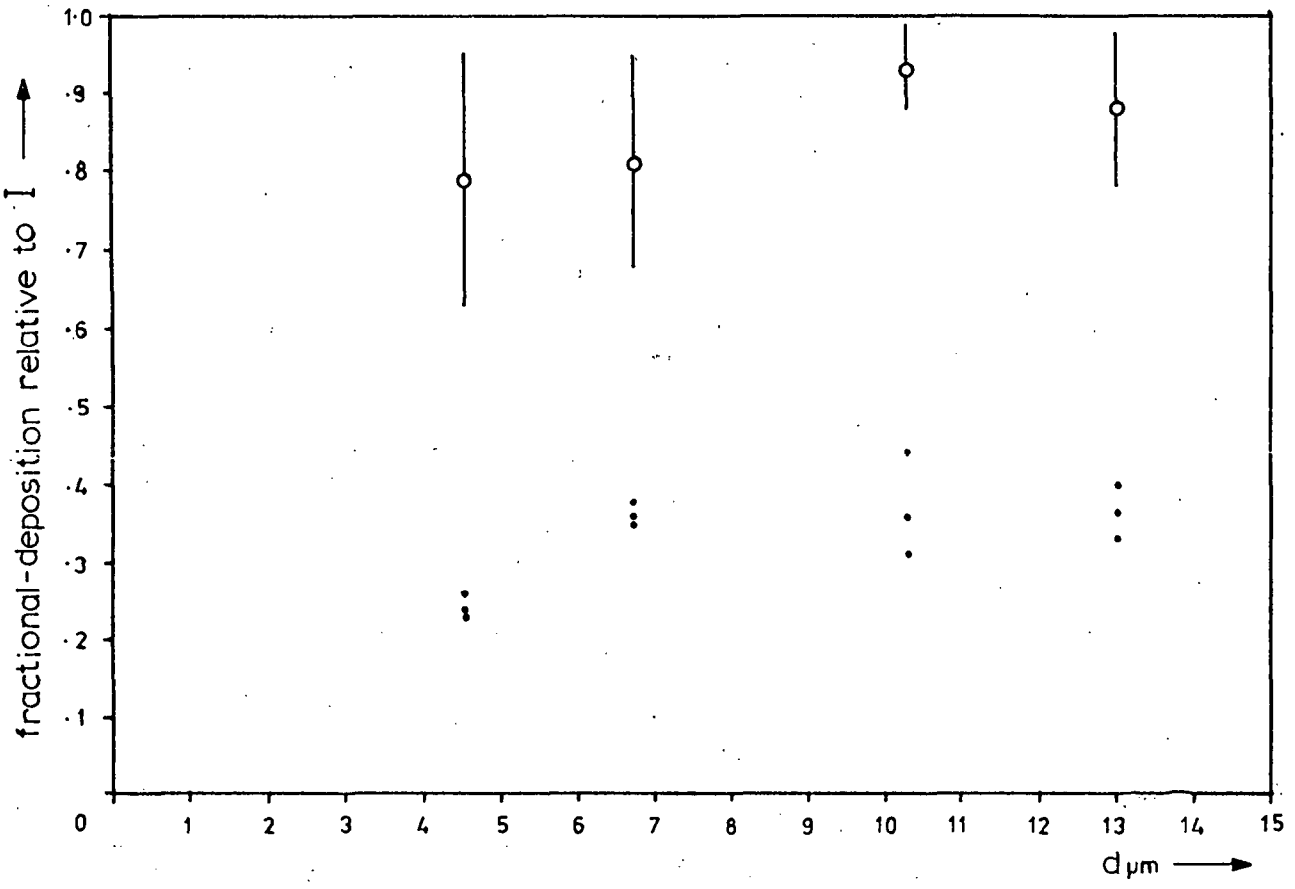

Figure 4.2.4: $f_c(x)$ vs particle diameter (μm). Bars on $f_o(x)$ indicate 95% confidence limits about mean.

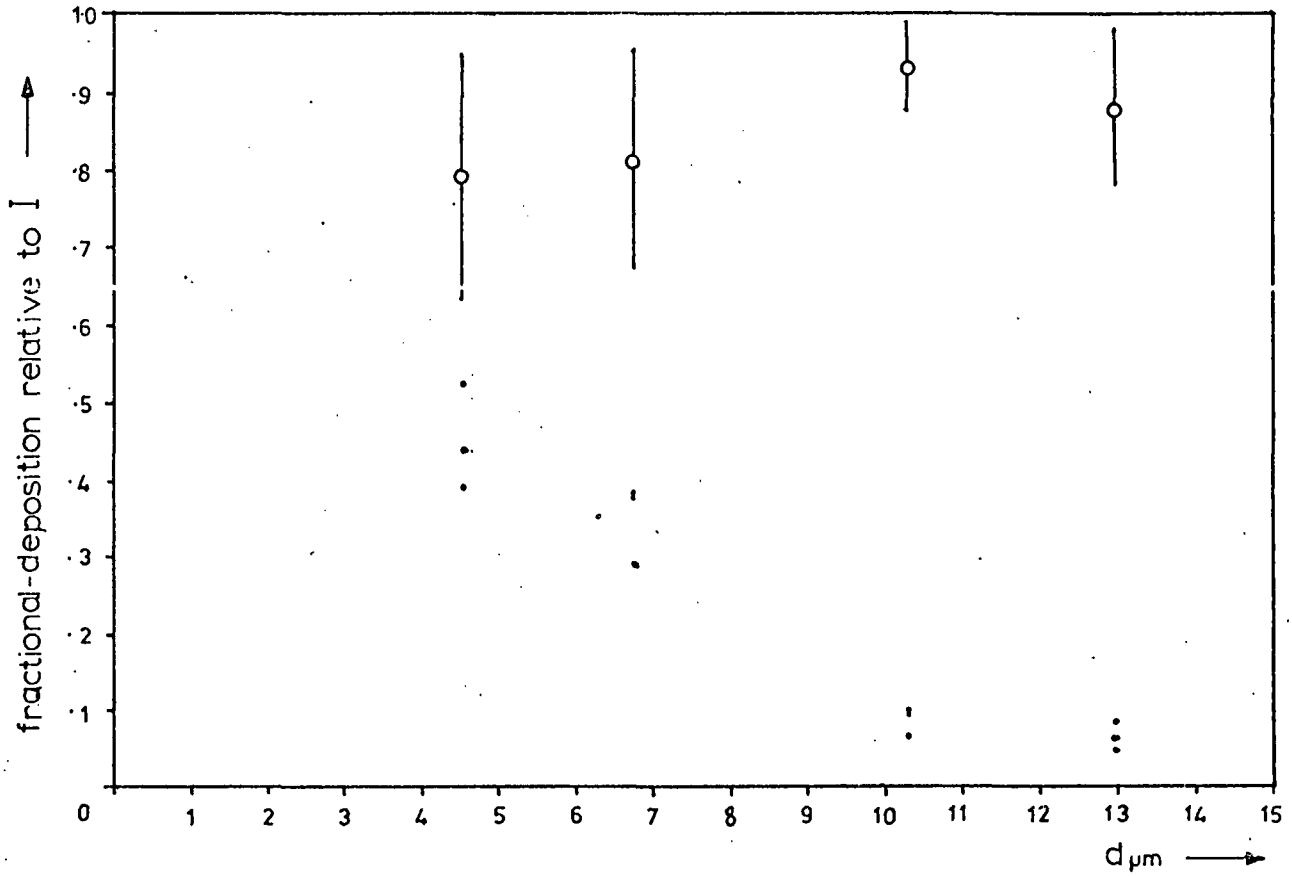

Figure 4.2.5: $f_R(I)$ vs particle diameter (μm). Bars on $f_D(I)$ indicate 95% confidence limits about mean.

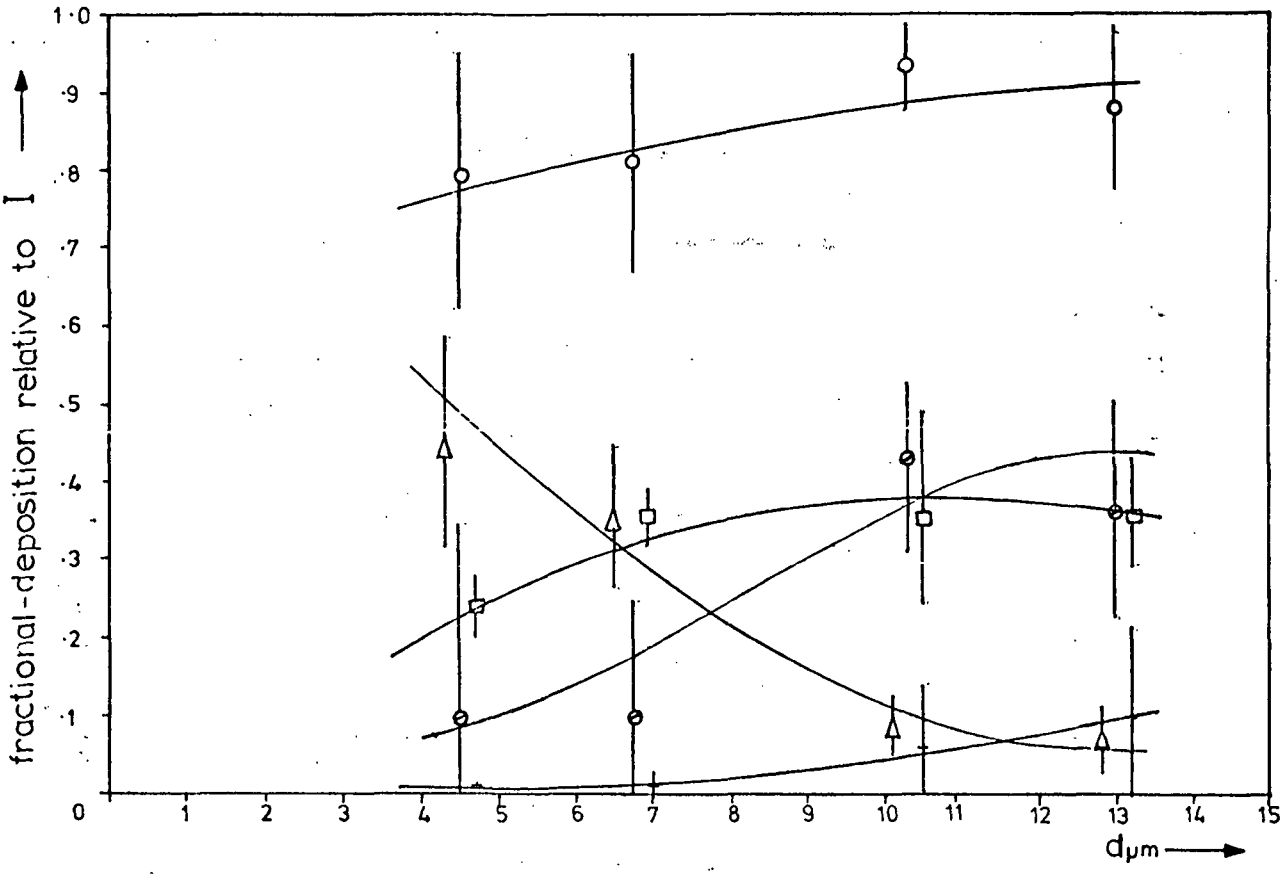

fW(I)

fS(I)

fC(I)

fR(I)

fD(I)

Figure 4.2.6(A): Average values of $f_W(I)$, $f_S(I)$, $f_C(I)$, $f_R(I)$ and $f_D(I)$, vs particle diameter (μm). Bars indicate 95% confidence limits about mean. Lines drawn by eye-fit.

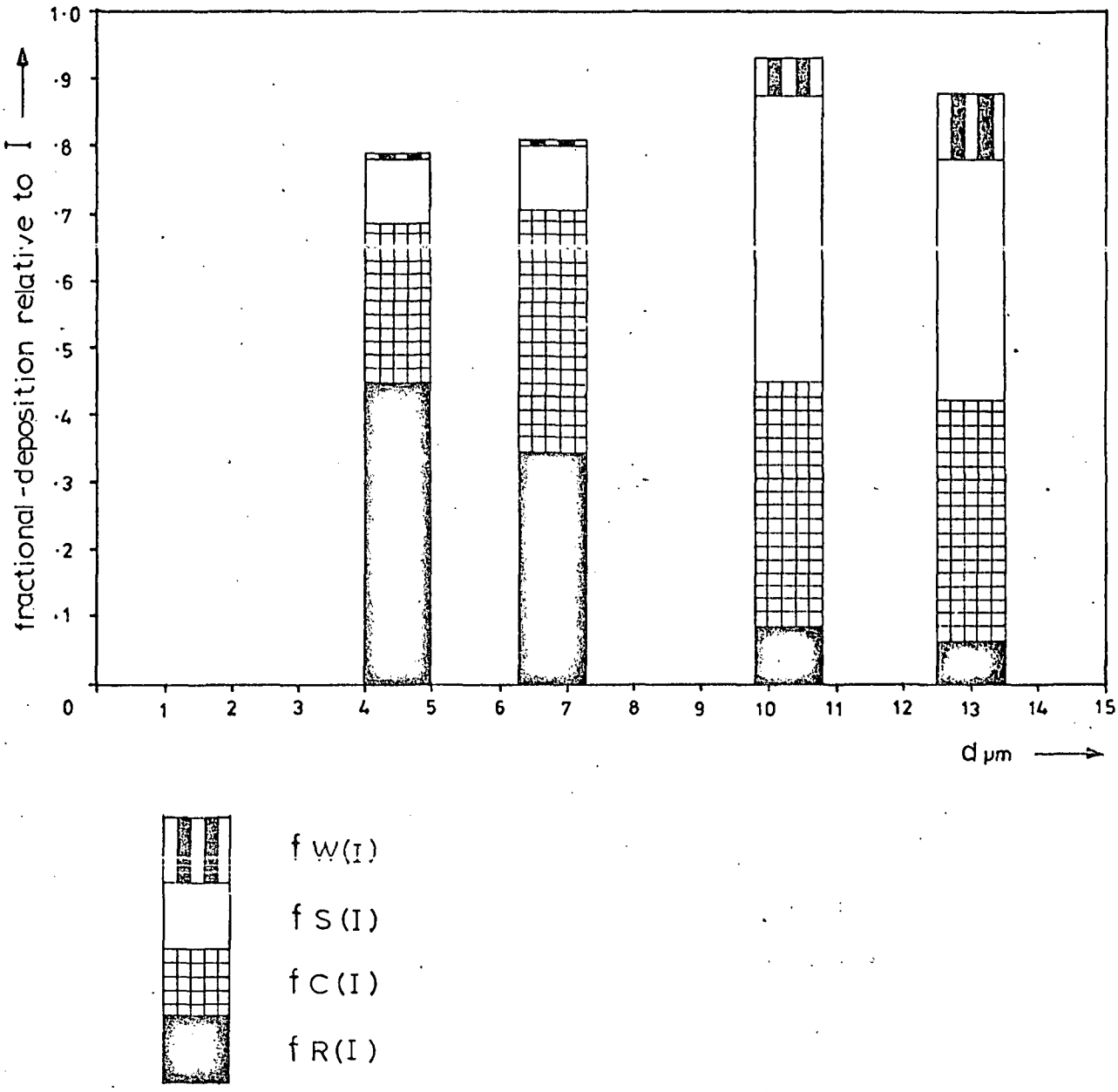

Figure 4.2.6(B): Average values of $f_W(I)$, $f_S(I)$, $f_C(I)$ and $f_R(I)$, vs particle diameter (μm), expressed in histogram form.

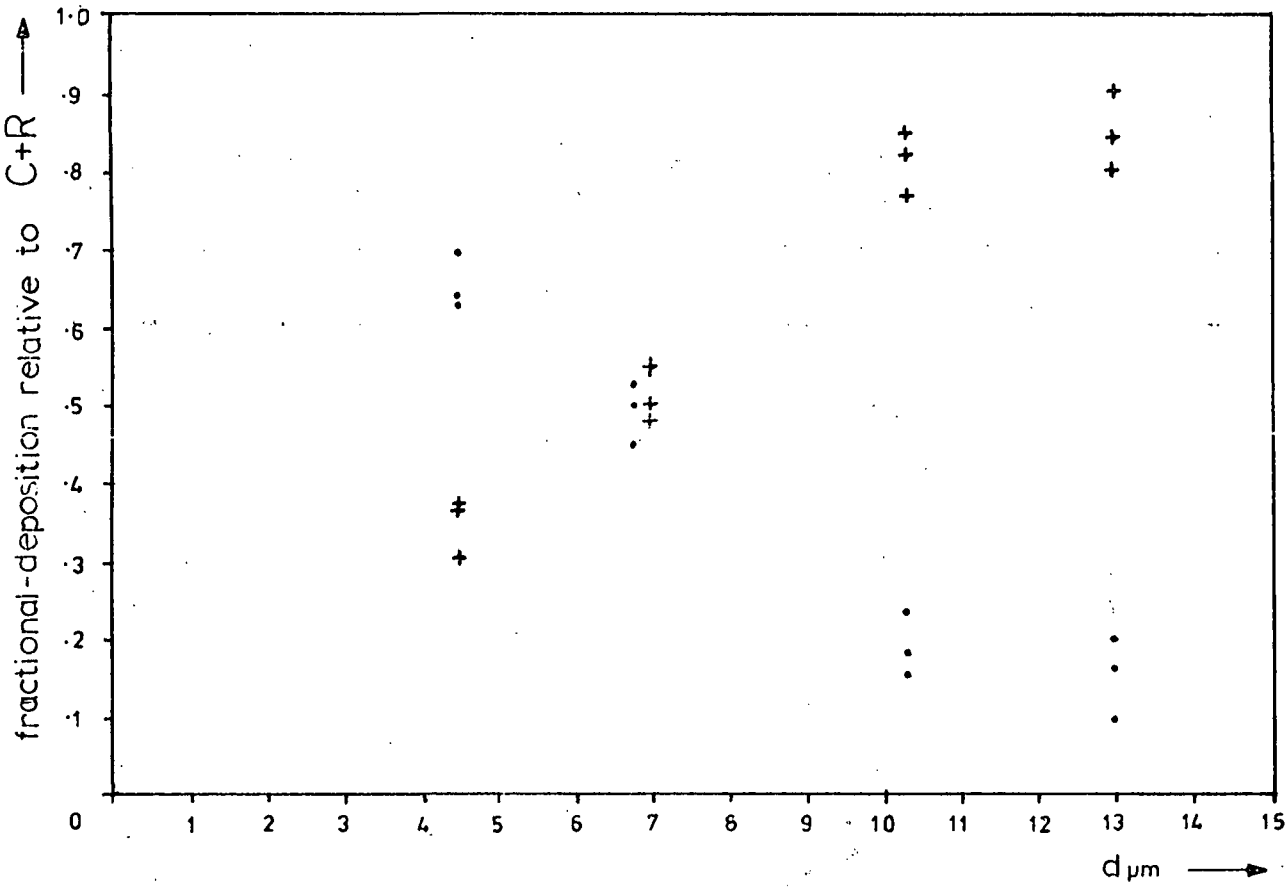

• fR(C+R)

+ fC(C+R)

Figure 4.2.7: $f_{C(C+R)}$, $f_{R(C+R)}$ vs particle diameter (μm).

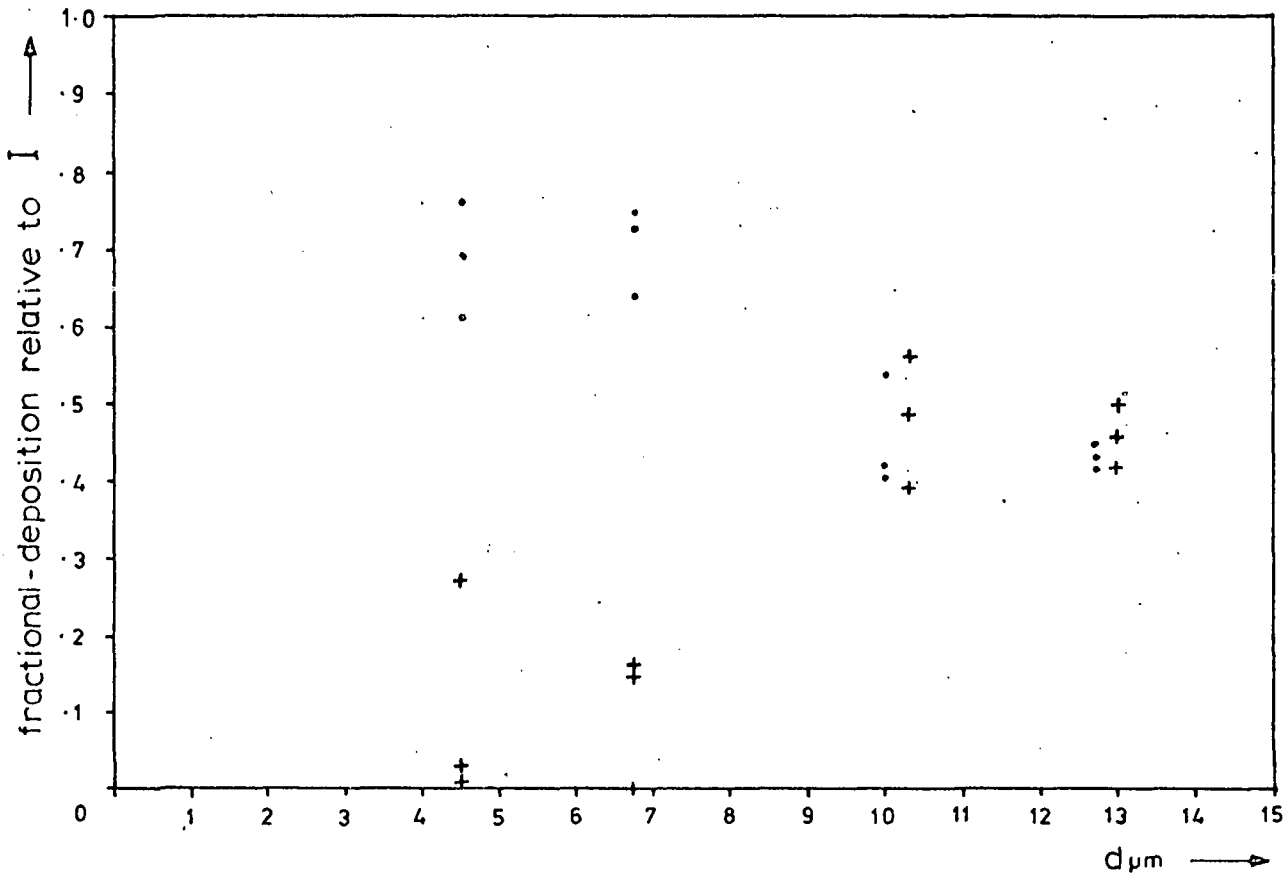

Figure 4.2.8: $f_{c+R}(x)$, $f_{w+s}(x)$, vs particle diameter (μm).

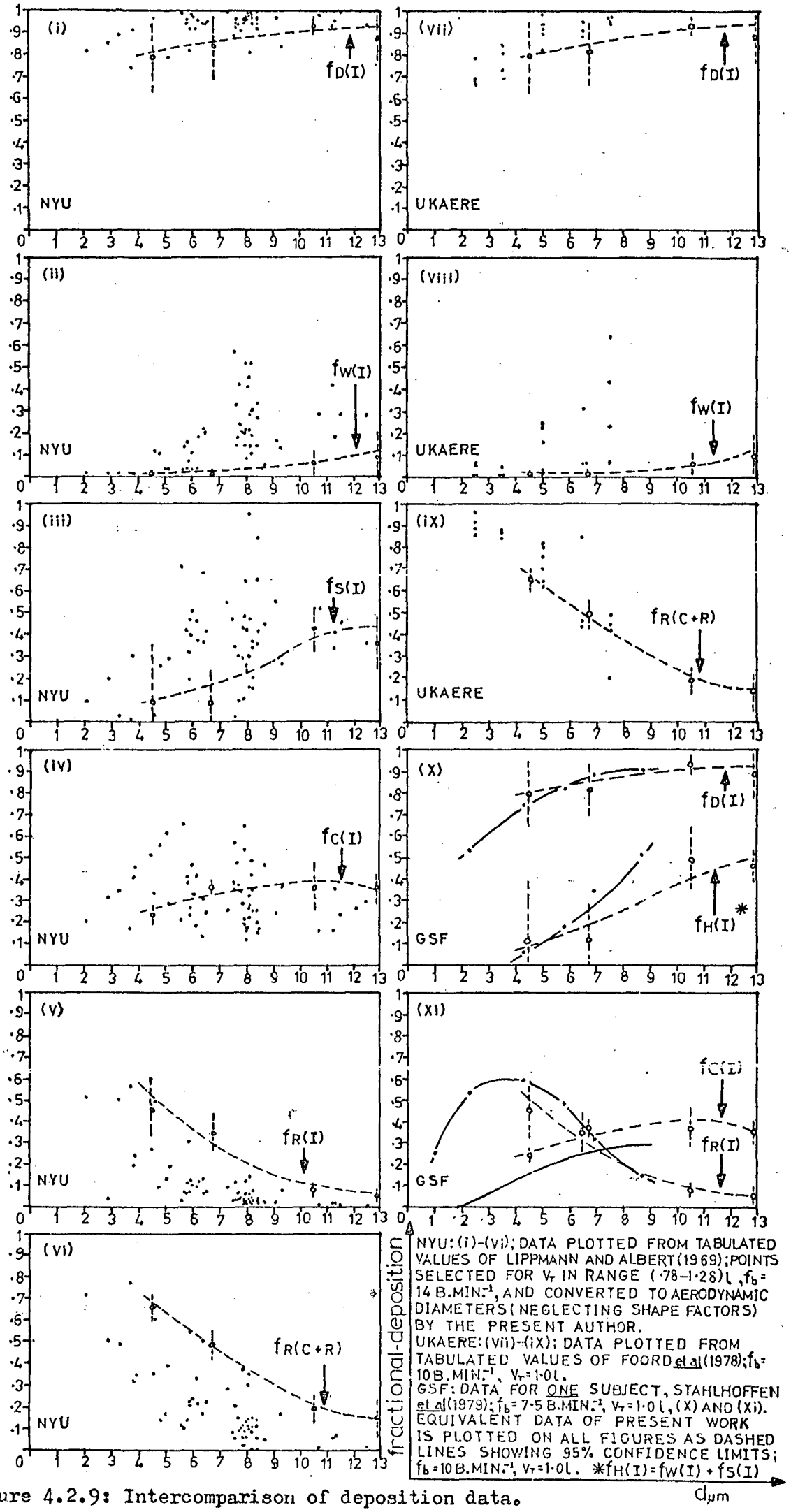

NYU: (i)-(vi); DATA PLOTTED FROM TABULATED VALUES OF LIPPMANN AND ALBERT (1969); POINTS SELECTED FOR V_T IN RANGE (·78–1·28) l, f_b = 14 B.MIN.$^{-1}$, AND CONVERTED TO AERODYNAMIC DIAMETERS (NEGLECTING SHAPE FACTORS) BY THE PRESENT AUTHOR.
UKAERE: (vii)-(ix); DATA PLOTTED FROM TABULATED VALUES OF FOORD et al (1978); f_b = 10 B.MIN.$^{-1}$, V_T = 1·0 l.
GSF: DATA FOR ONE SUBJECT, STAHLHOFFEN et al (1979); f_b = 7·5 B.MIN.$^{-1}$, V_T = 1·0 l, (X) AND (Xi).
EQUIVALENT DATA OF PRESENT WORK IS PLOTTED ON ALL FIGURES AS DASHED LINES SHOWING 95% CONFIDENCE LIMITS; f_b = 10 B.MIN.$^{-1}$, V_T = 1·0 l. *$f_H(I) = f_W(I) + f_S(I)$

Figure 4.2.9: Intercomparison of deposition data.

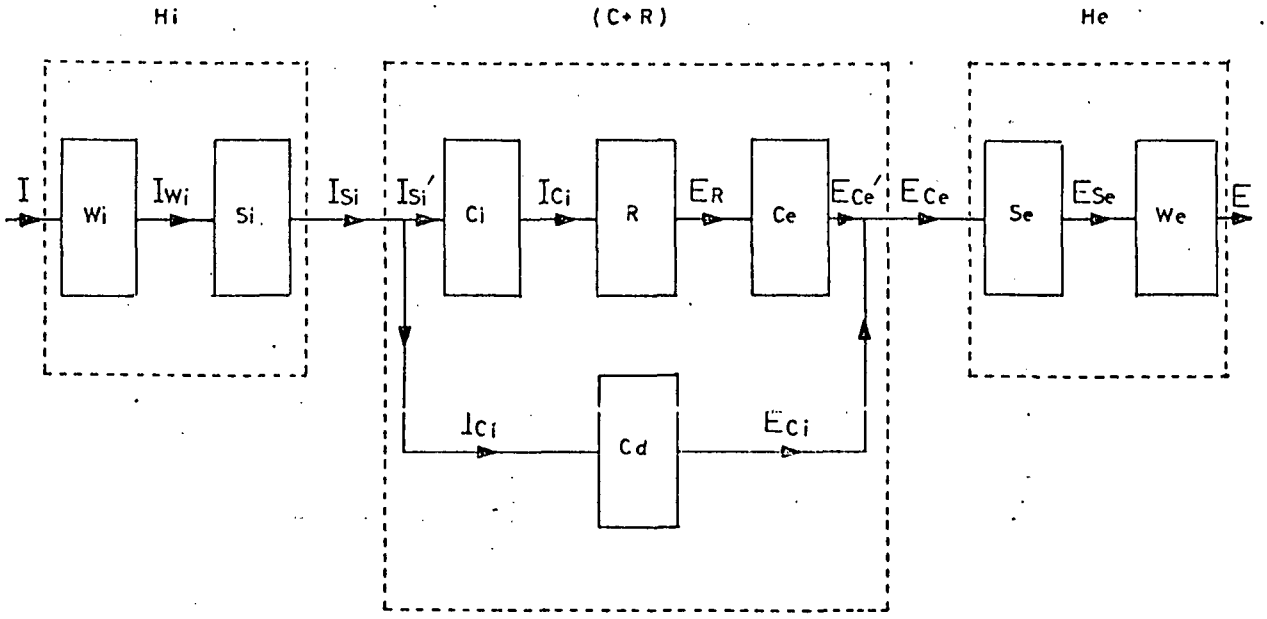

Figure 4.2.10: Lung model.

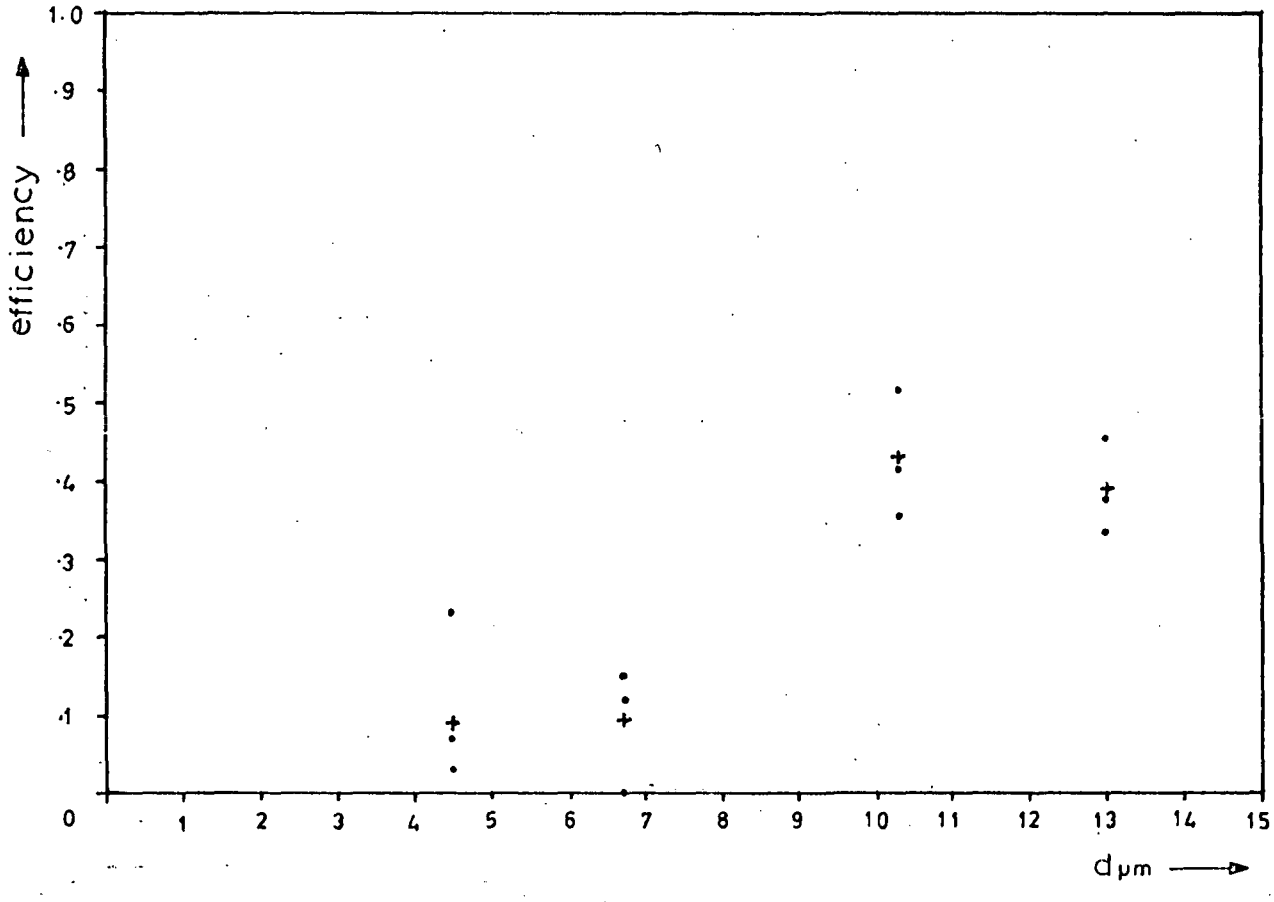

+ = mean

Figure 4.2.11: ϵ_H vs particle diameter (μm), q_2=1.

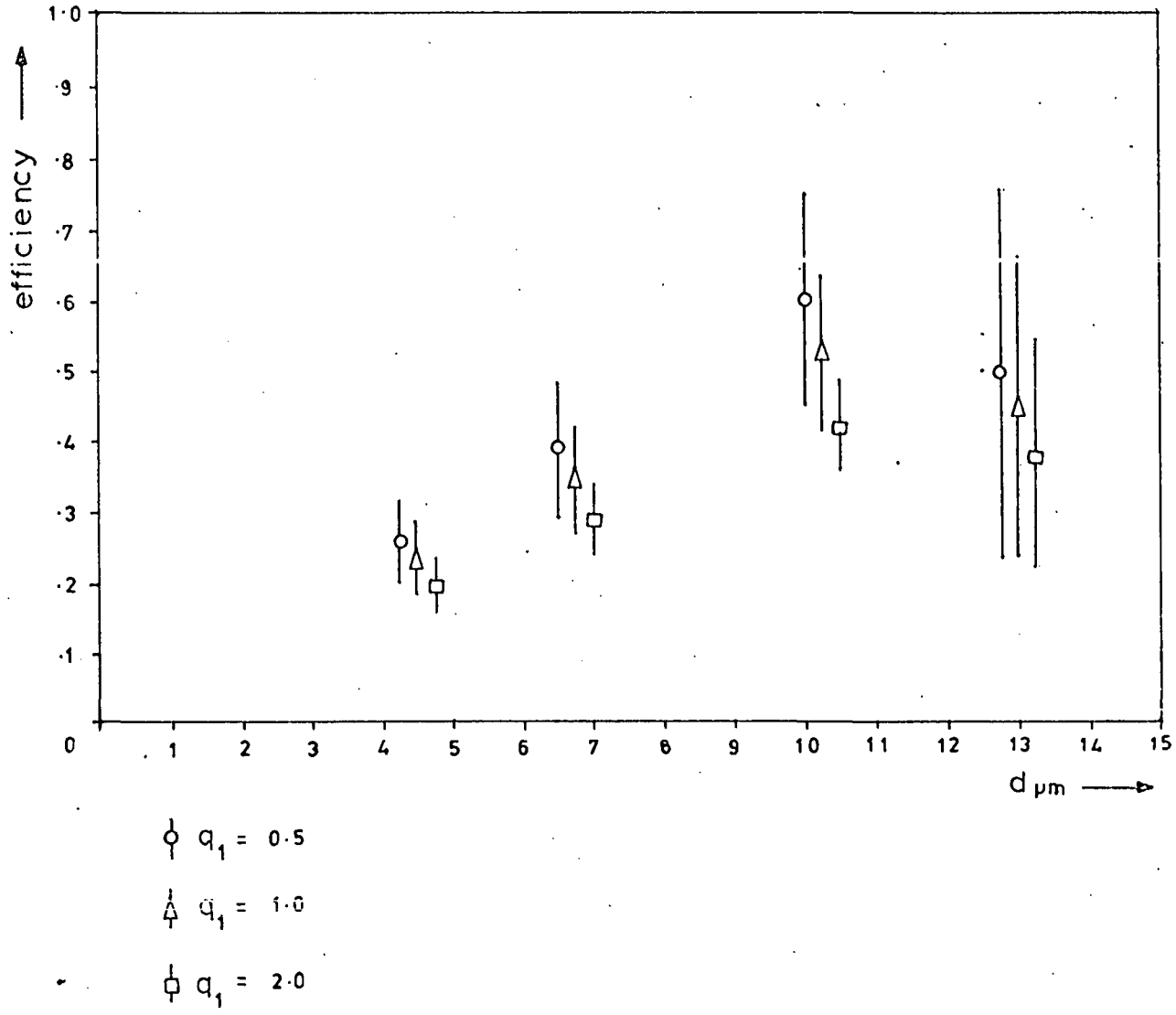

Figure 4.2.12: ϵ_c vs particle diameter (μm) for a range of q_1 values ($q_2 = q_3 = 1$). Bars indicate 95% confidence limits about mean.

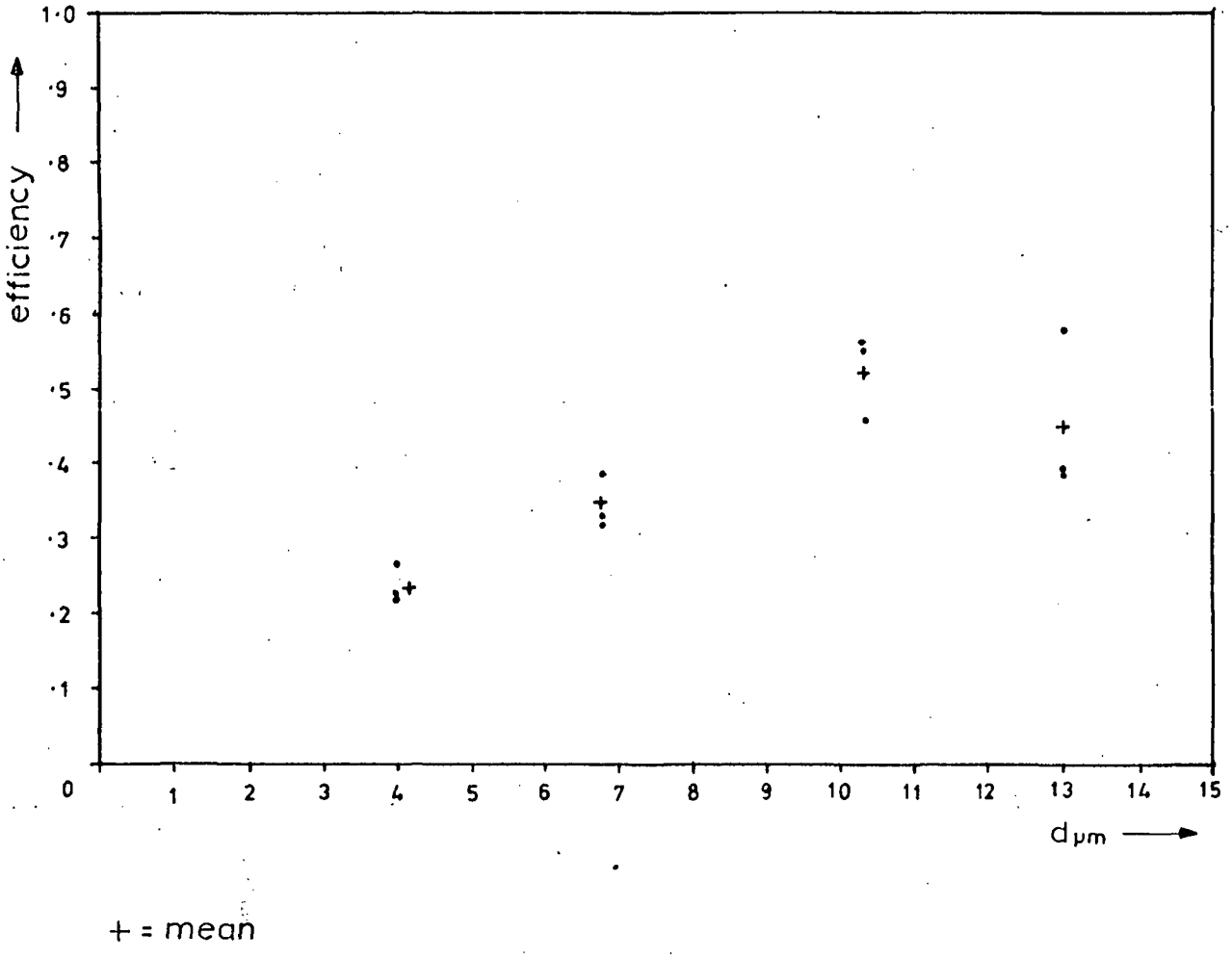

Figure 4.2.13: ϵ_c vs particle diameter (μm) $q_3 = q_2 = q_1 = 1$.

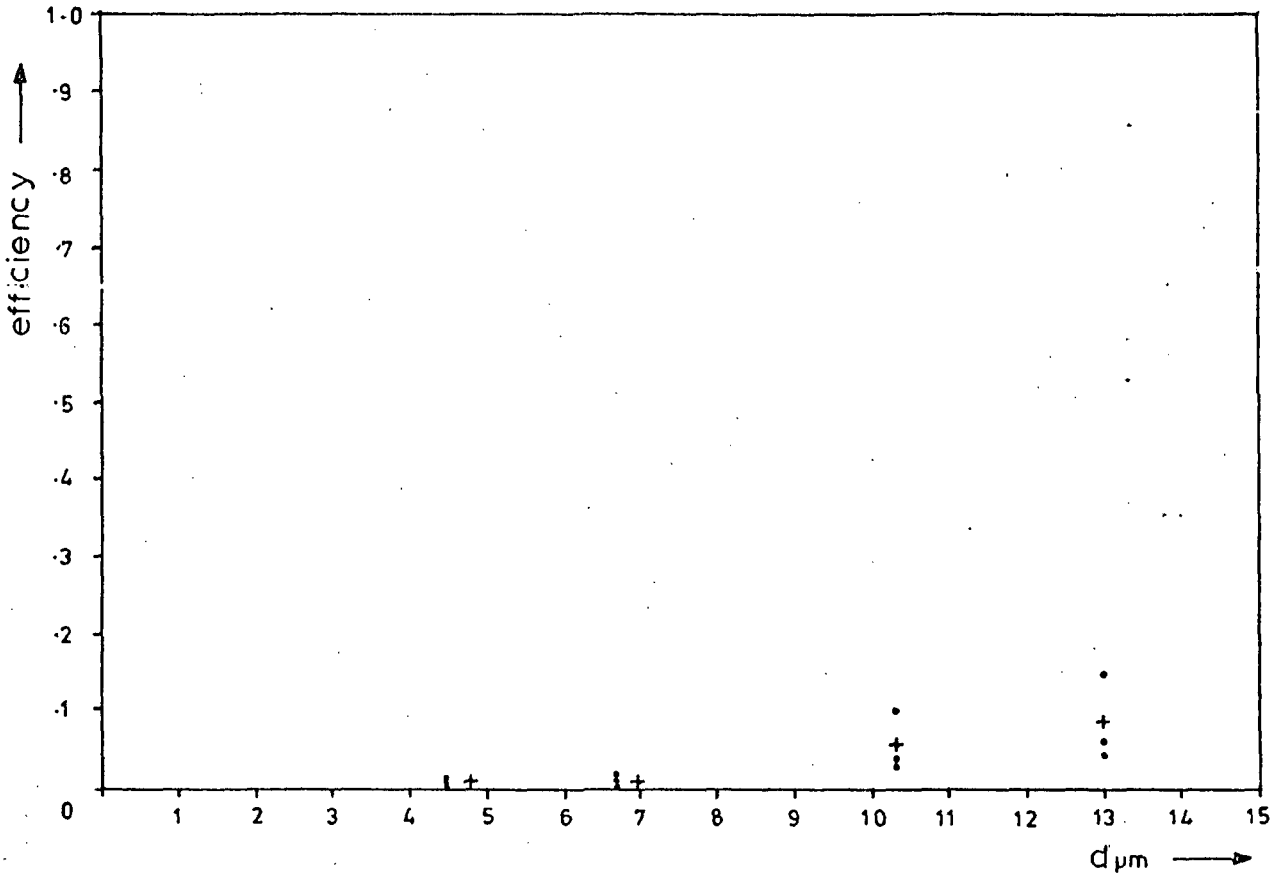

Figure 4.2.14: ϵ_w vs particle diameter. $q_3 = q_2 = q_1 = 1$.

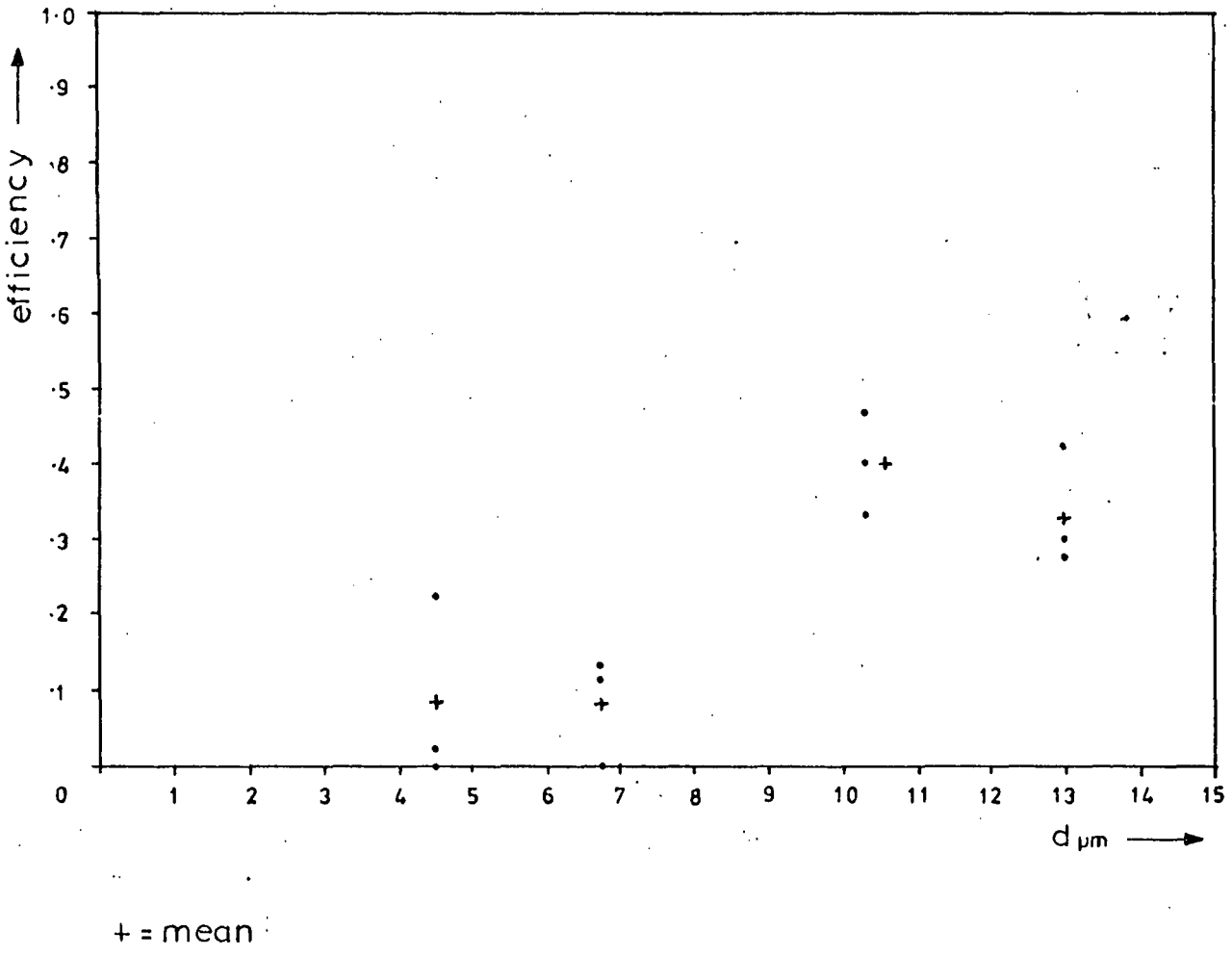

Figure 4.2.15: ϵ_s vs particle diameter (μm) $q_3 = q_2 = q_1 = 1$.

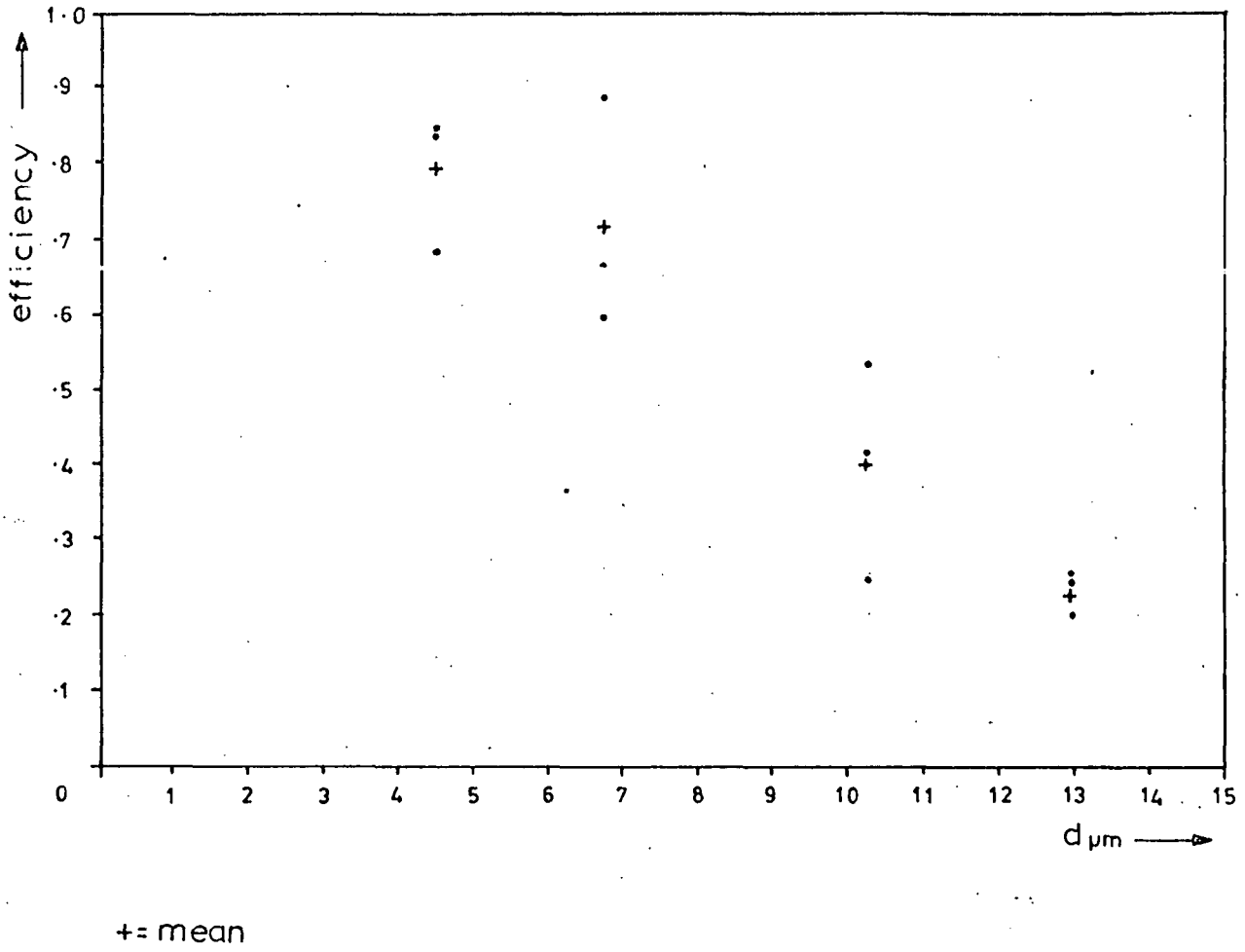

Figure 4.2.16: ϵ_R vs particle diameter (μm). $q_3 = q_2 = q_1 = 1$.

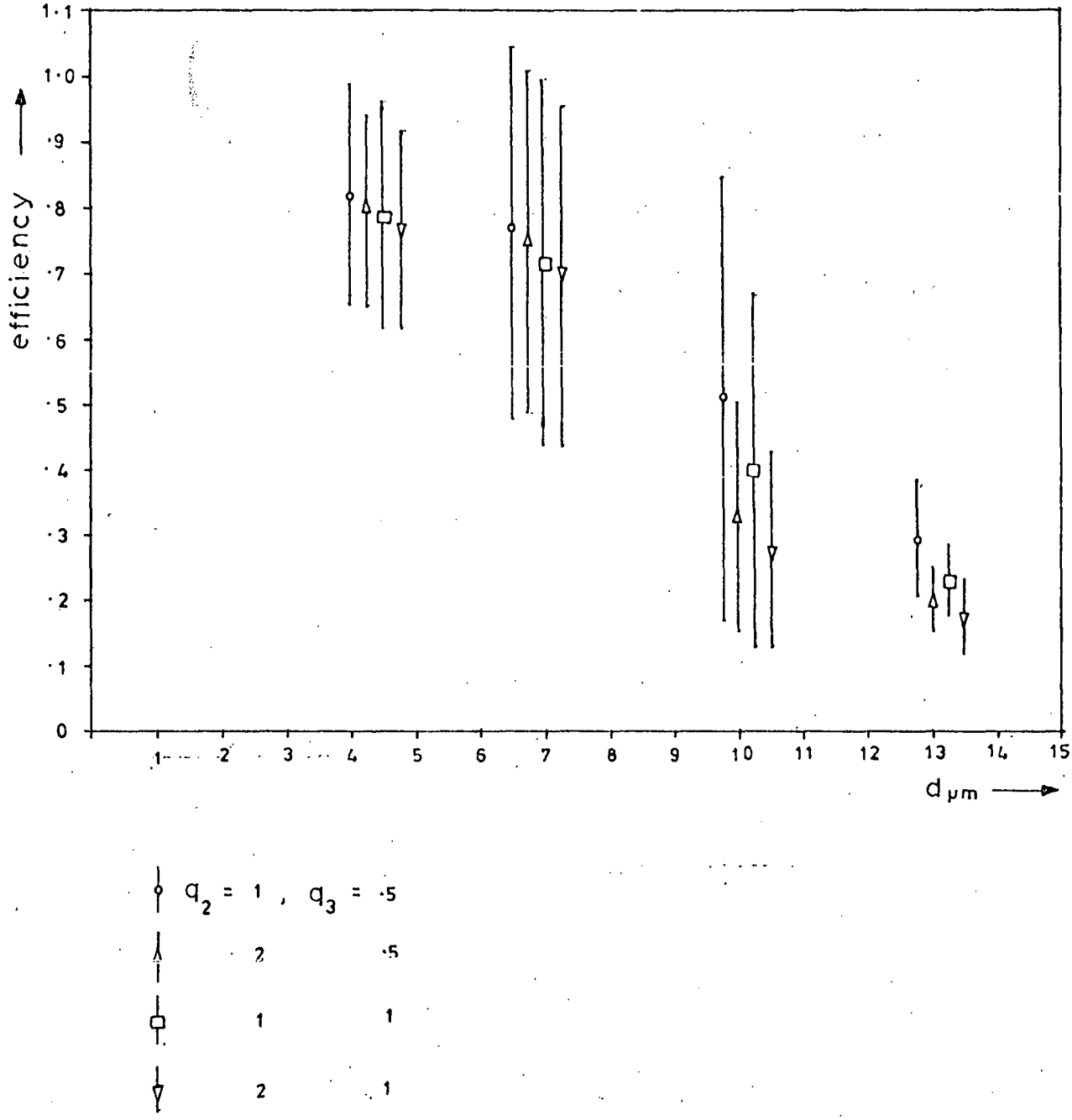

Figure 4.2.17: ϵ_R vs particle diameter (μm) for a wide range of assumptions. Bars indicate 95% confidence limits about mean.

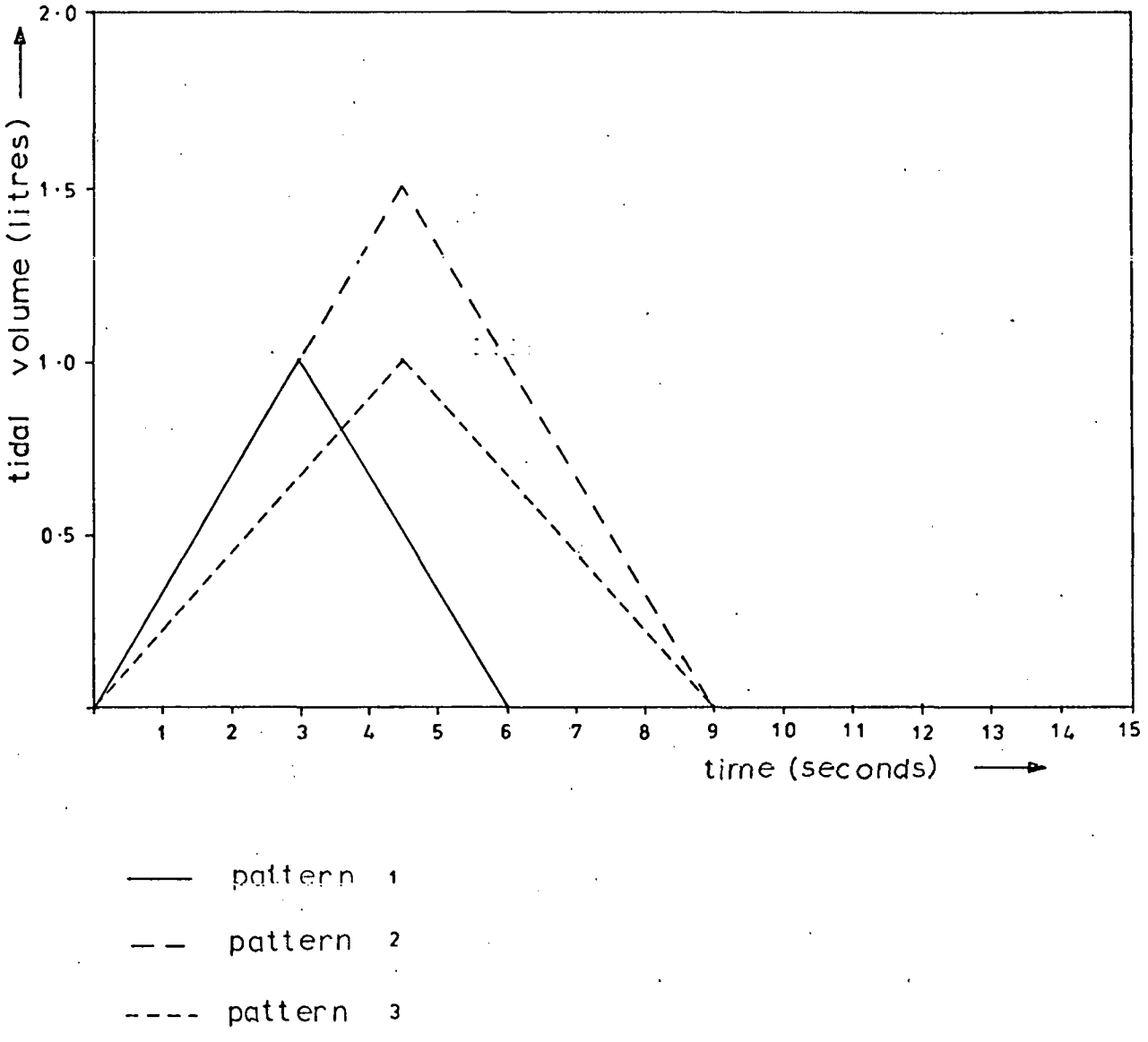

Figure 4.2.18: Breathing pattern study.

pattern	subject	$f_{D(I)}$	$f_{W(I)}$	$f_{S(I)}$	$f_{C(I)}$	$f_{R(I)}$
1. V_T = 1·0 l f_b = 9·80	DCFM	·7020	·0088	0	·2579	·4353
	AM	·7945	·0087	·0265	·2331	·5262
	AR	·8776	·0116	·2555	·2210	·3895
	group av.	·7914	·0097	·0940	·2373	·4503
2. V_T = 1·5 l f_b = 6·64	ATM	·8356	·0027	·0774	·1239	·6316
	FH	·755	·0005	·0371	·1869	·5321
	RH	·8292	0	·1780	·2084	·4428
	group av.	·8071	·0011	·0976	·1731	·5355
3. V_T = 1·0 l f_b = 6·78	VC	·8372	·0034	0	·3335	·5003
	MS *	·7308	·0044	·0639	·1623	·5002
	JV	·8466	·0010	·0204	·4456	·3796
	group av.	·8049	·0029	·0281	·3138	·4600

* average of 2 results

Table 4.2.3: Deposition fractions in variable breathing pattern study.

pattern	subject	f_b	t_{p1}	inh: exh	V_T	e.r.v.+ V_T
1.	DCFM	9·17	·70	1 : 2·20	1·0	n.d.
	AM	10·09	·62	1 : 2·50	1·0	3·17
	AR	10·15	·31	1 : 0·96	1·0	2·30
	group av.	9·80	·54	1 : 1·89	1·0	2·74
2.	ATM	6·77	·44	1 : 1·14	1·5	3·82
	FH	6·58	·35	1 : 1·18	1·5	4·54
	RH	6·57	·27	1 : 1·13	1·5	3·26
	group av.	6·64	·35	1 : 1·15	1·5	3·91
3.	VC	6·95	·66	1 : 1·48	1·0	3·78
	MS *	6·71	·37	1 : 1·05	1·0	3·00
	JV	6·67	·37	1 : 1·56	1·0	2·27
	group av.	6·78	·47	1 : 1·39	1·0	3·02

n.d. = not determined

* = average of 2 results

Table 4.2.4: Breathing conditions in variable breathing pattern study.

subject	$d_{\mu m}$	$f_{D(I)}$	$f_{W(I)}$	$f_{S(I)}$	$f_{C(I)}$	$f_{R(I)}$
MS 1	4·53	·7312	·0045	·0873	·1471	·4923
MS 2	4·66	·7304	·0042	·0405	·1783	·5074
MS av.	4·60	·7308	·0044	·0639	·1623	·5002
PT 1	10·21	·8920	·0269	·3358	·4605	·0688
PT 2	10·55	·9180	·0434	·5693	·2519	·0534
PT av.	10·38	·9050	·0352	·4525	·3537	·0636

A. Deposition fractions.

subject	f_b	t_{p1}	inh:exh	V_T	erv + V_T
MS 1	6·70	·29	1:1·09	1·0	3·00
MS 2	6·72	·44	1:1·01	1·0	3·00
MS av	6·71	·37	1:1·05	1·0	3·00
PT 1	10·20	·34	1:0·91	1·0	2·65
PT 2	10·22	·30	1:1·05	1·0	2·65
PT av	10·21	·32	1:0·98	1·0	2·65

B. Breathing conditions.

Table 4.2.5: Reproducibility of results.

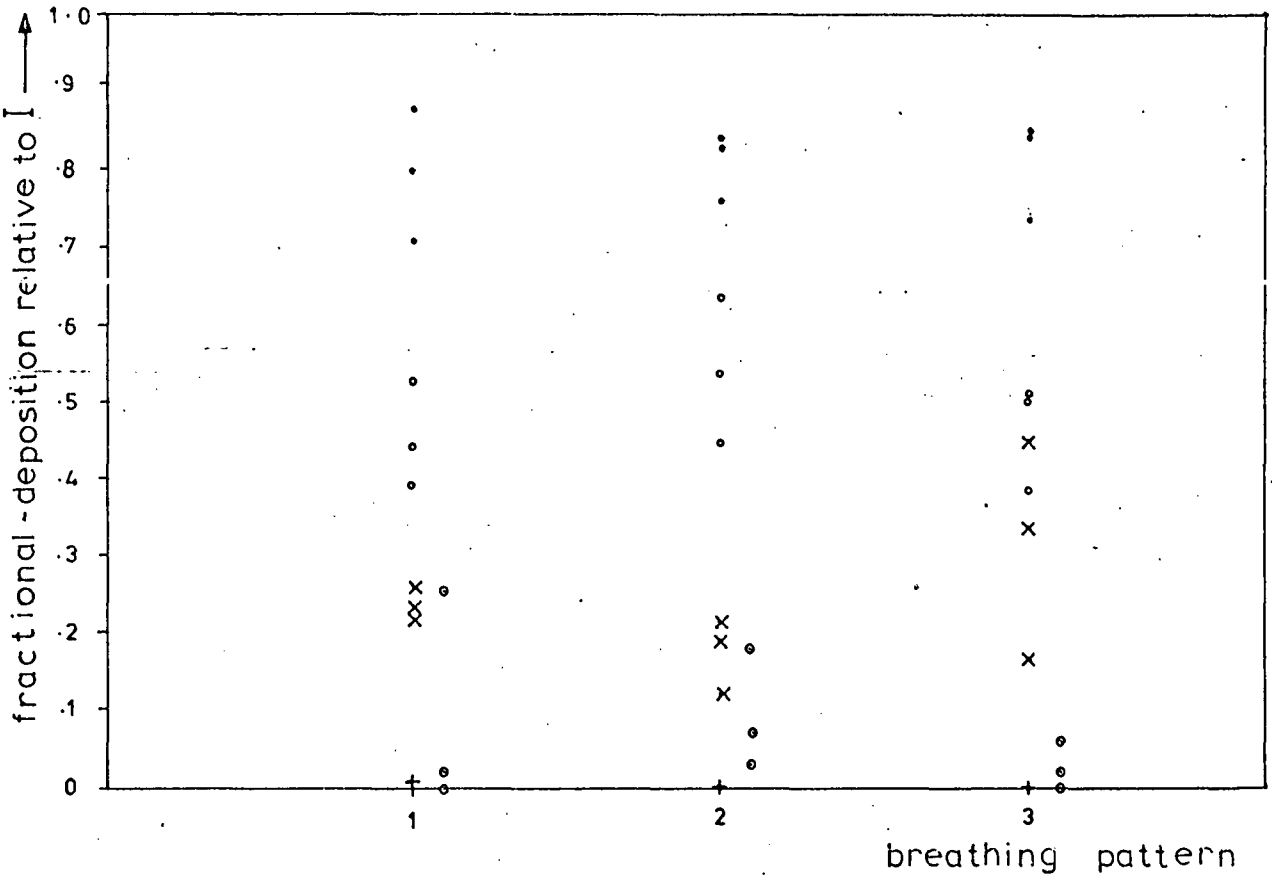

• fD(I)

+ fW(I)

∘ fS(I)

× fC(I)

∘ fR(I)

Figure 4.2.19: Breathing pattern results.

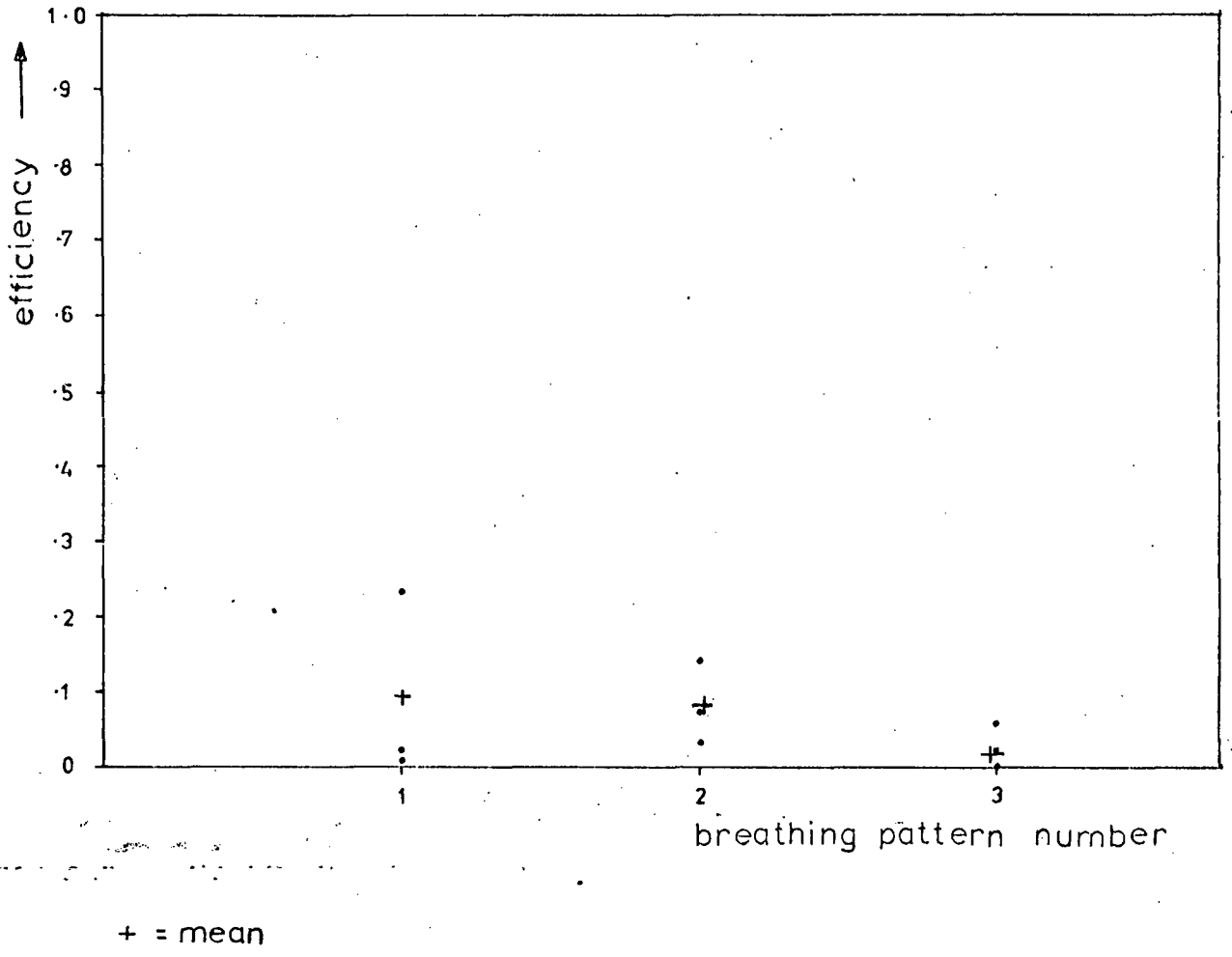

Figure 4.2.20: ϵ_H in breathing pattern study; $q_2 = q_1 = 1$.

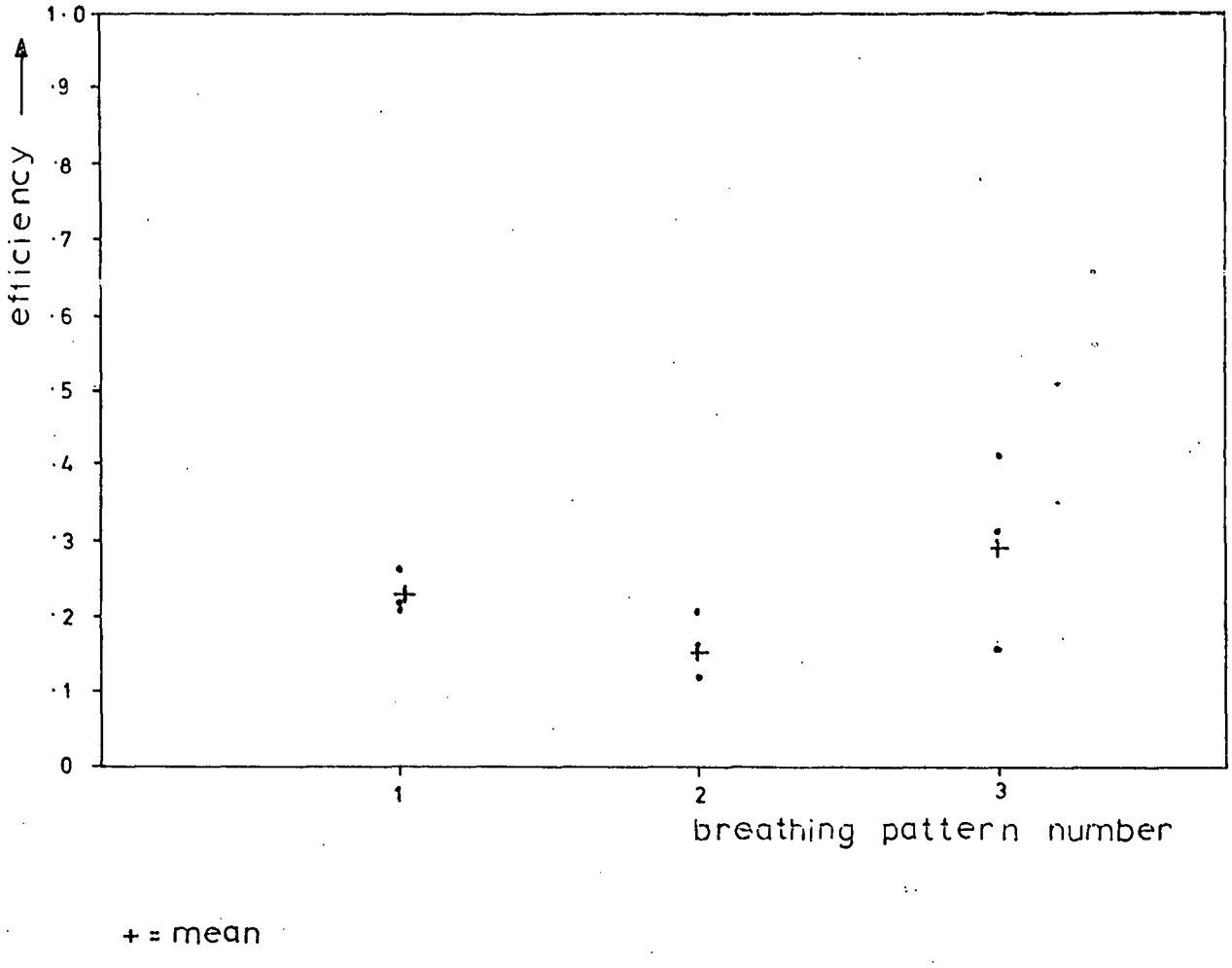

Figure 4.2.21: ϵ_c in breathing pattern study. $q_3 = q_2 = q_1 = 1$.

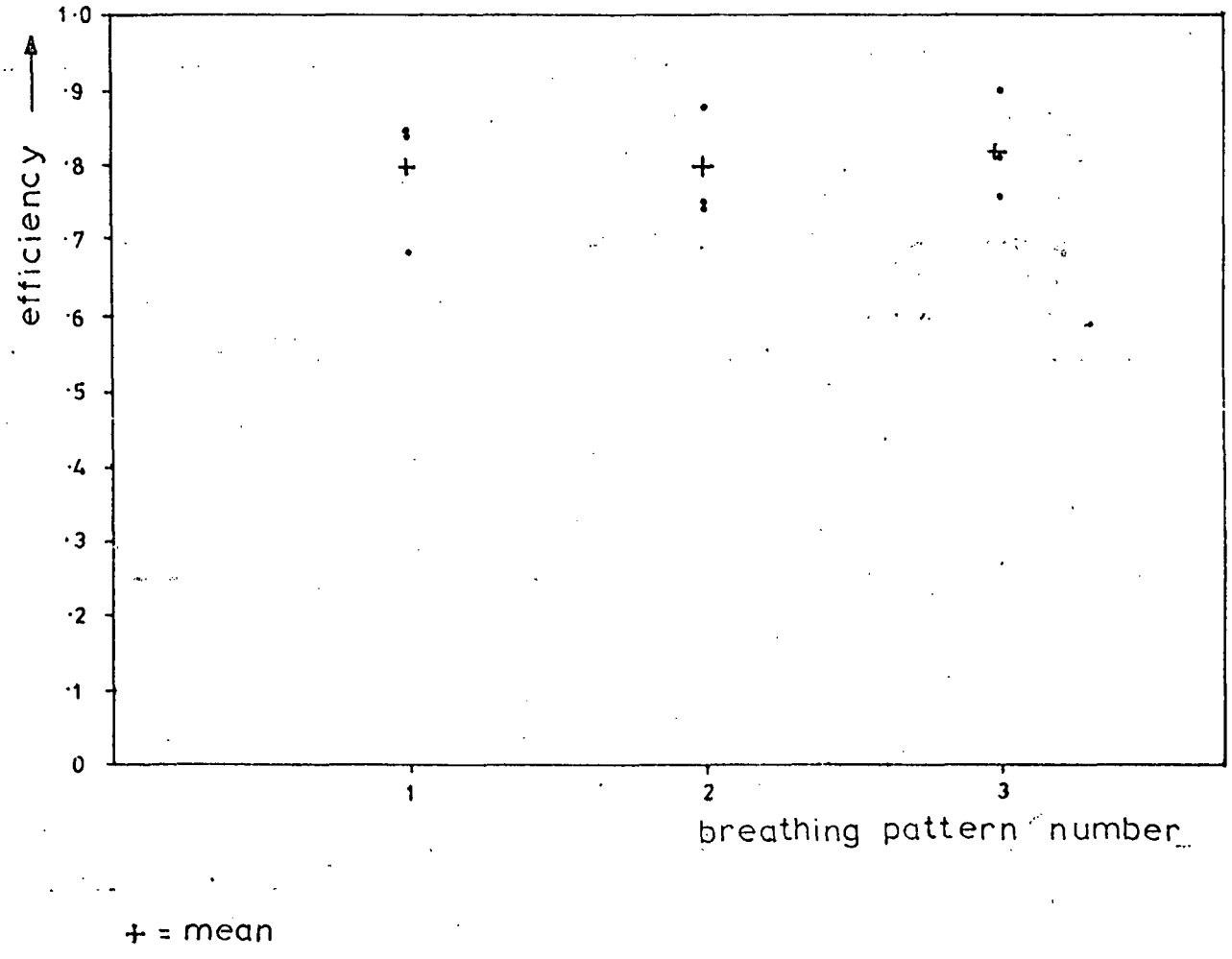

Figure 4.2.22: ϵ_R in breathing pattern study. $q_3 = q_2 = q_1 = 1$.

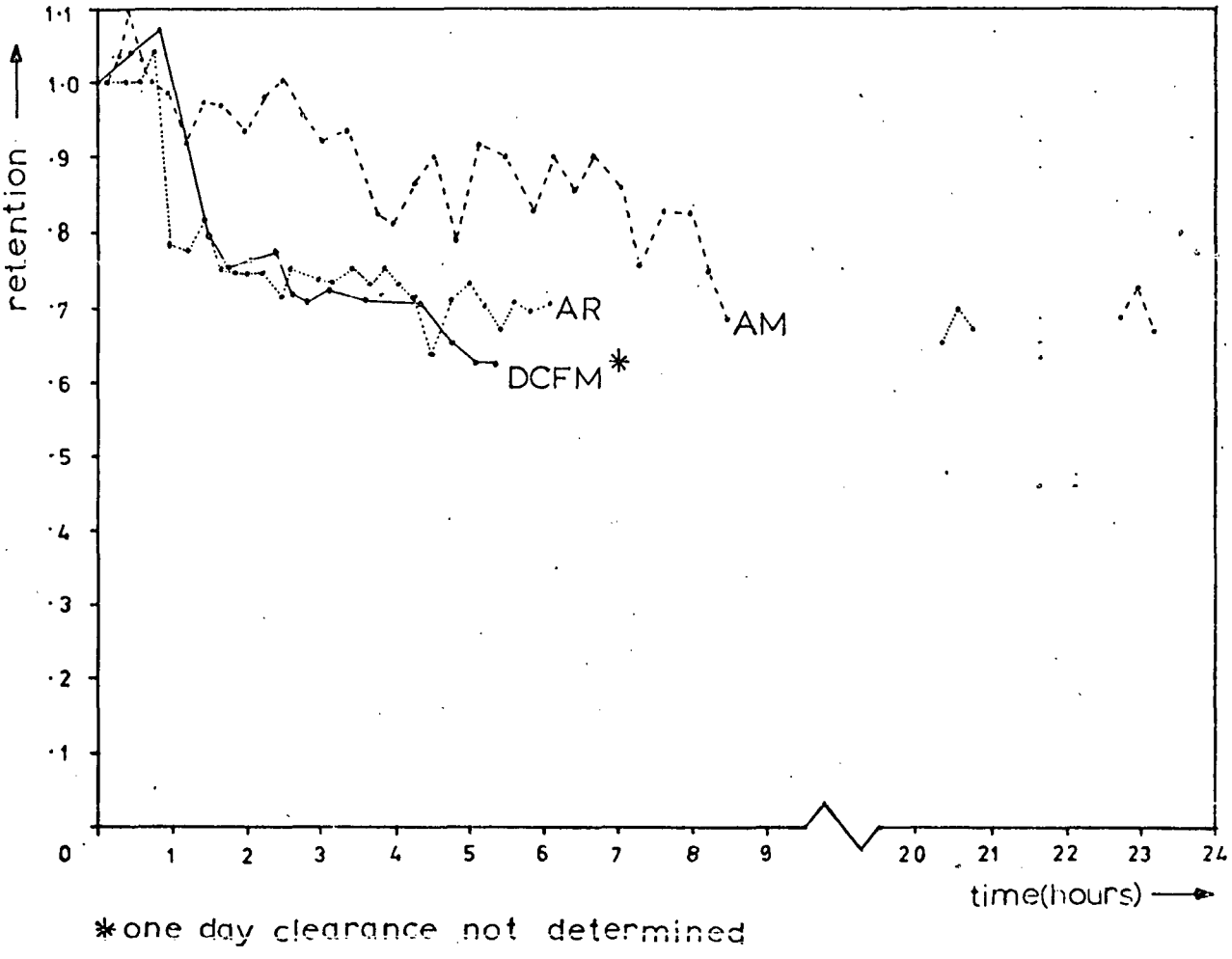

Figure 4.3.1: Clearance curves at $\bar{d} = 4{\cdot}5\,\mu m$.

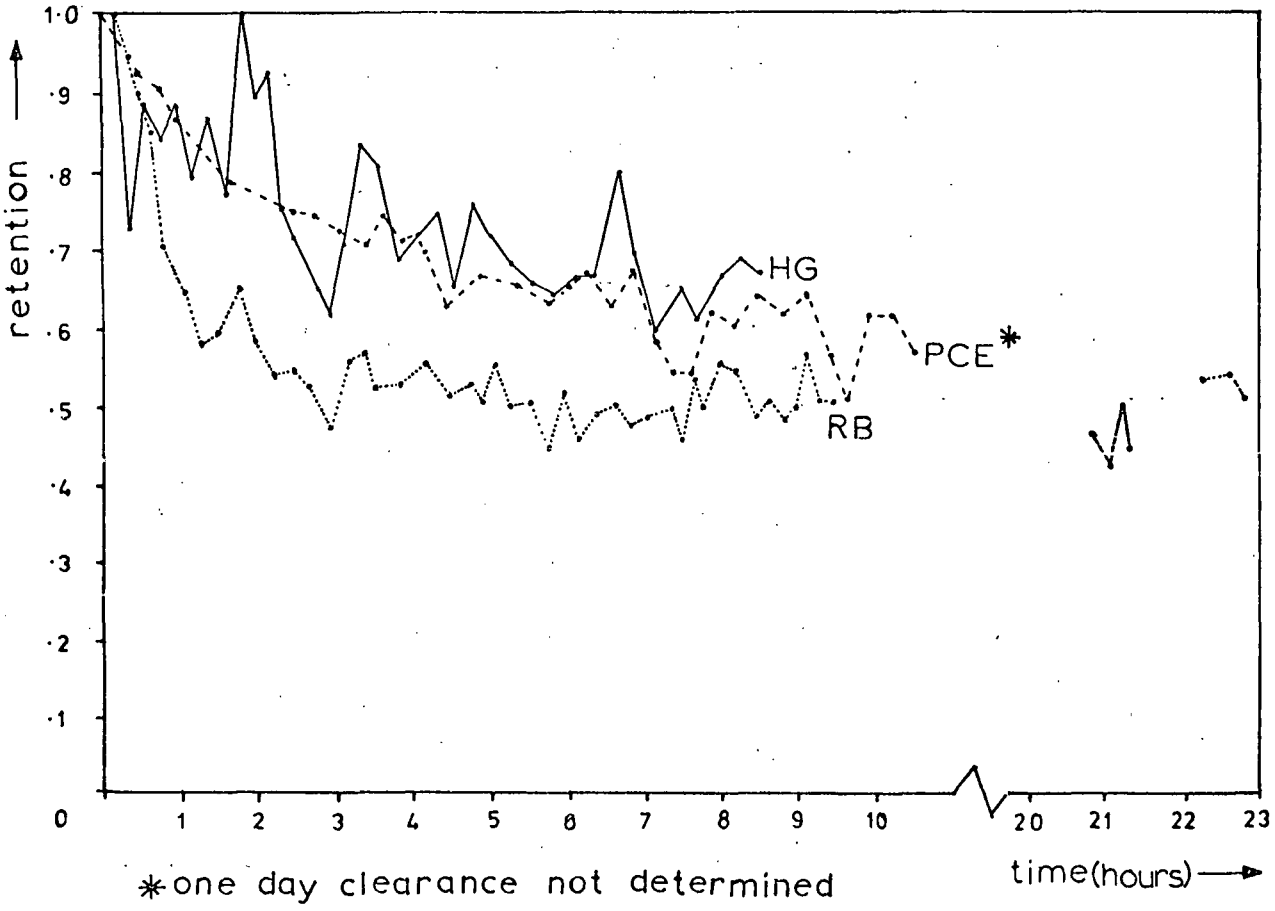

Figure 4.3.2: Clearance curves at $\bar{d} = 6{\cdot}7\ \mu m$.

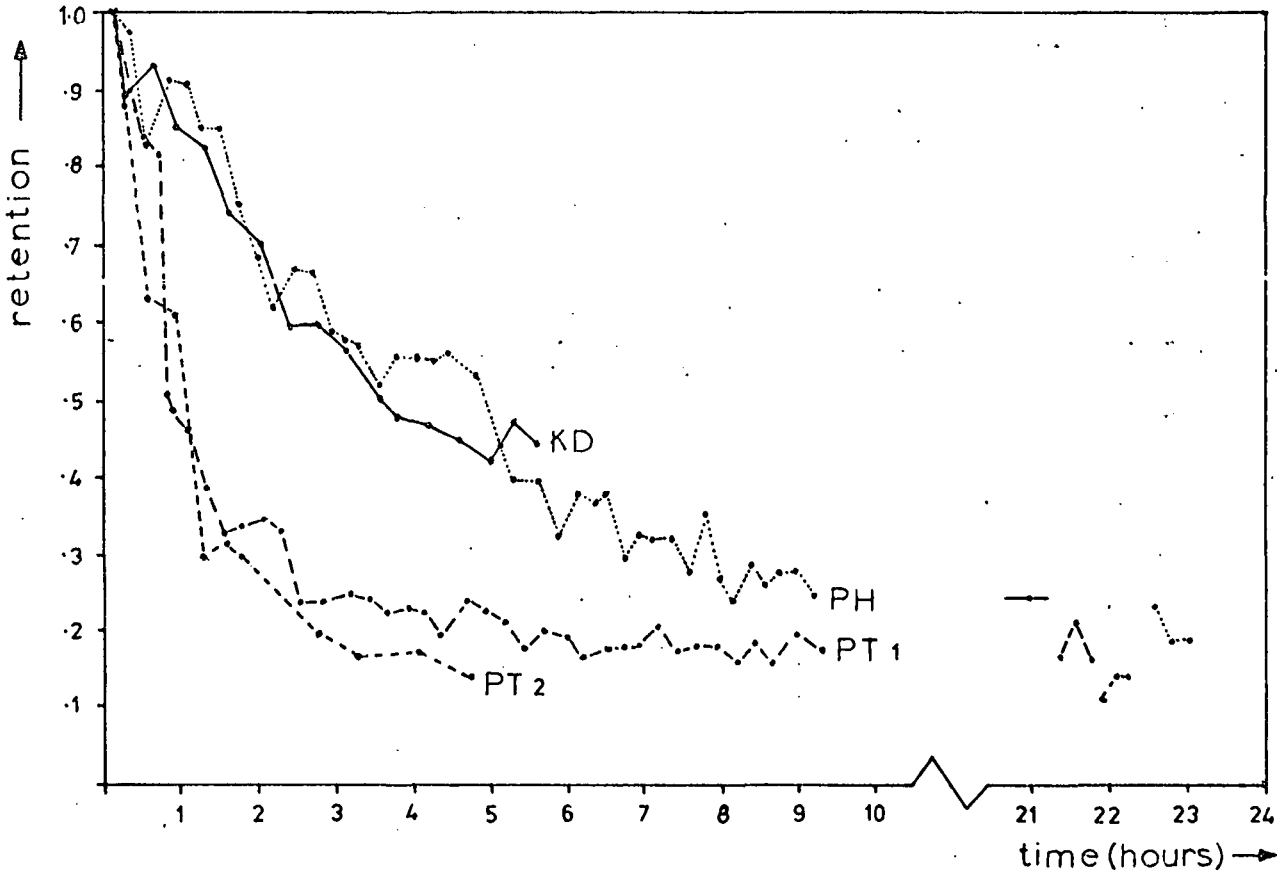

Figure 4.3.3: Clearance curves at $\bar{d}$ = 10·4μm.

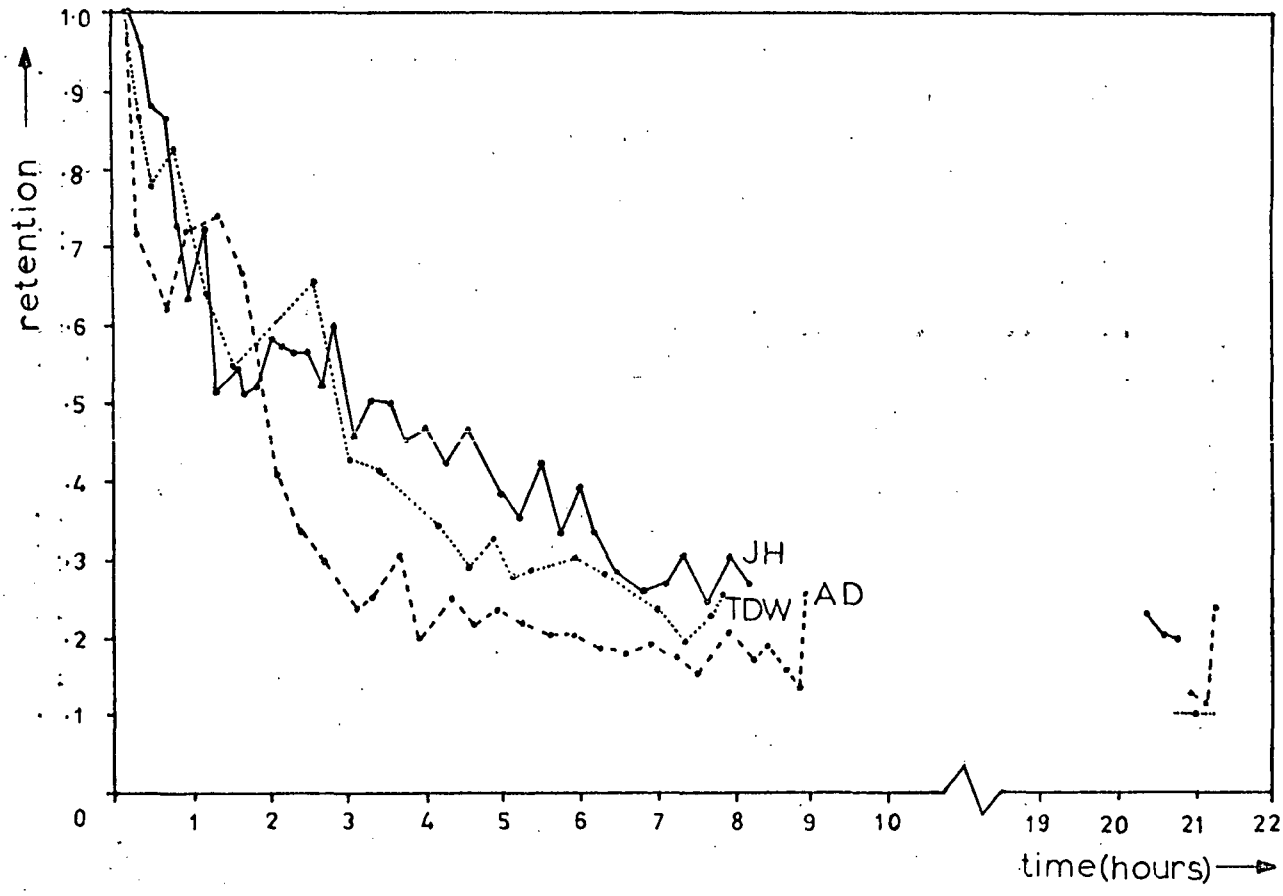

Figure 4.3.4: Clearance curves at $\bar{d}$ = 13μm.

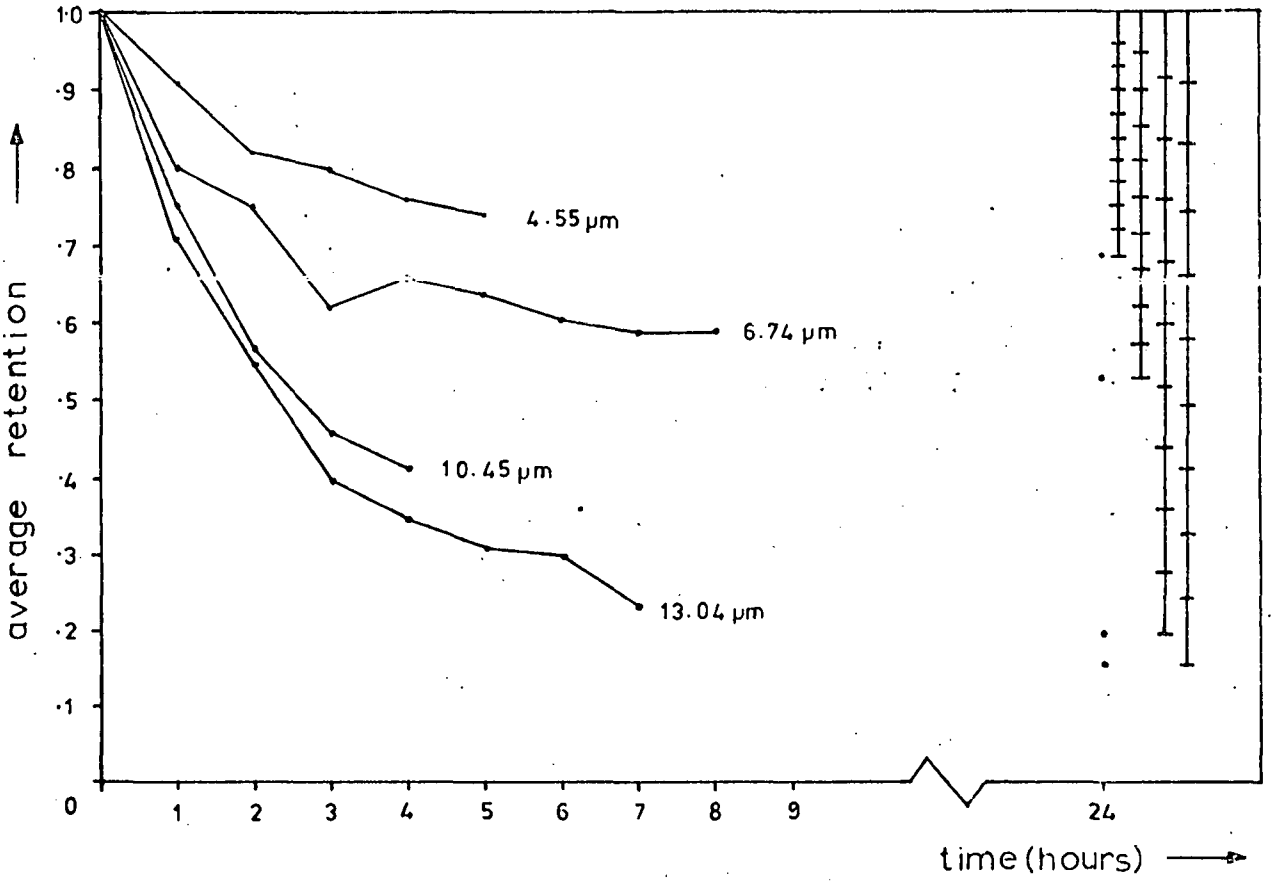

Figure 4.3.5: Averaged clearance curves, all sizes.

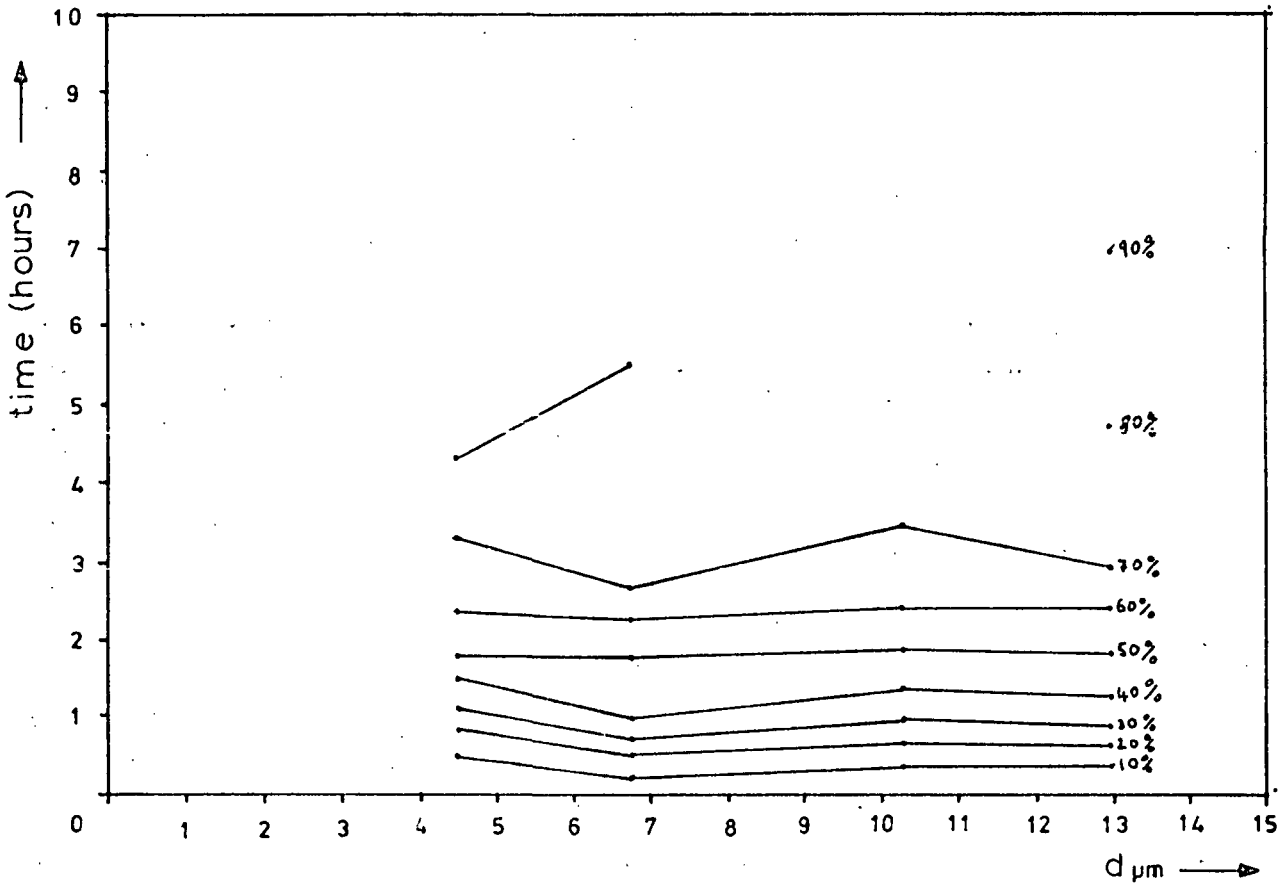

Figure 4.3.6: Time to clear particular percentages of initial deposit below larynx, 10 - 90%.

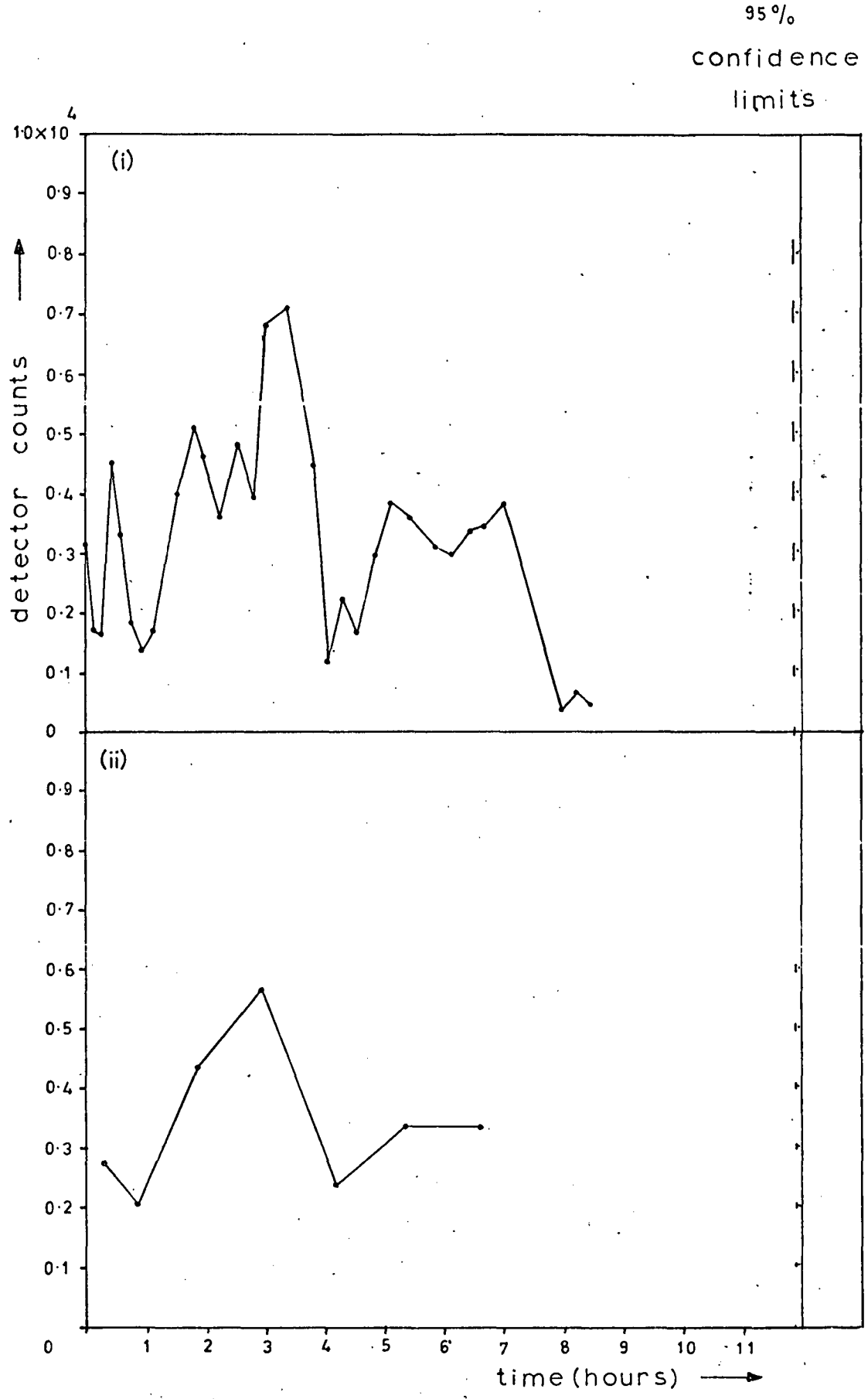

Figure 4.3.7: Single detector throat clearance curves.
Subject AM, $\bar{d} = 4 \cdot 58\ \mu m$.

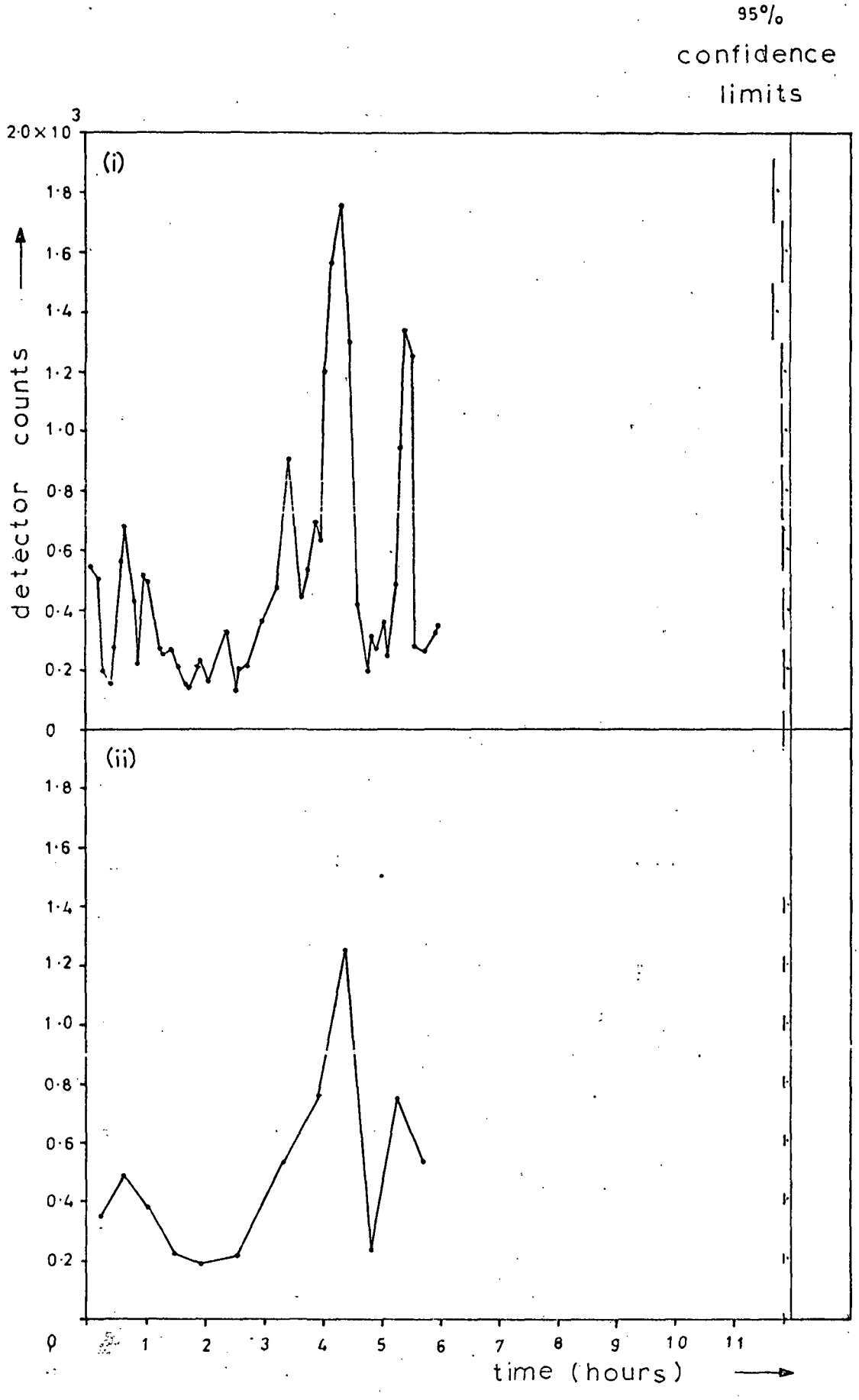

Figure 4.3.8: Single detector throat clearance curves.
Subject AR, $\bar{d} = 4 \cdot 53\ \mu m$.

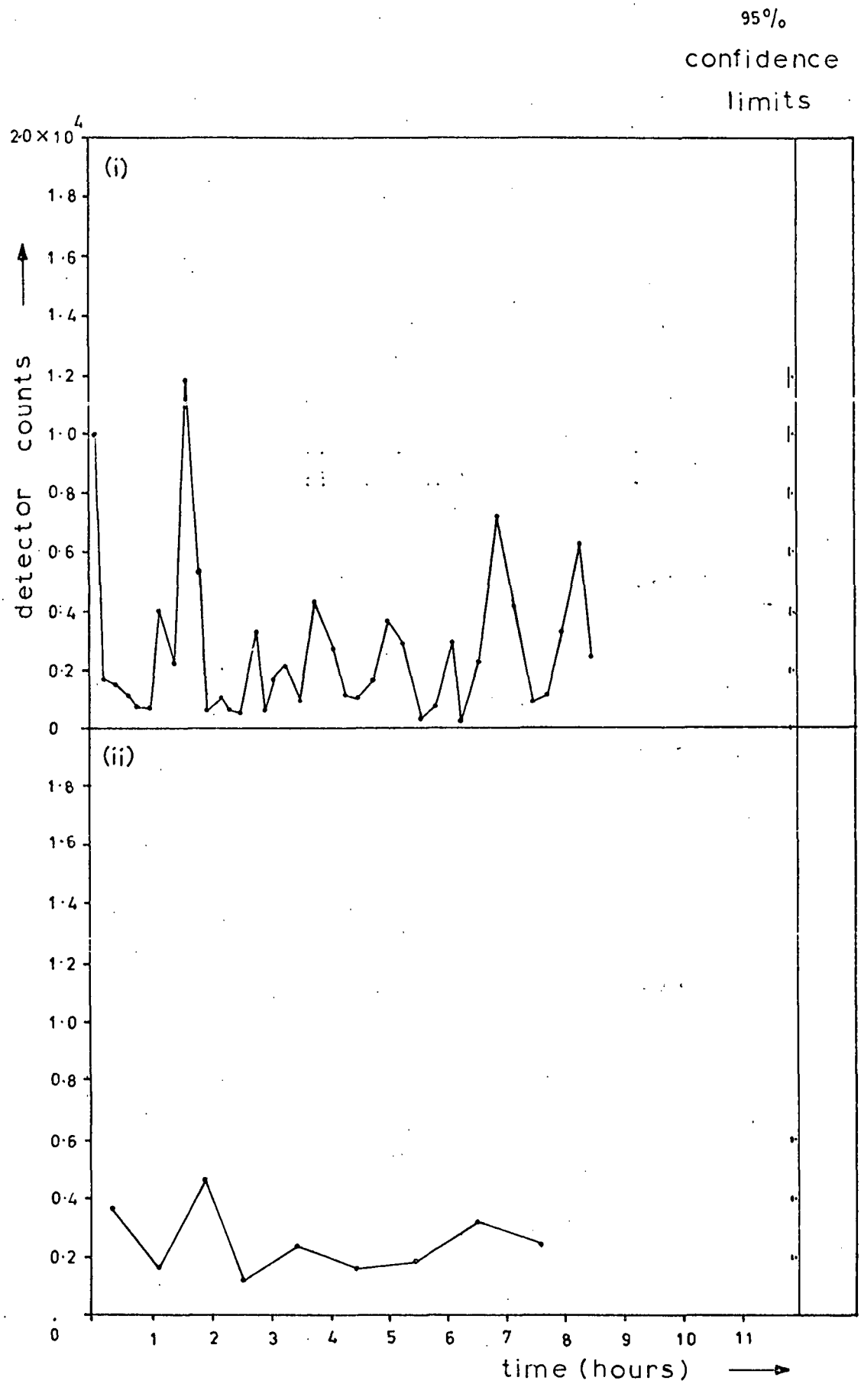

Figure 4.3.9: Single detector throat clearance curves.
Subject HG, $\bar{d}$ = 7·0 μm.

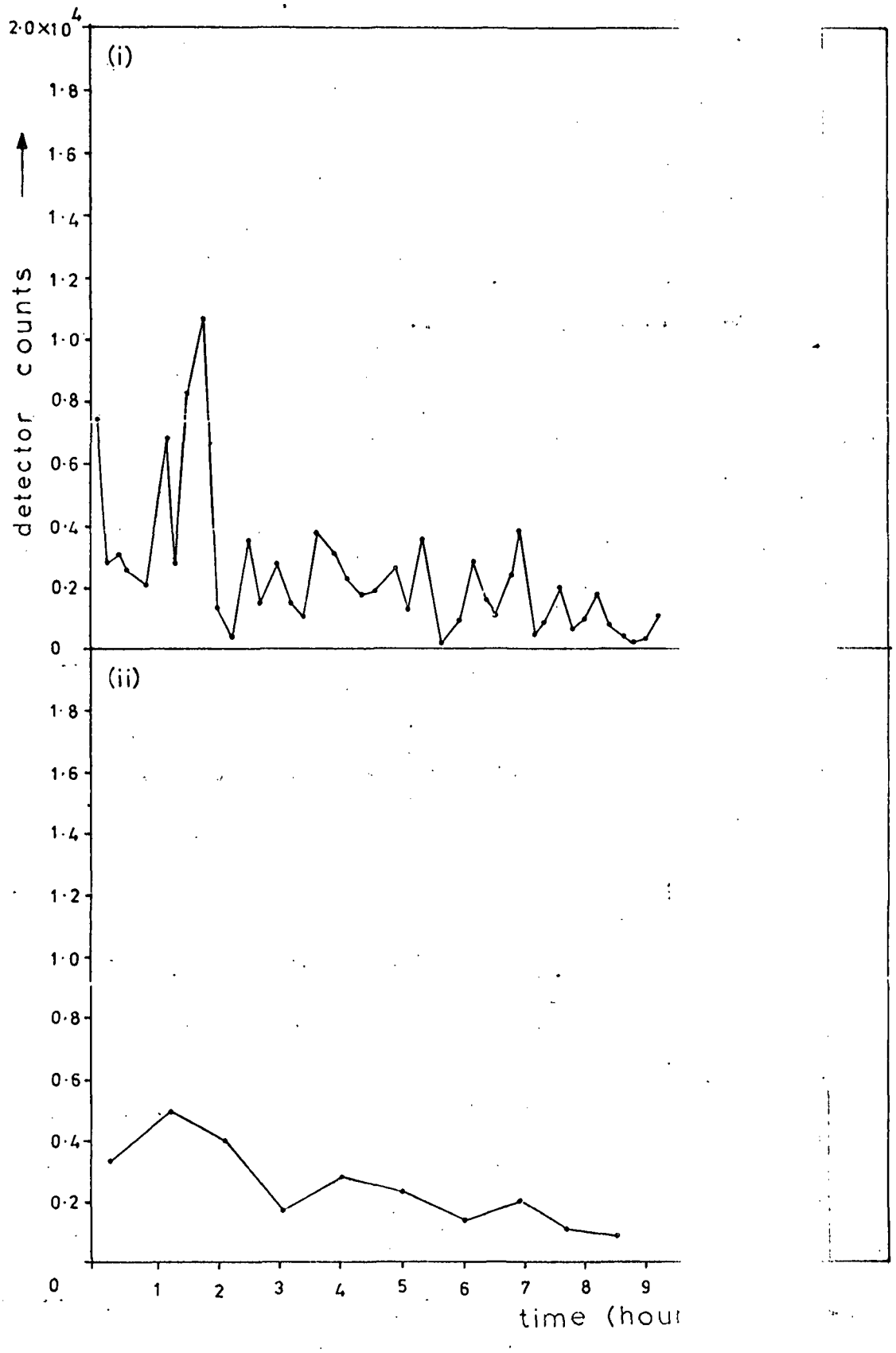

Figure 4.3.10: Single detector throat clearance curves.
Subject PH, $\bar{d}$ = 10·44 μm.

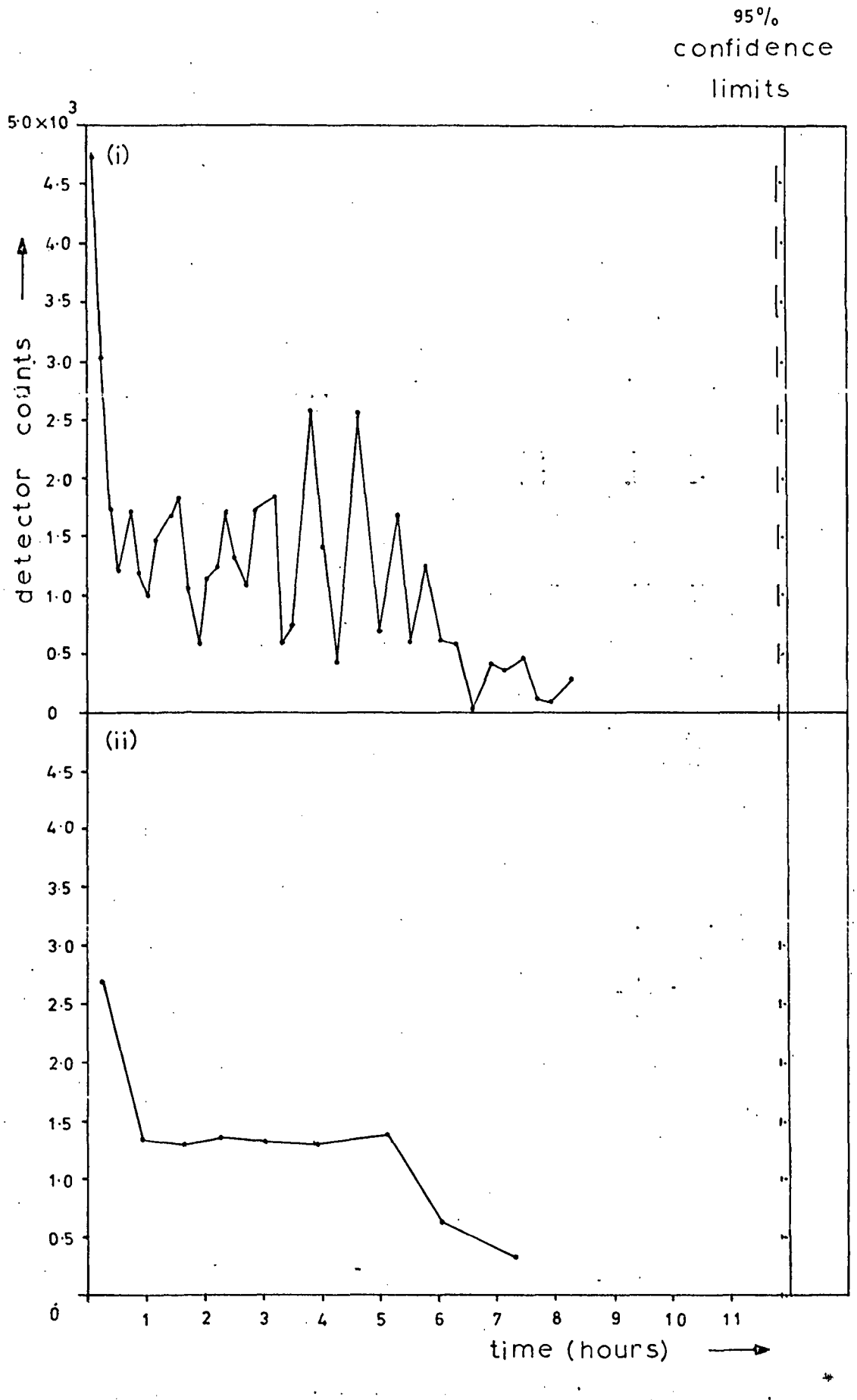

Figure 4.3.11: Single detector throat clearance curves.
Subject JH, $\bar{d}$ = 13·05 μm.

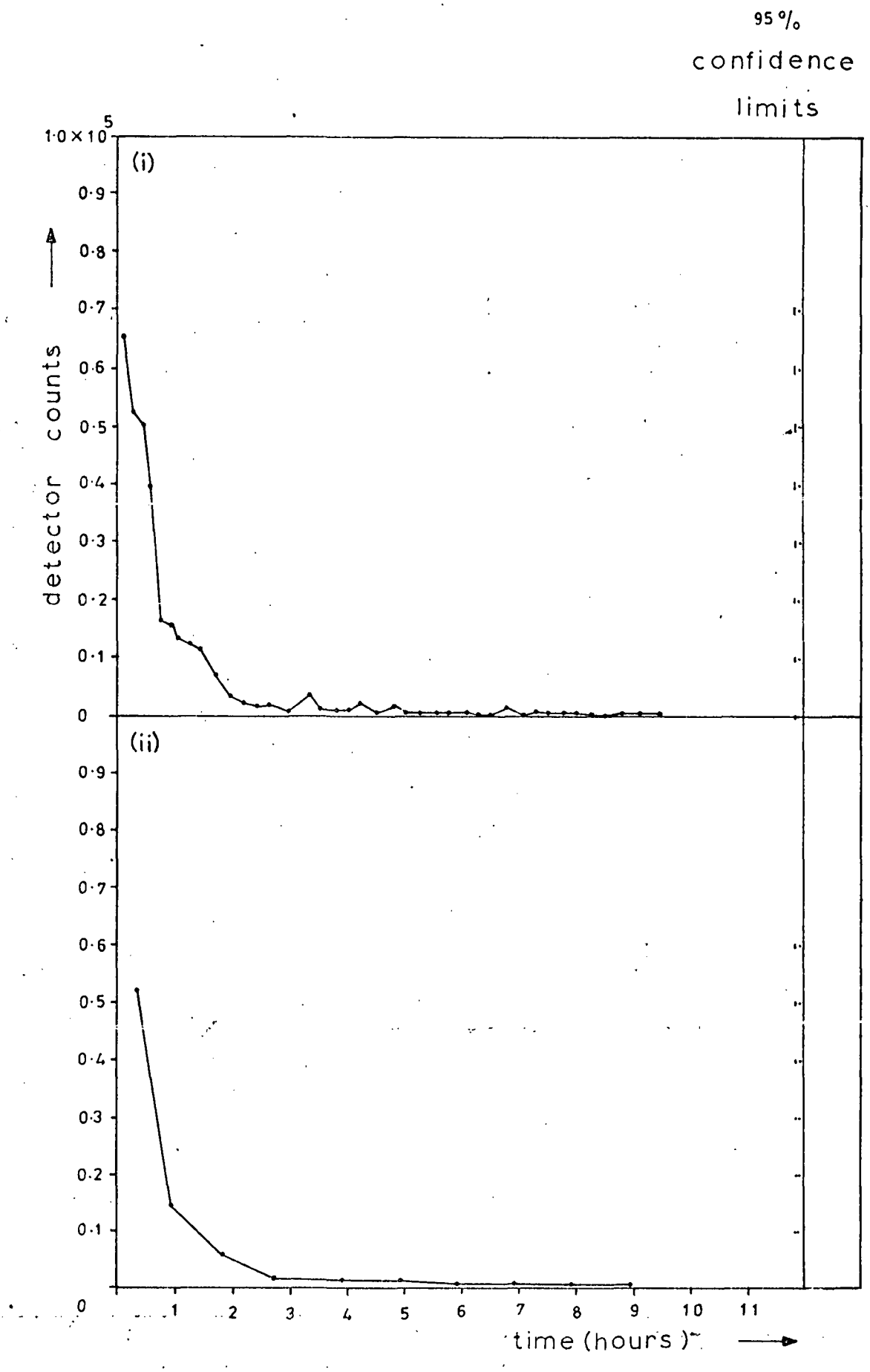

Figure 4.3.12: Single detector throat clearance curves.
Subject PT1, $\bar{d}$ = 10·21 μm.

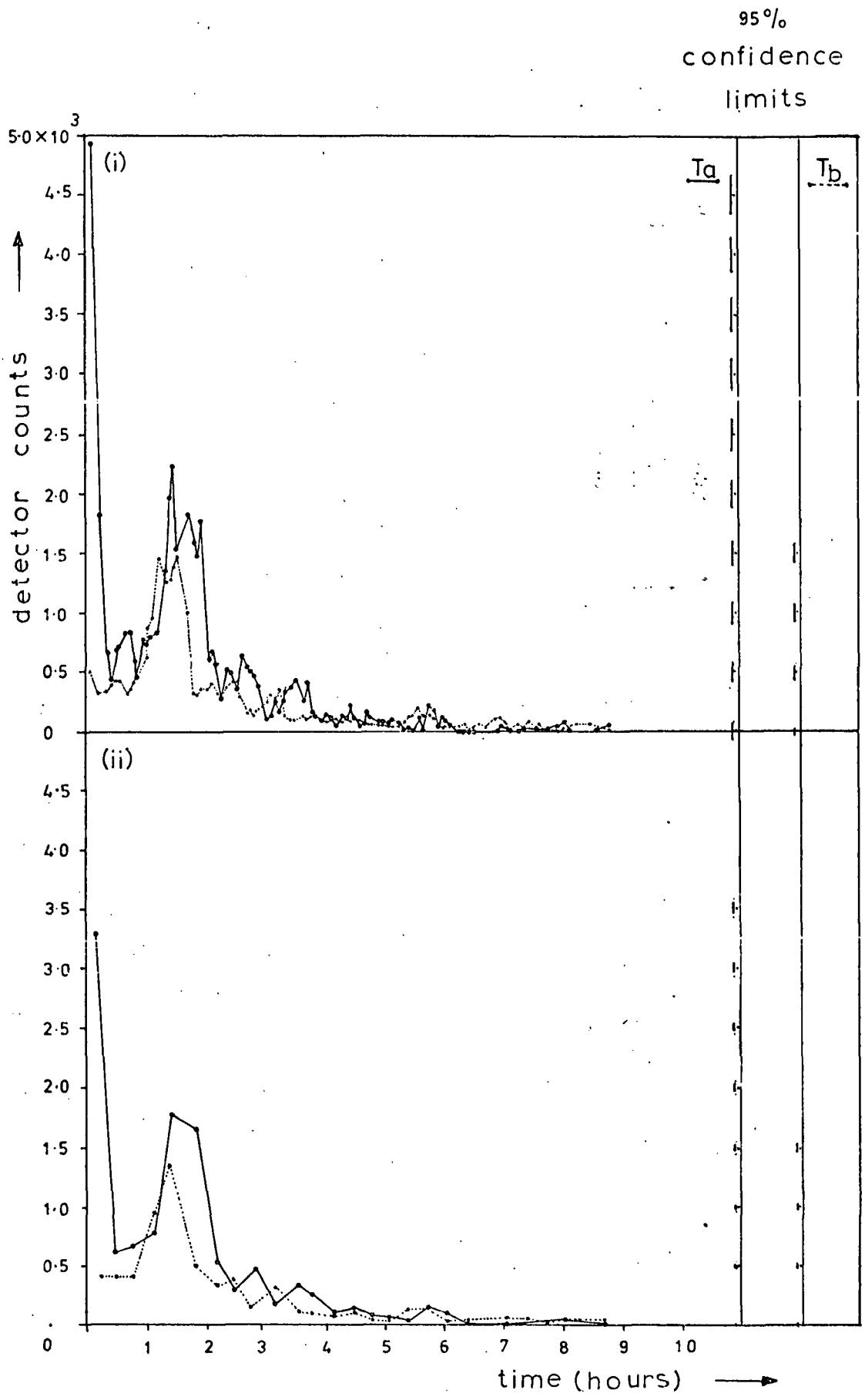

Figure 4.3.13: Double detector throat clearance curves.
Subject AD, $\bar{d}$ = 13 23 μm.

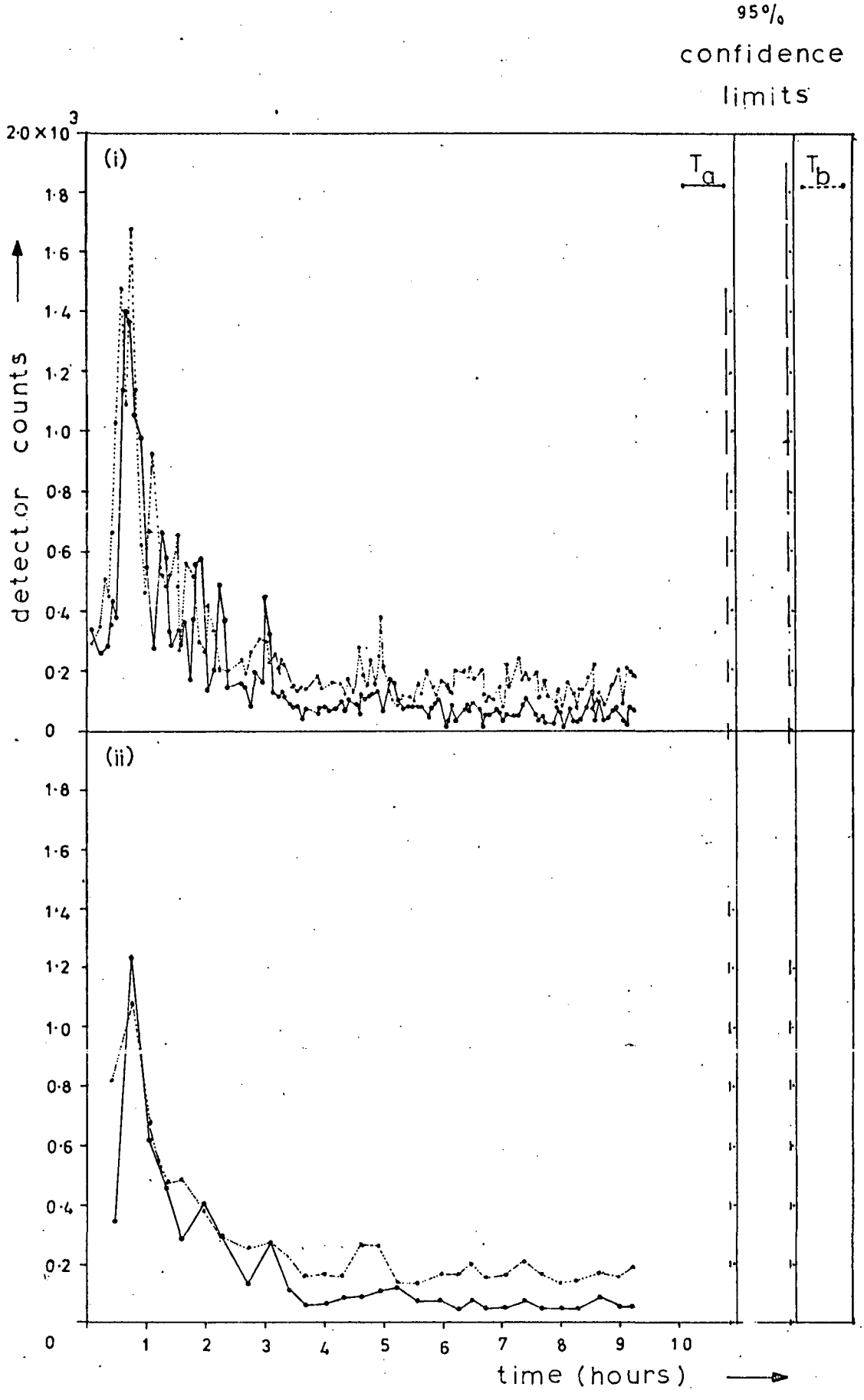

Figure 4.3.14: Double detector throat clearance curves.
Subject ATM, $\bar{d}$ = 4·50 μm.

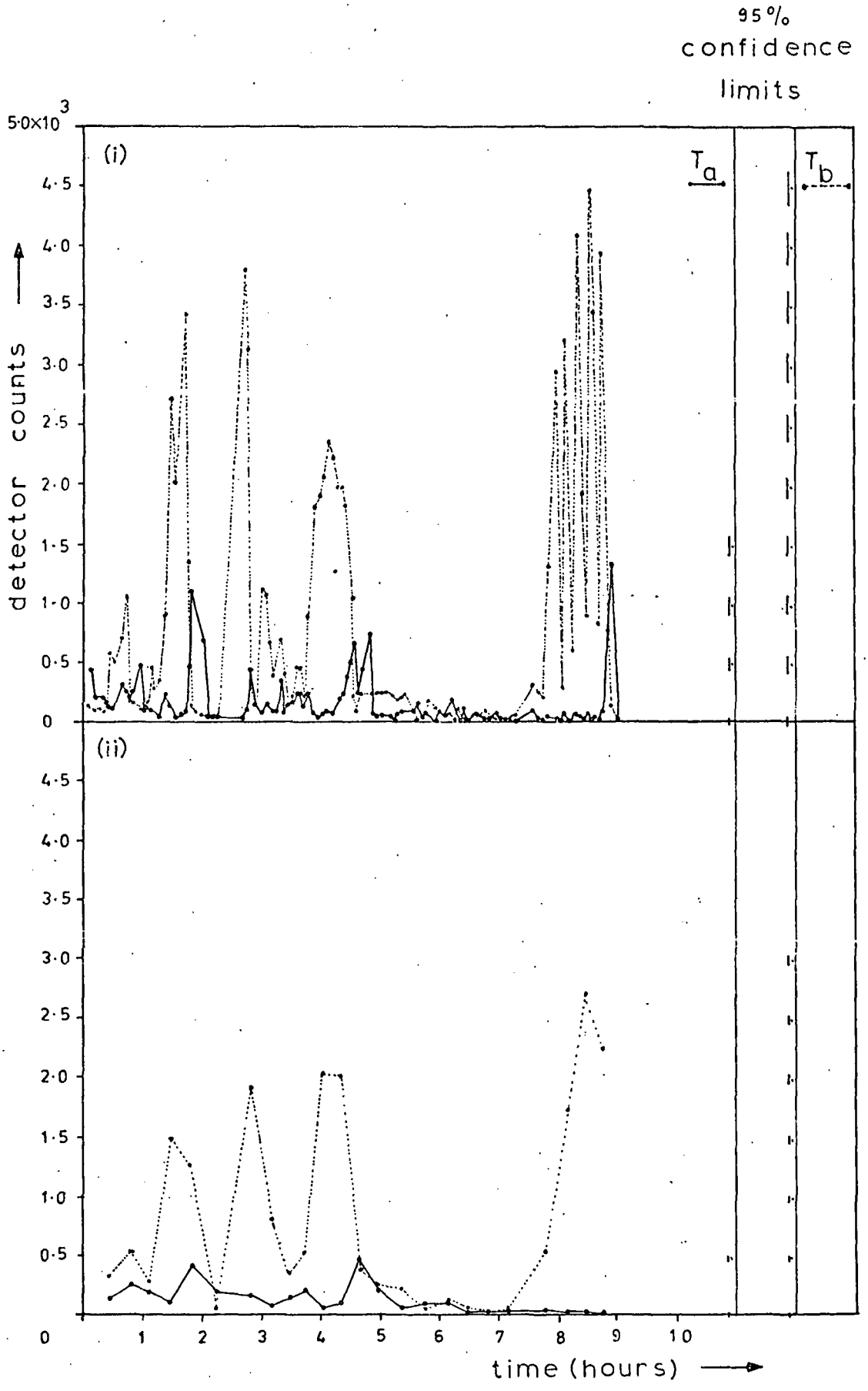

Figure 4.3.15: Double detector throat clearance curves.
Subject FH, $\bar{d} = 4 \cdot 49$ μm.

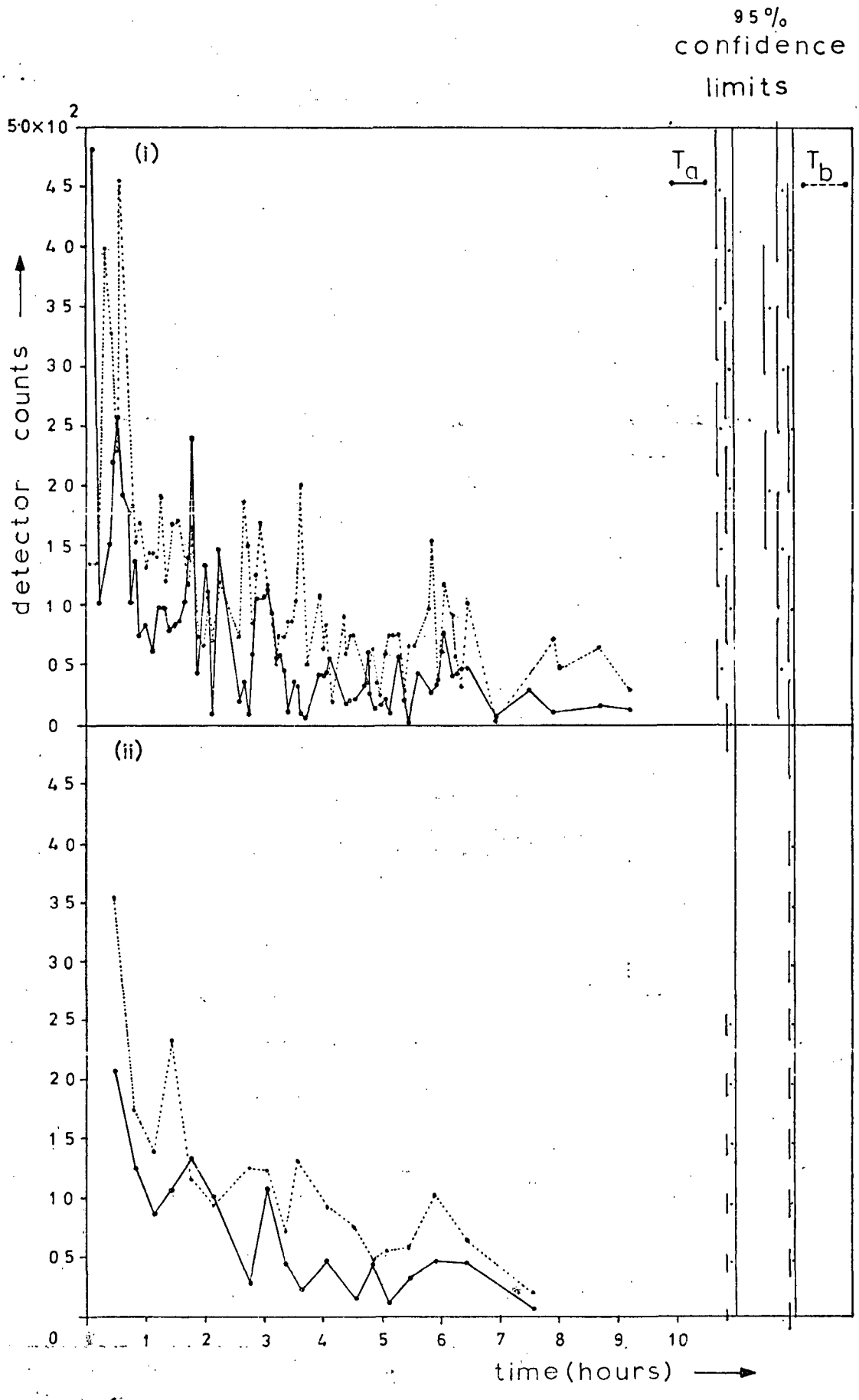

Figure 4.3.16: Double detector throat clearance curves.
Subject RH, $\bar{d}$=4·48 μm.

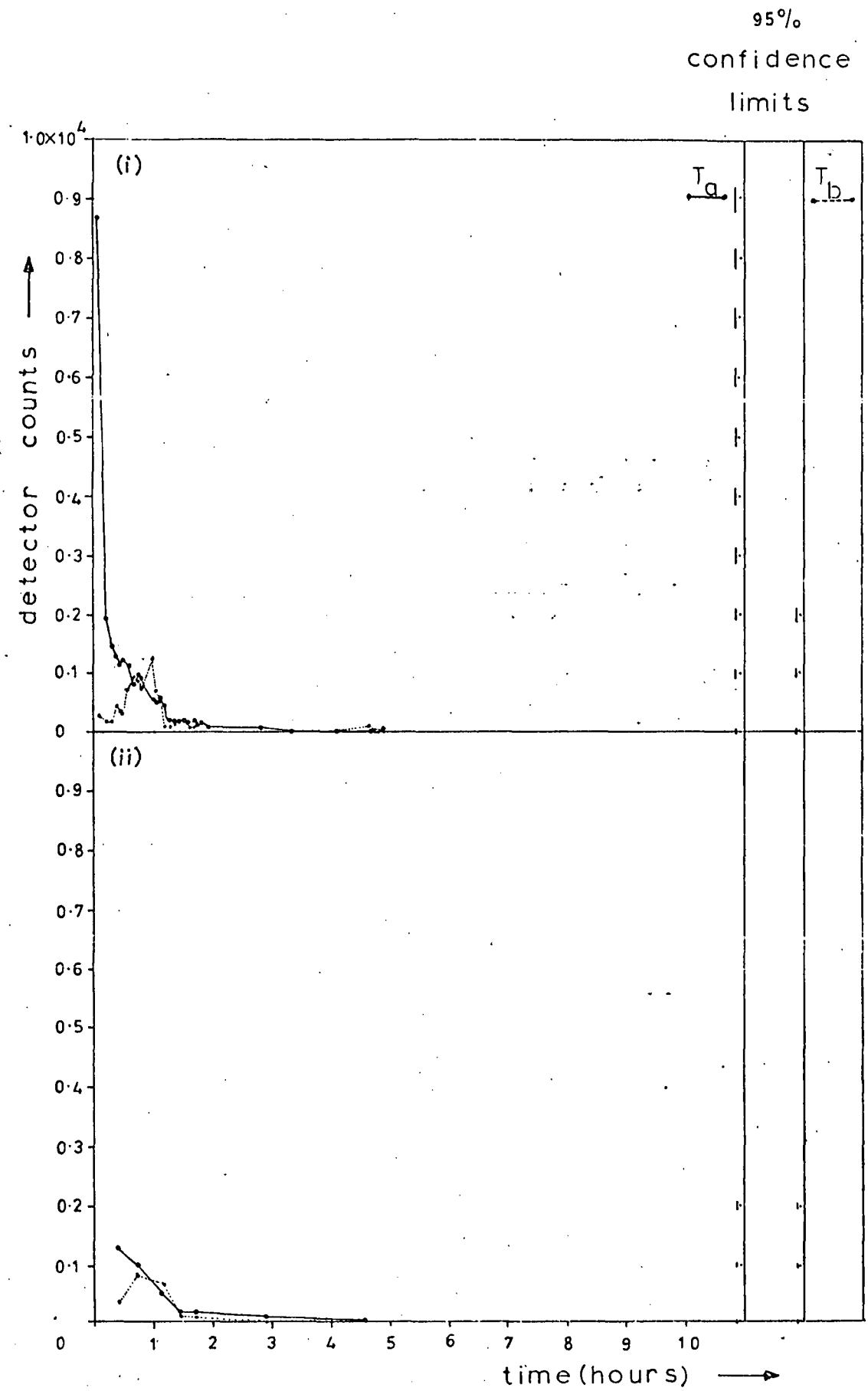

Figure 4.3.17: Double detector throat clearance curves.
Subject PT2, $\bar{d} = 10{\cdot}55\ \mu m$.

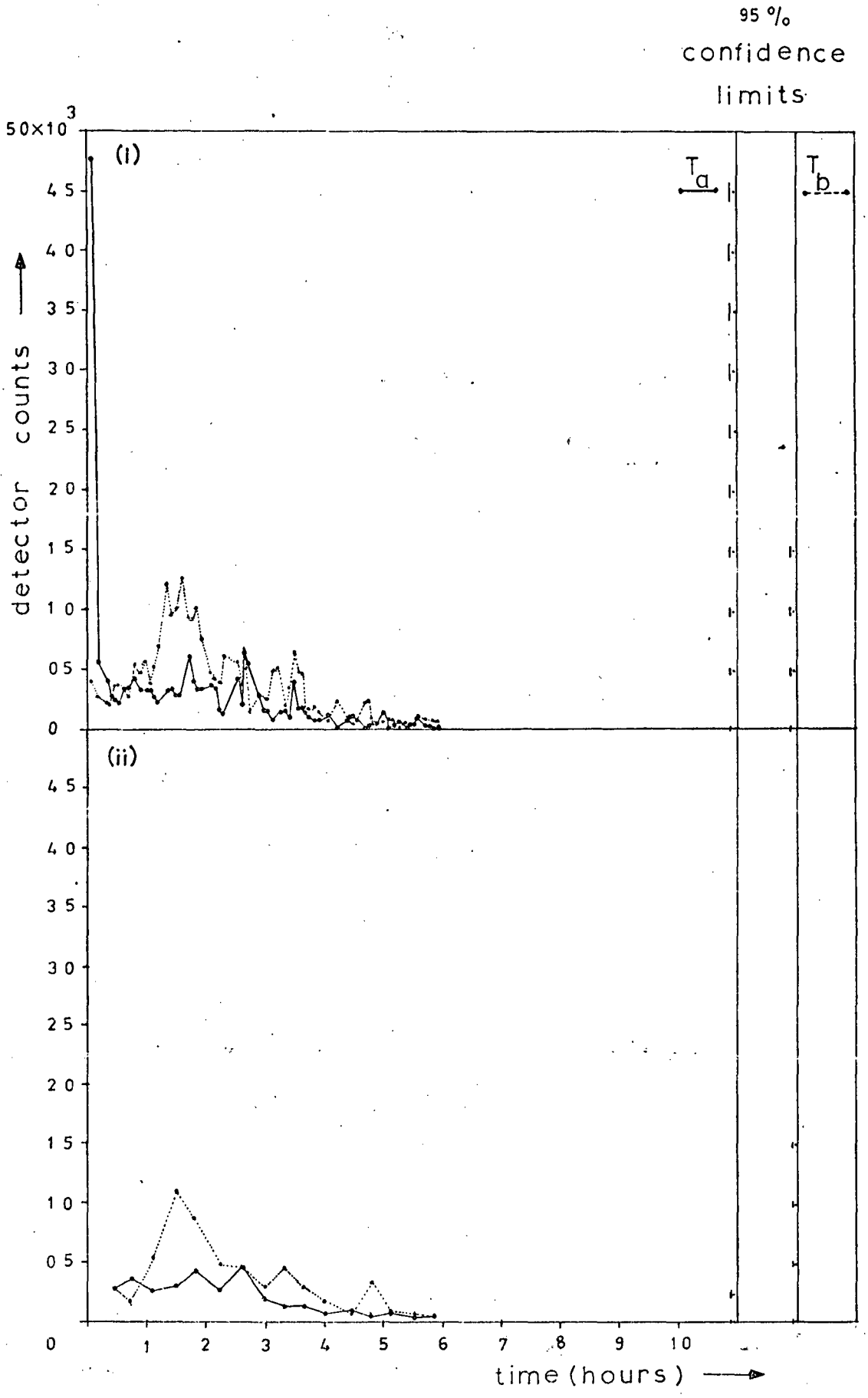

Figure 4.3.18. Double detector throat clearance curves.
Subject KD, $\bar{a}$ = 10·53 μm.

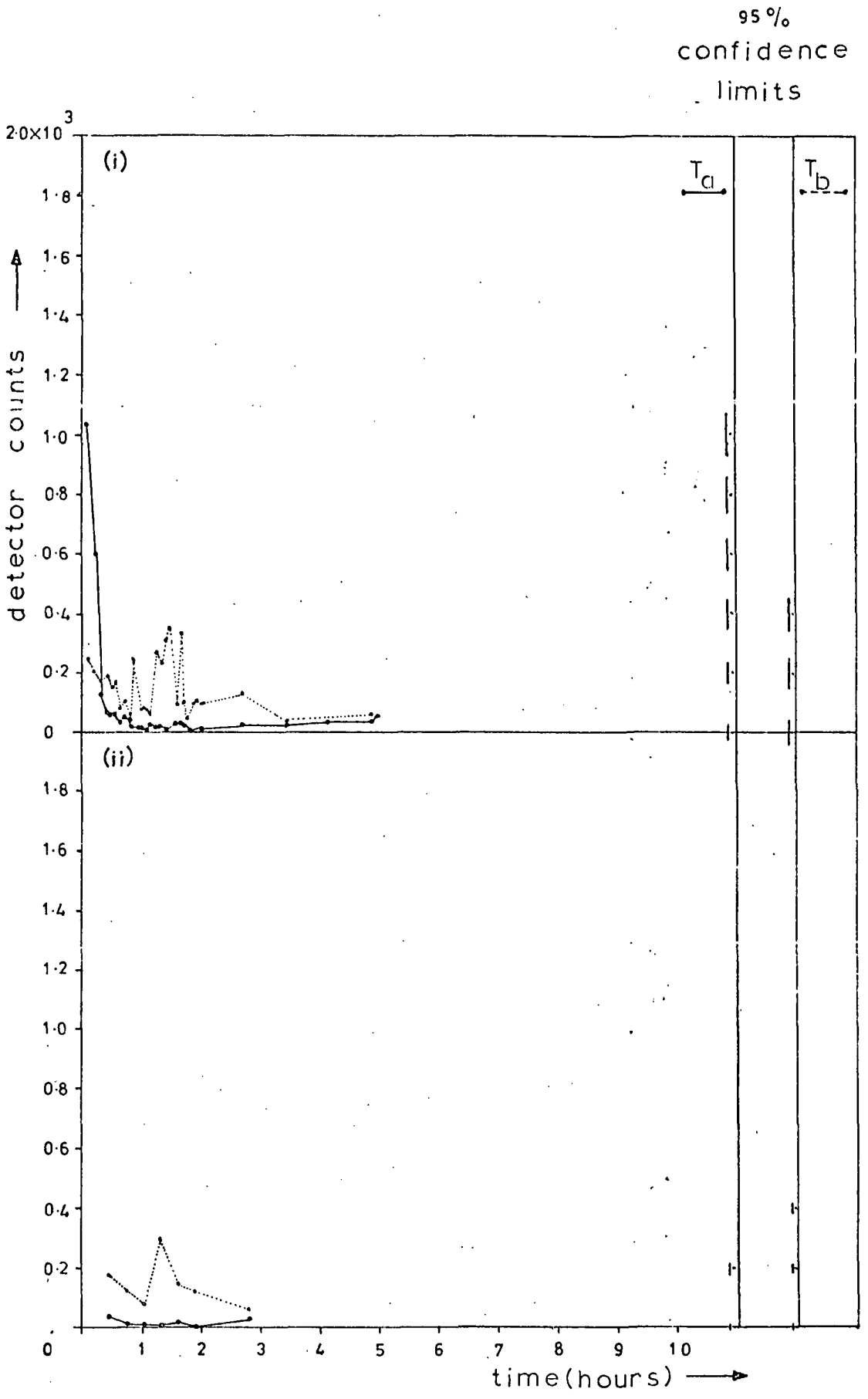

Figure 4.3.19: Double detector throat clearance curves.
Subject VC, $\bar{d} = 4 \cdot 58\ \mu m$.

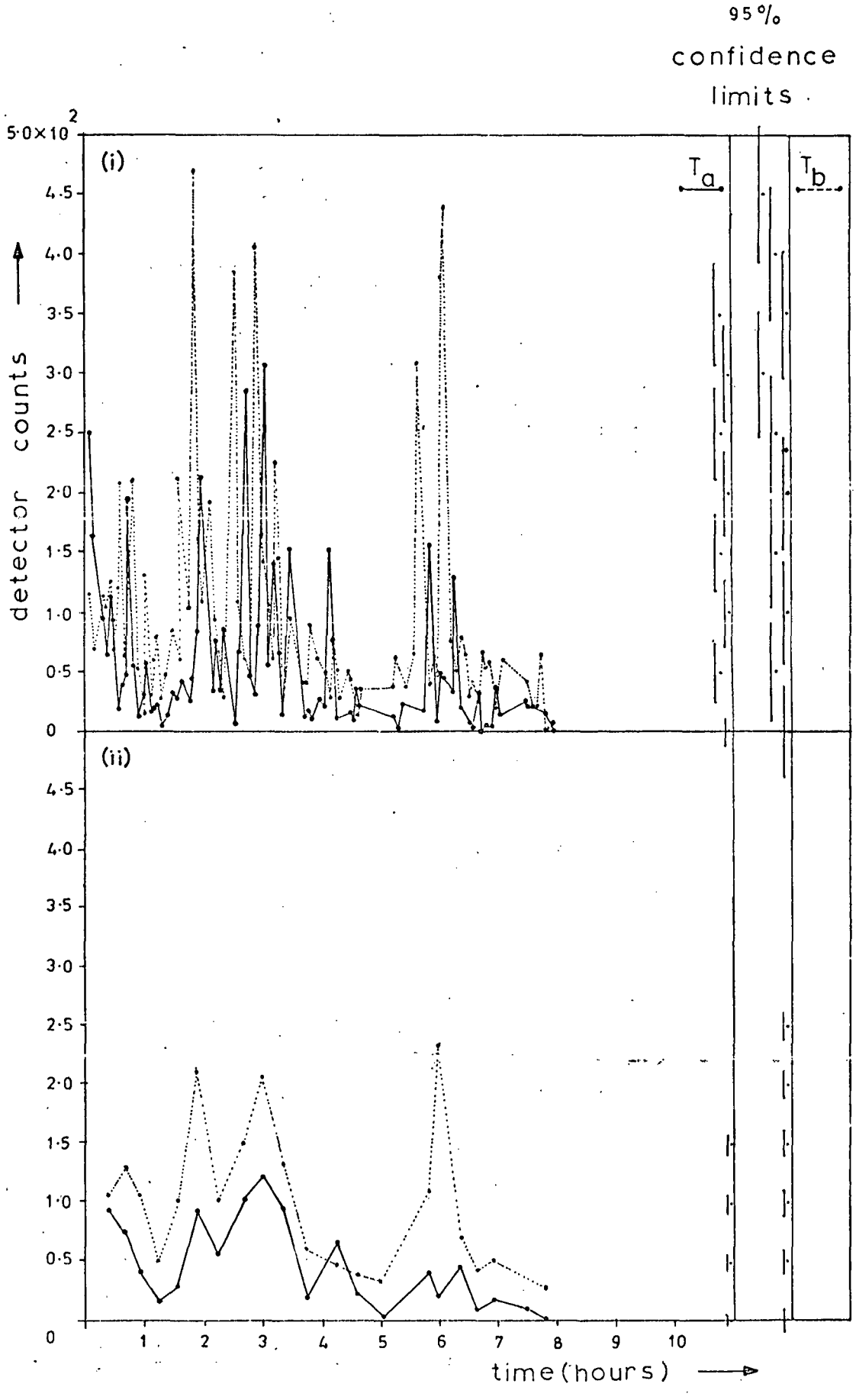

Figure 4.3.20. Double detector throat clearance curves.
Subject MS1, $\bar{d}$ = 4·53 μm.

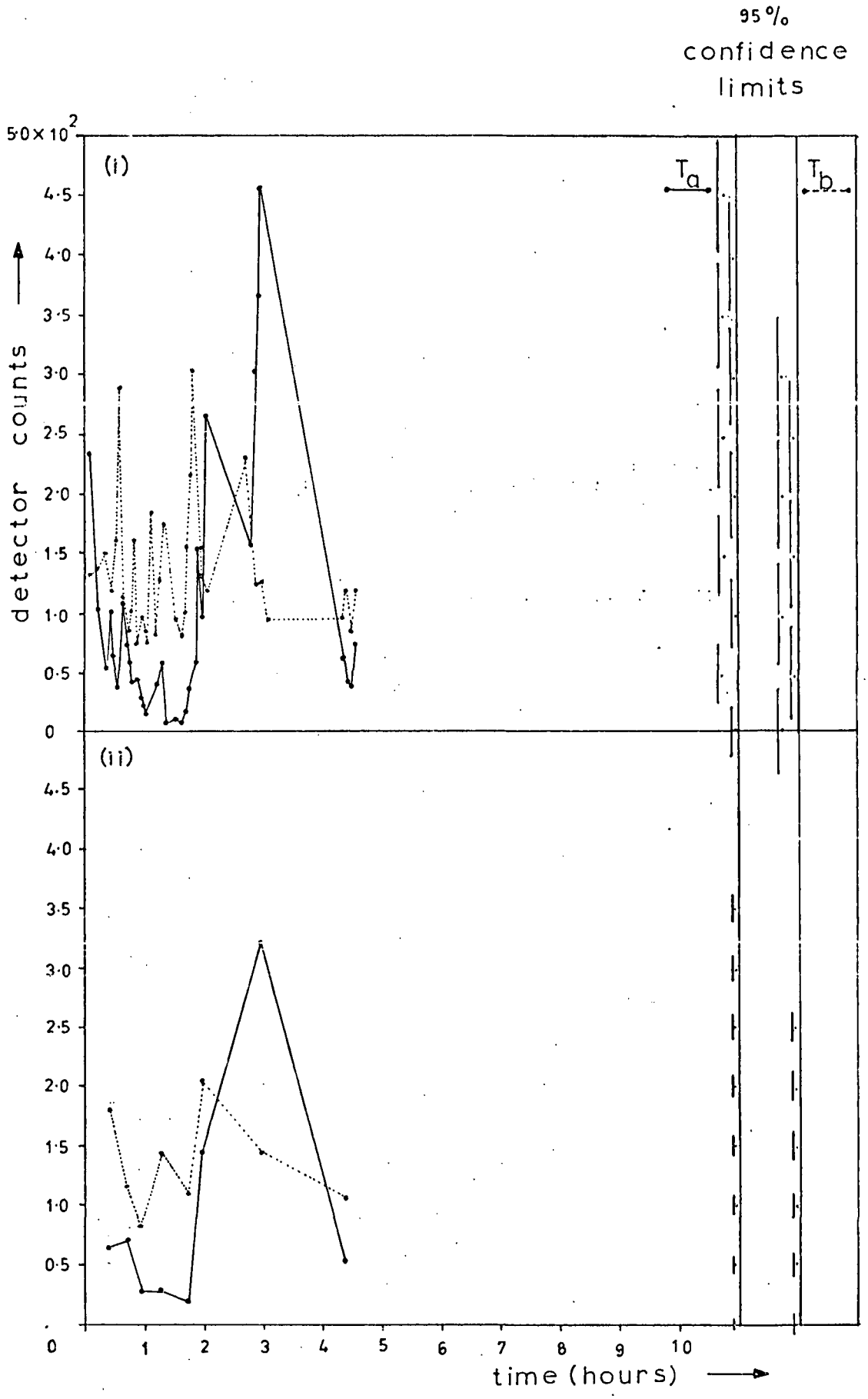

Figure 4.3.21: Double detector throat clearance curves.
Subject MS2, $\bar{d}$ = 4·66 μm.

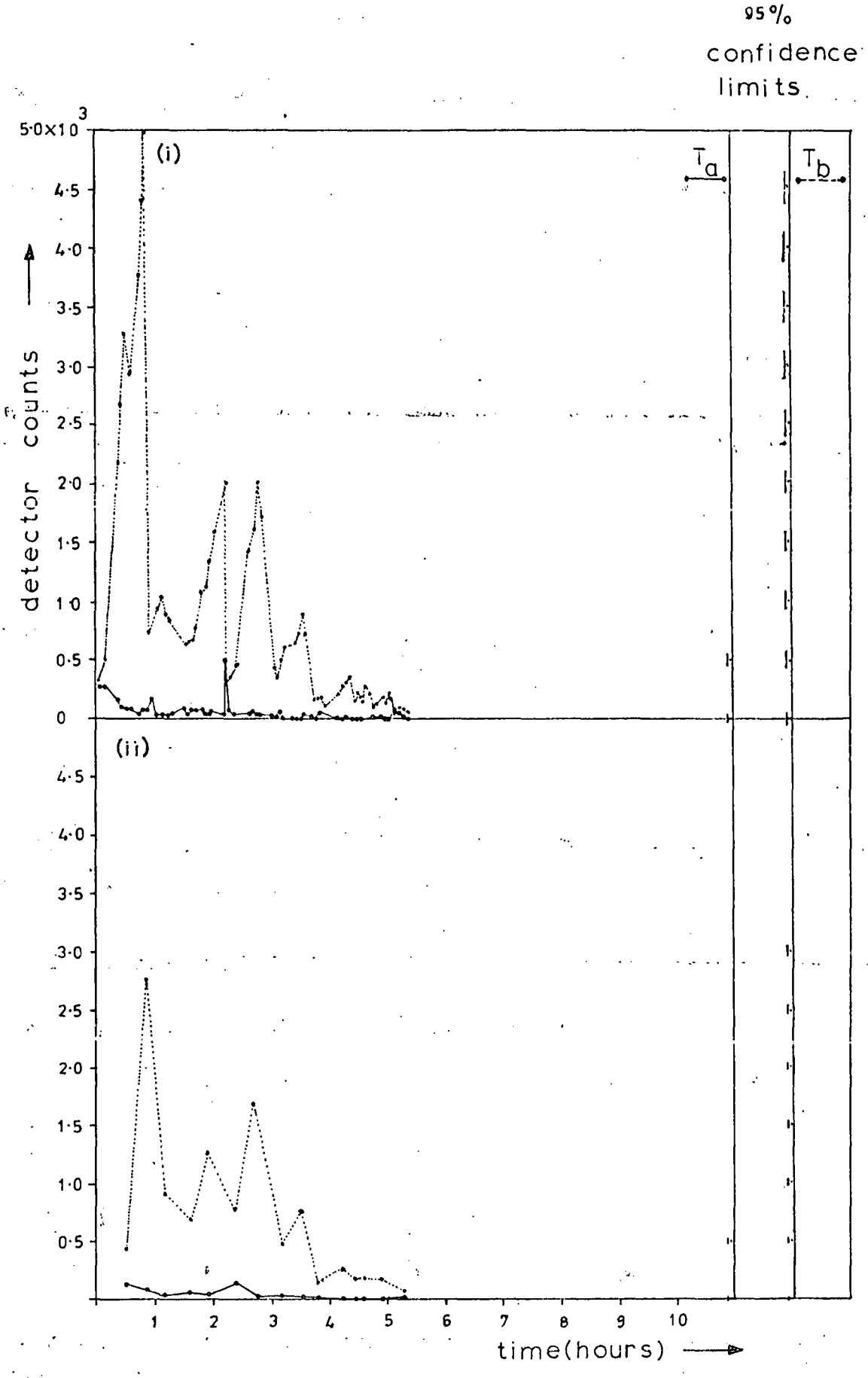

Figure 4.3.22. Double detector throat clearance curves.
Subject JV, $\bar{d}$ = 4·64 μm.

5. CONCLUSIONS AND RECOMMENDATIONS

It is doubtful whether much useful information may be obtained from the results of the present work on either the size fraction of respirable dust or the size fraction of dust which deposits on the dead space airways. The possible exception to this is the finding that the laryngeal/pharyngeal region is an important filtration mechanism, particularly at large particle sizes. In terms of absolute filtration efficiency it is rivalled only by the human nose (HEYDER and RUDOLF, 1977). However, while the results may add little to existing knowledge of the aerosol deposition characteristics in the human respiratory tract they may well subtract from it owing to the doubts cast on the results of other workers in the field who employ similar techniques. In particular, such work normally depends on the assumption of a nearly completely effective short-term removal of particles which initially deposited in the dead space airways (LIPPMANN and ALBERT, 1969: FOORD et al, 1978; STAHLHOFFEN et al, 1979). Agreement between the regional deposition results of the present work and the latter two of these groups is reasonable, in a limited range of comparison, particularly concerning the fractional clearance after about one day. This suggests that despite the widely differing techniques employed, reasonable 'accuracy'has been obtained in each case. Whether or not the same comments should apply in the case of total deposition must ultimately depend on a subjective evaluation of the techniques employed by each group. However, it is the regional deposition that is of most practical significance and until the doubts cast on the validity of such data are satisfactorily resolved the results of all groups should be regarded only as an upper deposition limit, in the case of respirable dust, and a lower deposition limit, in the case of the dust fraction which deposits on the dead space airways. Until then, the present respirable dust sampling criteria look reasonable (i.e. BMRC and ACGIH), but those recommended by the Task Group on Lung Dynamics (1966) seem too high in comparison with the results of the present work.

In the meantime, it is recommended that other techniques be employed, or invented, to define the true regional aerosol deposition characteristics in the human respiratory tract. In particular, the use of radio-opaque dusts shows great promise if a satisfactorily monodisperse test-aerosol can be produced. Such work has already indicated the possibility of very lengthy residence times on tantalum dust in the ciliated airways

of human volunteers (NADEL et al, 1970), but interpretation of the degree of aerosol penetrance is severely complicated by the poor quality of such aerosols (SMITH et al, 1976). An interesting incidental effect sometimes observed by experienced bronchographers is that the bronchographic medium can be rapidly distributed in patterns interpreted as alveolar filling (LEITH, 1977). This raises the possibility of a transfer of deposited particles from the dead space to the respiratory zones and should certainly be considered as a possible factor in interpreting the results of the present work.

Besides being of value in resolving questions on the experimental accuracy of the present results, there are other important reasons why the effectiveness of short-term clearance in the dead space airways merits further investigation. For example, if the residence times of dust in the dead space are far longer than is presently assumed, then the calculated radiation dose due to inhaled radionuclides may well be seriously underestimated. Such assumptions are also often involved in the determination of what is, ostensibly, long-term alveolar clearance in experimental animals (HATCH and GROSS, 1964).

The purely qualitative observations on the nature of clearance patterns in the present work also merit further investigation. The relevance of this phenomenon, besides possibly underlying some basic physical or biological mechanism, lies in the concentration of dust deposits at selected points in the lungs. Complications might arise, for example, in the interpretation of the regional deposition and clearance patterns of inhaled radioactive aerosols using scintillation cameras (LOURENCO et al, 1971).

ACKNOWLEDGEMENTS

I would like to gratefully acknowledge the helpful advice and criticisms rendered to me in the pursuit of this research by my supervisors Dr. D.C.M. Muir, Dr. M. Sudlow and Dr. P. Tothill. I would also like to thank; Mr. W.H. Walton, who conceived a method of performing the inhalation sampling, using a single spirometer, quite independently of a knowledge of the double spirometer configuration; Mr. G. Lynch and the IOM workshop who did a splendid constructional job on the total deposition apparatus; Dr. J. Hannan, whose advice and direct assistance in the development of the radioactive scanning techniques, computing and many other aspects of the research was most helpful; Mr. R.J. Aitken, whose considerable efforts in the development of techniques and during the long period of obtaining results were invaluable; Dr. R.G. Love for his helpful comments and advice on the physiological aspects of the study; Drs. N. Foord, of AERE, Harwell, and W. Stahlhoffen, of GSF, Frankfurt, for their free excahnge of unpublished data and their encouragement.

I would like to pay special thanks to my wife for the ungrateful task of deciphering my manuscript and to my daughter, Helen, for her mature forbearance during its preparation.

I thank the European Coal and Steel Community and the National Coal Board for their generous financial support and co-operation, particularly when it became necessary to allow extra time for completion of the research.

Finally, I would like to thank my eighteen subjects for their considerable time and efforts, for whom the experience of participating in the research was always an ordeal.

REFERENCES

ALBERT, R.E. and ARNETT, L.C. (1955) AMA Arch. Indus. Health, 12, 99.

ALBERT, R.E., LIPPMANN, M., PETERSON, H.T., BERGER, J., SANBORN, K., BOHNING, E. (1973) Arch. Intern. Med., 131, 115.

ALBERT, R.E., LIPPMANN, M., SPIEGELMAN, J., STREHLOW, W., BRISCOE, P., WOLFSON, P. and NELSON, N. (1967) Inhaled Particles II, pp 361-378. (Edited by Davies, C.N.), Pergamon Press, Oxford.

ALLEN, T. (1974) 'Particle Size Measurement', Ch. 4. Published by Chapman and Hall.

ALTSHULER, B. (1959) Bull. Math. Biophys., 21, 257.

ALTSHULER, B., YARMUS, L., PALMES, E.D. and NELSON, N. (1957) AMA Arch. Ind. Health, 15, 293.

ASSMUNDSSON, T. and KILBURN, K. (1970) Am. Rev. Resp. Dis., 102, 388.

BATEMAN, J.R.M., CLARKE, S.W., PAVIA, D. and SHEAHAN, N.F. (1978) J. of Physiol., 284, 55.

BAUMBERGER, J.P. (1923) J. Pharmacol. Exptl. Therap., 21, 47.

BLACK, A. and WALSH, M. (1970) Ann. Occ. Hyg. 13, 82.

BOOKER, D.V., CHAMBERLAIN, A.C., RUNDO, J., MUIR, D.C.F. and THOMSON, M.L. (1967) Nature (Lond.), 215, 30.

BRICARD, J. and PRADEL, J. (1966) In: 'Aerosol Science', Ch. 4, P.89. Published by Academic Press, New York.

BRISCOE, W.A., FORSTER, R.E. and COMROE, J.H.(Jr.) (1954) J. Appl. Physiol. 7, 27.

BROWN, C.E. (1931) J. Ind. Hyg. Toxicol., 13, 285.

BROWN, J.H., COOK, K.M., NEY, F.G. and HATCH, T. (1950) Am. J. Public Health, 40, 450.

CAMNER, P. (1971) Environ. Physiol., 1, 137.

CAMNER, P. and PHILIPSON, K. (1978) Arch. Env. Hlth, 33, 181.

COMROE, J.H., FORSTER, R.E., DUBOIS, A.B., BRISCOE, W.A. and CARLSEN, E. (1955) 'The Lung', p.358, Year Book Med. Pub. INC., Chicago, USA.

DALHAM, T. (1956) Acta. Physiol. Scanda., 36 (Supplement 123, p.89).

DAUTREBANDE, L. (1962) In: 'Microaerosols', p. 34. Published by Academic Press, New York.

DAUTREBANDE, L., BECKMANN, H. and WALKENHORST, W. (1957) AMA Arch. Ind. Health, 16, 179.

DAUTREBANDE, L., CARTRY, D., VAN KERKOM, J. and CEREGHETTI, A. (1954) In: 'Essai de Prevention de la Silicose', Union Minière du Haut, Katanga.

DAVIES, C.N. (1964) Annal. Occ. Hyg., 7, 169.

DAVIES, C.N. (1974) Chemistry and Industry (June 1st), 441.

DAVIES, C.N., HEYDER, J. and SUBBA RAMU, M.C. (1972) J. Appl. Physiol., 32, 591.

DAVIES, C.N., LEVER, M.J. and ROTHENBERG, J.S. (1977) Inhaled Particles IV, pp.151-162, (Edited by Walton, W.H.). Published by Pergamon Press, Oxford.

DENNIS, W.L. (1950) J. Sci. Instrum., 27, 1,950.

DENNIS, W.L. (1970) Inhaled Particles III, (Edited by Walton, W.H.), pp.91-103. Published by Unwin Bros., London.

DRINKER, P., THOMSON, R.M. and FINN, J.L. (1928) J. Ind. Hyg. Toxicol., 10, 13.

EHRET, R., KIEFER, H., MAUSHART, R. and MÖHRLE, G. (1964) In: 'Assessment of Radioactivity in Man', 1, 141.

FEW, J.D., SHORT, M.D. and THOMSON, M.L. (1970) Radiochem. Radional. Lett., 5, 275.

FOORD, N., BLACK, A., WALSH, M. (1977) In: Inhaled Particles IV, pp.137-148, (Edited by Walton, W.H.). Published by Pergamon Press, Oxford.

FOORD, N., BLACK, A. and WALSH, M. (1978) J. Aerosol Sci., 9, 343.

FRY, F.A. (1970) J. Aerosol Sci., 1, 135.

FUCHS, N. and SUTUGIN, A.G. (1966) In: 'Aerosol Science', (Edited by Davies, C.N.), Ch. 1, p.2.

GALEN, (between 129-199 AD) In: 'On the Usefulness of Parts of the Body', translated by M.T. May, Ithaca, N.Y., Cornell Univ. Press, 1968, Vol. II, p.525.

GOODMAN, R.M., YERGIN, B.M., LANDA, J.F., GOLINVAUX, M.H. and SACKNER, M.A. (1978) Am. Rev. Resp. Dis., 117, 205.

GORE, D.J. and PATRICK, G. (1978) Phys. Med. Biol., 23, 730.

GUNN, R. (1954) J. Meterol., 11, 339.

HAMILL, P. (1979) Health Phys., 36, 355.

HANNAN, J. (1978) Private communication.

HARPER, P.V., LATHROP, K.A. and GOTTSCHALK, A. (1966). In: 'Pharmacodynamics of some Technetium-99m Preparations', p.335, USAEC Report CONF-651111.

HATCH, T.F. and GROSS, P. (1964) In: 'Pulmonary Deposition and Retention of Inhaled Aerosols'. Published by Academic Press, New York.

HEYDER, J. (1971) Staub-Reinhalt Luft, 31, 11.

HEYDER, J., ARMBRUSTER, L., GEBHART, J., GREIN, E. and STAHLHOFFEN, W. (1975) J. Aerosol Sci., 6, 311.

HEYDER, J. and DAVIES, C.N. (1971) J. Aerosol Sci., 2, 437.

HEYDER, J., GEBHART, J., HEIGNER, G., ROTH, C. and STAHLHOFFEN, W. (1973) J. Aerosol Sci., 4, 191.

HEYDER, J. and RUDOLF, G. (1977) In: Inhaled Particles IV, pp.107-126, (Edited by Walton, W.H.). Published by Pergamon Press, Oxford.

HIDY, G.M. and BROCK, J.R. (1969) Environ. Sci. Tech., 3, 563.

HILDING, A.C. (1965) Med. Thorac., 22, 329.

HOLMA, B. (1967) Acta. Med. Scanda., suppl. 473.

HORSFIELD, K. and CUMMING, G. (1967) Bull. Math. Biophys., 29, 245.

JACOBSEN, M., RAE, S., WALTON, W.H. and ROGAN, J.M. (1971) Inhaled Particles III, pp.903-920, (Edited by Walton, W.H.). Published by Unwin Bros., England.

KILBURN, K.H. (1968) Am. Rev. Resp. Dis., 98, 449.

KOPS, J., DIBBETS, L., HERMANS, L. and VAN DE VATE, J.F. (1975) J. Aerosol Sci., 6, 329.

LANDAHL, H.D. (1950) Bull. Math. Biophys., 12, 43.

LANDAHL, H.D. and BLACK, S. (1947) J. Ind. Hyg. Toxicol., 29, 269.

LANDAHL, H.D. and HERRMANN, R.G. (1948) J. Ind. Hyg. Toxicol., 30, 181.

LANDAHL, H.D., TRACEWELL, T.N. and LASSEN, W.H. (1951) AMA Arch. Indust. Hyg. 3, 359.

LANDAHL, H.D., TRACEWELL, T.N. and LASSEN, W.H. (1952), AMA Arch. Ind. Hyg. Occupational Med., 6, 508.

LEITH, D.E. (1977) In: 'Respiratory Defense Mechanisms', Part II, Vol.5 of 'Lung Biology in Health and Disease', p.575. Published by Marcel Dekker INC., New York.

LIPPMANN, M. (1977) Handbook of Physiology, Section on Environmental Physiology, (Edited by Lee, D.H.K. and Murphy, S.). Published by Am. Physiol. Soc.

LIPPMANN, M. and ALBERT, R.E. (1969) Am. Ind. Hyg. Ass. J., 30, 257.

LIPPMANN, M. and ALTSHULER, B. (1976) In: 'Air Pollution and the Lung', p.43. Published by J. Wiley & Sons, New York.

LISTER, J. (1868) Brit. Med. J., 2, 53.

LOURENCO, R., KLIMEK, M.F. and BOROWSKI, D.J. (1971) J. Clin. Invest., 50, 1411.

LUCAS, A.M. and DOUGLAS, L.C. (1934) Arch. Otolaryngol., 20, 518.

MACKLEM, P.T. and MEAD, J. (1967) J. Appl. Physiol., 32, 460.

MAY, K.R. (1949) J. Appl. Phys., 20, 932.

MELANDRI, C., PRODI, V., TARRONI, G., FORMIGANI, M., ZAIACOMO, T. De, BOMPANE, G.F. and MAESTRI, G. (1977) Inhaled Particles IV, pp.193-201, (Edited by Walton, W.H.). Published by Pergamon Press, Oxford.

MERCER, T.T. (1973) In: 'Aerosol Technology in Hazard Evaluation', p.287 (re. Ch. 2), P.358 (re. Ch. 3). Published by Academic Press, New York.

MERCER, T.T. (1975) Hlth Phys., 29, 673.

MITCHELL, R.I. (1977) Inhaled Particles IV, pp. 163-170, (Edited by Walton, W.H.). Published by Pergamon Press, Oxford.

MORROW, P.E. (1977) 'Lung Biology in Health and Disease', Vol. 5, Part II.

MORROW, P.E., GIBB, F.R. and GAZIOYLU, K. (1965) Inhaled Particles II, pp. 351-359, (Edited by Davies, C.N.). Published by Pergamon Press, Oxford.

MORSY, S.M., ECKHARDT, B. and STAHLHOFFEN, W. (1978) Hlth Phys., 35, 325.

MUIR, D.C.F. (1967) J. Appl. Physiol., 23, 210.

MUIR, D.C.F. and DAVIES, C.N. (1967) Ann. Occup. Hyg., 10, 161.

MUIR, D.C.F., SWEETLAND, K. and LOVE, R.G. (1971) Inhaled Particles III, pp. 81 - 90, (Edited by Walton, W.H.). Published by Unwin Bros., England.

NADEL, J.A., WOLFE, W.G., GRAF, P.D., YOUKER, J.E., ZAMEL, N., AUSTIN, J.H.M., HINCHCLIFFE, W.A., GREENSPAN, R.H. and WRIGHT, R.R. (1970) New Eng. J. Med., 283, 281.

OGDEN, T.L. and BIRKETT, J.L. (1977) Inhaled Particles IV, pp. 93 - 105, (Edited by Walton, W.H.). Published by Pergamon Press, Oxford.

ORENSTEIN, A.J., (Ed.) (1960) Proc. Pneumoconiosis Conf., Johannesburg, 1959. Published by A. Churchill Ltd., London.

OWENS, J.S. (1923) Trans. Med. Soc., London, 45, 79.

PAVIA, D. and THOMSON, M.L. (1926) Ann. Occ. Hyg., 19, 109.

PHILIPSON, K. (1973) J. Aerosol Sci., 4, 51.

PORSTENDÖRFER, J., GEBHART, J. and RÖBIG, G. (1977), J. Aerosol Sci., 8, 371.

PROTECTION OF THE PATIENT IN RADIONUCLIDE INVESTIGATIONS (1971) ICRP PUBLICATION 17, Pergamon Press, Oxford.

PROCTOR, D.F. (1964) Handbook of Physiology, Respiration, Vol. 1, Ch. 8, (Edited by Fenn, W. and Rahn, H.). Published by Am. Physiol. Soc., Washington D.C.

PROCTOR, D.F. and SWIFT, D.L. (1971) Inhaled Particles III, pp. 59-69, (Edited by Walton, W.H.). Published by Unwin Bros., England.

ROGAN, J.M., ATTFIELD, M.D., JACOBSEN, M., RAE, S., WALKER, D.D. and WALTON, W.H. (1973) Br. J. Ind. Med., 30, 217.

RYLEY, D.J. (1959) Brit. J. of Appl. Phys., 10, 93.

SACKNER, M.A., ROSEN, M.J. and WARNER, A. (1923) J. Appl. Physiol., 34, 495.

SAITO, Y. (1912) Arch. Hyg. Bacteriol., 75, 134.

SAYERS, R.R., FIELDNER, A.C., YANT, W.P., THOMAS, B.G.H. and McCONNELL, W.J. (1924) Bur. Mines, Rept. Invest. No. 2661.

SCHLESINGER, R.B., BOHNING, D.E., CHEN, T.L. and LIPPMANN, M. (1977) J. Aerosol Sci., 8, 429.

SCHLESINGER, R.B. and LIPPMANN, M. (1972) Am. Ind. Hyg. Ass. J., 33, 237.

SCHOENBERG, M.D., GILMAN, P.A., MUMAW, V.R. and MOORE, R.D. (1961) Brit. J. Exp. Path., 42, 486.

SILVERMAN, L., LEE, G., PLOTKIN, T., SAWYERS, I.A. and YANCEY, A.R. (1951), Arch. Ind. Hyg. Occupational Med., 3, 461.

SLEIGH, M.A. (1977) In: 'Respiratory Defense Mechanisms', Part 1, Vol. 5, of 'Lung Biology in Health and Disease', p. 251. Published by Marcel Dekker, INC., New York.

SMITH, J.C., STITIK, F.P. and SWIFT, D.L. (1926) Am. Rev. Resp. Dis., 113, 515.

STAHLHOFFEN, W., ECKHARDT, B., GEBHART, J., HEYDER, J. and STUCK, B. (1979) J. Aerosol Sci., 10, 222.

STANESCU, D.C., PATTIJN, J., CLEMENT, J. and VAN DE WOESTIJNE, K.P. (1972) J. Appl. Physiol., 32, 460.

STÖBER, W. (1972) In: 'Assessment of Airborne Particles', p.249, (Edited by Mercer, T.T., Morrow, P. and Stöber, W.). Published by C.C. Thomas, Springfield, USA.

STUART, B.O. (1973) Arch. Intern. Med., 131, 60.

STURGESS, J. (1977) Am. Rev. Resp. Dis., 115, 819.

TAKAHASHI, K. and KUDO, A. (1973) J. Aerosol Sci., 4, 209.

TASK GROUP ON LUNG DYNAMICS (1966) Hlth. Phys., 12, 173. Report of Committee II of a Task Group of the ICRP, 1965.

TAULBEE, D.B. and YU, C.P. (1975) J. Appl. Physiol., 38, 77.

TOPPING, J. (1965) In: 'Errors of Observation and their Treatment', p.79. Published by Chapman and Hall Ltd., London.

TOTHILL, P. (1974) In: 'Instrumentation in Nuclear Medicine', Vol. 2. Published by Academic Press INC., New York.

TOTHILL, P. and GALT, J.M. (1971) Phys. Med. Biol., 16, 625.

TYNDALL, J. (1870) Proc. Roy. Inst. of Gt. Brit., 6, 1.

VAN ASS, A. (1977) Am. Rev. Resp. Dis., 115, 721.

VAN WIJK, A.M. and PATTERSON, H.S. (1940) J. Ind. Hyg. Toxicol., 22, 31.

WALKER, J.E.C., WEILS, R.E. and MERRILL, W. (1961) Am. J. Med., 30, 259.

WALSH, M., BLACK, A. and FOORD, N. (1977) J. Aerosol Sci., 8, 83.

WEIBEL, E.R. (1963) In: 'Morphometry of the Human Lung'. Published by Springer Press, Berlin.

WHITBY, K.T. and LUI, B.Y. (1966) In: 'Aerosol Science', (Edited by Davies, C.N.). Published by Pergamon Press, Oxford.

WHITBY, K.T., LUNDGREN, D.A. and PETERSON, C.M. (1965) Int. J. Air Wat. Poll., 9, 263.

WILSON, I.B. and LA MER, V.K. (1948) J. Ind. Hyg. Toxicol., 30, 265.

YEATES, D.B., ASPIN, N., LEVISON, H., JONES, M.T. and BRYAN, A.C. (1975) J. Appl. Physiol., 39, 487.

YU, C.P. (1977) J. Aerosol Sci., 8, 237.

YU, C.P. and CHANDRA, K. (1978) J. Aerosol Sci., 9, 175.

APPENDIX 1

The filter C_d is in effect comprised of two in-series filters C_{di} C_{de} say, possessing an aerosol deposition efficiency of ϵ_{cdi}, ϵ_{cde}, for inspiration and expiration, respectively.

Referring to Figure A.1,

$$\epsilon_{cd} = \frac{I_{cd} - E_{cd}}{I_{cd}} = \left[1 - \frac{E_{cd}}{I_{cd}}\right]$$

for simplicity suppose that,

$$\epsilon_{cde} = \frac{C_{de}}{I_{cd'}} = \epsilon_{cdi} = \frac{C_{di}}{I_{cd}} = \epsilon_{cd'}$$

$$\therefore E_{cd} = I_{cd'}(1 - \epsilon_{cd'})$$

and, $I_{cd'} = I_{cd}(1 - \epsilon_{cd'})$

$$\therefore \epsilon_{cd} = \left[1 - \frac{I_{cd}(1 - \epsilon_{cd'})^2}{I_{cd}}\right]$$

$$\therefore \epsilon_{cd} = 2\epsilon_{cd'} - \epsilon_{cd'}^2 \simeq 2\epsilon_{cd'} \quad \text{for small values of } \epsilon_{cd}$$

Since, assuming equal efficiencies in both directions of flow, it is necessary that,

$$\epsilon_{cd'} < \epsilon_c$$

$$\therefore \epsilon_{cd} < \sim 2\epsilon_c$$

$$\therefore 0 < q_1 < \sim 2$$

When, $q_3 \neq 1$, ϵ_{cd} cannot be related directly to ϵ_c, only to ϵ_{ci}, or ϵ_{ce}. When $\epsilon_{ci} > \epsilon_{ce}$, $q_1 > q_4$; when $\epsilon_{ci} < \epsilon_{ce}$, $q_1 < q_4$; when $q_3 = 1$, $\epsilon_{ci} = \epsilon_{ce} = \epsilon_c$, $q_1 = q_4$; conditions which are satisfied by the equation below, a simple approximation only.

$$q_4 = \frac{q_1 + q_3}{2} \qquad \ldots\ldots\ldots \text{ equation } 4.2.35$$

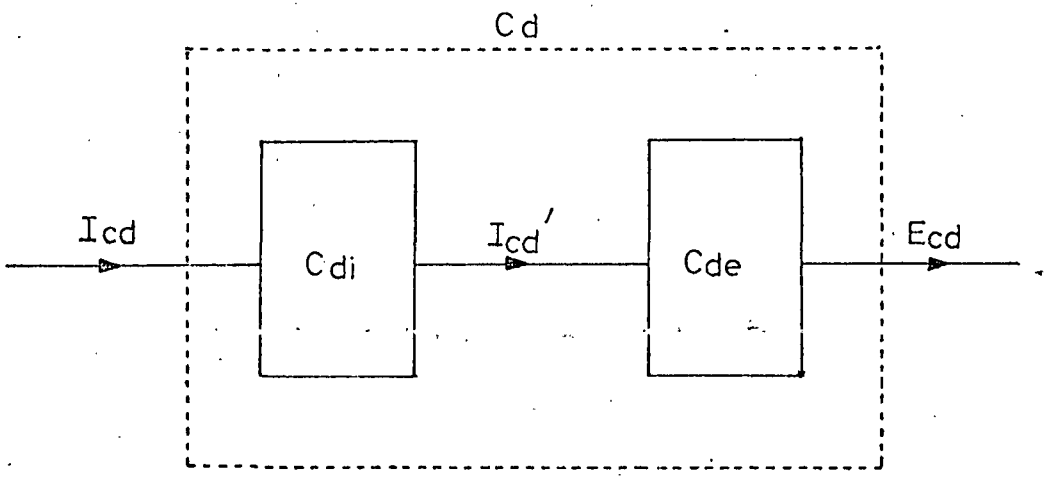

figure A.1 : filter Cd

APPENDIX 2

Now, $D = W_i + S_i + C_i + C_d + R + C_e + S_e + W_e$

$$\therefore f_D(I) = \frac{1}{I}\Bigg[\epsilon_w . I + \epsilon_s . I(1-\epsilon_w) + \epsilon_{ci} . Y'I(1-\epsilon_w)(1-\epsilon_s)$$

$$+ q_4 . \epsilon_{ci} . YI(1-\epsilon_w)(1-\epsilon_s)$$

$$+ \epsilon_R \Big(Y'I(1-\epsilon_w)(1-\epsilon_s) - \epsilon_{ci} . Y'I(1-\epsilon_w)(1-\epsilon_s) \Big)$$

$$+ \epsilon_{ce} \Big(Y'I(1-\epsilon_w)(1-\epsilon_s) - \epsilon_{ci} . Y'I(1-\epsilon_w)(1-\epsilon_s)$$

$$- \epsilon_R \Big(Y'I(1-\epsilon_w)(1-\epsilon_s) - \epsilon_{ci} . Y'I(1-\epsilon_{Hi}) \Big) \Big)$$

$$+ \epsilon_S \Big(Y'I(1-\epsilon_w)(1-\epsilon_S) - \epsilon_{Ci} . Y'I(1-\epsilon_w)(1-\epsilon_S)$$

$$- \epsilon_R \Big(Y'I(1-\epsilon_w)(1-\epsilon_s) - \epsilon_{ci} . Y'I(1-\epsilon_w)(1-\epsilon_s) \Big)$$

$$- \epsilon_{Ce} \Big(Y'I(1-\epsilon_w)(1-\epsilon_S) - \epsilon_{Ci} . Y'I(1-\epsilon_w)(1-\epsilon_S)$$

$$- \epsilon_R \Big(Y'I(1-\epsilon_w)(1-\epsilon_S) - \epsilon_{Ci} . Y'I(1-\epsilon_w)(1-\epsilon_S) \Big) \Big) \Big)$$

$$+ \epsilon_W \Big(Y'I(1-\epsilon_w)(1-\epsilon_S) - \epsilon_{Ci} . Y'I(1-\epsilon_w)(1-\epsilon_S)$$

$$- \epsilon_R \Big(Y'I(1-\epsilon_w)(1-\epsilon_S) - \epsilon_{Ci} . Y'I(1-\epsilon_w)(1-\epsilon_S) \Big)$$

$$- \epsilon_{Ce} \Big(Y'I(1-\epsilon_w)(1-\epsilon_S) - \epsilon_{Ci} . Y'I(1-\epsilon_w)(1-\epsilon_S)$$

$$- \epsilon_R \Big(Y'I(1-\epsilon_w)(1-\epsilon_S) - \epsilon_{Ci} . Y'I(1-\epsilon_w)(1-\epsilon_S) \Big) \Big)$$

$$- \epsilon_S \Big(Y'I(1-\epsilon_w)(1-\epsilon_S) - \epsilon_{Ci} . YI(1-\epsilon_w)(1-\epsilon_S)$$

$$- \epsilon_R \Big(Y'I(1-\epsilon_w)(1-\epsilon_S) - \epsilon_{Ci} . Y'I(1-\epsilon_w)(1-\epsilon_S) \Big)$$

$$- \epsilon_{Ce} \Big(Y'I(1-\epsilon_w)(1-\epsilon_S) - \epsilon_{Ci} . Y'I(1-\epsilon_w)(1-\epsilon_S)$$

$$- \epsilon_R \Big(Y'I(1-\epsilon_w)(1-\epsilon_S) - \epsilon_{Ci} . Y'I(1-\epsilon_w)(1-\epsilon_S) \Big) \Big) \Big) \Big)$$

$$+\epsilon_S\left(Y(1-\epsilon_W)(1-\epsilon_S) - q_4\cdot\epsilon_{Ci}\cdot Y(1-\epsilon_W)(1-\epsilon_S)\right)$$

$$+\epsilon_W\left(Y(1-\epsilon_W)(1-\epsilon_S) - q_4\cdot\epsilon_{Ci}\cdot Y(1-\epsilon_W)(1-\epsilon_S)\right.$$

$$\left.-\epsilon_S\left(Y(1-\epsilon_W)(1-\epsilon_S) - q_4\cdot\epsilon_{Ci}\cdot Y(1-\epsilon_W)(1-\epsilon_S)\right)\right)\Bigg]$$

Cancelling I and simplifying gives,

$$f_D(I) = \Bigg[\epsilon_W + \epsilon_S(1-\epsilon_W) + \epsilon_{Ci}\cdot Y'(1-\epsilon_W)(1-\epsilon_S)$$

$$+ q_4\cdot\epsilon_{Ci}\cdot Y(1-\epsilon_W)(1-\epsilon_S)$$

$$+\epsilon_R\left(Y'(1-\epsilon_W)(1-\epsilon_S)(1-\epsilon_{Ci})\right)$$

$$+\epsilon_{Ce}\left(Y'(1-\epsilon_W)(1-\epsilon_S)(1-\epsilon_{Ci})(1-\epsilon_R)\right)$$

$$+\epsilon_S\left(Y'(1-\epsilon_W)(1-\epsilon_S)(1-\epsilon_{Ci})(1-\epsilon_R)(1-\epsilon_{Ce})\right)$$

$$+\epsilon_W\left(Y'(1-\epsilon_W)(1-\epsilon_S)(1-\epsilon_{Ci})(1-\epsilon_R)(1-\epsilon_{Ce})(1-\epsilon_S)\right)$$

$$+\epsilon_S\left(Y(1-\epsilon_W)(1-\epsilon_S)(1-q_4\cdot\epsilon_{Ci})\right)$$

$$+\epsilon_W\left(Y(1-\epsilon_W)(1-\epsilon_S)(1-q_4\cdot\epsilon_{Ci})(1-\epsilon_S)\right)\Bigg]$$

putting,

$$P_1 = Y'(1-\epsilon_W)(1-\epsilon_S)$$

$$P_2 = P_1(1-\epsilon_{Ci})$$

$$P_3 = P_2(1-\epsilon_R)$$

$$P_4 = P_3(1-\epsilon_{Ce})$$

$$P_5 = P_4(1-\epsilon_S)$$

$$P_1' = Y(1-\epsilon_W)(1-\epsilon_S)$$

$$P_2' = P_1'(1-q_4\cdot\epsilon_{Ci})$$

$$P_3' = P_2'(1-\epsilon_S)$$

$f_D(I)$ becomes,

$$f_D(I) = \epsilon_W + \epsilon_S(1 - \epsilon_W) + \epsilon_{Ci}\left[P_1 + q_4 \cdot P_1' + q_3 \cdot P_3\right]$$

$$+\epsilon_R \cdot P_2 + \epsilon_S \cdot P_4 + \epsilon_W \cdot P_5 + \epsilon_S \cdot P_2' + \epsilon_W \cdot P_3'$$

$$\therefore f_D(I) = \epsilon_W\left[1 + P_5 + P_3'\right] + \epsilon_S\left[1 - \epsilon_W + P_4 + P_2'\right]$$

$$+ \epsilon_{Ci}\left[P_1 + q_4 \cdot P_1' + q_3 \cdot P_3\right] + \epsilon_R \cdot P_2 \quad \text{.... equation 4.2.48}$$

HEAD OFFICE:

Research Avenue North,
Riccarton,
Edinburgh, EH14 4AP,
United Kingdom
Telephone: +44 (0)870 850 5131
Facsimile: +44 (0)870 850 5132

Tapton Park Innovation Centre,
Brimington Road, Tapton,
Chesterfield, Derbyshire, S41 0TZ,
United Kingdom
Telephone: +44 (0)1246 557866
Facsimile: +44 (0)1246 551212

Research House Business Centre,
Fraser Road,
Perivale, Middlesex, UB6 7AQ,
United Kingdom
Telephone: +44 (0)208 537 3491/2
Facsimile: +44 (0)208 537 3493

Brookside Business Park,
Cold Meece,
Stone, Staffs, ST15 0RZ,
United Kingdom
Telephone: +44 (0)1785 764810
Facsimile: +44 (0)1785 764811

Email: iom@iom-world.org